Benjamin K. Nyilitya

Nitrate source apportionment in surface and groundwater of the Lake Victoria basin in Kenya

Thesis submitted in fulfillment of the requirements for the degree of Doctor of Philosophy (PhD) in Bioscience Engineering: Environmental Sciences and Technology

Dutch translation of the title

Identificatie van nitraatbronnen in oppervlakte en grondwater in het bekken van het Victoriameer in Kenia

ISBN Number: 9789463573580

Citing this PhD

Nyilitya B. K. (2020). Nitrate source apportionment in surface and groundwater of the Lake Victoria basin in Kenya. PhD Thesis, Faculty of Bioscience Engineering, Ghent University, Belgium

Promotors

Prof. dr. ir. Pascal Boeckx
Department of Green Chemistry and Technology (ISOFYS)
Faculty of Bioscience Engineering
Ghent University, Belgium

Prof. dr. ir. Stephen Mureithi
Department of Land Resource Management and Agricultural Technology
Faculty of Agriculture
University of Nairobi, Kenya

Board of Examiners
Prof. dr. ir. Peter Bossier **(Chairman)**
Department of Animal Sciences and Aquatic Ecology
Faculty of Bioscience Engineering
Ghent University, Belgium

Prof. dr. ir. Peter Goethals
Department of Animal Sciences and Aquatic Ecology
Faculty of Bioscience Engineering
Ghent University, Belgium

Prof. dr. ir. Stefaan De Neve
Department of Environment
Faculty of Bioscience Engineering
Ghent University, Belgium

Dr. Fredrick Tamooh
Department of Zoological Sciences
Kenyatta University, Kenya

Prof. dr. Lutz Breuer
Department of Landscape, Water and Biogeochemical Cycles
Justus Liebig University Giessen, Germany

Dean of the Faculty of Bioscience Engineering, Ghent University
Prof. dr. ir. Marc Van Meirvenne

Rector of Ghent University
Prof. dr. ir. Rik Van de Walle

Table of Contents

Acknowledgements vii
List of abbreviations x
Summary xiv
Samenvatting xvii
Chapter 1. Introduction 1
1.1 Lake Victoria basin 2
1.1.1 Drainage 3
1.1.2 Ecosystem services 6
1.2 Why a focus on nitrate? 8
1.3 Nutrient and Nitrate pollution 10
1.4 Impacts of excess nutrient discharge in the Lake Victoria basin, Kenya 16
1.5 Limited riverine and groundwater nitrogen studies in the Lake Victoria basin, Kenya 19
1.6 Solving the problem: a multi-tracer approach 23
1.7 Objectives, research questions and hypothesis 26
1.8 Thesis Outline 28
1.9 Sampling strategy 30
Chapter 2. Land use controls Kenyan riverine nitrate discharge into Lake Victoria – Evidence from Nyando, Nzoia, and Sondu Miriu river basins 32
2.1 Introduction 34
2.2 Materials and methods 36
2.2.1 Study area 36
2.2.2 Sampling and analysis 40
2.2.3 Statistics 45
2.3 Results and Discussion 45
2.3.1 Spatial clustering of sampling stations 45
2.3.2 Physicochemical and Isotopic characterization 49
2.3.2.1 In-situ parameters 49
2.3.2.2 Nyando catchment 51
2.3.2.3 Nzoia catchment 58

2.3.2.4 Sondu Miriu catchment 62
2.4 Conclusions 66
Chapter 3. Nitrate source apportionment in the complex Nyando tropical river basin in Kenya 68
3.1 Introduction 70
3.2 Material and methods 73
3.2.1 Study area 73
3.2.2 Sampling and analysis 76
3.2.3 Statistical analysis 80
3.3 Results and discussion 82
3.3.1 Hydrochemistry 82
3.3.2 Spatial-temporal NO_3^- concentrations 83
3.3.3 Multi tracer approach in identifying dominant nitrate sources 87
3.3.4 Estimating proportional contribution of potential NO_3^- sources to the river nitrate 96
3.4 Conclusions 99
Chapter 4. Tracking sources and fate of groundwater nitrate in Kisumu city and Kano plains in Lake Victoria basin, Kenya 101
4.1 Introduction 103
4.2 Materials and Methods 105
4.2.1 Study area 105
4.2.2 Water sampling and analysis 107
4.3 Results and discussion 111
4.3.1 Hydrochemistry 111
4.3.2 Spatial groundwater NO_3^- distribution and its controlling factors 115
4.3.3 Use of multi isotope and hydro-chemical methods to track sources of groundwater nitrate contamination and removal 117
4.4 Conclusions 125
Chapter 5. General conclusions and discussion 126
5.1 Key research findings 127
5.1.1 Land use controls Kenyan riverine nitrate discharge into Lake Victoria – Evidence from Nyando, Nzoia, and Sondu Miriu river basins 127

5.1.2 Nitrate source apportionment in the complex Nyando tropical river basin in Kenya 129

5.1.3 Tracking sources and fate of groundwater nitrate in Kisumu city and Kano plains in Lake Victoria basin, Kenya 131

5.2 Key factors influencing NO_3^- input into surface and groundwater in Lake Victoria basin, Kenya and the necessary remedial measures 132

5.3 Research gaps and future perspectives 141

5.3.1 Biogeochemistry research 141

5.3.2 Sustainable management 143

5.3.2.1 River basin characterization 144

5.3.2.2 River basin monitoring 145

5.3.2.3 Nitrate Policy 146

5.3.3 Related initiatives 147

References 149

Appendices 164

Curriculum Vitae 186

Acknowledgements

Pursuing a PhD is a challenging task especially when one is a husband, father and an employee. It is even complex when one undertakes the task far away from your wife, 3 children and motherland. This has been my status and case for the last four years of my PhD study in Belgium. It has therefore taken the guidance and support of colleagues, institutions, friends and family to make this dream a reality.

First, I would like to give my sincere gratitude to my promoter Prof. Pascal Boeckx for his insightful guidance and unwavering support throughout this period, which extends beyond the PhD duration. This dream started sometimes in Nov/2011 through a Research stay (thanks to VLIRUOS) but couldn't kickoff by then due to lack of funding. You still welcomed me in your laboratory in 2015 as an IAEA fellow, something which re-kindled this vision and kept it alive in me. You didn't give up on me despite the delays, until in 2016 when the breakthrough in funding was achieved. I remember the tough comments, which have always made the work better, and the inspiration which comes from a "very good" comment from you. I am indeed grateful Prof.

My heartfelt gratitude to my co-promoter, Prof. Stephen Mureithi. You have been a close career counsellor and a mentor to me. Your encouraging words and facilitation of the field studies have had a great impact in realizing this dream. I can't forget the fieldwork campaigns, in the steep and muddy terrains of mt. Elgon. Your resilience ensured that we got a way for the vehicle to pass where other motorists couldn't maneuver, and we reached those remote sample locations. Surely, Thanks a lot.

The ISOFYS team. Special thanks to Samuel Bode. I very well remember how you assisted in optimizing the sediments incubation experiment and training me on the use of the IC. You were available to assist in trouble-shooting any laboratory system or procedure within ISOFYS. To this I say THANK YOU. Many Thanks to Katja. You made sure that there was no nonsense in using the "special" weighing machines. I can't forget how you look on top of those IRMS systems - very dear machines to you. For sure, my IRMS data was never late, thanks our dear sister. My appreciation to Stijn. Remembers how you demonstrated to me the bacterial denitrification technique, such a tedious procedure yet you performed it with the strength reminiscent of your stature. You made sure that, we were done with the bacterial conversions of this work before

moving-on to your current position, all the best in your career endeavors. To Erick, remembering that morning when I landed in Brussels for the first time, and you received and ushered me to the city of Gent. Thanks for your kindness. To Marijn, I salute your prowess in modelling software and the fast responses and solutions you give, keep it up. Special appreciation to My PhD colleagues - Joseph, Ben, Isaac and Scientific support staff - Thomas and Lodewijk, for the warmth and friendly atmosphere you provide at ISOFYS. Wishing you the best in your career pursuit. Special gratitude to Saskia, you do your work with a friendly attitude, passion and great concern. I am indeed grateful for all the arrangements ranging from, travel itinerary, room bookings and not to forget the departmental bike which was always available for me. My wife always remember your kindness, may you continue to shine in that office.

I am forever grateful to VLIRUOS-Belgium for: first, funding me for a three month (pre-doc) Research stay to develop this research concept; and very importantly, funding my PhD studies to completion through the TEAM project "Improved management for nitrate pollution in the Lake Victoria catchment of Kenya - ZEIN2016PR423. Indeed you are transforming and changing lives.

I appreciate the Cabinet Secretary and Principal Secretary of the Ministry of Water, sanitation and Irrigation – Kenya, for the facilitation and support as an employee of the Ministry during this period. Special appreciation to the Director of National Water Resources Management (Mr. Crispin Juma) for your encouraging support. Thanks to my colleagues at the Water quality and Research divisions (to name a few: Bernard Karicho, Agnes Mbugua, Simintei Kooke, Mware Kinyua, Daudi Kamau, John Okungu), you have been quite supportive. Special thanks to Dr. Kennedy K'oreje (CWTL-WRA), God used you in such a humble way when you sent the email contacts of Pascal, you can now see the results, am forever grateful my brother.

Great appreciation to the University of Nairobi (Department of LARMAT), for hosting and supporting me while performing field studies and laboratory analysis. Special thanks to Bedan Waithaka, you were not only the field driver but a friend and colleague at work. Driving the vehicle and assisting in field measurements to you wasn't overworking but teamwork. Enjoy your hobbies in retirement with peace and God's blessings. Thanks to Kimotho, the energetic laboratory technologist at LARMAT. Elias Odundo, you're the best field technician I have ever worked with. I marvelled your skills on *in situ* equipment calibration and the zeal you portray at work. It is my

prayer that your career dreams will be achieved one day, never give up. Seme and Okumu - the hydrological technologists (WRA- Kisumu & Kakamega), not even the mighty waters of Nyando and Nzoia could scare you not to determine the river flows, I am grateful.

And now to my family who have sacrificed enormously for this dream to be achieved. Eunice, the only one, and my better half. Words may fail me, but we share this achievement. You have endured long periods of my absence with the kids and you kept them happy and satisfied. You were even ahead of me in the PhD class, yet you didn't waiver in your roles. God bless you sweetheart. My Children – Esther, Timothy and Rehema, Thanks for forbearance. I hope my absence didn't discourage your academic and career goals but it will spur vigour and passion to develop your God-given talents and skills. You can do better.

To God be the Glory

List of abbreviations

ANOVA	Analysis of Variance
BH	Borehole
CA	Commercial Agriculture
CAN	Calcium ammonium Nitrate fertilizer
DAP	Di Ammonium Phosphate fertilizer
D	Dry
DO	Dissolved Oxygen
DON	Dissolved Organic Nitrogen
EAC	East Africa Community
EC	Electrical Conductivity
EW	End Wet
GDP	Gross Domestic Product
GIS	Geo Information System
HCA	Hierarchical Cluster Analysis
HDPE	High Density Polyethylene
HSD	Honestly Significant Difference
IAEA	International Atomic Energy Agency
IC	Ion Chromatogram
INMS	International Nitrogen Management Systems
IRMS	Isotope Ratio Mass Spectrometer
KNBS	Kenya National Bureau of Statistics
LVB	Lake Victoria Basin
LVBC	Lake Victoria Basin Commission
LVND	Lake Victoria Nitrate Directive
LVEMP	Lake Victoria Environmental Management Project
MA	Mixed Agriculture
MODIS	Moderate resolution Imaging Spectroradiometer
MQ	MilliQ
M&S	Manure and Sewage

NF	Nitrate Fertilizers
NF&R	Ammonium in Fertilizer/Rain
NP	Nitrate in precipitation
NPK	Nitrogen Phosphorous Potassium fertilizer
PVC	Polyvinyl Chloride
PW	Peak Wet
RI	Residential/ Industrial
S	Sugarcane
SIAR	Stable Isotope Analysis in R
SN	Soil Nitrogen
SSA	sub-Saharan Africa
SW	Start Wet
T	Tea
TF	Tea/ Forest
TN	Total Nitrogen
TU	Tea/ Urban
U	Urban
VSMOW	Vienna Standard Mean Ocean Water
WHO	World Health Organization
WRA	Water Resources Authority

Chemical compounds/ symbols

B	Boron
Ca^{2+}	Calcium
Cl^{-}	Chloride
Cs_2BO_2	Cesium borate
HCl	Hydrochloric acid
HCO_3^{-}	Hydrogen carbonate
K^{+}	Potassium
KCl	Potassium Chloride
KNO_3	Potassium Nitrate
Mg^{2+}	Magnesium
$MgClO_4$	Magnesium perchlorate
N	Nitrogen
N_2	Nitrogen gas
Na^{+}	Sodium
NaOH	Sodium hydroxide
NH_4^{+}	Ammonium
NH_4OH	Ammonium hydroxide
$(NH_4)_2SO_4$	Ammonium Sulphate
NO_2^{-}	Nitrite
NO_3^{-}	Nitrate
N_2O	Nitrous Oxide
O_2	Oxygen gas
PO_4^{3-}	Phosphate
SO_4^{2-}	Sulphate
TN	Total Nitrogen
TP	Total Phosphorus
$\delta^{11}B$	Stable isotope of boron with mass 11
$\delta^{15}N$	Stable isotope of nitrogen with mass 15
$\delta^{18}O$	Stable isotope of oxygen with mass 18

Units

℃	Degree Centigrade
cm	Centimeter
ha	Hectare
KM	Kilometer
L	Liter
M A S L	Meters Above Sea Level
meq	Milli equivalent
mg	Milli gram
mm	Milli meter
µg	Micro gram
µm	Micro meter
µS	Micro Siemens
t	Tones
‰	Per mill

Summary

Eutrophication of the waters of Lake Victoria has increasingly become a major threat to the water quality and ecosystem service of Africa's largest freshwater body. This is closely linked to rapid increase in human population and socio-economic activities in its basin which generates excess nutrient deposition into the Lake. Nitrate (NO_3^-) is one of the major nutrients associated with eutrophication of water bodies and whose concentration levels in Lake Victoria are reportedly on the increase. However, recent spatiotemporal data and information on NO_3^- concentrations, discharge, distribution and sources in the Lake's basin is scanty. The Lake is shared by the three East Africa Community partner states: Kenya, Uganda and Tanzania. The Kenyan side of the basin contributes around 38% of the total riverine flow into the lake, hence it's significant to the Lake's hydrology. With the overall objective to identify and apportion NO_3^- sources at the Kenyan side of the Lake's basin, this study investigated spatiotemporal NO_3^- concentrations, sources, discharge and fate in both surface and groundwater resources of the basin. Here, we apply a state-of-the-art approach by integrating hydrochemical, multi isotope (δ^{15}N- and δ^{18}O-NO_3^-, and δ^{11}B) and a Bayesian isotopic mixing model to identify and apportion NO_3^- sources and study biogeochemical processes.

The study was carried out in three distinct river basins of the Kenyan side of the basin (Nyando, Nzoia, and Sondu Miriu) and groundwater in Kisumu city and its surrounding Kano plains. The findings show that land use patterns in the basin influences riverine NO_3^- concentrations and discharge. Specifically, human population density and unsustainable intensification of agricultural practices were the predominant factors determining NO_3^- levels in the river basins. This was evidenced by the highly populated and intensively cultivated mixed agriculture land use zone of the Nyando basin recording significantly higher NO_3^- levels while the upstream zones of the river basins, characterized by low human activities, recorded lower NO_3^- values. However, *In situ* attenuation of NO_3^- was observed in the downstream catchments and was likely more intense in the dry season due to reduced water discharge volumes and longer water residence time. Further studies are required to investigate the potential biogeochemical processes including denitrification, nitrification, and annamox, among others. River NO_3^- delivery into the Lake is governed by river water discharge volume, basin size, and season. Therefore, of the three river basins studied, the

largest and high water-yielding River Nzoia, recorded the highest NO_3^- delivery into the Lake, followed by Sondu Miriu and Nyando river basins in that order.

The Lake Victoria basin in Kenya is characterized by a complex land use system where agricultural activities, industries and residences are mixed, or small holder farms that encroach forest and wetland areas. It can therefore be complicated to differentiate nonpoint sources of pollution in the river basins. Nevertheless, by coupling hydrochemistry, multi-isotope tracers and a Bayesian isotopic mixing model, the potential sources of river NO_3^- discharge were identified and quantified. Moreover, the added value of integrating this multi-tracer approach is demonstrated in this work for application in complex river basins of the sub-Saharan Africa. Especially, boron isotope ($\delta^{11}B$) data was quite useful here by overcoming the limitations faced when using $\delta^{15}N$- and $\delta^{18}O$-NO_3^- alone, thus enabling the differentiation of manure and sewage sources in both surface and groundwater. Manure was identified as the major source of riverine NO_3^- input in the basin, dominating the mixed agriculture, sugarcane and the residential/industrial land use zones. Sewage sources dominated river NO_3^- in the urban land use, in addition to being a major source in the residential/industrial and sugarcane land uses during the dry season. Soil nitrogen was the other key riverine NO_3^- source, which dominated the tea and forest land use zones, and was also the dominant source in the basin during the agriculturally dormant 'short rains' season. Inorganic fertilizers on the other hand, were the main sources of river NO_3^- in the large-scale tea and commercial flower farming zones.

Groundwater NO_3^- concentration and sources varied spatially and seems to be largely controlled by human population density. Shallow wells located in Kisumu city and boreholes in Ahero town showed significantly high NO_3^- concentration compared to those located in the rural Kano plains. Approximately 63% of the boreholes and 75% of the shallow wells exceeded the drinking water WHO threshold for NO_3^- and NO_2^- during the study period. Sewage was established to be the main source of groundwater NO_3^- pollution in Kisumu's informal settlements, in Ahero town and in boreholes located in populated neighborhoods. Manure on the other hand, was the main NO_3^- source in boreholes and shallow wells located in the Kano area and those in newly planned estates around Kisumu. NO_3^- isotope enrichment corresponding to a NO_3^- concentration decrease was evident in the dry season, indicating that *in situ* denitrification might be responsible for the NO_3^- decrease. However, a partial nitrification process could be taking place concurrently, which might

be responsible for an increase in NO_2^- concentrations observed in the dry season. However, these potential biogeochemical processes in groundwater needs to be further investigated.

Findings from this study reveal the main activities, which controls NO_3^- input into the water resources of the basin. The use of animal manure in mixed farming systems and free range livestock keeping are common practices in the basin, responsible for the observed dominance of the manure NO_3^- source. In addition, inadequate and outdated sewage treatment infrastructure is a characteristic of most urban centers in the basin, which results in discharge of untreated wastewater into freshwater resources. Furthermore, human encroachment of forests, wetlands and poor land management practices have been rampant in the basin, triggering high soil erosion rates and nutrient losses. Therefore, the requisite policy guidelines and intervention strategies should be developed and implemented in the basin, in order to control excess NO_3^- discharges and ensure sustainable water and ecosystem services.

Samenvatting

Eutrofiëring van het Victoriameer is in toenemende mate een grote bedreiging geworden voor de waterkwaliteit en ecosysteemdiensten van het grootste zoetwaterlichaam van Afrika. Dit hangt nauw samen met een snelle toename van de menselijke bevolking en sociaal-economische activiteiten in het stroomgebied, die een overmaat aan nutriënteninput in het meer veroorzaken. Nitraat (NO_3^-) is een van de belangrijkste voedingsstoffen die de eutrofiëring van waterlichamen veroorzaakt en waarvan de concentratie in het Victoriameer toeneemt. Echter, recente ruimtelijke gegevens en informatie over NO_3^--concentraties, -lozing, -distributie en -bronnen in het bekken van het meer zijn schaars. Het meer wordt gedeeld door de drie partnerstaten van de Oost-Afrikaanse Gemeenschap: Kenia, Oeganda en Tanzania. De Keniaanse kant van het bekken draagt ongeveer 38% bij aan de totale rivierinstroom in het meer, en is dus belangrijk voor de hydrologie van het meer. Met als algemene doelstelling het identificeren en identificeren van NO_3^--bronnen aan de Keniaanse kant van het bekken van het meer, onderzocht deze studie spatiotemporale NO_3^--concentraties, -bronnen, -afvoer en *sinks* in zowel oppervlakte- als grondwater van het bekken. Hier passen we een *state-of-the-art* benadering toe door hydrochemische, multi-isotoop (δ^{15}N- en δ^{18}O-NO_3^- en δ^{11}B) en een Bayesiaans isotoop mengmodel te integreren om NO_3^--bronnen te identificeren en toe te wijzen en biogeochemische processen te bestuderen.

De studie werd uitgevoerd in drie verschillende stroomgebieden aan de Keniaanse kant van het bekken (Nyando, Nzoia en Sondu Miriu) en het grondwater in de stad Kisumu en de omliggende Kano-vlaktes. De bevindingen tonen aan dat landgebruikspatronen in het bekken de NO_3^--concentraties en afvoer via rivieren beïnvloeden. Met name de bevolkingsdichtheid en de niet-duurzame intensivering van landbouwpraktijken waren de belangrijkste factoren die de NO_3^- niveaus in de stroomgebieden bepaalden. Het dichtbevolkte en de intensief gecultiveerde zone met gemengd landgebruik in het Nyando-bekken vertoonde aanzienlijk hogere NO_3^--niveaus, terwijl de stroomopwaartse zones van de stroomgebieden, gekenmerkt door lage menselijke activiteiten, lagere NO_3^--concentraties vertoonden. Echter, *in situ* verwijdering van NO_3^- werd waargenomen in de stroomafwaartse stroomgebieden en was waarschijnlijk intenser in het droge seizoen als gevolg van verminderde watervolumevolumes en dus een langere waterverblijftijd. Verdere studies zijn nodig om de mogelijke biogeochemische processen, waaronder denitrificatie, nitrificatie en annamox, te onderzoeken. De afgifte van NO_3^- door rivieren in het meer wordt

bepaald door het afvoervolume van het rivierwater, de omvang van het bekken en het seizoen. Van de drie onderzochte rivierbekkens registreerde de rivier met het grootset debiet (Nzoia) daarom de hoogste NO_3^--afgifte in het meer, gevolgd door de stroomgebieden van Sondu Miriu en Nyando.

Het bekken van het Victoriameer in Kenia wordt gekenmerkt door een complex landgebruik waar landbouwactiviteiten, industrieën en woningen worden gemengd, of kleine boerenbedrijven die bos- en moerasgebieden binnendringen. Het is daarom ingewikkeld om difuse bronnen van vervuiling in deze stroomgebieden te differentiëren. Niettemin werden door de koppeling van hydrochemie, multi-isotoop tracers en een Bayesiaans isotoop mengmodel de potentiële bronnen van NO_3^--lozing in de rivier geïdentificeerd en gekwantificeerd. Bovendien wordt de toegevoegde waarde van de integratie van deze multi-tracer-aanpak aangetoond en opent perspectieven voor toepassing in complexe stroomgebieden van Sub-Sahara Afrika. Vooral de gegevens van boorisotopen ($\delta^{11}B$) waren nuttig om de beperkingen te overwinnen die werden ondervonden bij het gebruik van $\delta^{15}N$- en $\delta^{18}O$-NO_3^-, waardoor de differentiatie tussen mest- en afvalwaterbronnen van NO_3^- in zowel oppervlakte- als grondwater mogelijk werd. Mest werd geïdentificeerd als de belangrijkste bron van NO_3^--input in rivieren van het bekken en domineerde de gemengde landbouw, het suikerriet en de residentiële / industriële landgebruikszones. Afvalwater van huishoudens domineerden in het stedelijke landgebruik, mas was ook een belangrijke bron van NO_3^- in het residentiële / industriële en suikerrietlandgebruik tijdens het droge seizoen. Bodemstikstof was de andere belangrijke NO_3^--bron in de thee- en bosgebieden en was ook de dominante bron in het bekken tijdens 'korte regenseizoen' waarin minimale landbouwactiviteiten plaatsvinden. Anorganische meststoffen waren daarentegen de belangrijkste bronnen van rivier NO_3^- in de grootschalige thee- en commerciële bloementeeltzones.

De concentratie en bronnen van grondwater NO_3^- varieerden ruimtelijk en lijken grotendeels te worden gedreven door bevolkingsdichtheid. Ondiepe waterputten in de stad Kisumu en boorputten in de stad Ahero vertoonden een significant hoge NO_3^--concentratie vergeleken met die in de landelijke Kano-vlakten. Ongeveer 63% van de boorputten en 75% van de ondiepe waterputten overschreed tijdens de onderzoeksperiode de WHO-drempel voor drinkwater voor NO_3^- en NO_2^-. Afvalwater van huishoudens is de belangrijkste bron van NO_3^--vervuiling van het grondwater in de informele nederzettingen van Kisumu, in de stad Ahero en in boorgaten in dicht bevolkte buurten. Dierlijke mest was daarentegen de belangrijkste NO_3^--bron in boorgaten en ondiepe

putten in het Kano-gebied en in nieuw geplande woongebieden rond Kisumu. In grondwater nam de aarijking van isotopen in NO_3^- toe met een gelijktijdige afname van de NO_3^--concentratie en in dit vooral in het droge seizoen. Dit fenonmeen geeft aan dat *in situ* denitrificatie verantwoordelijk zou kunnen zijn voor de daling van NO_3^-concentratie in grondwater. Er kan echter tegelijkertijd een partieel nitrificatieproces plaatsvinden, wat verantwoordelijk kan zijn voor een toename van de NO_2^--concentraties. Deze potentiële biogeochemische processen in grondwater moeten echter verder worden onderzocht.

De bevindingen uit dit onderzoek onthullen de belangrijkste activiteiten, die de NO_3^--toevoer in bekken van het Victoriameer regelen. Het gebruik van dierlijke mest in gemengde landbouwsystemen en het houden van dieren met vrije uitloop is een gangbare praktijk in het bekken, die verantwoordelijk is voor de waargenomen dominantie van mest als NO_3^--bron. Bovendien is een ontoereikende en verouderde rioolwaterzuiveringsinfrastructuur een kenmerk van de meeste stedelijke centra in het bekken, wat resulteert in lozing van onbehandeld afvalwater in zoetwaterbronnen. Bovendien is de menselijke aantasting van bossen, wetlands en slechte landbeheerpraktijken in het bekken wijdverbreid, wat leidt tot hoge erosiepercentages en verlies van plantenvoedingsstoffen. Daarom moeten dringend beleidsrichtlijnen en interventiestrategieën voor het stroomgebied worden ontwikkeld en geïmplementeerd om de toenemende NO_3^--lozingen te beheersen en duurzame beheer van water- en ecosysteemdiensten te waarborgen.

Chapter 1. Introduction

1.1 Lake Victoria basin

Background information

Lake Victoria is the second largest fresh water lake in the world and Africa's largest fresh water body with a surface area of approximately 68,000 km^2 (Lung'ayia et al., 2001). It is shared by three East African countries (Fig. 1.1): Tanzania, with a surface area share of 33,756 km^2 (49%), Uganda with a share of 31,001 km^2 (45%), and Kenya with a share of 4,113 km^2 (6%). It has a drainage basin area of 193,000 km^2 spread over five coutries: Tanzania, with a basin area share of 84,920 km^2 (44%), Kenya, with a share of 42,460 (22%), Uganda, with a share of 30,880 (16%), Rwanda, with a share of 21,230 (11%) and Burundi, with a share of 13,510 (7%).

It is a relatively shallow lake for its area, with an average depth of 40 m and a maximum depth of 80 m (LVEMP, 2005). The lake straddles the equator between latitudes 3°12'S – 0°30'N and longitudes 31°40' – 34°50'E, and at an altitude of 1,134 m a.s.l. The Lake Victoria Basin (LVB) experiences an equatorial climate with sub-humid temperatures ranging between 15 and 30°C, influenced by the relatively high elevation of the Lake and its mountains (Nyeko-Ogiramoi et al., 2013). Rainfall in the basin averages around 1300mm, varying from 886 mm in the low-lying lakeshore areas to 2600 mm in the highlands. The mean evaporation rate ranges between 1100 – 2050 mm per year, which decreases with increasing altitude but in some months exceeds rainfall (Nyeko-Ogiramoi et al., 2013). The population of the basin was estimated at 45 million in 2015 (WorldBank, 2018). However, it has been projected to grow to around 60 million in 2020 because of a high population growth rate and in-migration caused by the attraction of the lake's resources (Bremner et al., 2013). The population density is around 300 persons per km^2, much higher than Africa's average of 36 persons per km^2 (see Figure 1.2), and a population growth rate >3% per annum (Muyodi et al., 2010).

Figure 1.1. Map of the Lake Victoria basin showing the Lake surface area and drainage basin area within its five riparian countries: Kenya, Uganda, Tanzania, Rwanda and Burundi (LVEMP, 2006)

1.1.1 Drainage

Water input into the Lake consists of: rain over the lake's surface, estimated at 82% of the Lake's water and catchment (rivers) discharges accounting for 18% (COWI, 2002). The LVB is drained by several rivers originating from the three riparian countries as shown in Table 1.1. Table 1.1 also gives average river water discharges and their percentage contributions determined using long term monitoring data from 1950 to 2000 (COWI, 2002; LVEMP, 2005). The largest of all rivers is R. Kagera which has tributaries from Rwanda and Burundi and contributes about 33.5% of the total riverine inflow to Lake Victoria. Based on long term monitoring of inflow (catchment discharge, rainfall over the lake) and outflow (evaporation over the lake and White Nile outflow) data, a water mass balance of the lake was estimated

(COWI, 2002). Catchment inflow was 778. 3 $m^3 s^{-1}$ (Table 1.1) while rain over the Lake amounted to 3631 $m^3 s^{-1}$. Water outflow by evaporation over the lake's surface was estimated at 3330 $m^3 s^{-1}$ and outflow through the White Nile amounted to 1046 $m^3 s^{-1}$. The groundwater contribution to the Lake water balance was assumed to be negligible. Furthermore, studies have shown that the contribution of groundwater to the Lake water balance is <1% of the total inflows (Owor et al., 2011) This leaves a small positive inflow of 33 $m^3 s^{-1}$, which reportedly accounted for the Lake level rise of about 1.0 m between January 1950 and December 2000 (COWI, 2002).

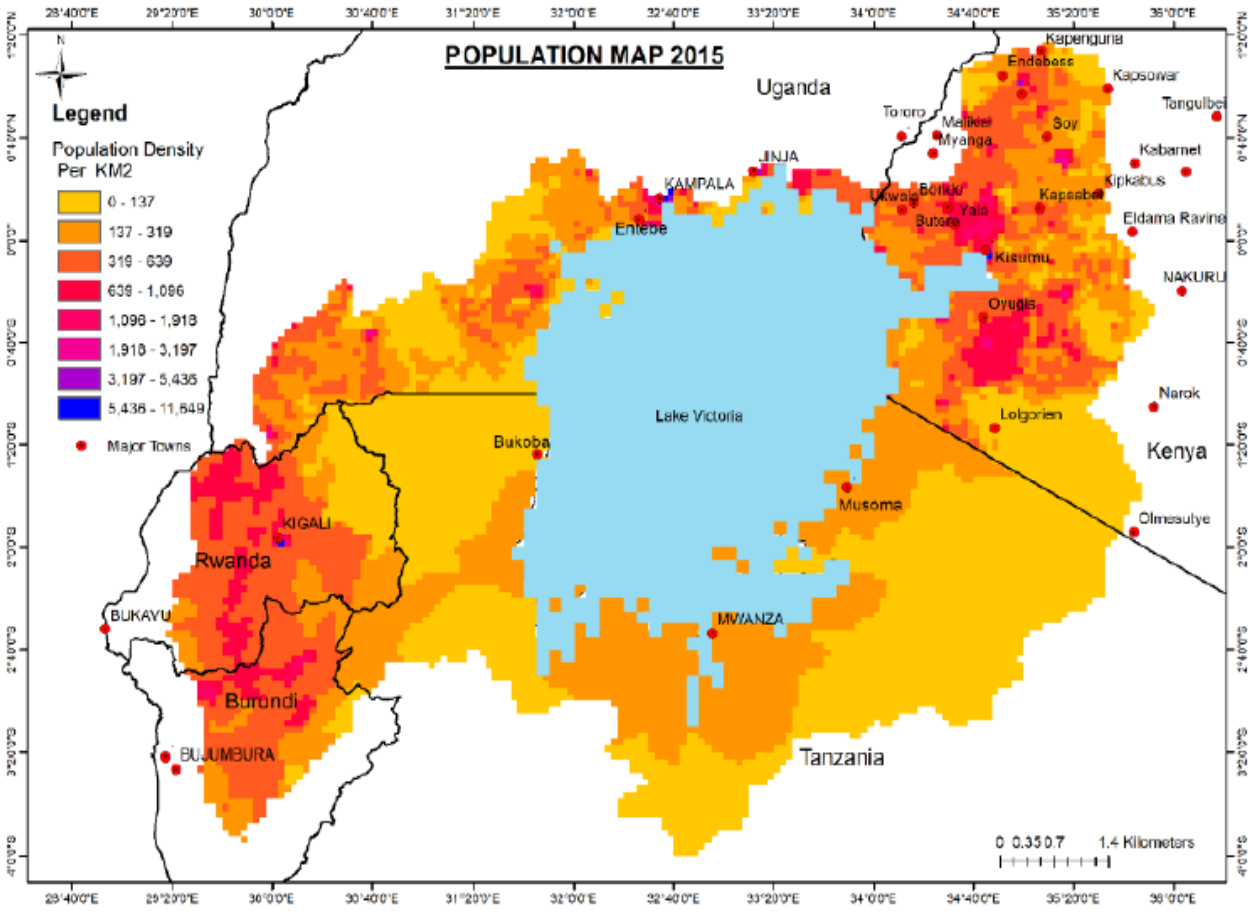

Figure 1.2. Lake Victoria basin population map for 2015, showing the population density (people per km^2) distribution in its five riparian countries: Kenya, Tanzania, Uganda, Rwanda, and Burundi (WorldBank, 2018)

Although Kenya holds only 6% share of the Lake surface area, comprising mainly the Winam gulf (Fig. 1.1), its basin contributes for 38% (292.1 $m^3 s^{-1}$, Table 1.1) of the total catchment inflow. This is exclusive of the Mara River, a trans-boundary river which originates in the Mau water tower in Kenya but discharges into Lake Victoria through Tanzania, contributing 4.8% of the total catchment inflow.

Table 1.1. Rivers draining the Lake Victoria basin. Discharge values are long term average water discharges computed from river gauging measurements during the period 1950 – 2000. The basin area represents the total basin area of each of the five riparian countries (COWI, 2002)

Country	**River basin**	**Discharge ($m^3 s^{-1}$)**	**Percentage (%)**	**Basin area (km^2)**
Kenya	Nzoia	115.3	14.8	42,460 (22%)
	Nyando	18	2.3	
	Sondu Miriu	42.2	5.4	
	Gucha Migori	58	7.5	
	Yala	37.6	4.8	
	Sio	11.4	1.5	
	South Awach	5.9	0.8	
	North awach	3.7	0.5	
	Sub-total	**292.1**	**37.6**	
Tanzania	Mara*	37.5	4.8	84,920 (44%)
	Grumeti	11.5	1.5	
	Mbalageti	4.3	0.5	
	E. shore stream	18.6	2.4	
	Simiyu	39.0	5.0	
	Magogo moame	8.3	1.1	
	Nyashishi	1.6	0.2	
	Issanga	30.6	3.9	
	S. shore stream	25.6	3.3	
	Biharamulo	17.8	2.3	
	W. shore stream	20.7	2.7	
	Kagera*	260.9	33.5	
	Sub-total	**476.4**	**61.2**	
Uganda	Bukora	3.2	0.4	30,880 (16%)
	Katonga	5.1	0.7	
	N. shore stream	1.5	0.2	
	Sub-total	**9.8**	**1.3**	
	Total Average inflow	**778.3**	**100.0**	
Rwanda				21,230 (11%)
Burundi				13,510 (7%)

* Kagera and Mara are Transboundary Rivers. Kagera crosses over Burundi, Rwanda, Uganda and Tanzania. Mara crosses over Kenya and Tanzania (see Fig. 1.1).

1.1.2 Ecosystem services

The lake and its catchments are valued for its socio-economic potential in addition to its immense ecological values. It supports the livelihoods of about one third of the population living in its riparian countries (>45 million) by providing basic needs and services like food, fresh water and transport. In addition, it is a great economic resource to the regional economies by providing energy (hydroelectric power stations), transport, potable and commercial water supply, wildlife and tourism, minerals, cash crops, trade and industry, and fishery among others, making it a core to regional integration and development of East Africa (Fig. 1.3). Being the source of the White Nile, it is an important asset of the Nile River basin countries.

Figure 1.3. Some ecosystem services of Lake Victoria including transport, fishing, birds, wildlife, wetlands and tourism via its scenic beaches

The basin is rich in fish resources and wildlife diversity. It has been reported (COWI, 2002) that Lake Victoria supports the most productive fresh water fishery in the world with an annual fish yield exceeding 300,000 tons, worth ca. 600 million US dollar annually. This is dominated

by the Nile perch (*Lates niloticus*) and the Nile tilapia (*Oreochromis niloticus*) species. However, due to eutrophication of the lake waters and over fishing, fish populations in the Lake have been on the decrease (Ochumba, 1990; Sitoki et al., 2010). The basin has a rich diversity of wildlife (including endangered animals like Sitatunga, de Brazza monkeys, Faschons hartebeests, reptiles and birds). It has also tourist attraction sites such as national parks, game reserves, and scenic sites. In addition, it has mineral resources like graphite, limonite, copper, gold, iron, limestone, soapstone, tin and nickel (LVEMP, 2006). The lake shores are covered by extensive wetlands which play an important role in hydrological stability and ecosystem productivity of the basin. Socio-economically, wetlands are a source of fish, raw materials for handicrafts, and outdoor recreation to the riparian communities. They are home to a diversity of wildlife including various bird species, mammals (hippopotamus) and reptiles. In addition, wetlands are dominated by the papyrus vegetation, which acts as nutrient filters of water entering the lake (Odada et al., 2006; Raburu et al., 2012). The nutrients are removed through incorporation into the plant tissues of the wetland vegetation, accumulation into wetland sediments and in the case of nitrogen, through denitrification in the root zone of the wetland vegetation (Kansiime et al., 2007; Nyenje et al., 2010).

However, the Lake Victoria ecosystem health has undergone drastic changes in the last five decades, mainly driven by a high population growth, land use change and economic activities taking place in its catchment. Land subdivision into small-holder farms, forest and wetland encroachment, development of commercialized agriculture, urbanization and industrialization have exerted considerable pressure on land, vegetation and water resources (Raburu et al., 2012; Wang et al., 2012). These anthropogenic activities have led to serious negative environmental impacts on the basin such as deforestation, accelerated soil erosion, incremental wetland loss, and elevated sewage discharges which triggers uncontrolled discharge of nutrients into the Lake resulting in eutrophication of the Lake waters (Lung'ayia et al., 2001; Scheren et al., 2000).

1.2 Why a focus on nitrate?

Eutrophication is a term commonly used to describe the biological effects caused by nutrient enrichment in aquatic ecosystems. It is closely associated with increasing nitrogen (N) and phosphorus (P) concentrations in water, but N attracts more attention because it often limits primary production in water bodies, and also because of the far much high global application of N-based inorganic fertilizers as compared to phosphorus (Glibert et al., 2005). The understanding of the sources of nutrient discharge, distribution, and potential biogeochemical processes is key in controlling the impacts of eutrophication in water bodies. There are several methods used in the determination of sources of nutrient pollution in water. These include, traditional source identification methods which are based on combining water quality assessment data and land use data. On the other hand, water quality models are widely used by environmental and water regulatory institutions around the world for management, planning and pollution control.

The most commonly used models include: SWAT (Soil Water and Analysis Tools), WASP (Water Quality Analysis Simulation Program), SIMCAT (simulation of catchments), TOMCAT (Temporal/Overall Model for Catchments), BASINS (Better Assessment Science Integrating Point and Nonpoint Sources), MIKE II, QUAL 2E, QUASAR, ISIS (Cox, 2003; Gao and Li, 2014). Water quality models integrated with remote sensing and geographical information systems (GIS) data includes the export coefficient model which has been applied to study nonpoint source nutrient pollution (Do et al., 2011; Johnes, 1996; Mattikalli and Richards, 1996). The model estimates solute loading at the outlet of a watershed using land use data, fertilizer application rates and export coefficients. The DRASTIC model is also a GIS-based method used for groundwater pollution vulnerability assessment (Mfumu Kihumba et al., 2017; Shirazi et al., 2012). However, a major shortcoming of most of these models is that they are developed for a particular purpose and no one model can provide all the desired functions (Gao and Li, 2014). In addition, models contain assumptions and limitations which may result in large deviation between the facts and the simulation. Therefore, users tend to use

a combination of models to solve multiple water quality problems. Other commonly used methods for water quality assessment are multivariate statistical techniques (Barakat et al., 2016; Pejman et al., 2009). Although these methods are straight forward in application, they are limited in apportioning the contribution of several potential sources of pollution to a water body, while most statistical models rarely consider groundwater contribution (Xia et al., 2018). In addition, these methods are limited in unravelling nutrient transformation mechanisms which are crucial in understanding the fate of nutrients in a water body (Gao and Li, 2014).

However, this study focuses on the nitrate (NO_3^-), to apply a state-of-the-art approach which integrates multiple isotopes ($\delta^{15}N$, $\delta^{18}O$-NO_3^-, $\delta^{11}B$), hydrochemistry and a Bayesian mixing model (mixSIAR) to study NO_3^- discharge, pollution sources and biogeochemical processes on the Kenyan side of the Lake Victoria Basin. This technique is the first of its kind in the region and shall provide highly missing data and information necessary for improving policy guidelines and implementing mitigation strategies for control of excess NO_3^- discharge in the basin. It is noteworthy that the other N species (organic N, ammonium (NH_4^+)), and phosphate (PO_4^-) significantly contribute to eutrophication of water bodies. To this effect, studies on nutrient concentrations (including total nitrogen (TN) and total phosphorus (TP)) have been done in the Kenyan part (Winam gulf) of Lake Victoria (Gikuma-Njuru et al., 2013b; Lung'ayia et al., 2001; LVEMP, 2005). However, no study has been undertaken to investigate the sources of NO_3^- pollution, discharge and distribution on the Kenyan part of the Lake's basin. This could partly be attributed to lack of appropriate technology to identify and quantify nonpoint sources of nutrient pollution. Therefore, due to the existing data and technical knowledge gap, this work focuses on the NO_3^-, and implements the state-of-the-art methodology (see section 1.6 for further details) which has successfully been implemented in other regions of the world in NO_3^- source apportionment and biogeochemical investigations (Mayer et al., 2002; Meghdadi and Javar, 2018; Widory et al., 2013; Xue et al., 2012; Yevenes et al., 2016; Zeng and Wu, 2015; Zhang et al., 2018b).

1.3 Nutrient and Nitrate pollution

Elevated NO_3^- input into a water body causes degradation of water quality and consequently contributes to affecting its ecosystem health. High amounts of NO_3^- in aquatic environments lead to eutrophication, which is manifested through propagation of dense algal blooms, aquatic weeds like water hyacinth in Lake Victoria, and development of anoxic zones. In addition to causing water quality decline in fresh water resources, eutrophication is associated with a decrease in fish populations and as a result it lowers the ecosystem service (Lung'ayia et al., 2001; Ochumba, 1990). To human health, a high NO_3^- uptake is a risk for methemoglobinemia (blue baby syndrome) in children and for cancer following long term exposure (Kendall et al., 2007). In addition, epidemiological studies have linked prenatal NO_3^- exposure of > 5 mg L^{-1} per day (in drinking water) to birth defects in the offspring. This includes: neural tube defects (Brender et al., 2013), central nervous system defects (Arbuckle et al., 1988), and congenital heart defects (Cedergren et al., 2002). The World Health Organization (WHO) has put the maximum allowable NO_3^- concentration at 50 mg L^{-1} in potable water; but recent findings by Schullehner et al. (2018) report an increased colorectal cancer risk already at NO_3^- concentrations as low as 3.9 mg L^{-1}.

In the tropical Sub-Saharan Africa (SSA), NO_3^- contamination of both surface water and groundwater is emerging as major threat to freshwater availability (Nyenje et al., 2010; White et al., 2017). This is driven by the high population growth rate, urbanization and an economic boom happening in these countries. Rural to urban migration in SSA has led to rapid growth in urban population and industrialization as people look for better opportunities (White et al., 2017). It is reported that urban cities in SSA countries have grown in population at an average rate of 4.0% per year in the past 20 years compared to the global annual urban population growth rate projected to be between 1.4 and 1.8% (WHO, 2015). The main environmental challenge posed by urbanization in SSA has been lack of corresponding investment in urban waste water management infrastructure. As a result, untreated urban sewage, characteristically high in concentration of organic N and other dissolved inorganic species (NO_3^-, NH_4^+, PO_4^{3-},

nitrite (NO_2^-)), ends up contaminating fresh water resources. For instance, in East Africa, major cities sprawling around Lake Victoria, such as Kampala, Kisumu, Entebbe, and Mwanza (Fig. 1.1) lack adequate sanitation systems due to low financial investments in current wastewater treatment technologies (Wang et al., 2012). In addition, the urban poor residents in these cities often depends on natural systems (rivers, lakes) for livelihoods, which gives rise to unplanned urban settlements (slums) around these resources, resulting in untreated sewage discharges into these water resources (Benkovitz et al., 1996; White et al., 2017).

On the other hand, the need for food sustainability in SSA (where many still suffer malnutrition) has led to the adoption of both organic and inorganic fertilizer use to boost crop productivity. Such intensive agricultural practices increase NO_3^- leaching into water bodies (Maghanga et al., 2013). Human encroachment and settlement in natural habitats like forests, wetlands and riparian areas is a major land degrading practice in the LVB. It is associated with nutrient loading into the lake (Odada et al., 2006). This has reportedly resulted into about 60% of the Lake's basin being affected by land degradation processes, resulting into elevated soil erosion, collapsing of river banks, siltation of water reservoirs and high sediment deposition into Lake Victoria (Raburu et al., 2012). The situation has been exacerbated by human encroachment of wetlands destroying their nutrient buffering capacity and importance for biodiversity. Studies report that major wetlands around Lake Victoria such as the Nakivubo wetland (Uganda), the Nyando wetland and the Yala swamp (Kenya) have been extensively encroached and converted into farming and human settlement areas (Kansiime et al., 2007; Raburu et al., 2012).

The scope of this study is the Kenyan side of the Lake Victoria drainage basin (Fig. 1.1), and the discussion will now focus on this part of the basin to highlight its status regarding nutrient discharges into the Lake.

The Kenyan part of the basin is quite significant for the Lake's hydrology and water quality because of its substantial riverine contribution (38%, Table 1.1). Due to its economic relevance,

the Kenyan side of the basin is one of the densely populated regions in the LVB, as shown in Fig. 1.2. According to the 2019 Kenya Population Census report, LVB, Kenya has a population of over 12 million people (KNBS, 2019). High population and economic growth have led to land use patterns in the basin, being deviated from natural landscapes to anthropogenic systems (Twesigye, 2011). For instance, encroachment of the Mau forest, which is the water source of Rivers: Nyando, Sondu Miriu, and Mara, led to massive deforestation, conversion of natural habitats to farmlands, and loss of biodiversity (Shepherd et al., 2000). It has been reported that about 7,084 ha of Mau forest land and 1,029 ha of pristine forests of Mt. Elgon (source of River Nzoia and Sio) were cleared between 2000 and 2003 (LVBC, 2007). The deforestation resulted into bare lands and even made worse by poor agricultural practices in escarpments (Slope: 19 – 43º). This led to increased runoff and high water turbidity being witnessed in the tributary rivers and the lake (Ntiba et al., 2001). It has been reported that sedimentation in Lake Victoria is contributed mostly by the Kenyan rivers and the river Kagera in Tanzania (Odada et al., 2006). Satellite imagery shows clear contrasts in the colouration of the Winam gulf waters relative to the main Lake Victoria (Fig. 1.4). It appears that the brownish colouration originates from the tributary rivers, especially the Nyando River mouth and extends to the rest of the gulf. In addition, the current state of forest encroachment by small scale farms and the resulting effects of highly turbid water in Lake Victoria at the Nyando river mouth can be seen in Fig. 1.5a & b.

Urbanization in the LVB, Kenya has seen a rapid growth and industrialization in major cities like Kisumu (Kenya's third largest city), Eldoret, Kakamega, Bungoma, Kitale, and Kericho. Agro-based activities (sugarcane, tea, coffee, rice, maize, tea) as well as other manufacturing activities are based in these cities. However, lack of a corresponding investment in the necessary wastewater treatment infrastructure in these urban centers outstretches existing sewage treatment plants (Wang et al., 2012). This often results in raw sewage containing high levels of organic N, the inorganic N species (NO_3^-, NH_4^+, NO_2^-), and PO_4^- being discharged

into the Lake and its tributary rivers as reported by Okungu and Opango (2004) and Omosa et al. (2012).

Figure 1.4. A satellite image showing the waters in the Winam gulf relative to the main Lake Victoria. Brown colouration is dense at the Nyando river mouth (Google Earth image, dated 21/ 02/2020).

Rapid urban population growth has resulted in proliferation of informal settlements (slums) which are not connected to formal sewer lines, but depends mainly on pit latrines and landfills for waste disposal (Wright et al., 2013). This makes groundwater highly vulnerable to pollution from these onsite systems. In Kisumu, for instance, groundwater is the main water source for urban slum dwellers and for the surrounding rural population. This is because, surface water is either not affordable or not accessible in these areas (Okotto-Okotto et al., 2015). Most slum residents depend on shallow wells because they are cheap to construct at household level. However, they are dung to the same depth (< 5 meters) as pit latrines therefore, making the water highly vulnerable to contamination from human wastes (Wright et al., 2013).

Agriculture is the mainstay of the Kenyan economy and the Lake basin is home to major cash crops like tea, sugarcane, wheat, cut flowers, coffee, and maize. Population pressure coupled

with the demand for food security has intensified agricultural activities in the region, though in an unsustainable way. As a result, there has been a rapid rise in acreage of land under both large-scale and small-scale farming, while mechanized farming and the use of inorganic fertilizers are increasing (Maghanga et al., 2013; Twesigye, 2011). This has a double impact on NO_3^- loss because some of the agricultural land has been hived from land previously occupied by forest or wetlands which naturally buffers the lake from excess nutrient deposition (Raburu et al., 2012). For instance, Fig. 1.5c & d show commercial flower and tea farms in the headwater catchments of R. Nyando and R. Sondu Miriu, respectively, where agrochemicals including inorganic fertilizers are intensively applied. Inorganic fertilizers used in the basin are mainly NH_4^+ and NO_3^- based (NPK, DAP, CAN, $(NH_4)_2SO_4$, and urea) and have been shown to influence the river NO_3^- content (Maghanga et al., 2013).

(a) (b)

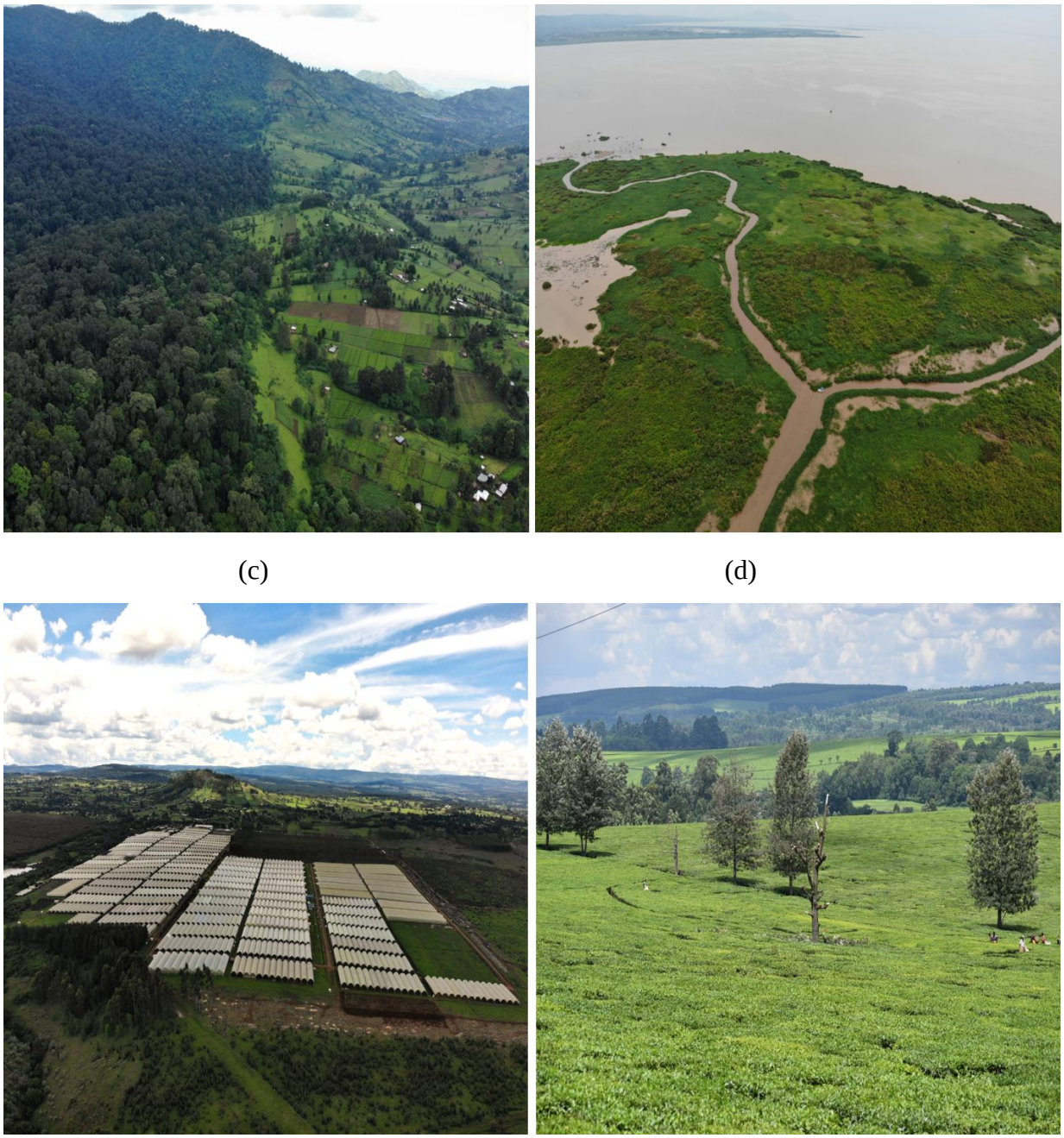

(c) (d)

Figure 1.5. Small-scale mixed farms and residences in the escarpment Kipkoil forest of the Nyando catchment (a); highly turbid R. Nyando water at the Lake Victoria river mouth (b); commercial flower farming in the upstream Nyando-Kipchorian tributary (c); commercial tea farming in the Ainapkoi tributary of Sondu Miriu catchment (d).

1.4 Impacts of excess nutrient discharge in the Lake Victoria basin, Kenya

Indicators of eutrophic conditions in Lake Victoria were observed as early as 1927 – 1928 when algal blooms were reported in some parts of the Lake by Worthington (1930). However, prolonged deep-water anoxia is reported to have begun in the 1960's and became more persistent in the 1970's when also algal population abundances increased across the lake (Talling, 1966; Verschuren et al., 2002). At the same time, limnology studies conducted in the Lake since that period of the 1960's show an increasing concentration trend for the key eutrophication-causing nutrients: NO_3^- and PO_4^- (Gikuma-Njuru and Hecky, 2005; Lung'ayia et al., 2001; Ochumba and Kibaara, 1989; Sitoki et al., 2010; Talling, 1966). Table 1.2 shows a summary of the evolution of NO_3^- concentration in the Winam gulf (Kenyan part) of Lake Victoria. It shows a continuous increase in NO_3^- over time from mean concentrations below 100 µg L^{-1} reported by Talling (1966), to levels above 1000 µg L^{-1}, which we recently obtained during our preliminary studies (Nyilitya et al., 2016). PO_4^- on the other hand, has been observed to increase in the gulf, from 4 µg L^{-1} (PO_4–P) reported by Talling (1966) to 57 µg L^{-1} (PO_4–P) reported by Sitoki et al. (2010). It should be noted here that nutrient data in the LV basin in Kenya for the last one decade is rare, and this motivated our study.

Table 1.2. NO_3^- concentrations in the Winam gulf of Lake Victoria (latitude 0º 6' – 0º 33' S, longitude 34º 12'–34º 51' E) as reported in different research studies within six consecutive decades.

Period	**NO_3^- (µg L^{-1})**	**Reference**
1960 – 1962	66 - 128	Talling and Talling (1966)
1975	35.4	Melack (1976)
1989	110±96	Gophen et al. (2001)
1998	295±195	Lung'ayia et al. (2001)
2000 – 2004	213±95	LVEMP (2005)
2004	360±54	Sitoki et al. 2010
2008 – 2009	289±360	Sitoki et al. 2012
2015 – 2016	1061±1070	Nyilitya et al. 2016

Consequently, there has been clear impacts observed on the physical, chemical and biological conditions of the Lake (Juma et al., 2014). Notable impacts associated with excess deposition of nutrients in the lake include the occurrence of dense algal blooms which have become increasingly dominated by the potentially-toxic blue-green algae species (Muyodi et al., 2010). Water hyacinth, on the other hand, has become a regular menace blocking water ways and ports and affecting transportation and fisheries (Lung'ayia et al., 2001). Secchi transparencies, which are an indicator of the clearness of the lake (the higher the value of Secchi, the better the lake water) show a decreasing trend. The highest Secchi values of 1.3 – 1.5 m in the Winam gulf were reported by Worthington (1930), while recently Simiyu et al. (2018) reported values between 26 and 85 cm in the gulf. Increase in chlorophyll *a* concentration in the lake is another key indicator of eutrophication. Early data indicated low chlorophyll *a* concentrations (3.0 – 4.6 µg L^{-1}), but concentrations have risen tremendously, with recent studies reporting values ranging between 274 – 4382 µg L^{-1} (Simiyu et al., 2018). In addition, studies by Juma et al. (2014), using moderate resolution imaging spectroradiometer (MODIS) analysis, show an increasing aquatic vegetation in the Winam gulf from 64,564 ha in the year 2000 to 438,891 ha in 2010. Furthermore, studies have linked eutrophication of the lake to the large-scale fish mortalities and decline in fish populations (Kolding et al., 2008; Lung'ayia et al., 2001; Ochumba, 1990). The researchers reported that the high rate of algal blooms growth limits light penetration in the lake, clogged gills of the fish and prompted the formation of hypoxic zones in the deeper waters, resulting in fish mortalities and low fish productivity of the Lake. This has had a significant socio-economic impact in Kenya since the fishing industry has been a major foreign exchange earner for the country with LVB fisheries contributing more than 95% of the total fish produced in Kenya (LVEMP, 2005). In addition, about 1 million people on the Kenyan side are directly or indirectly supported by the fish sector (LVEMP, 2005).

The lake is used for transport within the East African riparian states and as a source of potable water for the surrounding cities and population. However, a dense water hyacinth regularly covers whole bays as seen in Figure 1.6 of the Kisumu port in the period between December

2016 and May 2017. The water hyacinth infestation regularly affects water transport between Kisumu and the other lake shore cities in the region. In addition, dense water hyacinth growth normally clogs water intake points and filtration systems of the city's water service provider (Fig. 1.6 (inset)). This not only increases the treatment costs but it also lowers the production capacity of the water service provider (LVEMP, 2005). As a consequence, piped water in Kisumu city (3rd largest city in Kenya) is either inaccessible or unaffordable to the majority of the urban poor, who's other option is shallow groundwater. As earlier stated, the shallow groundwater quality is highly compromised due to the inadequate sewage infrastructure in the city (Wright et al., 2013).

At national level, the degradation of water quality in the Lake Victoria basin happens against the backdrop that Kenya is a water scarce country with a per capita fresh water endowment of approximately 527 m^3 against the UN standard of above 1000 m^3 for countries which are not water stressed (JICA, 2013). The Lake basin accounts for 60% of the country's fresh water resources and supports the livelihood of one third of the country's population (CRA, 2011). Generally, the increase in nutrient concentration triggers a cascade of environmental and socio-economic impacts and leads to loss of biodiversity.

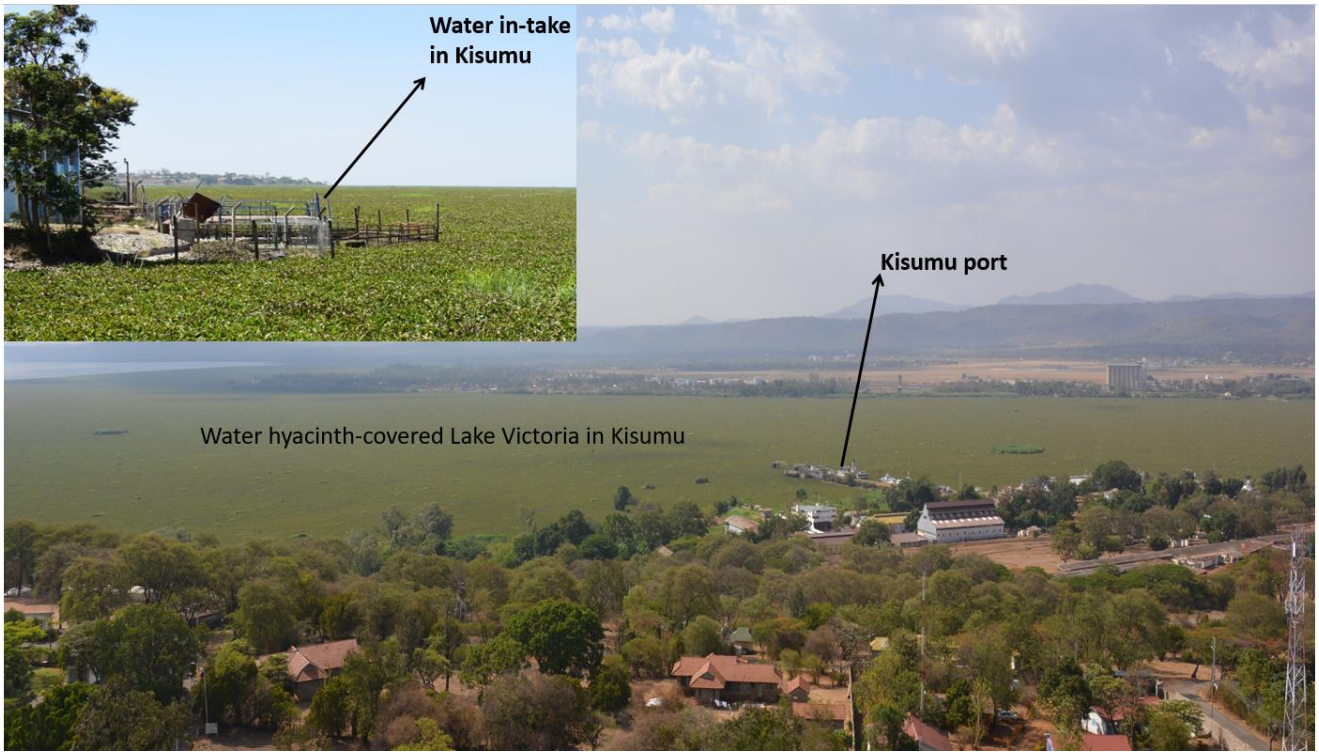

Figure 1.6. Water hyacinth-cover over Lake Victoria in Kisumu, blocking the Kisumu port and the water in-take point (inset) of the Kisumu water and sewerage company in February, 2017.

1.5 Limited riverine and groundwater nitrogen studies in the Lake Victoria basin, Kenya

Environmental management of the basin is mandated to the Lake Victoria Basin Commission (LVBC), which is a regional institution of the East Africa Community (EAC) member states. LVBC coordinates the Lake Victoria Environmental Management Project (LVEMP) in each of the EAC member states through which water quality monitoring in the basin is conducted. At national level, the Ministry of Water & Irrigation (Kenya), through its Water Resources Authority (WRA), undertakes catchment water resources management activities. However, relevant nitrogen (N) studies in the basin largely consists of work done through LVEMP. Available N data in the rivers reports total nitrogen (TN) concentrations, but it is lacking information with regard to spatiotemporal distribution of N concentration in river basins and also values of mineral N species (i.e. NO_3^-, NO_2^- and NH_4^+).

Table 1.3 shows the annual TN discharge of each river basin and the annual TN discharge from the Kenyan side of Lake Victoria basin, conducted under LVEMP from 2000 – 2004. It should be noted that relevant nutrient data from LVEMP for the last one and half decade is lacking due to the destruction of their Kisumu laboratory during the 2007 – 2008 post-election violence in Kenya. In addition, the project's activities have been focused on intervention programs like rehabilitation of sewage treatment infrastructure of major cities, tree planting, and wetland protection, among others (WorldBank, 2018). The TN discharges (Table 1.3) were estimated from the mean river water discharge and mean TN concentrations of each river basin at the river mouth (COWI, 2002; LVEMP, 2005). TN concentrations ranged from 0.8 mg L^{-1} recorded in the North Awach River, to 1.9 mg L^{-1} recorded in the Nyando River. The higher TN values obtained in the Nyando River were attributed to sewage discharges from several sugarcane and allied industries as well as from urban centers it drains through. However, the Nzoia River recorded the highest TN discharges into Lake Victoria due to the high water discharge volumes experienced in the catchment (Table 1.3). The Sondu Miriu River, on the other hand, recorded the highest TN per unit area. This could be linked to the large-scale commercial tea farming which occupies a large part of the catchment and where inorganic fertilizers are regularly used. Seasonally, the study reported the highest TN concentrations during the wet season months (April and October) as a result of agricultural inputs and increased soil erosion.

Table 1.3. Annual total nitrogen (TN) discharge into Lake Victoria by Kenyan rivers, estimated from the mean water discharge (measured at river mouth) and mean TN concentration of each river basin during the 2000 – 2004 monitoring period (COWI, 2002; LVEMP, 2005).

River	Mean discharge ($m^3 s^{-1}$)	Basin area (km^2)	Mean TN ($mg L^{-1}$)	Annual TN discharge ($t yr^{-1}$)	TN per unit area ($kg km^{-2} yr^{-1}$)
Nzoia	115.3	12852	1.09	3963.3	308.4
Nyando	18.0	3652	1.9	1078.5	295.3
Sondu Miriu	42.2	3508	1.22	1623.6	462.8
Sio	11.4	1437	0.85	305.6	212.7
Yala	37.6	3357	1.06	1185.7	353.2
Gucha Migori	58.0	6600	1.36	2487.6	376.9
North Awach	3.7	1985	0.77	89.8	45.2
South Awach	5.9	3156	1.6	297.7	94.3
Total	**292**	**36,547**		**11,032**	

The work by LVEMP (2005) estimated the relative contributions of catchment (riverine) and atmospheric deposition to the Lake's N input. From atmospheric (wet and dry) deposition, they obtained a TN contribution of 22,424 tones yr^{-1} while the catchment (Table 1.3) contributed 11,032 tones yr^{-1} to the Lake. This implies that atmospheric deposition contributed about 70%, while river catchment discharge accounted for 30% of the annual N input into the Kenyan side of the Lake Victoria basin. For the whole Lake Victoria basin, (COWI, 2002) had reported 102,150 (66%) and 53,430 (34%) tones TN yr^{-1} for atmospheric and catchment depositions respectively. Scheren et al. (2000), on the other hand, reported 85,513 (72%) and 33,892 (28%) tones TN yr^{-1} for atmospheric and catchment depositions respectively for the whole basin. However, the atmospheric N deposition rate for the Kenyan side of the basin (LVEMP, 2005), which amounts to 54.5 kg N ha^{-1}, is high compared to similar studies in West Africa (Galy-Lacaux and Delon, 2014) and the Congo Basin (Bauters et al., 2018) which have reported 6 – 15 and 18.2 kg N ha^{-1} respectively. The Lake Victoria basin-Kenya study was conducted in only one site, Kisumu, which is not entirely representative of the basin and therefore might

have been overestimated. Nevertheless, the intense human activities in the Kenyan side of the basin and Kisumu in particular, like untreated urban sewage and industrial emissions are expected to significantly increase atmospheric N fluxes and deposition. In addition, biomass burning (charcoal and burning of sugarcane plantations during harvest) is very common in the surrounding Kano and the Nandi forests. These activities are linked to the increase in atmospheric N fluxes in African tropical ecosystems (Bauters et al., 2018; Chen et al., 2010).

Generally, these studies (COWI, 2002; LVEMP, 2005; Scheren et al., 2000) are similar regarding the relative contribution of the two main sources (atmospheric deposition and catchment discharges) to the N input into the Lake. However, such data is limited qualitatively and quantitatively and is too general to be relied on for the development of targeted N control measures. This is because, normally, there are several potential N sources at the river catchment scale ranging from anthropogenic to natural sources and they require to be identified and apportioned. In addition, it's important to generate spatial-temporal N data from both catchment and atmospheric deposition, and which includes the mineral N species (NO_3^-, NO_2^- and NH_4^+).

Studies on groundwater nutrient pollution in the Lake Victoria basin in Kenya has been focused on Kisumu city (Oiro, 2012; Okotto-Okotto et al., 2015; Wright et al., 2013). However, data on the spatial-temporal NO_3^- concentrations in the city and the rural areas is rare. In addition, no study has attempted to discriminate between the potential sources of NO_3^- pollution in the region.

Therefore, given the intense human activities in the basin coupled with insufficient water quality data, initiatives by the LVBC and other national environmental institutions to control excess nutrient discharge in the basin have been less effective (Juma et al., 2014). One of the main factors limiting these initiatives in the basin is limited amount of data and information on nutrient (NO_3^-, NH_4^+, PO_4^-) concentrations, their discharge mechanisms and potential sources in the river basins. Because of the impact eutrophication has caused to the socio-economic

wellbeing and biodiversity in the basin, most of the research done in the basin concerning NO_3^- was concentrated in the Lake (Gikuma-Njuru et al., 2013a; Gikuma-Njuru and Hecky, 2005; Lung'ayia et al., 2001; Sitoki et al., 2010; Stager et al., 2009). Recently, environmental management efforts and further research have been focused on point NO_3^- sources like urban and industrial effluents as well as nutrient buffering and removal systems aimed at controlling point sources (Agwanda and Iqbal, 2019; Kansiime et al., 2007; Musungu et al., 2014; Nyenje et al., 2010). In addition, research aimed at identifying the fate and transport mechanism of nutrients in the region is very rare. This limits water resources management and policy institutions in developing targeted intervention strategies for the control of excess nutrient discharge in the basin. Therefore, it is needful to investigate spatiotemporal nutrient concentrations and distribution in the basin, and to establish their potential sources and associated transformation mechanisms. Such information will enable water and environmental policy making institutions in the region to implement targeted intervention measures to control excess discharge of nutrients in the catchment.

The focus of this study is on the NO_3^-. This is because, amongst the other nutrients, NO_3^- is a major water contaminant which is highly influenced by human activities and land use changes, as is being witnessed in the LV basin, Kenya. In addition, and as earlier stated, the health and environmental effects associated with NO_3^- cannot be underestimated especially in a region with serious data and information gaps like the Lake Victoria basin. Therefore, studying NO_3^- levels, its distribution and potential sources will be a good indicator of the impacts human activities have had on the water quality of the basin, and will help in awareness creation and implementation of targeted intervention measures.

1.6 Solving the problem: a multi-tracer approach

The commonly used approach in the management and control of surface and/or ground water NO_3^- has been based on monitoring data and comparing these against threshold values: i.e. WHO limit of 50 mg L^{-1} for NO_3^- (Widory et al., 2013). However, based on chemical data

alone, it is generally hard to distinguish to what extent different sources (at a catchment scale) are contributing to the observed NO_3^- level in a water body. For instance, apportionment of non-point sources of NO_3^- is extremely difficult based on monitoring data; even by increasing the number of monitoring stations.

Research has demonstrated the use of isotopes to precisely identify and apportion NO_3^- sources in addition to studying major biogeochemical processes controlling NO_3^- concentrations in both surface and groundwater water (Kendall et al., 2007; Li et al., 2010; Panno et al., 2006; Widory et al., 2013; Xue et al., 2009). The use of nitrogen ($\delta^{15}N$) and oxygen ($\delta^{18}O$) isotope ratios of NO_3^- for source identification is based on the fact that potential NO_3^- sources such as inorganic fertilizers, manure, soil N, sewage and atmospheric deposition have distinct isotope signatures (i.e.; $\delta^{15}N$- and $\delta^{18}O$-NO_3^-) and therefore can be used to identify sources in a mixture as described and reviewed by Xue et al. (2009). In addition to source identification, isotopic composition of NO_3^- provides important information about N transformation mechanisms such as denitrification and nitrification. For instance, kinetic isotope effects during denitrification preferably convert lighter isotopes (^{14}N and ^{16}O) to N_2 and N_2O, causing an enrichment of the heavy isotopes (^{15}N and ^{18}O) in the residual NO_3^-, while NO_3^- concentration decreases (Fukada et al., 2003; Mayer et al., 2001). Furthermore, a general linear relationship indicating an enrichment of $\delta^{15}N$ relative to $\delta^{18}O$ by a factor of between 1.3:1 and 2.1:1 supports evidence for *in situ* denitrification (Kendall et al., 2007; Mengis et al., 1999).

However, mixing of multiple NO_3^- sources (point and non-point sources) is the key process controlling NO_3^- delivery to water bodies. Given that different NO_3^- sources have a distinctive isotopic ($\delta^{15}N$- and $\delta^{18}O$-NO_3^-) signature, their mixing results in intermediate isotopic values, consequently masking the source signal. The mixing effect can be amplified or even biased by superimposition of N transformation processes (nitrification, denitrification), which alter the NO_3^- isotope signal of the source through isotopic fractionation. These processes may complicate NO_3^- source apportionment based on isotope composition alone.

Boron (B) is ubiquitous in nature and usually co-migrates with NO_3^- in many environmental systems. The large range of B isotope ($\delta^{11}B$) ratios observed in nature enables clear contrasts to be made between boron sources; especially discriminating between animal manure sources and sewage or inorganic fertilizer sources. Furthermore, B is not affected by N transformation processes except may-be during adsorption-desorption interactions with clay minerals, iron and aluminum oxide surfaces (Bassett et al., 1995; Vengosh et al., 1994). Research has shown the added value of coupling NO_3^- and B isotope ($\delta^{15}N$, $\delta^{18}O\text{-}NO_3^-$, and $\delta^{11}B$) ratios to improve on NO_3^- source discrimination especially when NO_3^- transformation processes are involved (Erostate et al., 2018; Meghdadi and Javar, 2018; Seiler, 2005; Widory et al., 2013, 2005; Xue et al., 2013). In addition, researchers have developed and implemented an isotopic mixing model, mixSIAR, which uses a Bayesian framework for estimating possible proportional source contributions and determines the probability distribution for the proportional contribution of each source to the mixture (Parnell et al., 2010; Xue et al., 2012). The integration of hydro-chemistry data complements isotopic techniques in NO_3^- source apportionment because chemical constituents arising from anthropogenic sources tend to dominate those from natural sources. Therefore, valuable information about NO_3^- sources is obtained when $\delta^{15}N$ and $\delta^{18}O\text{-}NO_3^-$ data are linked with concentrations of major anions (Cl^-, SO_4^{2-}, HCO_3^-) and Cations (Na^+, K^+, Ca^{2+}, Mg^{2+}) in water (Liu et al., 2006; Min et al., 2002; Spruill et al., 2002). For instance, Cl^- is a conservative ion in water, which unlike the NO_3^-, it is not affected by biogeochemical processes taking place in a water body. Cl^- is therefore, a good indicator of these processes and also used in tracing anthropogenic solute sources (Li et al., 2010).

The key tools used in this study includes, multi-isotope ($\delta^{15}N$, $\delta^{18}O\text{-}NO_3^-$, $\delta^{11}B$), hydrochemistry, and a Bayesian mixing model (mixSIAR) to address the existing knowledge gap on NO_3^- discharge and sources in the Lake Victoria basin in Kenya.

1.7 Objectives, research questions and hypothesis

The overall objective of this PhD is to identify and apportion NO_3^- pollution sources in the Lake Victoria basin of Kenya, by studying the spatiotemporal variation of the concentration, source apportionment, discharge and fate of NO_3^- in both surface and groundwater resources.

The research questions, hypotheses and specific objectives of this study are presented below for each of the three main research topics.

Land use controls Kenyan riverine nitrate discharge into Lake Victoria – Evidence from Nyando, Nzoia, and Sondu Miriu river basins

The main research questions for this topic are:

1. What is the role of land use on river NO_3^- concentrations and sources?
2. Are biogeochemical processes affecting NO_3^- concentrations in rivers?

It was hypothesized that land use intensity has a strong effect on river NO_3^- concentrations and sources, but *in situ* denitrification attenuates NO_3^- along the river.

The specific objectives are:

1. Hydrochemical and isotopic ($\delta^{15}N$- and $\delta^{18}O$-NO_3^-) characterization of three major river basins (Nyando, Nzoia, and Sondu Miriu) in Lake Victoria basin, Kenya;
2. To determine the role of land use on river NO_3^- concentration and sources;
3. To determine the potential for N transformation mechanisms taking place along the river channels.

Nitrate source apportionment in the complex Nyando tropical river basin in Kenya

The main research questions:

1. What are the main sources of riverine NO_3^- input in the Lake Victoria basin, Kenya?
2. What is the proportional contribution of different potential NO_3^- sources?
3. What is the benefit of integrating isotopic, hydro-chemical and mixSIAR techniques in NO_3^- source apportionment of a tropical SSA river basin?

The overarching working hypothesis was that animal manure and sewage are the main sources of river NO_3^- input, but source contributions vary spatially and seasonally.

The specific objectives are:

1. Isotopic characterization of the potential NO_3^- sources in Lake Victoria basin, Kenya;
2. To study the spatiotemporal variability of NO_3^- discharge from different land use systems in a river basin, and develop long-term time series;
3. To apportion NO_3^- sources in a mixed SSA river basin;
4. To demonstrate the added value of integrating multi-isotopic ($\delta^{15}N$- and $\delta^{18}O$-NO_3^-, and $\delta^{11}B$), hydrochemical and mixSIAR approach to constrain NO_3^- sources in a tropical SSA river basin;
5. Propose management and governance guidelines to mitigate excess NO_3^- discharge and eutrophication of surface water in Lake Victoria basin, Kenya.

Tracking sources and fate of groundwater nitrate in Kisumu city and Kano plains in Lake Victoria basin, Kenya

The key research questions are:

1. What is the current status of groundwater quality regarding NO_3^-?
2. What are the dominant groundwater NO_3^- pollution sources?
3. Do *in situ* attenuation processes affect groundwater NO_3^- concentration?

The main hypothesis was that sewage is the leading source of groundwater pollution in the basin, but *in situ* denitrification could reduce NO_3^- loading.

The specific objectives are:

1. To establish the level of the current NO_3^- pollution in urbanized versus rural aquifer systems of the basin;
2. To constrain the sources of groundwater NO_3^- pollution in the Lake Victoria basin, Kenya;
3. To identify biogeochemical processes affecting mineral N concentration in the groundwater of the basin;
4. To propose management and governance guidelines to mitigate NO_3^- pollution of groundwater in the basin.

1.8 Thesis Outline

Chapter 2. "Land use controls Kenyan riverine nitrate discharge into Lake Victoria – Evidence from Nyando, Nzoia, and Sondu Miriu river basins".

In order to establish the main land use characteristics in the Lake Victoria basin in Kenya, this chapter demonstrates a land use clustering approach based on hierarchical cluster analysis (HCA) of physico-chemical parameters and land use maps for three major river catchments (Nyando, Nzoia, Sondu Miriu) of the LVB in Kenya. The three river basins are hydrologically distinct and were selected as such, to represent the main land use patterns of the LVB, Kenya. The chapter discusses baseline spatiotemporal NO_3^-, $\delta^{15}N\text{-}NO_3^-$, and $\delta^{18}O\text{-}NO_3^-$ data in each of the three river basins, makes comparisons, establishes the role of land use on riverine NO_3^- discharge and identifies the dominant NO_3^- sources based on hydro-chemical and isotopic ($\delta^{15}N$-, $\delta^{18}O\text{-}NO_3^-$) characteristics. Laboratory-based tests for the potential of occurrence of *in situ* denitrification in riverbed sediments from the study area are presented and discussed in this chapter.

Chapter 3. "Nitrate source apportionment in the complex Nyando tropical river basin in Kenya".

Due to the mixed nature of human activities in the Lake Victoria basin in Kenya, it can be complicated to clearly apportion the main sources of nutrient pollution in river basins as witnessed in chapter 2, for the implementation of targeted control measures. The Nyando river basin exemplifies the larger Lake Victoria basin and was selected for further field monitoring and detailed analysis. Therefore, this chapter presents an in-depth study (using 2 year field monitoring data) applying multi tracers (δ^{15}N-, δ^{18}O-NO_3^-, and δ^{11}B, hydrochemistry) and the isotope mixing model "mixSIAR" to apportion NO_3^- sources in the Nyando river basin. The benefit of integrating δ^{11}B in differentiating between manure, sewage and inorganic fertilizer NO_3^- sources in surface water is displayed in this chapter. Together with affirming the potential NO_3^- sources, the study quantified proportional NO_3^- source contributions, spatially and seasonally in the basin.

Chapter 4. "Tracking sources and fate of groundwater nitrate in Kisumu city and Kano plains in Lake Victoria basin, Kenya".

Groundwater in the region is highly used especially among the urban low income earners and the rural area residents. However, inadequate sanitation systems in the region together with increasing manure and fertilizer application in Kisumu and its surroundings Kano plains make groundwater resources highly vulnerable to surface water contaminants. This chapter discusses findings of a study conducted in Kisumu city and the surrounding Kano plains to assess groundwater quality, NO_3^- concentrations, identify the potential sources and associated biogeochemical processes for *in situ* attenuation of NO_3^-. The study goes further to demonstrate the added value of using the boron isotope (δ^{11}B) to discriminate between manure and sewage NO_3^- sources in groundwater.

Chapter 5. "General Conclusions and Discussion". The chapter presents a summary of the key findings based on the research questions in each of the preceding research chapters. It further gives an integrated discussion of the NO_3^- sources, proposes remedial measures for informing policy, and identifies research and policy gaps for further work.

1.9 Sampling strategy

In order to generate sufficient data/information which is representative of the Kenyan side of the LVB, three major river basins were selected for surface water monitoring studies. These rivers: Nyando, Nzoia, and Sondu Miriu, are hydrologically distinct, and account for approximately 60% of the total Kenyan riverine inflow into Lake Victoria (LVEMP, 2005). The selection of water sampling stations in these basins was conducted with the help of the LVEMP and WRA who are responsible for environmental and water resources management in the basins. The aim was to establish a spatial network covering the major land use patterns in the main tributaries of the rivers and is further described in chapter 2.

Field monitoring campaigns were carried out in the three river basins during four seasons: (1) the agriculturally productive wet period between May – July, 2016 marked as "peak wet" (PW) season, (2) the "end of wet" (EW) season in September, 2016, (3) the "dry" (D) season in December, 2016, and (4) the transition period from dry to wet season in March, 2017 marked as "start of wet" (SW) season. Through the analysis of water physicochemical data from these stations using hierarchical cluster analysis (HCA), the monitoring stations in each river basin grouped into homogeneous clusters which were named based on the common land use activity of each cluster. The HCA analysis is presented in chapter 2. This was in order to provide a description of the spatiotemporal NO_3^- discharge and distribution in the basins, assess the role of land use on NO_3^- discharge, and make comparisons in these three basins. This data is presented and discussed in chapter 2.

Given the diversity of land use in the Nyando river basin, which is characteristic of tropical

African river basins, the Nyando basin was selected for in depth NO_3^- source apportionment study. Therefore, river water sampling and monitoring continued in the Nyando stations during the same seasons (described above) until May, 2018, making a total of nine seasons of field monitoring in the Nyando basin. This in depth data analysis is discussed in chapter 3.

Due to the significance of groundwater as a portable water source for the low income urban slum dwellers in Kisumu city and rural residents in the Kano plains area, it is important to establish the groundwater quality status of the region, identify likewise NO_3^- pollution sources and potential biogeochemical processes taking place in these aquifers. The aim in the selection of groundwater monitoring stations was to cover the unconfined shallow aquifers and the deeper confined or unconfined aquifers spatially distributed within Kisumu and the Kano plains area. With the help of the WRA, groundwater stations were identified and selected from shallow wells (depth < 10 m) and boreholes (depth > 15 m) spatially distributed within the two locations. Sampling was conducted during the wet season between May and July, 2017, and during the dry season in February, 2018. This data is presented and discussed in chapter 4.

In addition, sampling of the potential sources of NO_3^- in the region was necessary in order to determine their isotopic ($\delta^{15}N$-, $\delta^{18}O$-NO_3^-, and $\delta^{11}B$) signatures for NO_3^-source apportionment. The potential sources include sewage, manure, inorganic fertilizers, precipitation and soil N. Sewage effluents were sampled from the inlet point of sewage treatment plants located in major towns (Kisumu, Eldoret, Kakamega, Bungoma, Kericho), sugarcane factories (Muhoroni, Mumias, Chemelil, Nzoia), agrochemical and lime factories. Manure was sampled from cow, goat and sheep collected from animal droppings in the basin. Inorganic fertilizers samples of the commonly used types (CAN, DAP, NPK, urea) were purchased from farmers and suppliers. Precipitation samples were collected from rainfall stations in Ahero, Kakamega and Kericho towns, while soil N samples were collected by filtering suspended soil sediments in river water using 11 µm filters. For the determination of the potential for occurrence of denitrification in riverbeds, superficial sediment samples were taken randomly in the river basins.

Chapter 2. Land use controls Kenyan riverine nitrate discharge into Lake Victoria – Evidence from Nyando, Nzoia, and Sondu Miriu river basins

This chapter has been published as

Nyilitya, B., Mureithi, S., Boeckx, P., 2020. Land use controls Kenyan riverine nitrate discharge into Lake Victoria – evidence from Nyando , Nzoia and Sondu Miriu river catchments. Isotopes Environ. Health Stud. 56, 170 – 192.

https://doi.org/10.1080/10256016.2020.1724999

Abstract

Nitrate (NO_3^-) sources and discharge were investigated using isotopic and hydro-chemical analyses in three river catchments draining Lake Victoria basin, Kenya. Hierarchical cluster analysis grouped Nyando, Nzoia and Sondu Miriu River stations into clusters corresponding to major land use classes of the catchments. Mixed agriculture (MA) in Nyando showed higher NO_3^- compared to the other land uses. The NO_3^- levels obtained (0.1–11.6 mg L^{-1}) are higher than those reported in previous studies. Hydrochemistry support isotopic data indicating that: NH_4^+-based fertilizers and soil N were the major NO_3^- sources in tea dominated areas with average $\delta^{15}N$, $\delta^{18}O$ of 6.5 ± 1.3‰, 6.7 ± 2.3‰, respectively; manure/sewage were the main source in MA areas with average $\delta^{15}N$, $\delta^{18}O$ of 8.4 ± 2.4‰, 7.8 ± 5.4‰, respectively; and sewage was the likely source in urban, residential & industrial areas recording average $\delta^{15}N$, $\delta^{18}O$ of 10.0 ± 2.4‰, 6.9 ± 3.7‰, respectively. The $\delta^{15}N$ between land uses were significantly different ($p < 0.0001$) while $\delta^{18}O$ were similar ($p = 0.4$). Seasonally, inorganic/organic fertilizers influenced river NO_3^- mostly in the wet cropping season. Lower NO_3^- concentrations observed in Nyando and Sondu Miriu during dry or start-wet season could be a result of *in situ* denitrification. General waste water management and sanitation strategies should be implemented and good agricultural practices established in the basin to control excess NO_3^- discharge

Key Words

Nitrate pollution, Lake Victoria, Kenya, Stable isotopes, Hydro-chemistry, Land-use

2.1 Introduction

Nitrate (NO_3^-) pollution of surface and groundwater resources has become a worldwide environmental problem threatening fresh water resources in many parts of the world (Sacchi et al., 2013). High NO_3^- concentrations in aquatic environments can cause eutrophication and at the same time pose health risks to humans such as methemoglobinemia in children (blue baby syndrome) and cancer following long term exposure (Kendall et al., 2007)]. Consequently, the World Health Organization (WHO) has set a limit of 50 mg L^{-1} NO_3^- for drinking water, although recent findings by Schullehner et al. (2018) report increased colorectal cancer risk at drinking water NO_3^- concentrations as low as 3.9 mg L^{-1}. Increasing input of NO_3^- into water bodies is attributed to intensive land use practices such as increased use of N-containing organic and inorganic fertilizers, industrial and urban discharges, and elevated atmospheric N deposition (Benkovitz et al., 1996).

However, in the Lake Victoria, Africa's largest fresh water body (surface area: 68,000 km^2) (Sitoki et al., 2010), a ca. 10-fold increasing trend in NO_3^- concentration has been reported over a period of ca. 50 years: studies done in 1965 (Talling, 1966) yielded 66 – 128 µg L^{-1}, in 1990 (Gophen et al., 1995) 110±96 µg L^{-1}, in 1998 (Lung'ayia et al., 2001) 295±195 µg L^{-1}, in 2002 (Gikuma-Njuru and Hecky, 2005) 213±95 µg L^{-1}, and in 2009 (Sitoki et al., 2010) 437±161 µg L^{-1}. This has resulted in eutrophication of Lake Victoria with increasing levels of reactive N in water bodies (UNEP and WHRC, 2007) and in turn fuelled the rapid proliferation of water hyacinth (*Eichhornia crassipes*) and decrease in fish population (Lung'ayia et al., 2001). This happens against the backdrop that the Lake is a great socio-economic resource of the East African Community (EAC) partner states for fisheries, tourism, transport, water, and energy among others, and a core to East Africa regional integration and development.

The Kenyan catchment contributes around 40% of the surface water inflow of Lake Victoria and is estimated at about 292.1 $m^3 s^{-1}$ (COWI, 2002). The catchment is drained by several rivers, major ones being River Nyando, Nzoia and Sondu Miriu. The rivers drain diverse land uses, ranging from pristine forests, commercial agricultural areas (tea, sugarcane, maize and

horticulture), mixed smallholder agriculture with livestock farming, urban centres, industrialized towns and wetlands. The basin is subjected to both a high population growth rate (>6% p.a.) and fast urbanization, due to the economic importance of its fresh water resources for domestic, agricultural and industrial purposes. The population pressure and economic development have led to land use change in the basin, which has in turn negatively impacted ecosystems (Juma et al., 2014). The basin, therefore, epitomizes a land degradation problem caused by deforestation, forest encroachment by smallholder farms, biomass burning (charcoal production) and poor land management practises. This has led to modification of physical, chemical and biological characteristics of rivers and as a consequence also Lake Victoria. This has been exemplified via remote sensing and demonstrated by an extending sediment plume in the Winam Gulf covering about 40 km^2 from the Nyando river mouth (ICRAF, 2003).

Therefore, given the environmental challenges and health risks posed by the uncontrolled discharge of NO_3^- into Lake Victoria, there is an important need to understand NO_3^- concentrations, sources and discharge by its tributary river catchments. Riverine nitrogen has been reported as the second most important source (after atmospheric deposition) of nitrogen loading into the Lake, estimated at 16% (Juma et al., 2014; Zhou et al., 2014). Previous studies on this part of the Lake Victoria basin have focused on limnology and nutrient enrichment of the Lake waters which has revealed an increasing NO_3^- concentration trend (Gikuma-Njuru and Hecky, 2005; Lung'ayia et al., 2001). With the effects of eutrophication threatening the lake's ecosystem, recent emphasis has been on impact mitigation. As such, research and environmental management efforts in the basin have been focused on point NO_3^- sources like urban and industrial effluents as well as nutrient buffering and removal systems (Kansiime et al., 2007; Nyenje et al., 2010). However, data on riverine NO_3^- discharge in Lake Victoria and other tropical lakes in Sub-Saharan Africa is scanty, and no study has attempted to investigate NO_3^- discharge and its sources from diverse land use of the major river catchments (Nyando, Nzoia, Sondu Miriu), draining the Kenyan part of the Lake Victoria basin.

The common approach in NO_3^- pollution management is monitoring concentrations in water with a comparison against threshold values, i.e. WHO limit of 50 mg L^{-1}. However, this method does not provide information on sources of $NO_3^-$and limits dedicated mitigation strategies. Research has demonstrated added value of using dual isotopes of NO_3^- ($\delta^{15}N$-, $\delta^{18}O$-NO_3^-) to distinguish between sources of NO_3^-, which is based on the fact that potential sources such as inorganic fertilizers, sewage, manure, soil nitrogen and atmospheric deposition have distinct isotopic characteristics (Kendall et al., 2007; Xue et al., 2009). Moreover, studies have integrated $\delta^{15}N$-, $\delta^{18}O$-NO_3^- with hydrochemistry to study NO_3^- sources in large river basins; e.g. Yili river of the Taihu Lake watershed, China (Zeng and Wu, 2015), Mississippi and Illinois river basins in the USA (Panno et al., 2006), and rivers draining watersheds in North-eastern USA (Mayer et al., 2002). As far as we are aware, this study is the first of its kind in tropical Africa, and integrates physicochemical data, hierarchical cluster analysis and isotopic methods to quantify and understand NO_3^- discharge contribution from different land use areas to riverine NO_3^-. Specifically, this study provides 1) information on potential NO_3^- sources (based on hydrochemistry, $\delta^{15}N$- and $\delta^{18}O$-NO_3^- data), and 2) baseline hydro-chemical data of Kenyan river draining into Lake Victoria. It is hypothesized that land use intensity has a dominant effect on river NO_3^- concentrations and sources. All together our findings can contribute to start establishing dedicated management plans for NO_3^- discharge mitigation in the basin.

2.2 Materials and methods

2.2.1 Study area

The study was conducted in three river catchments: Nyando, Nzoia and Sondu Miriu draining the Kenyan side of Lake Victoria (Fig. 2.1). River Nyando (Fig. 2.1b) is 153 km long and originates from western Mau and Nandi hills. It drains a catchment area of 3,590 km^2, has an average discharge rate of 18 m^3 s^{-1} and drains into the Winam Gulf of Lake Victoria (COWI, 2002). Key land use patterns in the Nyando catchment include the pristine Mau forests,

commercial tea, sugarcane, horticultural flower farms, mixed agriculture, mushrooming urban centres, industries and wetlands at the river mouth. River Nzoia (Fig. 2.1c), on the other hand, is the largest one of the three rivers. It originates from Cherengani hills with tributaries from Mt. Elgon and drains a catchment area of 12,709 km^2. Having a length of 334 km and an average discharge rate of 115.3 m^3 s^{-1}, the River Nzoia provides the second largest tributary flow to Lake Victoria after the river Kagera in Rwanda (COWI, 2002). River Nzoia drainage network consists of diverse land uses including mixed agriculture in the upstream catchments, major urban centres, commercial sugarcane, maize and wheat farming and agro-based industries. River Sondu Miriu (Fig. 2.1d) has its headwaters in the south-western block of the Mau complex, drains a catchment area of 3508 km^2 with an average discharge rate of 42.2 m^3 s^{-1} (COWI, 2002) and drains into the Winam Gulf of Lake Victoria. River Sondu Miriu drainage area consists of natural forests at the head water catchment. Planted forests and commercial tea estates occupy the midstream, while mixed agriculture and a hydroelectric power generation plant are the major land use in the downstream before its entry into Lake Victoria.

(a)

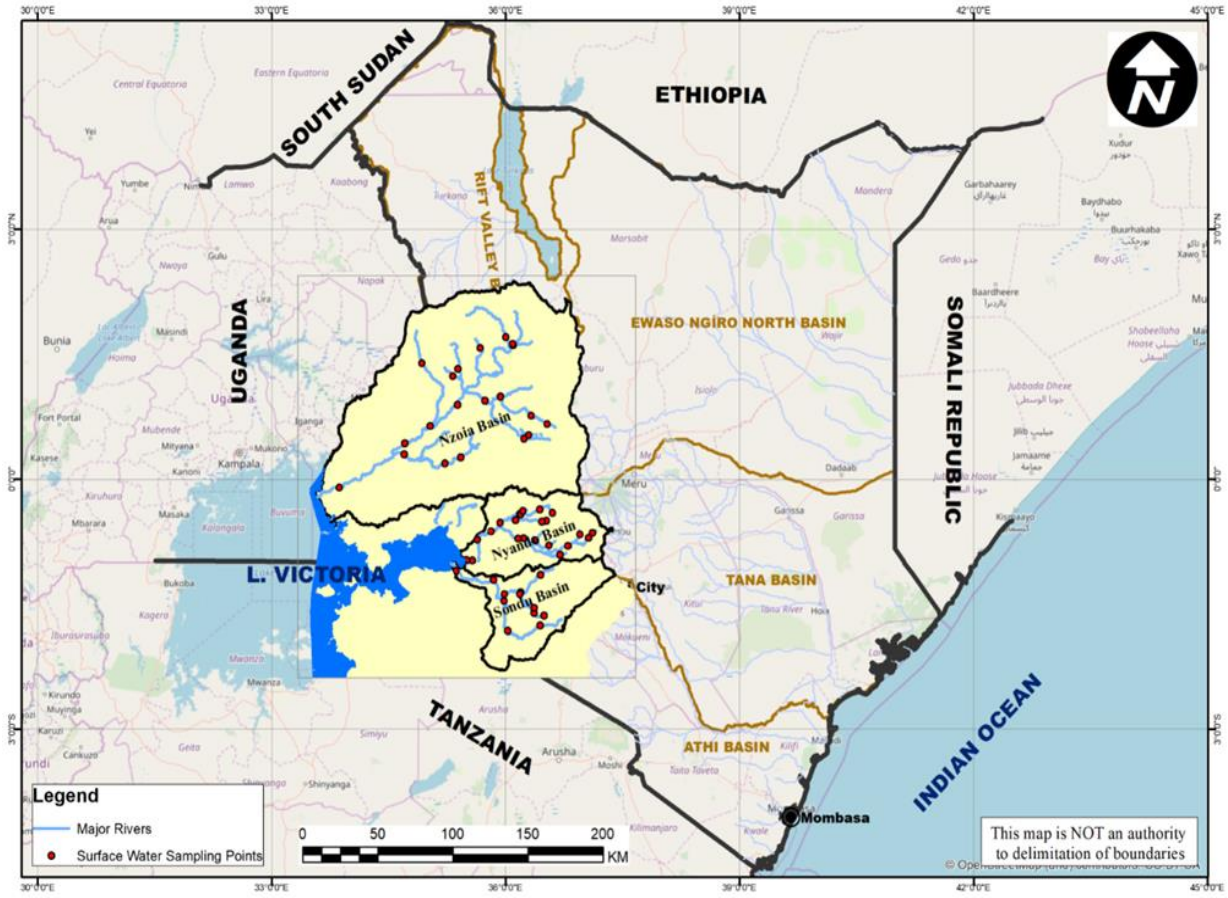

Figure 2.1 Map of Kenya in East Africa with inset: study area with major rivers and sample points (a), Land use maps of the river Nyando (b), Nzoia (c) Sondu Miriu (d) catchments of Lake Victoria basin, Kenya; spatial sampling stations are indicated by bullets and labelled using HCA cluster IDs, are for Nyando, MA1–MA5: mixed agriculture, RI1–RI7: residential and industrial, S1- S8: sugarcane, TF1–TF3: tea and forest; for Nzoia, CA1–CA10: commercial agriculture, MA1–MA7: mixed agriculture, U1–U4: urban; and for Sondu Miriu, MA1–MA4: mixed agriculture, T1–T6: tea, TU1–TU2: tea and urban.

(b)

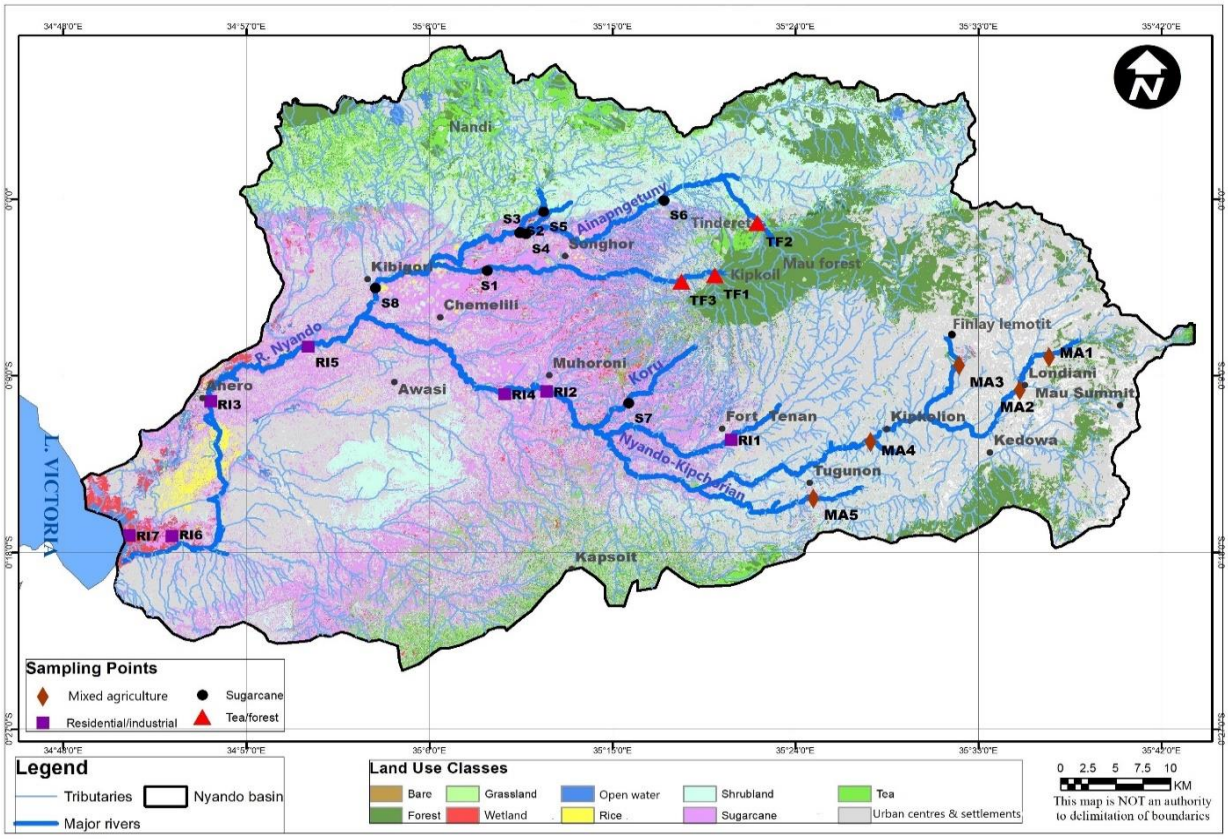

(c)

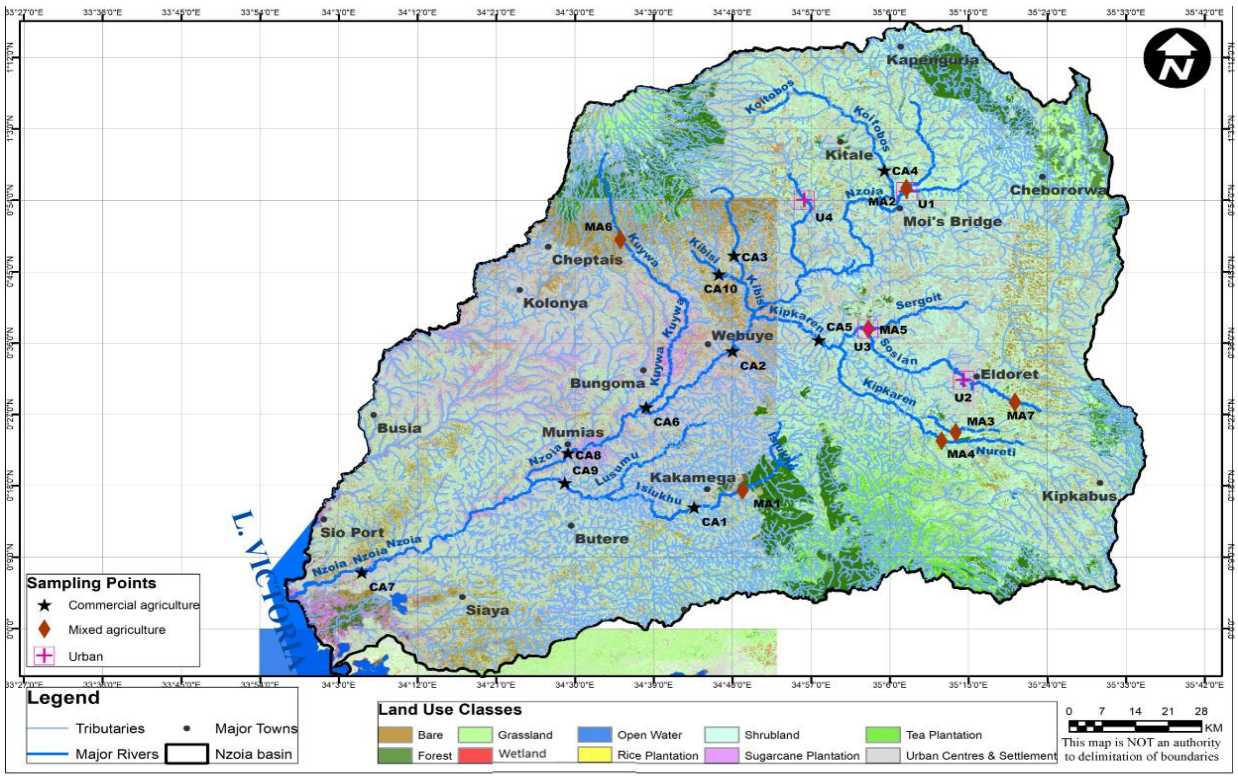

Figure 2.1 continued.

(d)

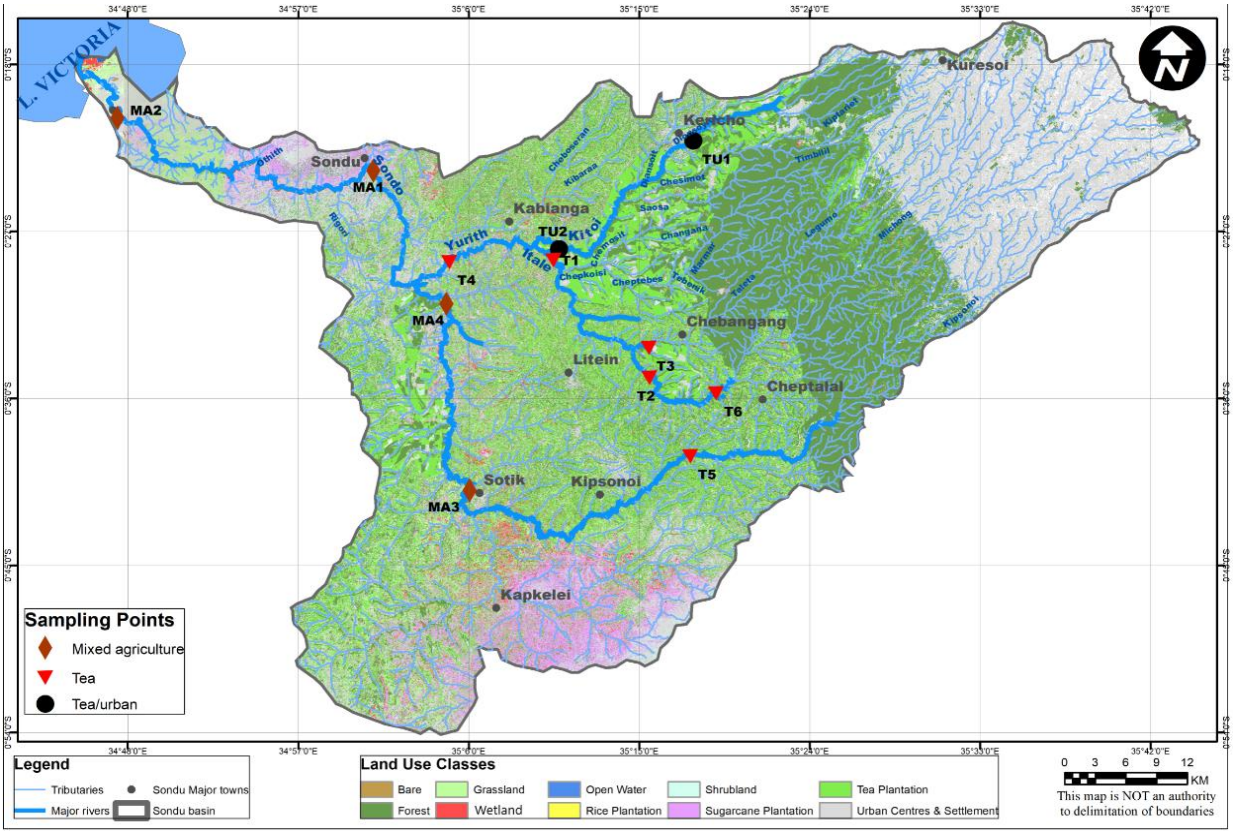

Figure 2.1 continued.

The study area experiences a long rains season between March and July and a short rainy season between September and November. However, during the study period, the area experienced erratic rainfall pattern compared to the long-term pattern (Fig. 2.2). Unusually low rainfall were experienced in the months of October and December, and a general temperature increase (>0.5°C) was observed comparing the sampling period to the long term data. These weather anomalies may be associated to the impacts of global warming which is not only limited to changes in temperature but also alters rainfall amount, distribution and pattern (IPCC, 2007).

2.2.2 Sampling and analysis

Selection of field sampling stations was done in consultation with the Lake Victoria Basin Commission's Environmental Management Project (LVEMP) and the Water Resources Authority (WRA) who run the Lake Victoria basin water quality monitoring network. Spatial

sampling stations in the Nyando catchment were identified and located in a headwater catchment consisting of pristine forest and commercial tea estate, commercial sugarcane estates, horticultural farm, mixed agriculture (which according to this study refers to: smallholder agriculture ca. < 5 ha and livestock keeping), industrial and urban centres, and wetland and river mouth. In the more expansive Nzoia catchment, stations were spatially distributed across the main channel, first and second order streams covering commercial sugarcane farms and sugar factories, large maize and wheat farms (ca. ≥ 5 ha), mixed agriculture, urban and industrial centres. In the Sondu Miriu catchment where tea farming is the major agricultural activity, stations were spatially spread covering mixed agriculture (maize, beans, sorghum, livestock) at lower reaches, tea growing (commercial and smallholder) at the midstream to upstream zone, and the urbanized Kericho town area.

A spatiotemporal sampling strategy was carried out at 23 sampling stations for along River Nyando, 21 stations in River Nzoia, and 12 stations in River Sondu Miriu. To capture seasonal variation in NO_3^- discharge, grab sampling was carried out in four seasons: 1) during an agricultural productive, wet period from May to July, 2016, marked as 'peak wet' (PW) season, 2) during the 'end of the wet' (EW) season in September, 2016, 3) during the 'dry season' (D) in December, 2016 and 4) at the transition period from dry to wet season in March 2017, marked as 'start of wet' (SW) season (Fig. 2.2).

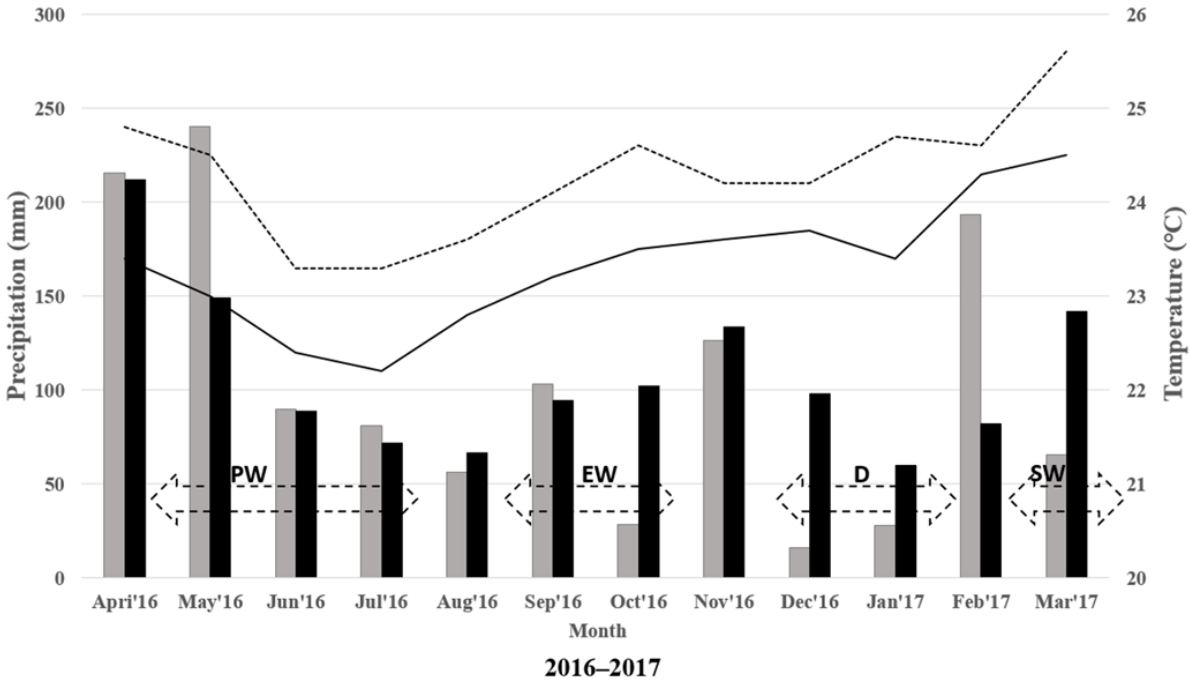

Figure 2.2. Monthly average rainfall and temperature registered at the Ahero (Kisumu) weather station. Long term (1967-1994) and study period (2016-2017) data are given for precipitation 2016-2017 (grey bars), precipitation 1967 - 1994 (black bars), temperature 2016-2017 (dotted line), and temperature 1967-1994 (full line); sampling periods include: peak wet cropping season (PW), end of wet season (EW), dry season (D), start of wet season (SW); Source: Kenya Meteorological Department.

In the field, water was taken as a grab sample in 200 mL high density polyethylene (HDPE) bottles, pre-filtered onsite (11 µm Whatmann filters) and stored in an insulated cooler box containing ice cubes for transportation to the laboratory for physicochemical and isotopic analysis. Duplicate samples for cation analysis were taken in 100 mL HDPE bottles, pre-filtered and acidified to pH 2 using dilute nitric acid. *In situ* measurements included temperature (T), electrical conductivity (EC), pH, dissolved oxygen (DO) and river water discharge measurements. These *in situ* parameters (T, EC, pH, DO) were measured in every sampling station using a multi-parameter sensor (2FD47F-Multi3430, WTW, Germany). River discharge measurements were carried out using a universal current flow meter (F1, Hydrokit, Germany) at the last sampling station before river mouth to estimate NO_3^- discharge of the river catchments into Lake Victoria. Superficial riverbed sediment samples were taken in polythene bags from select stations using an Ekman grab sampler (Eijkelkamp, Netherlands) mounted on a bridge, then stored in an insulated cooler box containing ice cubes for transportation to the

laboratory. In the laboratory, all water samples were filtered through 0.45 µm membrane filters and stored frozen (-17°C) awaiting analysis. Laboratory determination of Na^+, K^+, Ca^{2+}, Mg^{2+}, NH_4^+, NO_3^-, Cl^-, SO_4^{2-} and PO_4^{3-} concentrations was carried out using an ion chromatograph (930 Compact IC Flex, Metrohm, Switzerland). The $\delta^{15}N$– and $\delta^{18}O$–NO_3^- values were determined by the "Bacterial denitrification method" (Casciotti et al., 2002; Sigman et al., 2001; Xue et al., 2009), which allows for simultaneous determination of $\delta^{15}N$ and $\delta^{18}O$ of N_2O produced from the conversion of NO_3^- by denitrifying bacteria, which naturally lack N_2O-reductase activity. The $\delta^{15}N$ and $\delta^{18}O$ analysis of the produced N_2O was carried out using a trace gas preparation unit (ANCA TGII, SerCon, UK), coupled to an isotope ratio mass spectrometer (IRMS) (20-20, SerCon, UK). The N_2O sample was flushed out of the sample vial using a double-hole needle on an auto-sampler. Water was removed using a combination of nafion dryer and $MgClO_4$ scrubber. By cryogenic trapping and focusing, the N_2O was compressed onto a capillary column (CP-Poraplot Q 25 m, 0.32 mm id, 10 µm df, Varian, US) at 35ºC and subsequently analyzed by IRMS. The subsequent stable isotope data were expressed as delta (δ) units in per mil (‰) notation relative to the respective international standards:

$$\delta_{sample}\ (‰) = \left[\frac{R_{sample}}{R_{standard}} - 1\right] \times 1000 \qquad 2.1$$

Where R_{sample} and $R_{standard}$ are the $^{15}N/^{14}N$ or $^{18}O/^{16}O$ ratio of the sample and the standard for $\delta^{15}N$ and $\delta^{18}O$, respectively. The $\delta^{15}N$ values are reported relative to N_2 in atmospheric air (AIR) and $\delta^{18}O$ are reported relative to Vienna Standard Mean Ocean Water (VSMOW). Three internationally recognized reference standards, USGS32 (180.0 ± 1.0‰ for $\delta^{15}N$, 25.7 ± 0.4‰ for $\delta^{18}O$), USGS34 (-1.8 ± 0.2‰ for $\delta^{15}N$, -27.8 ± 0.4‰ for $\delta^{18}O$), and USGS35 (2.7 ± 0.2‰ for $\delta^{15}N$, 56.8 ± 0.3‰ for $\delta^{18}O$), were used to normalize the raw $\delta^{15}N$ and $\delta^{18}O$ values (based on a N_2O reference gas tank) to the AIR and VSMOW scale. USGS32 and USGS34 were used for normalization of the $\delta^{15}N$ value and USGS34 and USGS35 for the $\delta^{18}O$. The amount of NO_3^- in samples and references were matched (i.e. 20 nmol) which corrects for nonlinearity of the IRMS and blanks associated with the procedure. An in-house KNO_3 laboratory standard

(9.9‰ for $\delta^{15}N$, 24.3‰ for $\delta^{18}O$), was analyzed together with the samples for quality control. Measurement batches were only accepted if measured $\delta^{15}N$ and $\delta^{18}O$ values of the laboratory standard were within 0.4 and 0.5‰ of our accepted values, respectively. If standard deviation on replicate samples was higher than 0.3 and 0.4 for $\delta^{15}N$ and $\delta^{18}O$, respectively, the sample was reanalyzed. More details are provided in Casciotti et al. (2002), and Xue et al. (2009).

In order to determine the potential for occurrence of denitrification in the river beds, a laboratory experiment using superficial river bed sediments from the study area was set up as described by Dhondt et al. (2003). Twenty gram of dried and sieved (2 mm) river-bed sediments were weighed into a 500ml Schott bottle. 300ml of water solution (MQ water containing 20 µM $CaCl_2$) was added and the bottles sealed with bottle caps containing two holes fitted with pipes to flush the bottle (both sediment and airspace) using N_2 gas to remove O_2 from the system. After 2 days of anaerobic pre-incubation, Nitrapyrin was added as nitrification inhibitor at a concentration of 120 mg kg^{-1} dry soil. In the current study, no external carbon source was added other than the natural organic carbon of the sediments. Therefore, NO_3^- was added to the solution based on the sediment carbon content to ensure an electron donor: electron acceptor ratio which promotes denitrification in the system. Samples of the soil suspension were taken with a syringe at regular time intervals (0, 4, 8, 24, 30 and 48hours) and analyzed for NO_3^-. The sediment samples which showed NO_3^- reduction with time were further analyzed for $\delta^{15}N$ and $\delta^{18}O$ to demonstrate NO_3^- reduction can potentially occur in the river bed thereby biasing isotopic signature of NO_3^-. This relationship is expressed by a Rayleigh equation:

$$\delta_s = \delta_0 + \varepsilon \ln(f) \qquad 2.2$$

Where δ_0 is the initial $\delta^{15}N–NO_3^-$ value, δ_s is the $\delta^{15}N–NO_3^-$ value in the remaining NO_3^-, f is the fraction of the remaining NO_3^- and ε is the isotope enrichment factor.

2.2.3 Statistics

Water physicochemical dataset of spatial sampling stations was analyzed using hierarchical cluster analysis (HCA). The data for HCA (agglomeration schedule) analysis was first standardized by subtracting the mean value and dividing by the standard deviation of the parameter in order to eliminate the influence of different units between variables. HCA was performed on the data sets (using the following variables: Na^+, K^+, Ca^{2+}, Mg^{2+}, NO_3^-, Cl^-, SO_4^{2-}, pH, EC, T and DO) by means of the Ward's method using squared Euclidean distances as a measure of similarity in order to cluster sampling stations into homogeneous groups. The results were presented in a dendrogram showing the clusters and their proximity with a reduction in the dimensionality of the original data set. Hierarchical cluster analysis (HCA) has been applied in the past for surface and groundwater quality assessment and land use segmentation (Barakat et al., 2016; Kamtchueng et al., 2016; Pejman et al., 2009; Zhang et al., 2009). ANOVA with Tukey HSD tests ($p<0.05$ levels) were performed on the NO_3^-, $\delta^{15}N$ and $\delta^{18}O$ data to understand interactions between different land uses.

Major ionic constituents were plotted in piper tri-linear diagrams (Piper, 1944). These are a combination of anion and cation triangles with a diamond shape between them which is used to plot the analysis and whose position indicates the water type or water origin. Using the AquaChem (version 2014.2) software package, water types helped in understanding the processes controlling river water mineralization, which by extension indicates NO_3^- origin. In addition, NO_3^- versus Cl^- correlations were plotted to establish probable pathways controlling NO_3^- input in the river water (Widory et al., 2005).

2.3 Results and Discussion

2.3.1 Spatial clustering of sampling stations

River physicochemical data from a spatiotemporal sampling campaign in Nyando, Nzoia, and Sondu Miriu river catchments were analyzed using HCA which grouped sampling stations with

similar properties together. Figure 2.3a-c gives HCA output dendrograms grouping sampling stations for the Nyando catchment into four clusters, and for the Nzoia catchment and Sondu Miriu catchment into three clusters. The clusters, which in comparison to land use maps (Figure 2.1(b – d) corresponds to the major land use classes in the three river catchments informed the allocation of sample point identities (i.e. MA, S, T, CA…).

For the Nyando catchment (Fig. 2.3a and 2.1b), HCA grouped stations in the upper reaches of the Kipchorian tributary into cluster 1. The area lies at 1900–2300 m a.s.l. and is characterized by mixed agriculture (MA) area under food crop cultivation, a commercial horticultural flower farm, livestock keeping, and residential settlements. MA1, MA2, MA4 and MA5 are situated in an intensive agriculture and peri-urban area, while MA3 is located downstream of the commercial horticultural flower farm.

(a)

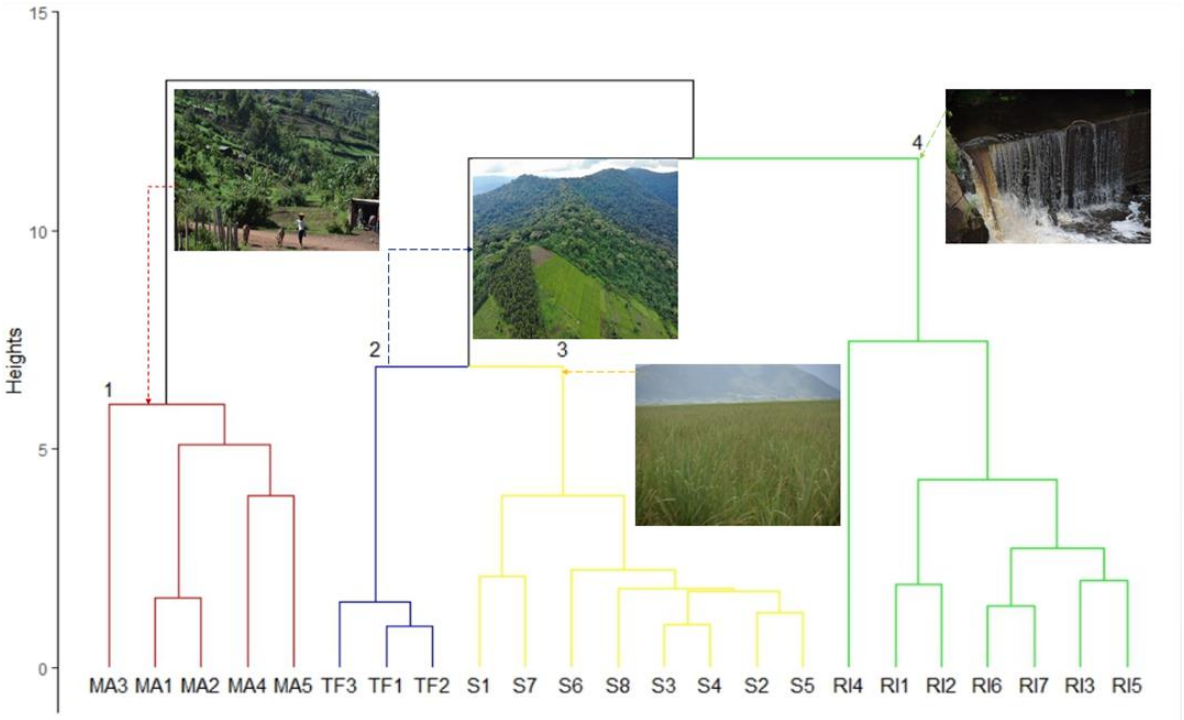

(b)

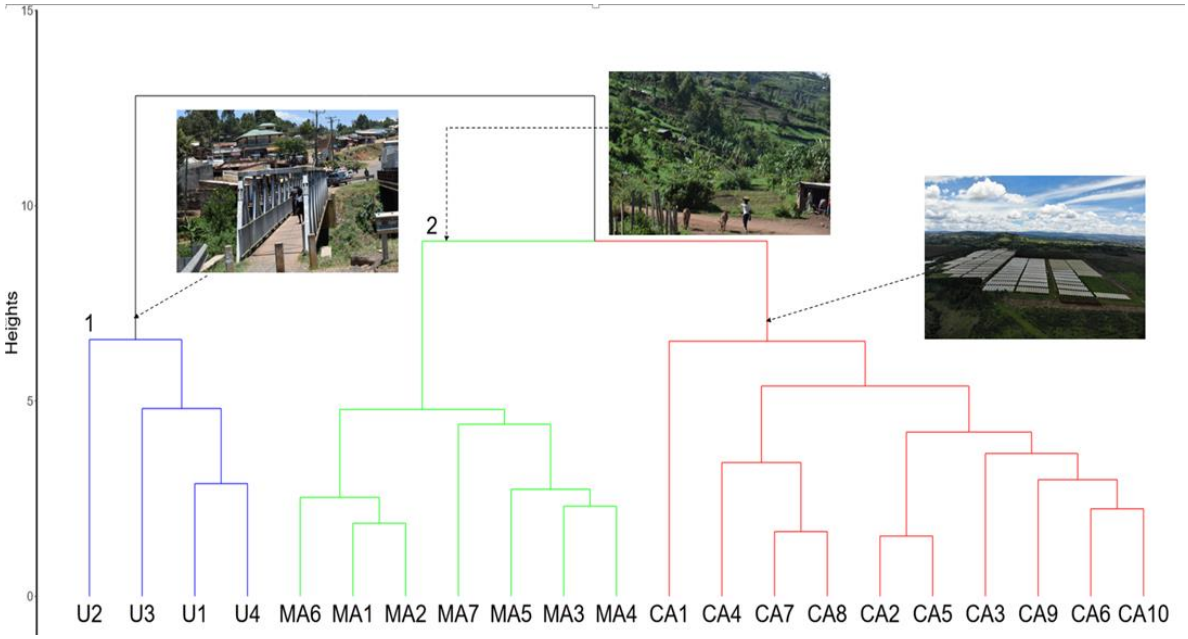

(c)

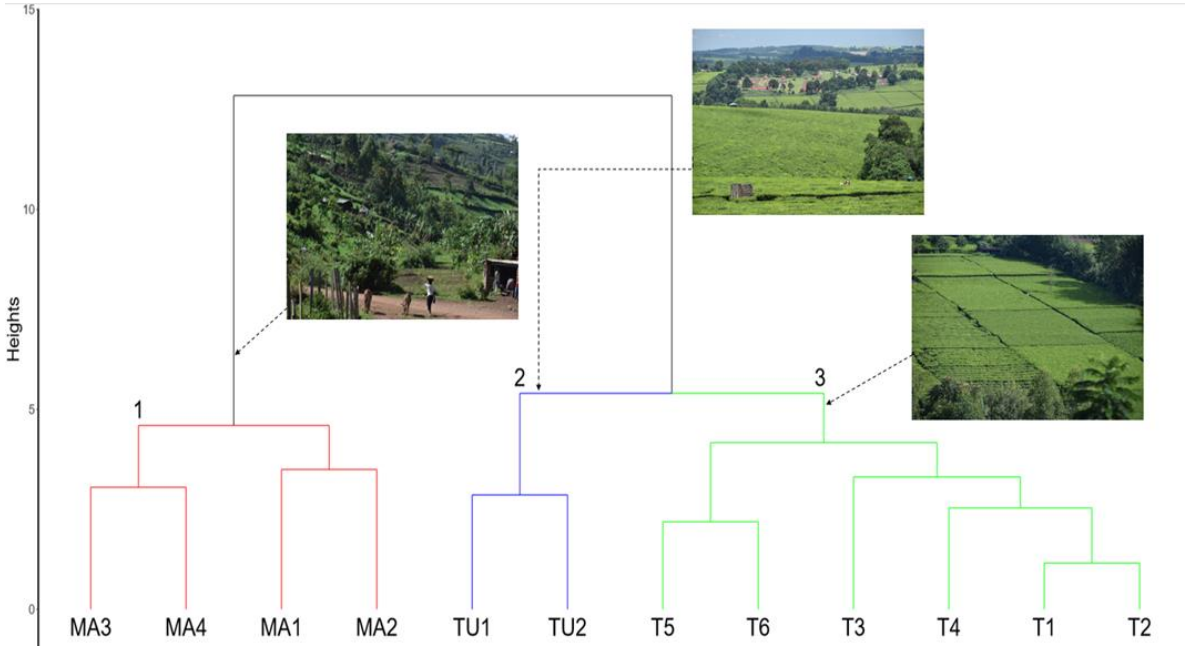

Figure 2.3. HCA cluster dendrograms (Ward's method, squared Euclidean distance) grouping sampling stations in the Nyando (a), Nzoia (b) and Sondu Miriu (c) river catchments; clusters are labelled by dominant land use i.e. MA: mixed agriculture, TF: tea and forests, S: sugarcane, RI: residential settlements and industrial, CA: commercial agriculture, U: urban, TU: tea and urban, T: tea.

Cluster 2 groups stations under tea and forest (TF1–TF3) located at the most upstream part of the catchment. TF1 is located in a pristine forest, which is part of the Mau complex, while TF2 is located in a commercial tea estate and TF3 in an area of smallholder mixed farms bordering the natural forest. Cluster 3 groups sample stations within the sugarcane belt (S1–S8) downstream of the tea area and forest. As can be observed from the HCA dendrogram, cluster 2 and cluster 3 areas have similar physicochemical properties and form one major group representing the river Ainapngetuny (Fig. 2.1b), one of the two main tributaries of River Nyando. Cluster 4 stations represent residential and industrial areas (RI1–RI7); they are located in the mid- to downstream reaches of the Nyando catchment. The area is characterized by relatively high populated residential and urban centers, agro-based industries (sugar, agrochemical, and lime factory), rice irrigation and affected wetlands.

For the Nzoia catchment (Fig. 2.3b and 2.1c), HCA grouped stations located in major urban centers like Eldoret and Moi's bridge towns into cluster 1 (U1–U4). These areas are characterized by sewage effluent discharges consisting of industrial and domestic waste. Cluster 2 consists of stations located in second and third order streams found in the upper reaches of the catchment whose common land use is mixed agriculture (MA) on small land parcels measuring $\leq$ 2 ha. Cluster 2 stations were also characterized by land degradation practices like deforestation and farming on steep slopes and un-terraced lands which leads to high soil erosion rates. Cluster 3 groups stations mainly under commercial agriculture (CA) of sugarcane, maize and/or wheat. Farms in cluster 3 consist of large-scale mechanized farms owned by state corporations like Nzoia and Mumias sugar companies which run sugarcane milling, ethanol and molasses production factories. In addition, the area has small scale farmers who have ventured into cash crops (sugarcane, wheat, maize) for commercial purposes. Furthermore, cluster 3 stations are located in the main Nzoia catchment and its first order streams.

For the Sondu Miriu catchment (Fig. 2.3c and 2.1d), HCA groups stations in mixed agriculture (MA) areas located in the downstream part of the main river (MA1, MA2) and the lower

reaches of the first order Kipsonoi tributary (MA3, MA4) into cluster 1. In this area, mixed agriculture (tea, maize, beans, sugarcane and sorghum), a hydropower dam, residential areas and livestock farming are the major land uses. HCA groups stations in the Ainapkoi tributary which drains a purely commercial tea area and the urbanized Kericho town into cluster 2 (TU). Cluster 3 consists of stations (T1-T6) in a predominantly tea growing area of the Chemosit basin. The area is characterized by small scale tea farms, commercial tea farms and planted forests. As observed in Fig. 2.3c, cluster 2 and 3 stations form one main group (tea area), distinct in physico-chemistry from the mixed agricultural area.

2.3.2 Physicochemical and Isotopic characterization

2.3.2.1 In-situ parameters

Table 2.1 presents a summary of *in situ* parameters obtained from the study area. Water EC values obtained in this study are within WHO standards for fresh water (< 500 µS cm^{-1}) ranging from a mean of 45 µS cm^{-1} in the tea land use of the Sondu Miriu catchment to 311 µS cm^{-1} in residential and industrial land use of the Nyando catchment. Moreover, the Nyando catchment portrayed higher EC values than the other two catchments. A neutral to slightly alkaline water pH (mean pH 6.9 − 8.3) was observed while DO values (6.4 − 7.9 mg O_2 L^{-1}) were sufficiently high for surface water and likely unfavourable for *in situ* denitrification processes (Nestler et al., 2011; Piña-Ochoa and Álvarez-Cobelas, 2006) (see further). Water temperature in the study area was influenced by altitude with the lowest mean water temperature of 17ºC recorded in the tea and forest (altitude: 1900–2200 m a.s.l), while the highest mean water temperature of 24ºC was observed in the residential and industrial located near shores of Lake Victoria (altitude: 1140–1300 m a.s.l).

Table 2.1. Summary of *in situ* parameters: pH, electrical conductivity (EC), temperature (Temp), dissolved oxygen (DO) per land use clusters (see Fig. 2.3 for explanation) in the three river catchments; river water and nitrate discharge values represents the last sampling point (before river mouth) for the Start wet (SW), Peak wet (PW), End wet (EW) and Dry (D) seasons.

River	Location	pH	EC (µS cm^{-1})	Temp (°C)	DO (mg O_2 L^{-1})		River water (m^3 s^{-1}) and nitrate (t day^{-1}) discharge			
							SW	PW	EW	D
Nyando	S	8.3±0.2	296±47	22±2	7.6±0.3	[1]	4.0	37.4	8.7	3.0
	TF	7.9±0.2	168±27	17±2	7.6±0.2					
	MA	7.2±0.9	184±52	18±3	7.0±0.6	[2]	0.8	6.2	1.5	0.06
	RI	8.1±0.3	311±104	24±2	6.4±1.8					
Nzoia	CA	7.6±0.3	123±29	22±2	7.4±0.6	[1]	41	187	149	26.6
	MA	7.3±0.3	90±21	18±2	7.3±0.6	[2]	17.7	22.2	33.5	5.2
	U	7.7±0.4	190±55	20±3	7.4±0.4					
Sondu Miriu	T	7.1±0.3	45±9	18±2	7.9±0.3	[1]	6.1	22.9	16.2	8.9
	TU	6.9±0.2	54±7	18±2	7.6±0.2	[2]	2.3	7.2	5.3	2.6
	MA	7.4±0.4	71±19	22±2	7.6±0.4					

[1] River water discharge [2] Nitrate discharge

The Nzoia catchment had the highest water discharge volumes during the study period, ranging 26 m^3 s^{-1} in the D season to 187 m^3 s^{-1} during the PW season. River Sondu Miriu water discharge ranged from 6.1 – 22.9 m^3 s^{-1} while the Nyando ranged from 3 – 37.4 m^3 s^{-1}. River nitrate discharge into the Lake Victoria were approximated from the river water discharge and NO_3^- concentration values (Table A1 – A3) at the last sampling station before the river mouth (Fig. 2.1). River Nzoia led in NO_3^- discharge into the Lake Victoria during the sampling period with a discharge of between 5.2 and 33.5 t day^{-1}, respectively. Sondu Miriu ranked second discharging between 2.3 and 7.2 t day^{-1} while the Nyando discharged between 0.06 and 6.2 t day^{-1}. A study by Okungu and Opango (2004), also reported the Nzoia catchment as leading source of total annual nutrient loading of Lake Victoria from the Kenyan side of the basin.

2.3.2.2 Nyando catchment

In order to characterize the river hydrochemistry under the different HCA determined land use areas of the Nyando catchment, major ions (Na^+, K^+, Ca^{2+}, Mg^{2+}, NO_3^-, HCO_3^- Cl^-, SO_4^{2-}) were plotted in piper diagrams (Piper, 1944) and presented in Figure 2.4a. A clear spatiotemporal variation in ionic constituents was observed in the Nyando catchment, which also indicates the dominant solutes and water types in this catchment. In the MA stations, dominance of alkali metals (Na^+, K^+) over alkaline earth metals (Ca^{2+}, Mg^{2+}) was found, while Cl^-+NO_3^- were the major anions giving a Na+K-Cl+NO_3 water type. Local geology normally influences dissolved river solutes and this is mainly reflected by base flow concentrations. However, the dominance of a Na+K-Cl+NO_3 water type in MA in all seasons suggests surface water contamination (Kamtchueng et al., 2016). In TF, alkaline earth metals dominated over the alkali metals, while Cl^-+NO_3^- and HCO_3^- were the major anions. In the diamond, TF plotted in the Ca+Mg-HCO_3 and Ca+Mg-Cl+NO_3 water type during the dry and wet seasons, respectively. A Ca+Mg-HCO_3 water type represents soil weathering (natural) sources (Ako et al., 2012) implying that the Ca+Mg-Cl+NO_3 water type observed in TF during wet seasons reveals influence by inorganic fertilizers applied in tea. Similar to TF, S showed a Ca+Mg-HCO_3 water type with an increase in Cl^-+NO_3^- during the wet seasons. RI seems to have both alkali (Na^+, K^+) and alkaline earth (Ca^{2+}, Mg^{2+}) metals in similar proportions. HCO_3^- was the major anion in RI but an increase of Cl^-+NO_3^- was again observed in the wet (PW, EW) seasons. The RI plotted in the Na+K-HCO_3 water type during the dry seasons and showed both Ca+Mg-HCO_3 and Na+K-Cl+NO_3 water types during the wet seasons.

The Cl^-+NO_3^- increase observed in Nyando catchment during wet seasons is likely related to agricultural inputs (inorganic/organic fertilizer) which are mainly applied during the wet cropping season in commercial tea, sugarcane, horticultural and mixed farming (Nyairo et al., 2015). The common fertilizer types used in the region are: NH_4^+ based NPK commonly applied in tea plantations; CAN and DAP commonly used in maize, wheat and beans; urea applied in

sugarcane farming; $(NH_4)_2SO_4$ in rice farming; and animal manure commonly broadcasted in mixed farming systems for subsistence (e.g. maize, beans, sorghum, millet).

(a)

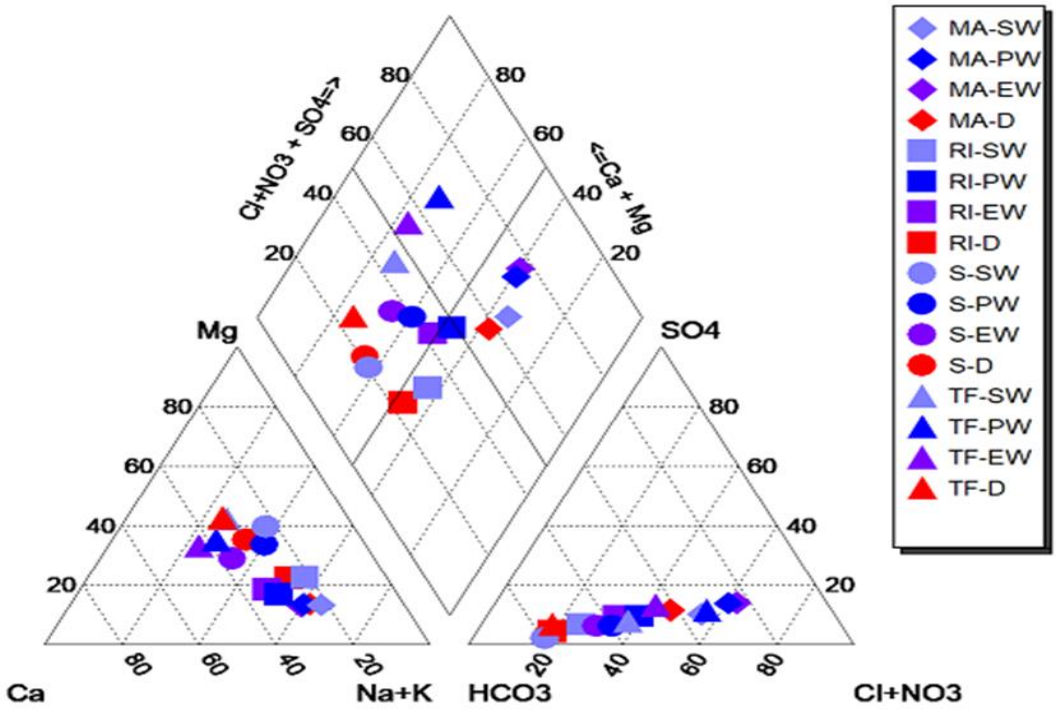

(b)

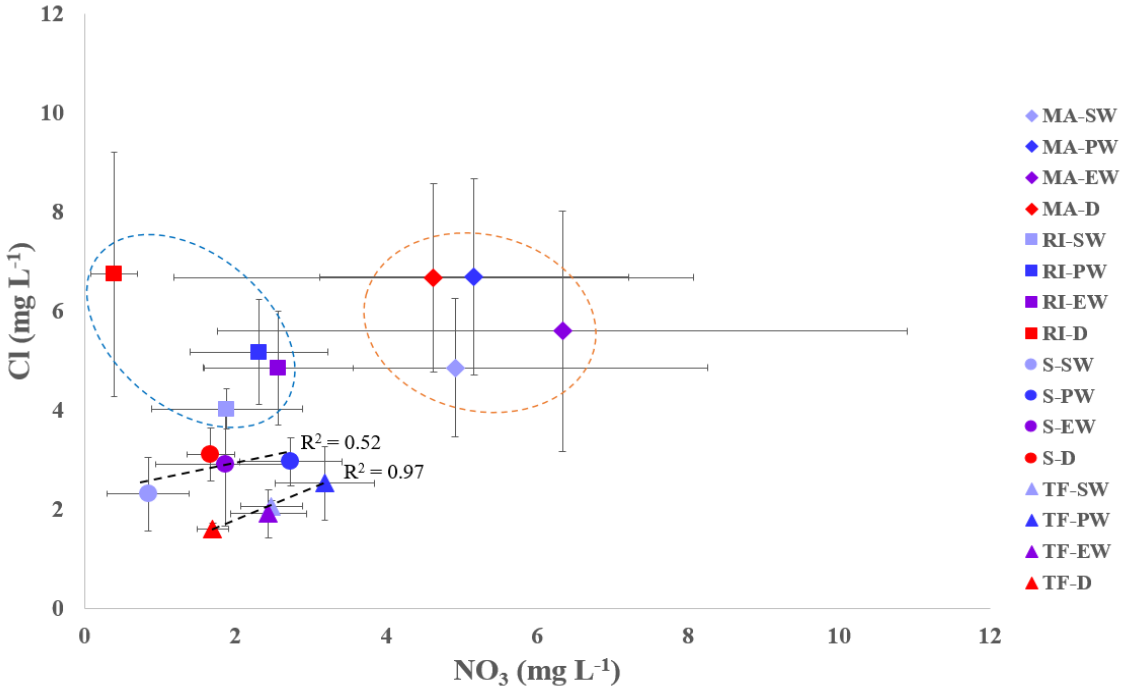
Cl (mg L-1)
NO3 (mg L-1)
R2 = 0.52
R2 = 0.97
MA-SW
MA-PW
MA-EW
MA-D
RI-SW
RI-PW
RI-EW
RI-D
S-SW
S-PW
S-EW
S-D
TF-SW
TF-PW
TF-EW
TF-D

(c)

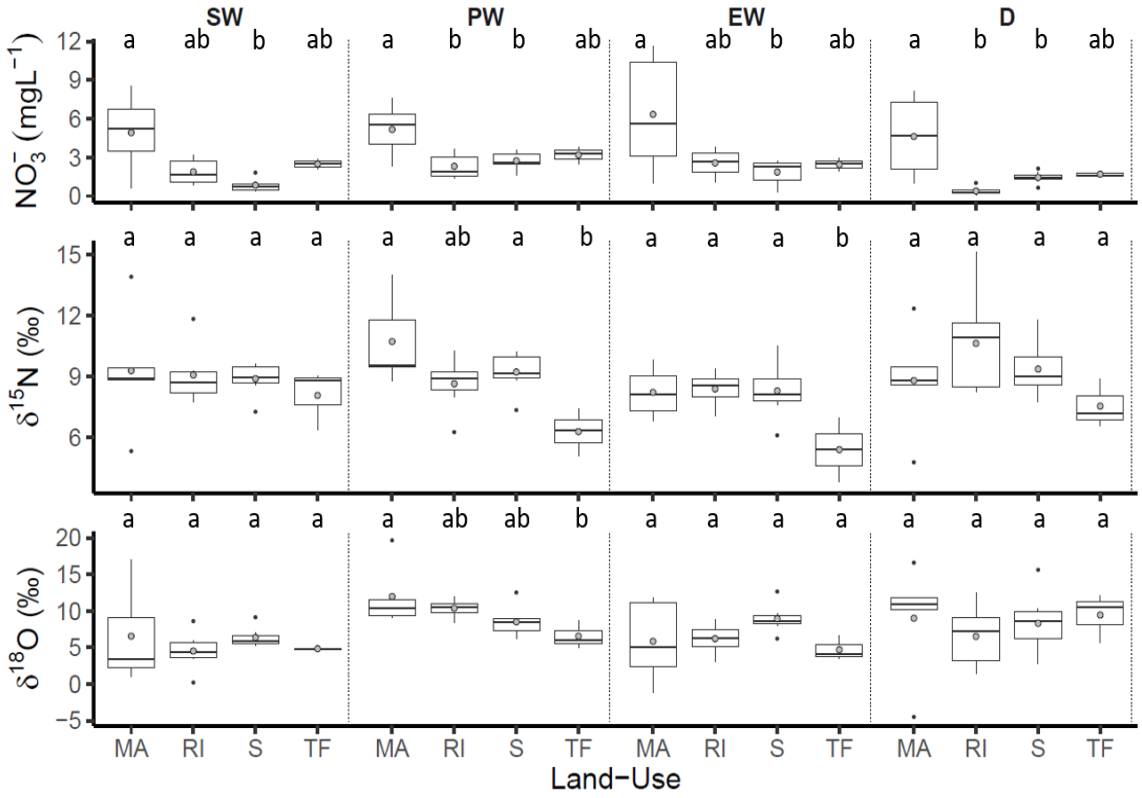

Figure 2.4. Nyando catchment: Piper trilinear plot of major cations and anions (in percent) for water characterization. Bullets represent land use clusters (see Fig. 2.3 for abbreviations), while colours represent selected sampling seasons (see Fig. 2.2 for abbreviations) (a); spatial temporal plot of mean Cl^- versus NO_3^- mean concentrations with standard deviations given as error bars and bullets represent land use clusters while colours represent seasons as described in (a) above (b); Ranges of NO_3^- concentration, $\delta^{15}N–NO_3^-$ and $\delta^{18}O–NO_3^-$ values obtained for different land use clusters in Nyando during start of wet (SW), peak wet (PW), end of wet (EW) and dry (D) seasons. Boxplots represent 25th, 50th, and 75th percentiles, whiskers represent 5th and 95th percentiles, black bullets represent outliers, and grey bullets represent mean values. Letters (a, b, c) represent ANOVA output with similar letters indicating non-significant difference ($p>0.05$) using Tukey HSD test (c).

Chloride behaves as a conservative ion in water whose concentration is not subject to physical, chemical and microbiological processes occurring within the river system and therefore a good indicator of anthropogenic impacts (Liu et al., 2006). Potential sources of Cl^- include natural sources (mineral dissolution), inorganic fertilizers (KCl), animal wastes and sewage effluents. The NO_3^- vs. Cl^- correlations can provide more information on NO_3^- sources, and help to identify removal processes via denitrification (Mengis et al., 1999; Widory et al., 2005). Figure

2.4b shows a plot of Cl^- versus NO_3^- in the Nyando catchment in which samples cluster into three groups. TF and S stations cluster closely together in a group which shows linear relationship (R^2 = 0.97, R^2 = 0.52 respectively) between Cl^- and NO_3^- pointing towards a contaminant source which causes a proportional Cl^- and NO_3^- increase from the dry to the peak wet season. The common source of Cl^- and NO_3^- should be the NPK fertilizer whose primary source of potassium (K) is potash (KCl). NPK is applied during the peak wet cropping season in the commercial tea and sugarcane farms. Furthermore, there was a clear separation of MA land use stations into a group with high Cl^- and NO_3^-. The MA land use is characterized by high population density living in an urbanizing area lacking effluent treatment infrastructure and practicing mixed farming of food crops and free-range livestock keeping. The area also has a commercial horticultural flower farm under irrigation. Both manure and inorganic fertilizers (NPK, CAN, DAP) are used in the area at a rate ranging between 25 and 75 kg N ha^{-1} yr^{-1} for planting and top dressing. This therefore, indicates that inorganic fertilizer losses, animal wastes and sewage discharges are major sources of the Cl^- and NO_3^- in MA.

RI stations, on the other hand, were separated in a group with high Cl^- but low NO_3^- concentration. RI is located in the downstream part of the Nyando catchment (Fig. 2.1b), which together with being a residential and relatively industrialized area, also has an irrigated rice farming zone and an extensive wetland towards the river mouth. As shown in Figure 2.4b, there seems a mechanism in RI which selectively consumes NO_3^- without affecting the Cl^- concentration. In spite of the high DO values (which don't favour denitrification) obtained in RI (Table1), denitrification in riparian zones has been reported to reduce NO_3^- load of stream water (Hill, 1996). As NO_3^- concentration decreases, denitrification causes an enrichment of $\delta^{15}N$-, $\delta^{18}O$– NO_3^- while NO_3^- concentration decreases in the remaining NO_3^- pool (Mengis et al., 1999). Denitrification is illustrated by the enriched $\delta^{15}N$–NO_3^- values ranging +8.2‰ to +15.1‰ observed in RI in the dry season corresponding to significantly low NO_3^- concentration ranging 0.1 – 1.0 mg L^{-1} (Figure 2.4c and Table A1). For instance, RI.3 RI.6 and RI.7 recorded very low NO_3^- values during the dry season: 0.2, 0.3 and 0.2 mg L^{-1} respectively corresponding

to $\delta^{15}N–NO_3^-$ of 8.3, 11.1 and 8.6 ‰ respectively which can be attributed to denitrification in the rice fields and the river mouth wetland. Furthermore, the average NO_3^- concentration in RI in the dry season (0.4 ± 0.1 mg L^{-1}) was significantly lower compared to the other land uses ($p = 0.03$) and seasons ($p < 0.0001$). On the other hand, the corresponding average $\delta^{15}N–NO_3^-$ (10.6 ± 6.3‰) was higher than average values obtained in the other land uses ($p = 0.09$) and seasons ($p = 0.009$).

MA land use recorded higher NO_3^- concentrations compared to the other land use clusters during the sampling period (Fig. 2.4c). The highest NO_3^- concentration (5.6 – 11.6 mg L^{-1}) were obtained in MA3 which drains a commercial horticultural flower farm. $\delta^{15}N–NO_3^-$ for MA points ranging +4.8‰ to +14‰ portray the dominance of manure and/or sewage NO_3^- source and was more pronounced (9.5‰ – +14‰) in the PW cropping season mainly due to animal manure application in the mixed farms. Nonetheless, $\delta^{18}O–NO_3$ values obtained in MA3: 17.0 (SW); 19.6 (PW) and 16.6 (D) lie in the nitrate fertilizer source range, +17‰ to +25‰ (Xue et al., 2009) and shows that inorganic fertilizers used in the irrigated commercial flower farm has impact on river water NO_3^- input in the MA land use. On the other hand, relatively low $\delta^{15}N–NO_3^-$ values ranging +3‰ to +7‰ which were obtained in TF during PW and EW seasons lie in the literature range for both soil N and ammonium-based fertilizer sources (Kendall et al., 2007). However, the lower $\delta^{18}O–NO_3^-$ observed in this land use during the wet seasons supports the inorganic fertilizer contribution assuming that the $\delta^{18}O–NO_3^-$ in rainfall is constant across all land uses during the wet season. In the TF, the ammonium-based fertilizer: NPK (25:5:5+5S) is most commonly used during wet seasons (PW, EW) for soil fertility improvement. It therefore suggests that, during the drier (D, SW) seasons, the $\delta^{15}N–NO_3^-$ (+6.4 – +9.0‰) and $\delta^{18}O–NO_3^-$ (+4.7 – +12.0‰) values obtained in the TF area originate from leaching of mineralized soil organic N in the dense natural forest. The isotope data supports the hydro chemical observations (Fig. 2.4a and b) thereby confirming that inorganic fertilizer loss in TF dominate river NO_3^- in the wet seasons while manure and sewage plus inorganic fertilizer (commercial horticulture) control river NO_3^- input in MA. The results also show the

leading influence of manure and sewage (urban, industrial) on river NO_3^- in the RI while inorganic fertilizers influence river NO_3^- in the S land use during the wet season.

However, *in situ* nitrate removal processes could be responsible for low NO_3^- values obtained in different parts of the catchment. Just as observed in RI stations, low NO_3^- contents (0.4 – 1.8 mg L^{-1}) were recorded in S land use during SW season which were below the natural forest value (background estimate: 2.9 mg L^{-1}) (Fig. 2.4c). Since this selective NO_3^- reduction in downstream Nyando (S, RI) cannot be caused by dilution as illustrated in Figure 2.4b, it appears that denitrification is the most probable pathway of the NO_3^- reduction. Similarly, low NO_3^- (0.6 mg L-1) was recorded in MA4 during SW season which was significantly low compared to other MA points. The dry periods (SW, D) appear to be favorable to denitrifcation mainly due to reduced water velocity which increases water residence time and contact with the river bed.

Results of laboratory denitrification experiments on river bed sediments demonstrate the relationship between NO_3^- loss (expressed as natural logarithm of the fraction of initial NO_3^- remaining in the sample) and increase in $\delta^{15}N$ (Fig. 2.5). River Nyando sediment samples: MA4, MA5 showed NO_3^- decrease from 9.5 mg L^{-1} and 79 mg L^{-1}, respectively at the start of the incubation to 0.1 mg L^{-1} and 2 mg L^{-1} after 24 and 48 hours of incubation, respectively. On the hand, $\delta^{15}N$ values increased from 13.7‰ (0 hours) to 25.8‰ (8 hours) for MA4 and from 6.5‰ (0 hours) to 22.3‰ (30 hours) for MA5 (Table A4). The $\delta^{15}N$ enrichment factor due to denitrification, ε, is equal to the slope of the linear relationship between the natural logarithm of the fraction of NO_3^- remaining in a system and the change in $\delta^{15}N$ (Fig. 2.5). The $\delta^{15}N$ enrichment factors obtained for the Nyando sediments were -17.5‰ and -17.2‰, respectively. These values are within the literature range (-3.0‰ to -29.4‰) of laboratory derived $\delta^{15}N$ enrichment factors for denitrification (Blackmer and Bremner, 1977; Dhondt et al., 2003; Wells et al., 2019). The sediment incubation results support the water chemistry and isotopic observations (Fig. 2.4b and c) to show that *in situ* denitrification is a potential process causing nitrate attenuation in River Nyando catchment. Consequently, the enrichment of $\delta^{15}N$–NO_3^-

due to denitrification may bias source apportionment, implying that manure/sewage may be overestimated.

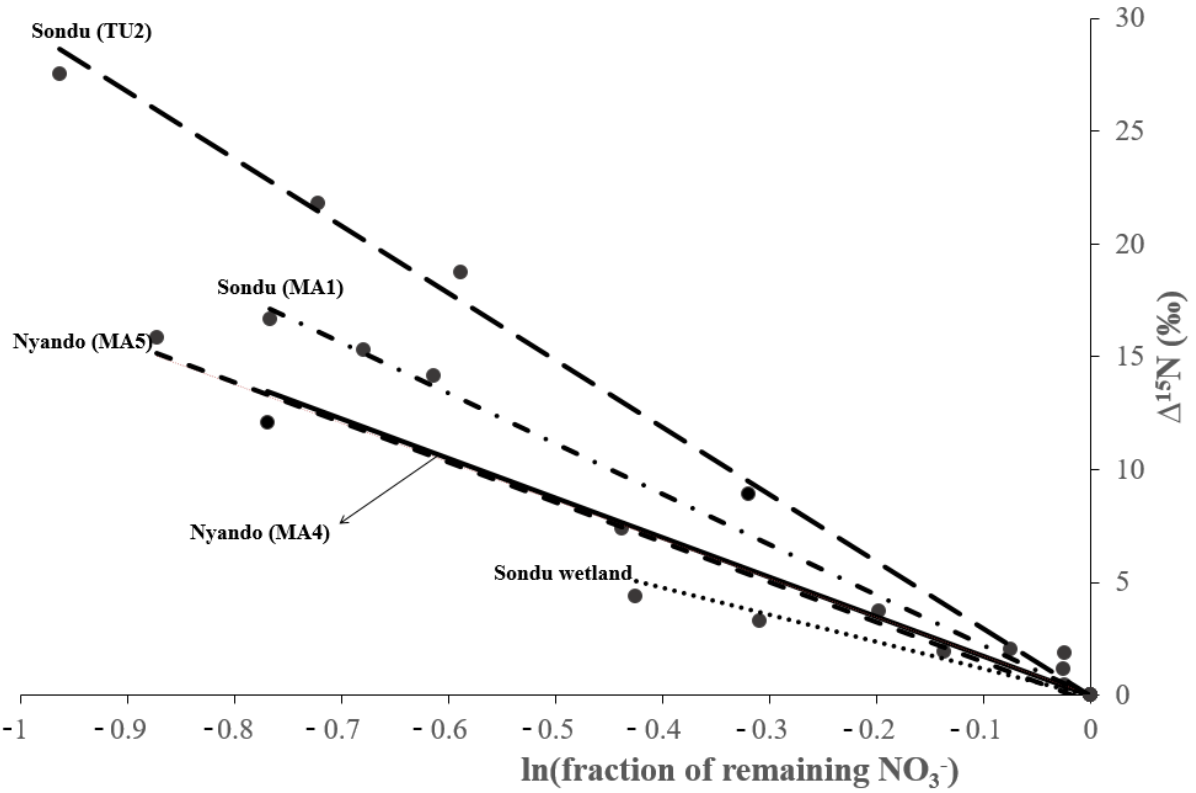

Figure 2.5. Determination of enrichment factors (ε , ‰) for potential denitrification in river bed sediments from Nyando and Sondu Miriu catchments. $\Delta^{15}N = \delta - \delta_o$, where δ represents $\delta^{15}N$ at time (t) and δ_o represents initial $\delta^{15}N$. Denitrification enrichment factors: Nyando, MA4, ε = –17.5‰; Nyando, MA5, ε = –17.2‰; Sondu, TU2, ε = –29.7‰; Sondu, MA1, ε = –22.3‰; Sondu wetland, ε = –11.9‰.

2.3.2.3 Nzoia catchment

In the Nzoia catchment, a spatiotemporal variation in hydro-chemical parameters was observed as well (Fig. 2.6a). Alkali metals were the dominant cations in U and MA land use stations while alkaline earth metals dominated CA. On the other hand, HCO_3^- dominance in CA and MA in the D season can be attributed to low water discharge levels (Table 2.1) which mainly consists of base flow solute levels while the $Cl^-+NO_3^-$ increase during PW season is associated with agricultural inputs (inorganic fertilizer, manure) during the wet cropping period.

(a)

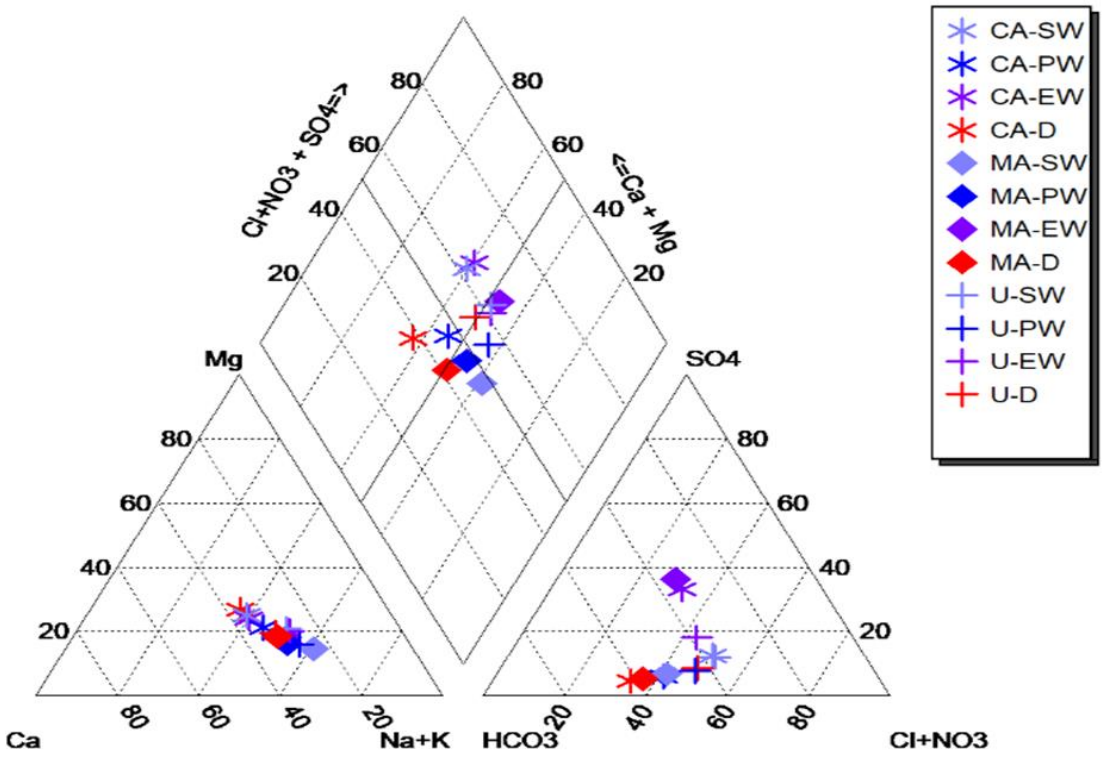
Cl+NO3 + SO4=>
<=Ca + Mg
Mg
SO4
Ca
Na+K
HCO3
Cl+NO3
80
60
40
20
CA-SW
CA-PW
CA-EW
CA-D
MA-SW
MA-PW
MA-EW
MA-D
U-SW
U-PW
U-EW
U-D

(b)

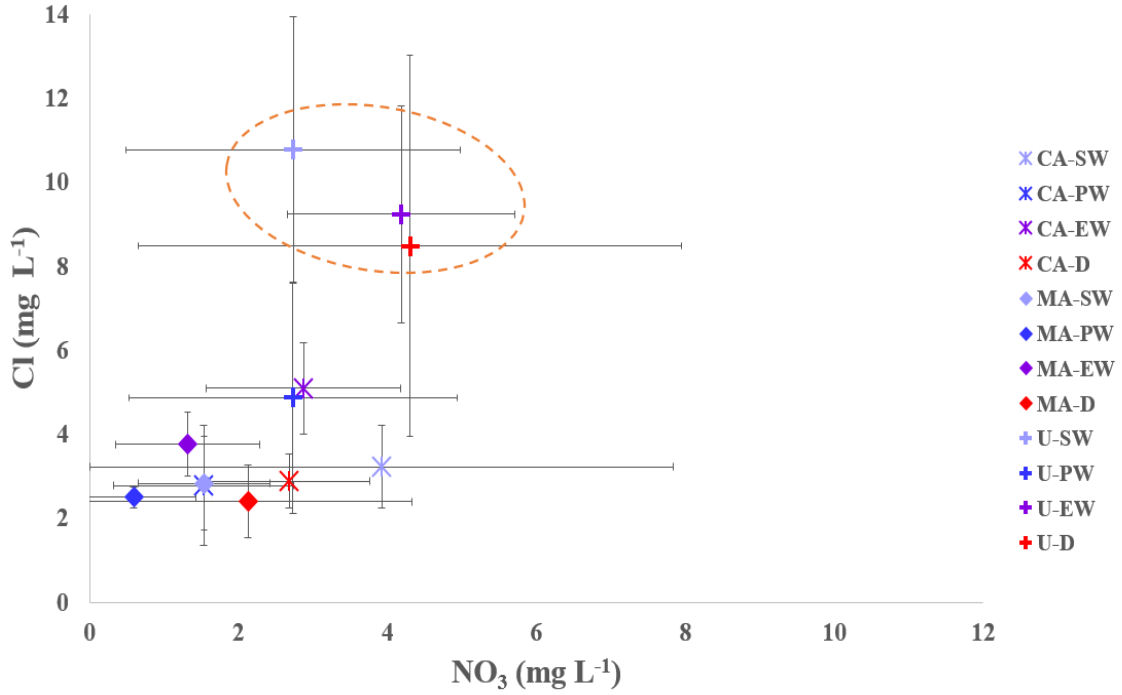
Cl (mg L-1)
NO3 (mg L-1)
0
2
4
6
8
10
12
14
CA-SW
CA-PW
CA-EW
CA-D
MA-SW
MA-PW
MA-EW
MA-D
U-SW
U-PW
U-EW
U-D

(c)

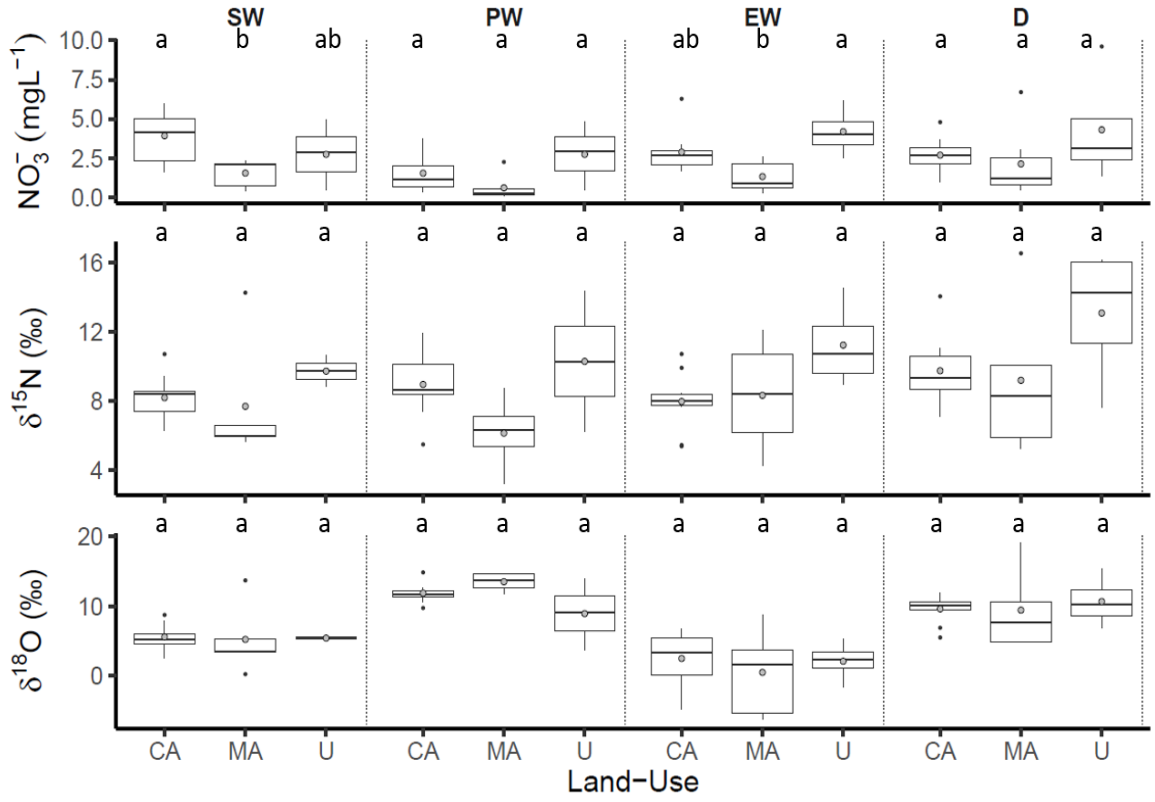

Figure 2.6. Nzoia catchment: Piper trilinear plot of major cations and anions (in percent) for water characterization. Bullets represent land use clusters (see Fig. 2.3 for abbreviations), while colours represent selected sampling seasons (see Fig. 2.2 for abbreviations) (a); spatial temporal plot of mean Cl^- versus NO_3^- mean concentrations with standard deviations given as error bars and bullets represent land use clusters while colours represent seasons as described in (a) above (b); Ranges of NO_3^- concentration, $\delta^{15}N–NO_3^-$ and $\delta^{18}O–NO_3^-$ values obtained for different land use clusters in Nzoia during start of wet (SW), peak wet (PW), end of wet (EW) and dry (D) seasons. Boxplots represent 25th, 50th, and 75th percentiles, whiskers represent 5th and 95th percentiles, black bullets represent outliers, and grey bullets represent mean values. Letters (a, b, c) represent ANOVA output with similar letters indicating non-significant difference ($p>0.05$) using Tukey HSD test (c).

However, CA and MA exhibited similar anion concentration in the EW season which can be attributed to reduced application of inorganic/organic fertilizers because two out of the three main crops (maize and wheat) grown in the catchment are under harvest in this season while only sugarcane (perennial crop) remains in the farms. This is unlike observed in the Nyando catchment where tea and sugarcane (both perennial) are the main crops, and normally under fertilizer application in both PW and EW. U stations displayed $Cl^-+NO_3^-$ as the dominant anion

in all seasons. Generally, the three land uses cluster around the center of the diamond, portraying Ca+Mg–HCO_3, Na+K–HCO_3, Na+K–Cl+NO_3 and Ca+Mg–Cl+NO_3 water types. As earlier mentioned, Ca+Mg–HCO_3 represents soil weathering/natural solute sources while Na+K–Cl+NO_3, Ca+Mg–Cl+NO_3, and Na+K–HCO_3 water types indicates anthropogenic contamination (Ako et al., 2012; Kamtchueng et al., 2016) either of sewage or organic/inorganic fertilizer origin. This implies that sources of ionic constituents in Nzoia catchment have similar contribution to the river mineralization.

A Cl^- versus NO_3^- plot for the Nzoia catchment (Fig. 2.6b) distinctly separates U (EW, D, SW) in a group having high Cl^- with corresponding lower NO_3^- concentration. However, U (PW) recorded relatively lower Cl^- concentrations, which can be attributed to dilution during the peak wet season when the river exhibits high water discharge (Table 2.1). In addition, U stations had relatively high NH_4^+ levels (1.9 – 2.5 mg L^{-1}) compared to CA and MA (< 0.1 mg L^{-1}). The relatively high Cl^- and NH_4^+ concentrations observed in U imply sewage contamination from major urban centers such as Eldoret, a major industrial hub in western Kenya. Just as alluded in several studies (Juma et al., 2014; Marwick et al., 2014; Wang et al., 2012) increase in population density and urbanization in Kenya, in the last two decades, has not been matched with the necessary planning and investment in sanitation infrastructure. This has led to the mushrooming of informal settlements "slums' and industrial hubs which has outstretched the existing sewage networks leading to discharge of raw or incompletely treated sewage into the rivers.

NO_3^- in the Nzoia catchment ranged from 0.1 mg L^{-1} in MA during the PW season to maximum of 9.6 mg L^{-1} in U during the dry season (Fig. 2.6c). CA and U recorded higher NO_3^- concentration in the SW and EW seasons respectively, but similar NO_3^- concentration was observed across the catchment in the PW and D seasons. The $\delta^{15}N–NO_3^-$ values ranged from +3.2‰ to +16.5‰ showing no significant difference in the catchment. However, the relatively higher $\delta^{15}N–NO_3^-$ values obtained in U (PW and D seasons) confirm sewage as the main source of the river NO_3^-, in agreement with hydro chemical findings (Fig. 2.6b). $\delta^{18}O–NO_3^-$ values in

the catchment are similar and generally lie in the nitrified N source range of -10‰ to +15‰ (Kendall et al., 2007; Mayer et al., 2001). However, the relatively higher $\delta^{18}O–NO_3^-$ values obtained during the PW season in CA and MA suggest increased inorganic fertilizer contribution during the wet cropping season, an observation which also agrees with hydrochemistry (Fig 2.6a).

2.3.2.4 Sondu Miriu catchment

In the Sondu Miriu catchment, alkali metals (Na^+, K^+) dominated over the alkaline earth metals (Fig. 2.7a), with Mg values below detection limit during the wet seasons (PW, EW). On the other hand, $Cl^-+NO_3^-$ were the dominant anions, therefore, giving $Na+K–Cl+NO_3$ as the main water type in Sondu Miriu catchment. An increase in $Cl^-+NO_3^-$ concentration was observed during PW season across the land uses with TU giving the highest $Cl^-+NO_3^-$ levels, an indicator of increased inorganic fertilizer contribution during the wet season and especially in the commercial tea farms. Given the main land use in this catchment was tea farming, it implies that the ammonium based inorganic fertilizer (NPK, 25:5:5+5S) which is the most commonly applied in tea farming contributes significantly to the $Na+K–Cl+NO_3$ water type, and has a higher influence during the wet seasons. The Cl^- versus NO_3^- plot (Fig. 2.7b) of the Sondu Miriu catchment, clearly separates TU in a group with high NO_3^- content without matching high Cl^- concentration. TU land use consisted of a zone covering approximately 20,000 ha under commercial tea plantation, which practiced aerial fertilizer application with an annual application rate of 38 – 63 kg N ha^{-1} (Jacobs et al., 2017). Hence, the relatively high NO_3^- levels corresponding to low Cl^- concentration observed in TU was due to the ammonium based NPK fertilizer type (25:5:5+5S) used whose potassium (K) form is $K(SO_4)_2$ and not potash (KCl).

NO_3^- in the Sondu Miriu catchment ranged from a minimum of 1.5 mg L^{-1} in T during the SW season to a maximum of 8.0 mg L^{-1} (Fig. 2.7c) in TU during the PW season. TU recorded generally higher NO_3^- levels in all seasons, while MA and T had similar concentrations in all but the SW season when T recorded the lowest concentration. This can be attributed to the

higher rate of inorganic fertilizer application in the commercial tea estates of the TU (38 – 63 kg N ha^{-1}) compared to the small scale tea farms of the T land use (13 – 30 kg N ha^{-1}), and mixed farms (MA) where animal manure is commonly applied (Jacobs et al., 2017). On the other hand, $\delta^{15}N–NO_3^-$ values in the Sondu Miriu catchment ranged from +2.8‰ in T to +9.6‰ in TU with MA giving significantly higher mean $\delta^{15}N–NO_3^-$ values during the PW and D seasons. The $\delta^{18}O–NO_3^-$ values ranged from +2.2‰ in T to +13.7‰ in MA. $\delta^{18}O–NO_3^-$ values in Sondu Miriu catchment were similar in all seasons except during the D season when TU gave significantly high values.

Given that MA land use of this catchment is characterized by rural residences purely lacking conventional sanitation infrastructure and free ranch livestock keeping, the higher $\delta^{15}N–NO_3^-$ values obtained during PW and D seasons (mean: +8.2‰ and 8.7‰, respectively) reveal increased river NO_3^- input from animal manure and domestic sewage sources. The high NO_3^- concentration reported in TU in all seasons supports hydro chemical observations (Fig. 2.7b) that the ammonium-based fertilizer 'NPK' commonly used in the commercial tea estates dominates river NO_3^- input. Sondu Miriu catchment generally portray a Na+K-Cl+NO_3 water type and lower $\delta^{15}N–NO_3^-$ values (relative to Nyando and Nzoia), implying that inorganic fertilizers are more dominating sources of river NO_3^-in the catchment. This agrees with Jacobs et al. (2017) who observed that land use strongly affects river NO_3^- in the Sondu Miriu River catchment. The authors also observed that river NO_3^- in land use areas, dominated by commercial tea plantations had higher NO_3^- concentrations than natural forest areas.

(a)

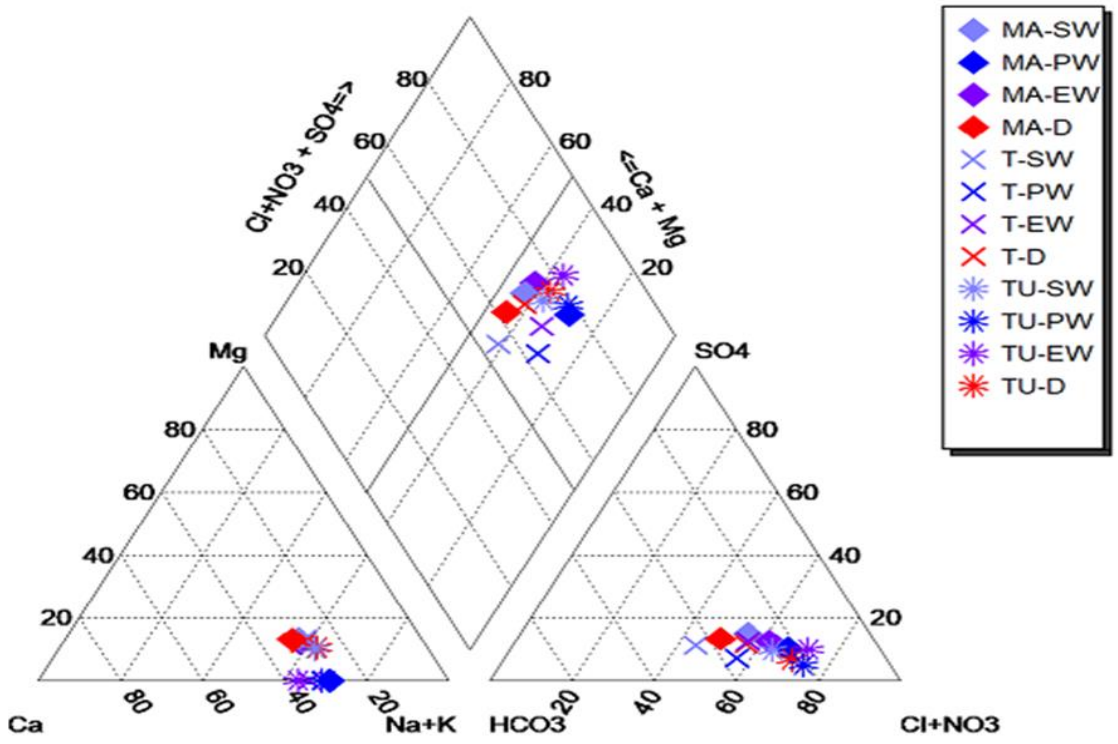
MA-SW
MA-PW
MA-EW
MA-D
T-SW
T-PW
T-EW
T-D
TU-SW
TU-PW
TU-EW
TU-D
Cl+NO3 + SO4=>
<=Ca + Mg
Mg
SO4
Ca
Na+K
HCO3
Cl+NO3

(b)

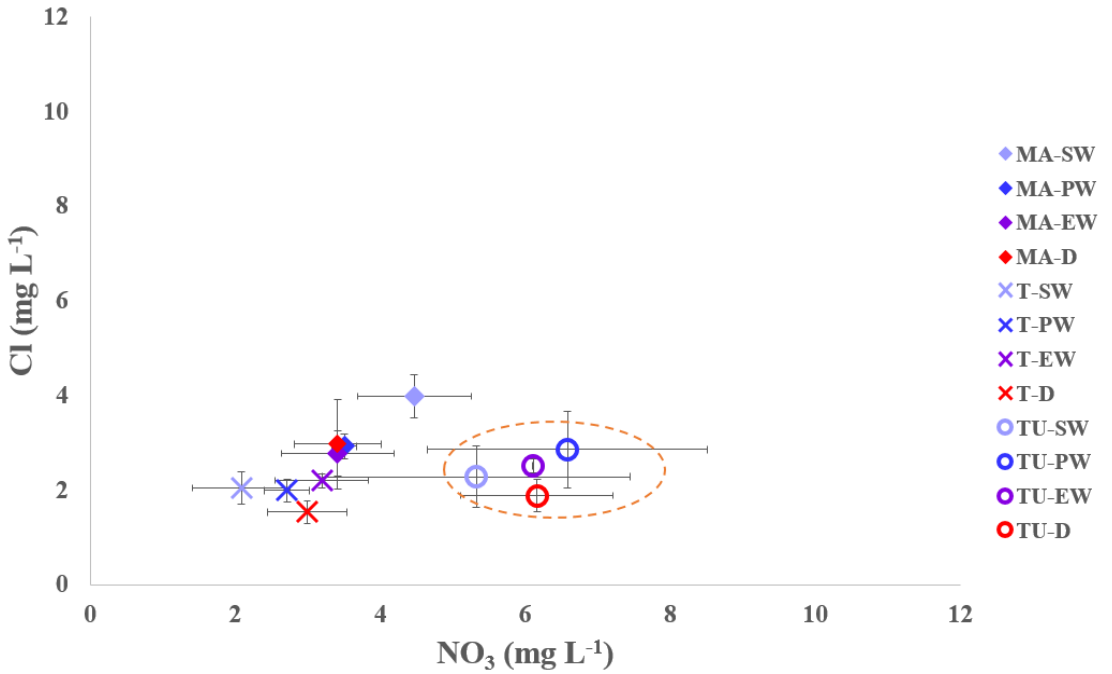
Cl (mg L-1)
NO3 (mg L-1)
MA-SW
MA-PW
MA-EW
MA-D
T-SW
T-PW
T-EW
T-D
TU-SW
TU-PW
TU-EW
TU-D

(c)

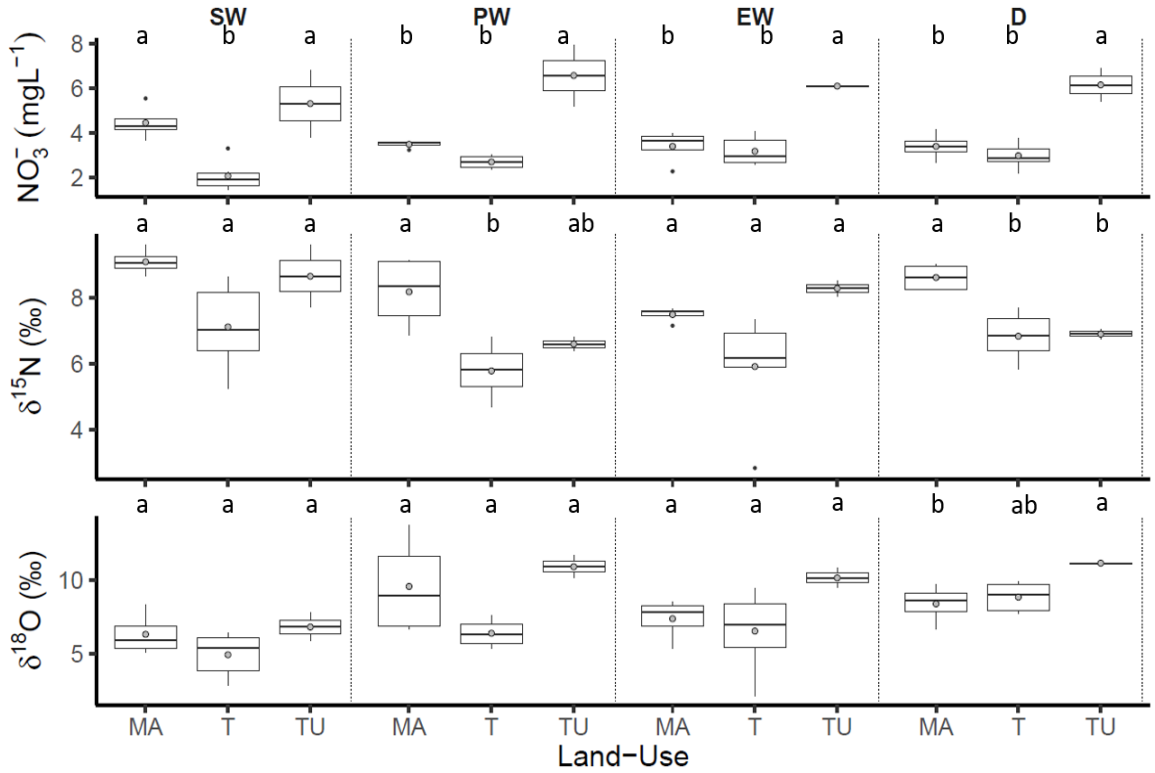

Figure 2.7. Sondu Miriu catchment: Piper trilinear plot of major cations and anions (in percent) for water characterization. Bullets represent land use clusters (see Fig. 2.3 for abbreviations), while colours represent selected sampling seasons (see Fig. 2.2 for abbreviations) (a); spatial temporal plot of mean Cl^- versus NO_3^- mean concentrations with standard deviations given as error bars and bullets represent land use clusters while colours represent seasons as described in (a) above (b); Ranges of NO_3^- concentration, $\delta^{15}N–NO_3^-$ and $\delta^{18}O–NO_3^-$ values obtained for different land use clusters in Sondu Miriu during start of wet (SW), peak wet (PW), end of wet (EW) and dry (D) seasons. Boxplots represent 25th, 50th, and 75th percentiles, whiskers represent 5th and 95th percentiles, black bullets represent outliers, and grey bullets represent mean values. Letters (a, b, c) represent ANOVA output with similar letters indicating non-significant difference ($p>0.05$) using Tukey HSD test(c).

Denitrification enrichment factors, ε, obtained from laboratory incubation of Sondu Miriu river sediments (Fig. 2.5) were -11.9‰ (wetland), -22.3‰ (MA1), and -29.7‰ (TU2). These values are within the range of laboratory derived $\delta^{15}N$ enrichment factors for denitrification reported by Wells et al. (2019). However, possible reason for variability in enrichment factors for denitrification amongst the sediments is difference in temperature or the organic carbon (electron donor) to nitrate (electron acceptor) ratio (Dhondt et al., 2003; Wells et al., 2019). Denitrification rate is assumed to have controlling influence on the enrichment factor, and also

denitrification is a first order reaction where low rates (caused by low quantity of electron donor) result into larger fractionations while high rates (high temperatures or high electron donor content) result into smaller fractionations (Mariotti, A; Germon, J; Lecrerc, 1982). For the current study, there was no temperature variation in the experiment (room temperature: 20°C), therefore, lower fractionations observed in the wetland sample is due to its higher carbon: nitrate ratio (Table A4). It is therefore likely that, denitrification is contributing to the relatively lower NO_3^- and enriched isotopic values obtained in these sections of the Sondu Miriu catchment. However, NO_3^- uptake by wetland vegetation (Dhondt et al., 2003; Lund et al., 1999) is the other potential NO_3^- reduction mechanism taking place in the study area.

Although river NO_3^- data in the Lake Victoria (Kenya) basin are limited, NO_3^- levels obtained in this study are higher than those available in literature for Kenyan river catchments in the basin: 1.3–7.2 mg L^{-1} (Jacobs et al., 2017), 0.16–0.38 mg L^{-1} (Nyairo et al., 2015), 5.3±1.3 mg L^{-1} (Kipkemboi et al., 2014), 0.8–1.0 mg L^{-1} (Okungu and Opango, 2004). Therefore, a clear indication of increasing NO_3^- concentration and discharge into Lake Victoria appears, which confirms the significant contribution of river catchments to the eutrophic conditions prevailing in the lake. From findings of this study, it appears that increasing river NO_3^-concentration in the basin is driven largely by manure losses from mixed agriculture, untreated sewage effluent (domestic and urban) discharges and inorganic fertilizer losses from commercial agriculture.

2.4 Conclusions

Physicochemical data of water from major river catchments in the Lake Victoria basin, Kenya, allowed clear separation and clustering of river water sampling stations corresponding to major land use classes of the catchments. The NO_3^- levels observed in this study are higher than those reported in preceding studies, indicating increasing NO_3^- concentrations in surface waters of the basin. In addition, our findings show that sources of NO_3^- and solute discharge in the river catchments vary with land use and seasons. Inorganic fertilizers and soil N are the main sources of riverine NO_3^- input in the predominantly tea growing land uses of Sondu Miriu and Nyando

river catchments, while both sewage and inorganic/organic fertilizers dominate in the mixed agriculture areas of the three catchments. The more urbanized areas (U, RI) displayed sewage as the dominant source of river NO_3^- input. Seasonally, inorganic/organic fertilizer losses dominate river NO_3^- input during the wet cropping season in the three catchments. However, laboratory derived $\delta^{15}N$ enrichment factors for river bed sediments are consistent with a potential active denitrification process, which could explain significantly low NO_3^- concentrations observed in the S and RI land use areas of the Nyando catchment (SW, D seasons) together with the relatively lower NO_3^- levels reported in Sondu Miriu catchment, but at the same time bias source apportionment. It's recommended that a future sampling and water quality monitoring network in the basin should be designed to capture the major land use patterns: sugarcane, tea, mixed agriculture, residential/industrial, urban and forests. A land-use based monitoring network will reduce the number of sampling stations and field costs. It also simplifies pollution control measures by focusing mitigating efforts on specific pollution impacts from each land use activity. To mitigate the increasing NO_3^- concentration trend, sewage and effluent collection and treatment facilities should be upgraded and extended to cover all urban, residential, and agricultural areas. In addition, soil fertility levels and other precision agricultural practices should be established in the basin in order to develop optimum fertilizer application rates for maximizing crop yields while at the same time minimizing nutrient losses into the rivers.

Chapter 3. Nitrate source apportionment in the complex Nyando tropical river basin in Kenya

This chapter has been submitted for publication and is undergoing review as

Nyilitya, B., Mureithi, S., Bauters, M., Boeckx, P. Nitrate source apportionment in the complex Nyando tropical river basin in Kenya. Journal of hydrology

Abstract

Excess nitrate (NO_3^-) discharge into fresh water resources poses detrimental effects on ecosystems and human health, yet the understanding of its potential sources is lacking in many parts of Sub-Saharan Africa. This study integrated hydrochemistry, multi-isotope tracers ($\delta^{15}N–NO_3^-$, $\delta^{18}O–NO_3^-$, $\delta^{11}B$) and a Bayesian mixing model (mixSIAR) to improve on the apportionment of multiple NO_3^- sources in the Nyando River basin of Lake Victoria, Kenya. River water was monitored spatially in the basin for hydro-chemical and isotopic parameters from July, 2016 to May, 2018. The data shows that NO_3^- concentrations in the basin are governed by the predominant land use. Mixed agriculture (MA) land use recorded significantly higher NO_3^- concentrations (8.8±10.6 mg L^{-1}), compared to other land use zones: residential & industrial (RI) 3.4±2.2 mg L^{-1}, sugarcane (S) 3.2±1.5 mg L^{-1} and tea & forest areas (TF) 3.0±1.1 mgL^{-1}. Stable isotope data and hydrochemistry complemented each other in identifying the potential NO_3^- sources and their spatial-temporal variation in the basin. Boron isotope ($\delta^{11}B$) data was categorically helpful in overcoming the limitations of $\delta^{15}N$-, $\delta^{18}O–NO_3^-$ to discriminate between manure and sewage sources. $\delta^{11}B$ specifically identified manure as the dominant source of river NO_3^- input in the MA, RI and S land use zones and also indicated soil N as the main river NO_3^- source in the TF land use. These findings were substantiated via nitrate source apportionment using a Bayesian isotopic mixing model which showed manure and/or sewage were the leading sources of river NO_3^- input in the basin, contributing 70% (MA), 65% (RI), 60% (S) and 46% (TF). Soil N ranked second with its highest proportional river NO_3^- contribution of 41%, recorded for the TF land use, followed by 29% (S), 24% (RI) and 18% (MA). Ammonium in fertilizers and/or rain was third contributing about 10% NO_3^- for all land uses, while NO_3^- fertilizers showed 1- 2% contribution across the basin. Nitrate in precipitation was the least NO_3^- source, contributing <1% across the basin. In order to control excess NO_3^- discharge in the basin, better guidelines for animal manure use, land conservation measures and improvement of sanitation systems should be prioritized.

Keywords: Nitrate apportionment, Nyando, River basin, stable isotopes, mixSIAR,

3.1 Introduction

Tropical catchments are being subjected to increasing population growth, urbanization, and increasing intensification of agricultural practices. It raises concern on nitrate (NO_3^-) pollution in river systems. The negative impacts associated with excess NO_3^- discharges in water bodies include eutrophication, proliferation of aquatic weeds and algal blooms, and consequently it causes the decline of local fish population and general disruption of aquatic ecosystems. Additionally, high NO_3^- levels in drinking water pose high risks to human health in form of both methemoglobinemia in infants (blue baby syndrome) and cancer (Kendall et al., 2007; Schullehner et al., 2018). As such, the World Health Organization (WHO) has defined 50 mg L^{-1} NO_3^- in potable water as the maximum concentration threshold.

An increasing demand for feeding a growing population has led to a sharp rise in agricultural production, and also the use of nitrogen (N) based compounds (inorganic/organic fertilizers) to boost agricultural production (Galloway et al., 2008). Therefore, the distribution and adoption of N-based inorganic fertilizers are becoming more common in the Sub-Saharan African (SSA) region, where traditionally animal manure was the main agricultural input for soil fertility improvement. The increase in N production and distribution, if not controlled, results in detrimental impacts on the receiving ecosystems. The situation in the SSA region is exemplified in the Lake Victoria basin, where insufficient sewage treatment systems and human encroachment of forests and wetlands result in elevated discharges of NO_3^- into surface water resources (Raburu et al., 2012; Wang et al., 2012).

Given the diverse nature of NO_3^- sources on a catchment scale, identification of the key NO_3^- sources becomes a prerequisite for effective NO_3^- control interventions. The Nyando River is one of the major rivers draining into Lake Victoria, the largest fresh water lake in Africa. River Nyando drains the Kenyan side of the Lake Victoria basin and is subjected to a variety of human-related pressures. It drains a diverse land use pattern including forests (pristine and planted), agricultural areas (commercial, mixed farming of crops and livestock), residential areas, urban and industrial centers and a wetland. Its headwater catchments are located in the

Mau forest complex, a major water tower of the Lake Victoria basin which experiences severe deforestation and human encroachment. For instance, it has been reported that about 7,084 ha of Mau forest land was cleared between the years 2000 and 2003 (LVBC, 2007). This triggers accelerated run-off in the upstream steep gradient areas during rain events, resulting in severe soil erosion and sediment deposition into Lake Victoria (ICRAF, 2003; Olang and Fürst, 2011).

Additionally, commercial tea farming dominates the upstream (Tinderet), while the midstream and the low lands of the Kano plains are under commercial sugarcane and rice farming where inorganic fertilizers are commonly applied (Maghanga et al., 2013; Twesigye, 2011). Mixed farming of food crops, sugarcane, and free-range livestock keeping is highly practiced in the river basin. Concurrently, the basin has a high population density, fast growing urban centers (Londiani, Muhoroni, Awasi, Ahero) and industries including sugar, agrochemical , rice, lime and cement production factories. Most of these urban centers lack conventional sewage treatment infrastructure while the industrial waste treatment facilities operate below capacity and often discharge untreated effluents into the Nyando river (Juma et al., 2014; LVEMP, 2005). On the other hand, the Nyando wetland at the river mouth, which acts as a natural nutrient pollution buffer zone to the lake, has been extensively reclaimed and converted into farmland and livestock feeding area (Raburu et al., 2012). Overall, the basin is a complex matrix of human land use systems, which all potentially impact the river chemistry and NO_3^- loads in their own way.

However, NO_3^- data from the river basin is highly limited, with an available study by Triest et al. (2012) reporting data only at a sub-basin scale. The Lake Victoria Basin Commission (LVBC) through its Lake Victoria Environmental Management Project (LVEMP) used to run a basin-wide water quality monitoring program in the period between 2000 and 2005 and generated a comprehensive nutrient dataset in terms of total nitrogen (TN) and total phosphorus (TP) (LVEMP, 2005). However, since that period, there has been an information gap in terms of N data from the LVEMP, and its activities are currently focused on intervention strategies to control pollution. But still, the available TN data is limited to be relied on for the

development of effective NO_3^- pollution control measures because NO_3^- is the main form of N associated with eutrophication and the causing of health-related risks (Kendall et al., 2007). Indeed, for a basin with a diverse land use and anthropogenic interferences like the Nyando, conventional hydrochemistry is insufficient neither for identifying the potential sources of river NO_3^- contamination nor for estimating the source contributions. Consequently, this hinders proper knowledge-based management guidelines to be introduced.

Therefore, an effective apportionment of NO_3^- pollution of the Nyando basin requires a land use-based understanding of the dominating NO_3^- sources and their associated contributions to the catchment level NO_3^- loads. Many studies have demonstrated the applicability of the dual isotopes of NO_3^- ($\delta^{15}N$, $\delta^{18}O$) and boron (B) ($\delta^{11}B$) to identify and apportion NO_3^- sources in water (e.g. Widory et al., 2013; Xue et al., 2009). Different NO_3^- sources (i.e. atmospheric N, soil N, mineral fertilizers, manure, and sewage) have distinguishable N ($\delta^{15}N$) and oxygen ($\delta^{18}O$) isotope signatures. However, N transformation processes (nitrification, denitrification) and mixing of several NO_3^- sources alter this signature of isotopes in NO_3^-, consequently complicating apportionment of NO_3^- sources. However, B is ubiquitous in nature and its isotope composition ($\delta^{11}B$) is largely not affected by NO_3^- transformation processes, except perhaps during adsorption-desorption interactions with clay minerals, iron and aluminum oxide surfaces (Bassett et al., 1995; Vengosh et al., 1994). In addition, $\delta^{11}B$ discriminates between manure and sewage sources, and therefore, can be used to improve source identification where mixing and transformation processes are involved (Widory et al., 2004). Consequently, the value of integrating $\delta^{15}N$-, $\delta^{18}O$-NO_3^- and $\delta^{11}B$ data in determining NO_3^- sources and associated transformation processes has been recently demonstrated (Nyilitya et al., 2020a; Widory et al., 2013; Xue et al., 2013). In addition, researchers have developed and applied an isotopic mixing model, mixSIAR, which uses a Bayesian framework to quantify proportional source contributions and determines the probability distribution for the proportional contribution of each source to the mixture (Matiatos, 2016; Parnell et al., 2010; Xue et al., 2012).

Therefore, this study integrates a multi isotope ($\delta^{15}N$-, $\delta^{18}O$–NO_3^-, $\delta^{11}B$), hydrochemical and mixSIAR approach to identify and apportion potential sources of NO_3^- input into the River Nyando. The state-of-the-art approach in a river catchment is the first of its kind in the region and should significantly contribute to the development of effective NO_3^- pollution control measures in the river basin.

3.2 Material and methods

3.2.1 Study area

The Nyando river basin lies between longitudes 34º47”E and 35º44”E, and latitudes 0º07”N and 0º20”S (Fig. 3.1b). It is 153 km long, originates from the Mau and the Nandi escarpments and drains an area of about 3,600 km^2 before its discharge into the Winam gulf of Lake Victoria. The altitude in the basin varies from 1134 m a.s.l at the Lake Victoria to about 3000 m a.s.l in the Mau and Nandi escarpments. The escarpment areas have a steep sloping topography with a slope ranging between 19–43º, while the lowlands in the Kano plains have a subdued topography and a slope of 0–4º. The Kano plain is a gently undulating alluvial plain (ranging 1135 – 1170 m a.s.l) at the base of the escarpments and occupies two-thirds of the lower half of the Nyando river basin (Raburu et al., 2012). The Nyando wetland is situated at the river mouth and along the shores of Lake Victoria covering an area of about 14.4 km^2 (Raburu et al., 2012).

The basin has a tropical moist climate, ranging from humid in the highlands to sub-humid in the low-lying Kano plains near the Lake. It experiences a bi-modal rainfall pattern with a long rain season occurring between March – July, while a short rain season occurs between September – November. The mean annual rainfall ranges from 1100 to 1600 mm with the upper reaches of the basin receiving higher amounts as compared to the middle and lower reaches. Mean annual minimum and maximum temperature are 16 and 29°C, respectively. The spatial variation in climate is attributed to altitude, proximity to the highlands and nearness to the

lakeshore. Soils in the highland areas consist of high silt and clay-containing soils (Ferrasols, Nitisols, Cambisols) while the lowlands have mainly alluvial soils which are highly vulnerable to soil erosion during the wet seasons (Olang and Fürst, 2011).

The river consists of two main tributaries: the Ainapngetuny, which originates from the Nandi hills; and the Kipchorian which originates from the Mau forests upstream of Londiani (Fig. 3.1b). The long-term annual average discharge of the Nyando river (based on river discharge data from the year 1950 to 2000) has been reported to be 18 $m^3 s^{-1}$ with peak discharges normally witnessed in April or early May (COWI, 2002). The basin has a diverse land use ranging from pristine and planted forests, commercial tea and sugarcane, mixed agriculture (food crops, cash crops), free range animal keeping, human settlements, industries and urban centers.

(a)

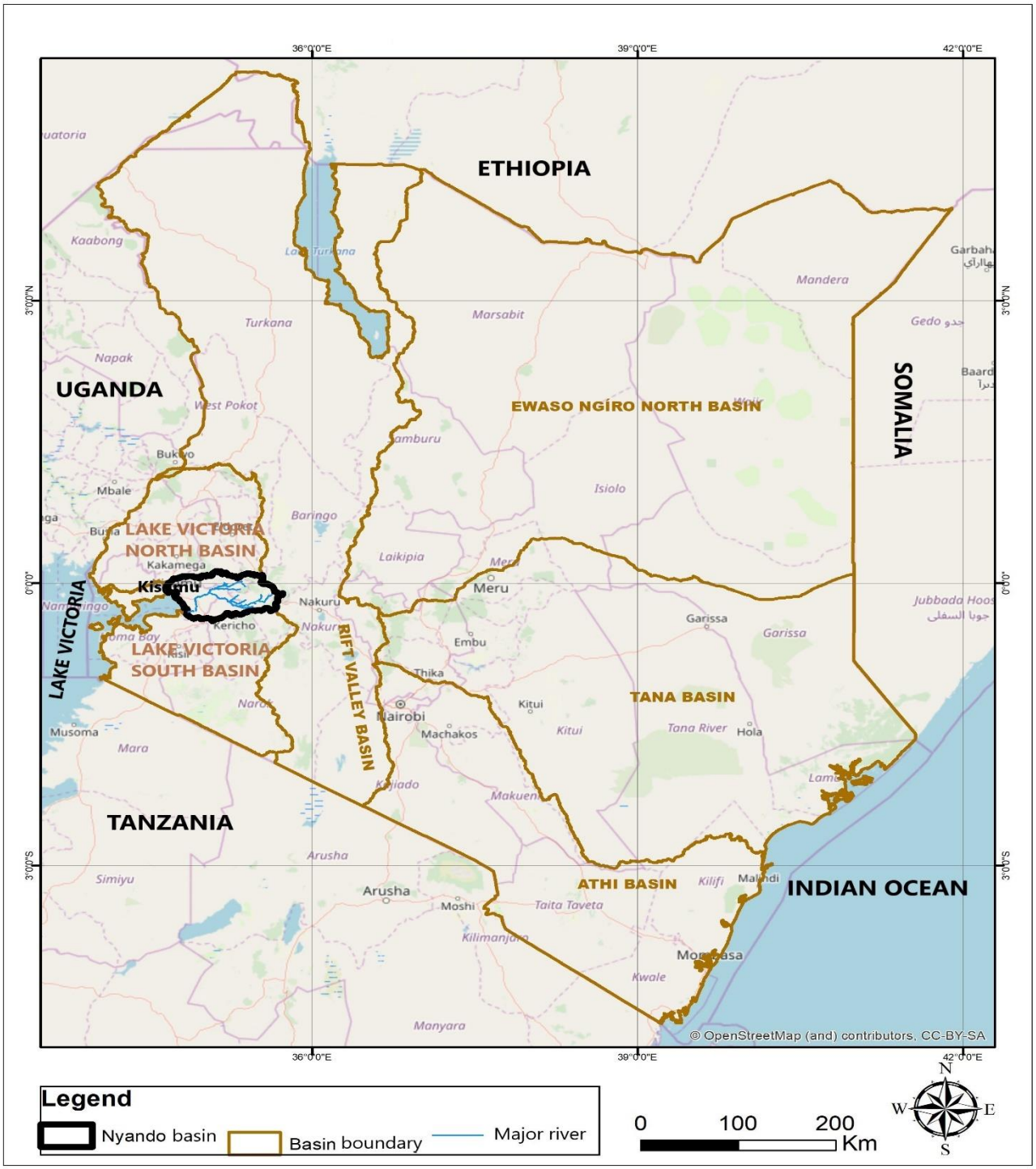
ETHIOPIA
UGANDA
SOMALIA
TANZANIA
INDIAN OCEAN
EWASO NGÍRO NORTH BASIN
LAKE VICTORIA NORTH BASIN
LAKE VICTORIA SOUTH BASIN
RIFT VALLEY BASIN
TANA BASIN
ATHI BASIN
LAKE VICTORIA
Kisumu
Nairobi
Nakuru
Meru
Mombasa
Arusha
Garissa
Kitui
Machakos
Embu
Thika
Kericho
Kakamega
Mbale
Musoma
Moshi
Malindi
Kilifi
Hola
Lamu
Marsabit
Isiolo
Turkana
Laikipia
Baringo
Mandera
Garbah
Gedo
Baard
Jubbada Hoos
Tana River
Taita Taveta
Kwale
Simiyu
Mara
Manyara
Kaabong
Napak
West Pokot
Samburu
Kajiado
Makueni
36°0'0"E
39°0'0"E
42°0'0"E
3°0'0"N
0°0'0"
3°0'0"S
© OpenStreetMap (and) contributors, CC-BY-SA
Legend
Nyando basin
Basin boundary
Major river
0
100
200
Km
N
S
E
W

(b)

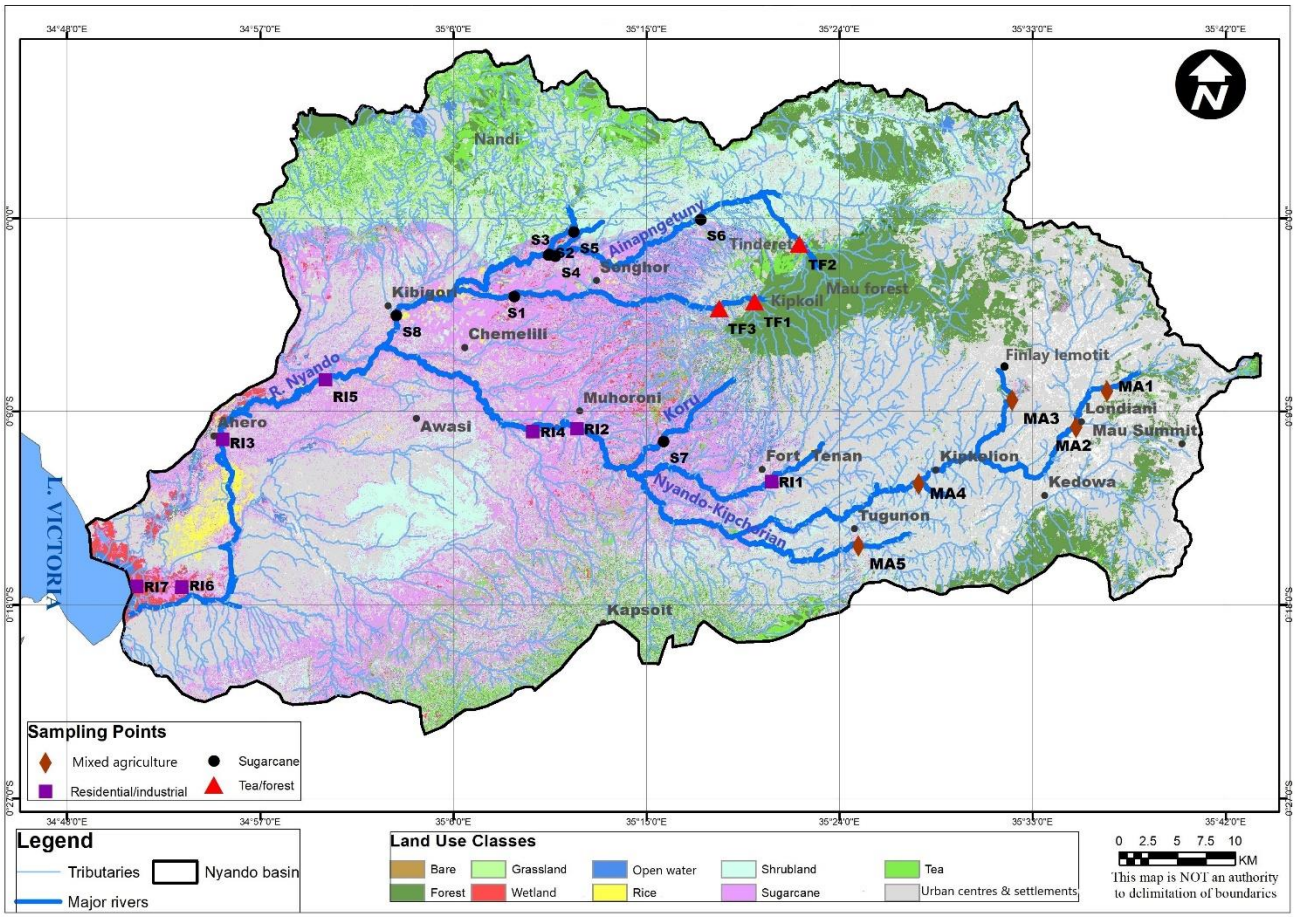

Figure 3.1. Map of Kenya with location of the Nyando basin in the Lake Victoria South basin, Kenya (a); Land use map of the river Nyando basin with spatial sampling stations indicated by bullets and labelled based on the main land use patterns, MA1–MA5: Mixed agriculture, RI1–RI7: Residential and Industrial, S1- S8: Sugarcane, TF1–TF3: Tea and Forest (b)

3.2.2 Sampling and analysis

For an effective basin-wide study in the Nyando River, spatially distributed sampling stations were identified along the main river and its tributaries and covering the key land use zones of the basin. In consultation with the Kisumu-based Water Resources Authority (WRA), a total of 23 sampling stations were set up covering pristine (Kipkoil) forest, commercial tea and sugarcane estates, horticulture, mixed agricultural areas (crops and livestock keeping), industrial and urban centres, wetland and river mouth (Fig. 3.1b). To study seasonal variability in isotopic and hydro-chemical parameters, sampling was conducted during four main seasons

per hydrological year: (1) the transition period between dry and wet season in March, marked as 'start wet' season (SW); (2) the agriculturally productive wet period between May – July, marked as 'peak wet' (PW); (3) during the 'end of the wet season' (EW) in September; and (4) in the dry season (D) in December as described in Nyilitya et al. (2020b). Field sampling was conducted for nine seasons consisting of 2 SW, 3 PW, 2 EW, and 2 D seasons from July 2016 to May 2018.

The sampling stations could be grouped into four clusters corresponding to the main land use classes in the basin. Therefore, the sample point labelling (Fig. 3.1b) is based on the four land use classes, which are: (1) mixed agriculture (MA) consisting of five stations (MA1 – MA5) in the upper reaches of the Kipchorian tributary, (2) residential & industrial (RI) consisting of seven stations (RI1 – RI7) located in the midstream Kipchorian tributary and the downstream reaches of the main Nyando river, (3) sugarcane (S) including eight stations (S1 – S8), seven of them located in the sugarcane belt in the mid – downstream reaches of the Ainapngetuny tributary and one in the Koru tributary, and (4) tea and forests (TF) consisting of three stations (TF1 – TF3) located in the Kipkoil forest and Tinderet commercial tea estates. The clustering was performed by analyzing water physico-chemical data from these stations using hierarchical cluster analysis (HCA) as described in earlier work by Nyilitya et al. (2020b).

In the field, water was taken as a grab sample in 200 mL high density polyethylene (HDPE) bottles, pre-filtered onsite using 11 µm filters (Whatmann, GE Healthcare Life Sciences, Chicago, IL, USA) and stored in an insulated cooler box containing ice cubes for transportation to the laboratory. Duplicate samples for cation analysis were taken in 100 mL HDPE bottles, pre-filtered and acidified to pH 2 using diluted hydrochloric acid. *In situ* measurements included temperature (T), electrical conductivity (EC), pH, dissolved oxygen (DO) and river water discharge measurements. The T, EC, pH, DO were measured in every sampling station using a multi-parameter sensor (2FD47F-Multi3430, WTW, Germany). In addition, the sampling of potential NO_3^- sources (sewage, manure, inorganic fertilizers, precipitation, and soil nitrogen) for the determination of endmember $\delta^{15}N$–, $\delta^{18}O$–NO_3^- and $\delta^{11}B$–B values was

conducted during these campaigns. Sewage effluents were sampled from the inlet point of sewage treatment plants located in major towns (Kisumu, Kericho), sugarcane factories (Muhoroni, Chemelil), agrochemical and lime factories. Manure was sampled from cow, goat and sheep collected from animal droppings in the basin. Inorganic fertilizer samples of the commonly used types (CAN, DAP, NPK, urea) were purchased from farmers and suppliers in the basin. Precipitation samples were collected from rainfall stations in Ahero, Kakamega and Kericho towns, while soil N samples were collected by filtering suspended soil sediments in river water using 11 µm filters (Whatmann, GE Healthcare Life Sciences, Chicago, IL, USA). In the laboratory, all samples were filtered again through 0.45 µm membrane filters and stored frozen (-17°C) awaiting analysis. Laboratory determination of Na^+, K^+, Ca^{2+}, Mg^{2+}, NO_3^-, NO_2^-, Cl^-, and SO_4^{2-} concentrations was carried out using an ion chromatograph (930 Compact IC Flex, Metrohm, Switzerland).

The $\delta^{15}N$– and $\delta^{18}O$–NO_3^- values were determined by the "Bacterial denitrification method" (Casciotti et al., 2002; Sigman et al., 2001; Xue et al., 2009), allowing simultaneous determination of $\delta^{15}N$ and $\delta^{18}O$ in N_2O produced from the conversion of NO_3^- by denitrifying bacteria, which naturally lack N_2O-reductase activity. The $\delta^{15}N$ and $\delta^{18}O$ analyses of the produced N_2O were carried out using a trace gas preparation unit (ANCA TGII, SerCon, UK), coupled to an isotope ratio mass spectrometer (IRMS) (20-20, SerCon, UK). The N_2O sample was flushed out of the sample vial using a double-hole needle on an auto-sampler. Water was removed using a combination of a nafion dryer and $MgClO_4$ scrubber. The N_2O was compressed onto a capillary column (CP-Poraplot Q 25 m, 0.32 mm id, 10 µm df, Varian, US) at 35°C by cryogenic trapping and focusing and subsequently analyzed by IRMS. The subsequent stable isotope data were expressed as delta (δ) units in per mil (‰) notation relative to the respective international standards:

$$\delta_{sample}\ (‰) = \left[\frac{R_{sample}}{R_{standard}} - 1\right] \times 1000 \qquad 3.1$$

Where R_{sample} and $R_{standard}$ are the $^{15}N/^{14}N$ or $^{18}O/^{16}O$ ratio of the sample and the standard for $\delta^{15}N$ and $\delta^{18}O$, respectively. $\delta^{15}N$ values are reported relative to N_2 in atmospheric air (AIR) and $\delta^{18}O$ are reported relative to Vienna Standard Mean Ocean Water (VSMOW). Three internationally recognized reference standards, USGS32 (180.0 ± 1.0‰ for $\delta^{15}N$, 25.7 ± 0.4‰ for $\delta^{18}O$), USGS34 (-1.8 ± 0.2‰ for $\delta^{15}N$, -27.8 ± 0.4‰ for $\delta^{18}O$), and USGS35 (2.7 ± 0.2‰ for $\delta^{15}N$, 56.8 ± 0.3‰ for $\delta^{18}O$), were used to normalize the raw $\delta^{15}N$– and $\delta^{18}O$– NO_3^- values (based on a N_2O reference gas tank) to the AIR and VSMOW scale. USGS32 and USGS34 were used for normalization of the $\delta^{15}N$ value and USGS34 and USGS35 for the $\delta^{18}O$. The amount of NO_3^- in samples and references were matched (i.e. 20 nmol), which corrects for nonlinearity of the IRMS and blanks associated with the procedure. An in-house KNO_3 laboratory standard (9.9‰ for $\delta^{15}N$, 24.3‰ for $\delta^{18}O$) was analyzed together with the samples for quality control. Measurement batches were only accepted if measured $\delta^{15}N$ and $\delta^{18}O$ values of the laboratory standard were within 0.4 and 0.5 ‰ of our accepted values, respectively. If standard deviation on replicate samples was higher than 0.3 and 0.4 for $\delta^{15}N$ and $\delta^{18}O$, respectively, the sample was reanalyzed. This method is well explained by Casciotti et al. (2002) and Sigman et al. (2001).

The water analysis technique for B and $\delta^{11}B$ is well covered by Tirez et al. (2010). Samples underwent a two-step chemical purification using Amberlite IRA-743-selective resin (method adapted from Gaillardet and Allgre (1995)). First, the sample (pH~7) was loaded on a Teflon PFA® column filled with 1 ml resin, previously cleaned with ultrapure water and 2N ultrapure NaOH. After cleaning the resin again with water and NaOH, the purified B was collected with 15 ml of sub-boiled HCl 2N. After neutralization of the HCl with Superpur NH_4OH (20%), the purified B was loaded again on a small 100 ml resin Teflon PFA® column. B was collected with 2 ml of HCl 2N. An aliquot corresponding to 2 mg of B was then evaporated below 70°C with mannitol ($C_6H_8(OH)_6$) in order to avoid B loss during evaporation (Ishikawa and Nakamura, 1990). The dry sample was loaded onto a tantalum (Ta) single filament with graphite (C), mannitol and cesium (Cs). $\delta^{11}B$ values were then determined by measuring the

$Cs_2BO_2^+$ ion (Spivack et al., 1987; Spivack and Edmond, 1986) by a thermal ionization mass spectrometer. The analysis was run in dynamic mode by switching between masses 308 and 309. Each analysis corresponded to 10 blocks of 10 ratios. Samples were always ran twice. Total B blank was less than 10 ng, corresponding to a maximum contribution of 0.2%, which is negligible. Seawater (IAEA-B1) was purified regularly in the same way, in order to check for possible chemical fractionation due to an uncompleted recovery of B, and to evaluate the accuracy and reproducibility of the overall procedure (Gonfiantini et al., 2003). Reproducibility was obtained by repeated measurements of the NBS951, and the accuracy was controlled with the analysis of the IAEA-B1 seawater standard ($\delta^{11}B$=38.6±1.7‰). Similar to N and O, B isotope ratios were expressed in delta (δ) units and a per mil (‰) notation relative to an international standard, NBS951.

3.2.3 Statistical analysis

Tests for spatiotemporal differences/similarities in hydro-chemical and isotopic parameters were done using ANOVA with Tukey (HSD) post hoc test, and $p < 0.05$ significance level was set to test the significance between the datasets.

To estimate proportional contributions of the potential NO_3^- sources, a Bayesian isotope mixing model implemented in R software and known as Stable Isotope Analysis in R (SIAR, mixSIAR version) was used. For a set of N mixture measurements on j isotopes and k sources, the mixing model can be expressed as provided by Parnell et al. (2010):

$$X_{ij} = \sum_{k=1}^{k} p_k\left(S_{jk} + C_{jk}\right) + \varepsilon_{ij} \qquad 3.2$$

$$S_{jk} \sim N(\mu_{jk}, \omega_{jk}^2)$$

$$C_{jk} \sim N(\lambda_{jk}, \tau_{jk}^2)$$

$$\varepsilon_{jk} \sim N(0, \sigma_j^2)$$

Where: X_{ij} is the isotope value j of the mixture i, in which i = 1, 2, 3,….N, and j = 1, 2, 3,…J; S_{jk} is the source value k of the isotope j, k = 1, 2, 3,…K and is normally distributed with a mean μ_{jk} and standard deviation ω_{jk}; p_k is the proportion of source k which needs to be estimated via the SIAR model; C_{jk} is the isotope fractionation factor for the j isotope of k source and is normally distributed with mean λ_{jk} and standard deviation τ_{jk}; and ε_{jk} is the residual error indicating the additional unquantified variation between individual mixtures and is normally distributed with mean 0, and standard deviation σ_j. More detailed explanation of the model is covered by Parnell et al. (2010).

In this study, two isotopes (j = 2: δ^{15}N-, δ^{18}O–NO_3^-) and five local NO_3^- sources (Fig. 3.4a: nitrate fertilizers (NF), ammonium in fertilizer/rain (NF&R), nitrate in precipitation (NP), soil nitrogen (SN), manure and sewage (M&S)) were used. The δ^{15}N-, δ^{18}O–NO_3^- values of locally collected sources were found to be in the literature range reported in Kendall et al. (2007), Mayer et al. (2001) and Xue et al. (2009). The mixSIAR model was applied to estimate proportional source contributions in the four land use areas of the Nyando river catchment in addition to determining seasonal trends in source contributions during the four main seasons (SW, PW, EW, D). Test for normality in the isotopic data of the five NO_3^- sources was done using the Kolmogorov-Smirnov test. The δ^{15}N and δ^{18}O values of the sources were normally distributed except for the δ^{15}N values of M&S sources.

Isotopic fractionations via denitrification in surface water was assumed to be absent (C_{jk}= 0). This is because:

1) denitrification causes exponential increase in δ^{15}N and δ^{18}O (in the ratio 2:1) with corresponding NO_3^- decrease (Fukada et al., 2003; Mayer et al., 2002; Mengis et al., 1999), isotope data in this study show more of a linear relationship between δ^{15}N- (and δ^{18}O) versus NO_3^-; and

2) DO values obtained in this study were sufficiently high (mean range: 6.6 – 7.4 mg O_2 L^{-1}) and not suitable for *in situ* denitrification (Piña-Ochoa and Álvarez-Cobelas, 2006).

3.3 Results and discussion

3.3.1 Hydrochemistry

Table 3.1 presents a statistical summary of hydrochemical and isotopic data obtained in the four main land use classes of the Nyando river basin. Water pH ranged from 5.1–8.7 with most samples showing a neutral to basic pH range (6.8–8.4). Water temperature ranged from 16.4ºC recorded at the high altitude (2200 m a.s.l) station MA1 (Fig. 3.1b) to 28.8 ºC recorded at the river mouth (RI7: 1135 m a.s.l). Dissolved oxygen values mainly ranged between 3.2–9.0 mg O_2 L^{-1}, except for a very low value of 0.1 mg O_2 L^{-1} obtained in the RI4 station. The latter station lies downstream of two factories: Muhoroni sugar company and Agro Chemical & Food company, which have been reported to discharge untreated industrial effluents into the river (LVEMP, 2005). Electrical conductivity (EC), on the other hand, ranged from 114–621 µS cm^{-1} and the majority was in the freshwater range (< 500 µS cm^{-1}).

For the major cations, Na^+ had the highest concentrations across the basin (3.2–47.2 mg L^{-1}) followed by, Ca^{2+} (2.6–7.5 mg L^{-1}), K^+ (1.5–69.4 mg L^{-1}) and Mg^{2+} (0.04–14.4 mg L^{-1}). Anions showed the following order: NO_3^- (0.1–56.3 mg L^{-1}) > Cl^- (0.9–13.3 mg L^{-1}) > SO_4^- (0.3–6.7 mg L^{-1}) > NO_2^- (0.01–0.75 mg L^{-1}). The dominant cation (Na^+) showed a spatial-temporal variation, recording significantly high concentrations ($p < 0.001$) in the MA and RI land uses compared to S and TF. In addition, dry seasons (D, SW) gave significantly high Na^+ ($p = 0.002$) concentrations than the wet seasons (PW, EW). This may indicate that Na^+ input in water is influenced by human activities in the MA and RI areas. This is supported by the Na/(Na+Cl) ratio of the water samples which ranged between 0.6–0.95. Na/(Na+Cl) ratios below 0.5 represents halite or albite dissolution (Zhang et al., 2015). The additional Na^+ source besides the geogenic sources (halite or albite dissolution) could be of anthropogenic nature. Ca^{2+} concentrations, on the other hand, were significantly higher ($p < 0.001$) in the downstream RI and S land uses than in the upstream MA and TF land uses. In addition, the dry seasons had significantly higher Ca^{2+} concentrations ($p < 0.001$) than the wet seasons, while the

Ca/(Ca+SO4) ratio (0.7–0.99) was greater than 0.5, for a single gypsum source. Other probable sources of Ca^{2+}, in this case, would be the geogenic sources, most likely carbonates.

Table 3.1. Summary statistics of hydro-chemical parameters in the four land use classes of Nyando river basin; letters on the land use mean represent ANOVA output with different letters indicating significant difference ($p < 0.05$) using Tukey HSD test

	Mixed agriculture (n=43)			**Residential & Industrial (n=61)**			**Sugarcane (n=67)**			**Tea & Forest (n=26)**		
	Min	**Mean**	**Max**	**Min**	**Mean**	**Max**	**Min**	**Mean**	**Max**	**Min**	**Mean**	**Max**
Na^{+} (mg L^{-1})	8.1	17.4±5.8^{a}	36.6	4.3	19.7±7.8^{a}	47.2	3.2	12.7±4^{b}	20.3	3.4	5.8±1.2^{c}	7.6
K^{+} (mg L^{-1})	3.7	7.2±2.1^{a}	11.4	2.2	9.6±9^{a}	69.4	1.9	4.5±1.3^{b}	9.0	1.5	2.9±1.3^{b}	8.3
Ca^{2+} (mg L^{-1})	2.6	8.7±3.3^{a}	20.5	4.1	13.9±5.5^{bc}	26.2	6.8	14.8±6.8^{b}	47.5	6.2	10.7±2.3^{ac}	15.7
Mg^{2+} (mg L^{-1})	0.0	2.5±1.6^{a}	6.9	1.1	5.2±2.7^{b}	12.8	0.0	7.1±2.8^{c}	14.4	3.6	6.1±1.5^{bc}	9.1
Cl^{-} (mg L^{-1})	1.9	6.2±2.5^{a}	13.3	2.0	4.6±1.4^{b}	12.3	1.4	2.9±0.9^{c}	5.1	0.9	1.7±0.5^{d}	3.2
NO_3^{-} (mg L^{-1})	0.6	8.8±10.6^{a}	56.3	0.1	3.4±2.2^{b}	7.5	0.4	3.2±1.5^{b}	7.4	1.6	3.0±1.1^{b}	5.2
SO_4^{2-} (mg L^{-1})	0.7	3.4±1.4^{a}	6.7	1.0	2.4±0.7^{b}	3.9	0.3	1.3±0.7^{c}	3.8	0.4	1.3±0.5^{c}	2.1
NO_2^{-} (mg L^{-1})	0.01	0.1±0.1^{a}	0.49	0.01	0.14±0.2^{a}	0.71	0.01	0.08±0.1^{a}	0.75	0.01	0.08±0.1^{a}	0.38
pH (–)	5.1	7.4±0.7^{a}	8.6	7.0	8.0±0.3^{b}	8.6	7.2	8.1±0.4^{bc}	8.7	6.9	7.8±0.3^{bd}	8.2
EC (µS cm^{-1})	95	172±47^{a}	299	142	257±96^{b}	621	148	254±59^{b}	424	92.0	154±35^{a}	213
Temp (°C)	14.2	18.2±2.5^{a}	24.0	18.4	23.2±2.4^{b}	28.8	17.5	21.4±1.7^{c}	26.5	15.3	17.1±1.5^{a}	20.8
DO (mg O_2 L^{-1})	5.1	6.8±0.7^{a}	8.2	0.1	6.6±1.5^{ab}	9.1	3.2	7.4±0.9^{ac}	9.0	4.3	7.3±1.1^{a}	8.5

3.3.2 Spatial-temporal NO_3^- concentrations

Figure 3.2 presents seasonal NO_3^- concentration data in each of the land use classes of the Nyando basin. NO_3^- concentrations ranged from 0.1 mg L^{-1}, recorded in RI4 during the dry season of 2016, to 56.3 mg L^{-1} obtained in MA3 during the start of the wet season in 2018. The highest concentrations in the basin were obtained for MA land use in all seasons, with 90% of all MA samples recording NO_3^- concentration above 4.0 mg L^{-1}. The mean NO_3^- concentrations in MA samples were significantly higher than the concentrations in the other land uses: RI ($p < 0.001$), S ($p < 0.001$) and TF ($p = 0.004$). In particular, the MA3 samples recorded peak

values ranging between 23 to 56.3 mg L^{-1} in the different sampling seasons (Fig. 3.2). The MA3 station is located in a stream which drains a commercial horticultural flower farm (Finlay lemotit, Fig. 3.1b) under irrigated greenhouse farming conditions, where NO_3^-- and NH_4^+-based fertilizers (CAN, DAP) are perennially applied (Nyilitya et al., 2020b). However, no seasonal differences in mean NO_3^- concentrations were observed in the MA land use, most likely due to the perennial anthropogenic activities in the area. The MA land use is mainly situated in the upstream part of the Kipchorian tributary (Fig. 3.1b) at an altitude ranging between 1900 – 2300 m a.s.l. It is a highly populated zone and most residents practice mixed farming of food crops (maize, beans, and potatoes) and livestock in small holder farms (< 5 ha), where the use of both animal manure and inorganic fertilizers to maximize yields is common. In addition, sanitation is a major challenge in the area since residences and urban centers in the vicinity (e.g. Londiani, Kipkelion, Fig. 3.1b) lack a formal sanitary system (Nyilitya et al., 2020b).

For RI land use, NO_3^- ranged from a minimum of 0.1 mg L^{-1} to a maximum value of 7.5 mg L^{-1}. Here, significantly lower NO_3^- concentrations were obtained during the dry season, recording an average value of 1.4 mg L^{-1} compared to 4.0, 3.9, and 4.3 for the SW, PW, and EW, respectively (Fig. 3.2). In the downstream part of the Nyando basin which is characterised by residential, industrial and urban areas, the NO_3^- concentration in RI was expected to be high during the study period. However, the dry season NO_3^- values were even lower than the background values. For instance, the average NO_3^- concentration in RI in the December 2016 dry season was 0.4 mg L^{-1}, which was lower than the natural forest sample (TF1) value of 1.9 mg L^{-1} in the same season (see Table A5). This may suggest NO_3^- removal to be taking place. For the S land use, NO_3^- ranged from 0.4 to 7.4 mg L^{-1}. Similar to the RI, significantly lower NO_3^- concentrations in the S land use were recorded during the dry season compared to the other seasons. NO_3^- in the TF land use ranged from 1.5 to 5.2 mg L^{-1}. There were no seasonal differences in NO_3^- concentrations observed in the TF land use, a trend which can be attributed to the relatively low human activities, implying fewer sources of NO_3^- contamination. Generally, the three land uses, RI, S, and TF, had similar NO_3^- concentrations.

Seasonally, both S and TF gave relatively higher NO_3^- concentrations in the wet seasons (PW, EW) than in the dry seasons (SW, D). This is unlike the case observed for the MA and RI land uses, which recorded similar concentrations in the four seasons with the exception of the low NO_3^- values obtained in RI (dry season). Normally, inorganic fertilizers (urea, NPK) are applied in tea and sugarcane plantations during the April – July (PW) and September – November (EW) seasons. This suggests that fertilizer use influences river NO_3^- directly in the S and TF land uses during the wet seasons. Similar studies by Maghanga et al. (2013) in the neighboring Nandi hills, monitored the effect of fertilizer application on NO_3^- concentration in streams, draining tea farms. They observed that fertilizer application contributed to stream water NO_3^- increase and reported higher values ranging between 22–36 mg L^{-1}.

NO_3^- studies done in the Nyando basin are limited to work done by Triest et al. (2012) at sub-basin level located in the RI land use. The study reported NO_3^- concentrations ranging between 1.2 mg L^{-1} in Ahero (RI3) and 2.4 mg L^{-1} measured downstream of Muhoroni (RI4). Their findings were lower than the current mean values obtained in RI for all seasons, except the dry season (Fig. 3.2). In comparison to previous studies in the Lake Victoria basin of Kenya, work done in the Chemosit sub-basin of the Sondu Miriu river basin reported mean NO_3^- concentrations ranging from 1.3±0.4 mg L^{-1} in natural forest to 7.1±2.6 mg L^{-1} in tea and forest plantations (Jacobs et al., 2017). The tea and forest plantation values were higher than the TF values obtained in this study. This can be attributed to the significantly large area occupied by commercial tea farms in the Chemosit sub-basin as compared to the smaller area of tea plantations (Tinderet tea estates) in the TF land use of the Nyando. The Mara river basin in Kenya, which has its origin at the western side of the Mau forest, reported NO_3^- concentrations between 3.5 and 8.5 mg L^{-1} for agricultural land use (Kipkemboi et al., 2014; Masese et al., 2017; Mwanake et al., 2019). The studies in the Mara basin obtained similar values to those obtained for RI and S in the current study but lower than the NO_3^- concentrations in MA. Studies done by Marwick et al. (2014) in the Athi-Galana-Sabaki river basin, draining the central and south-Eastern Kenya, reported similar NO_3^- concentrations (0.01 – 53.2 mg L^{-1})

while studies in the R. Tana in Kenya reports lower NO_3^- concentrations (1.2 ± 1.6 mg L^{-1}) (Bouillon et al., 2009). In comparison to other river basin studies in the sub-Saharan Africa, mean river NO_3^- values obtained in this study are higher than those reported for tropical rivers in Zambia (0.3 – 1.4 mg L^{-1}) (Kennedy et al., 2016), R. Pangani in Tanzania (2.1 – 3.1 mg L^{-1}) (Selemani et al., 2018), and Senegal river in West Africa (0.2 – 0.8 mg L^{-1}) (Mbaye et al., 2016). However, river NO_3^- in this study is in the range of values reported for the Vaal (1.0 – 5.0 mg L^{-1}) (Rensburg et al., 2019) and the Mvudi rivers (1.9 – 8.1 mg L^{-1}) (Edokpayi et al., 2015) of South Africa.

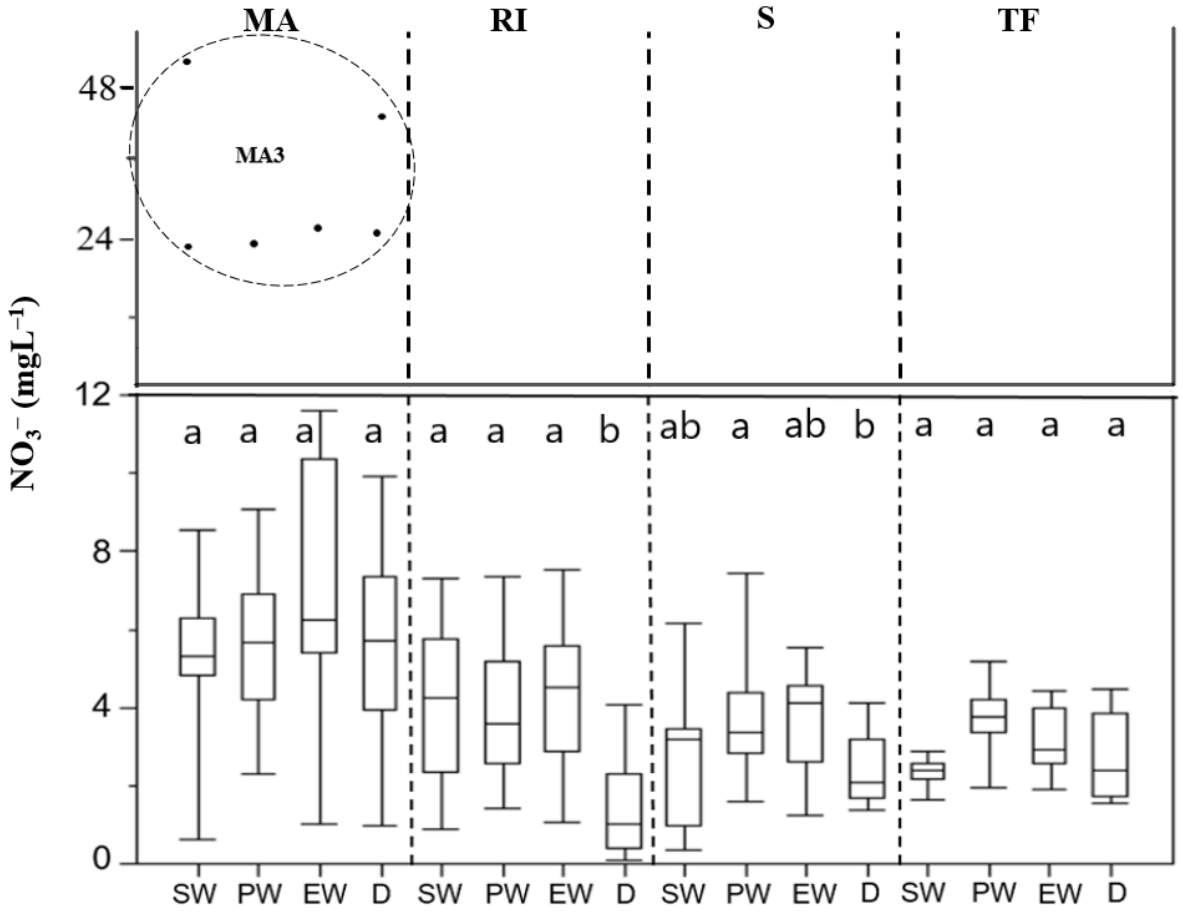

Figure 3.2. Seasonal NO_3^- concentration ranges in mixed agriculture (MA), residential & industrial (RI), sugarcane (S) and tea & forest land use areas of the Nyando river basin; seasons are: start wet (SW), peak wet (PW), end wet (EW), and dry (D), each season contains data from at least two monitoring campaigns (i.e. 2SW, 3PW, 2EW, 2D); letters represent ANOVA output with different letters indicating significant difference ($p < 0.05$) using Tukey HSD test, while dots in the upper part of the broken y-axis represent peak concentrations in the MA3 station

3.3.3 Multi tracer approach in identifying dominant nitrate sources

In this study, NO_3^- and B isotope data were applied in order to improve NO_3^- source apportionment in the different land use classes of the Nyando river basin. NO_3^- isotope values in the basin varied spatially as shown in Fig. 3.3. $\delta^{15}N–NO_3^-$ ranged from 3.8 to 15.1‰ in the basin with values obtained in TF being significantly lower compared to values of the other land uses. The highest $\delta^{15}N–NO_3$ were observed in MA and RI, recording mean values of 10.0 and 9.6‰, respectively. Mean values, ranging 8.7–10‰, obtained in S and MA, respectively, being dominated by agricultural activities, were lower than reported literature ranges for agricultural areas, 11–17‰ (Kellman and Hillaire-Marcel, 2003). However, the $\delta^{15}N–NO_3^-$ values in this study were in the range of similar river basin studies, 4–14‰ (Zeng and Wu, 2015), and 3–15‰ (Yevenes et al., 2016). $\delta^{18}O–NO_3^-$, on the other hand, ranged from -4.5‰ to +19.7‰ and gave similar values in most of the land use areas, except in TF, which recorded significantly lower values compared to the MA land use. $\delta^{18}O–NO_3^-$ values in the basin were in the nitrified NO_3^- range of –10 to +15‰ (Mayer et al., 2001; Xue et al., 2009), except for samples from a stream (MA3), draining a commercial flower farm, which recorded a mean value of 16.2‰ (Table A7).

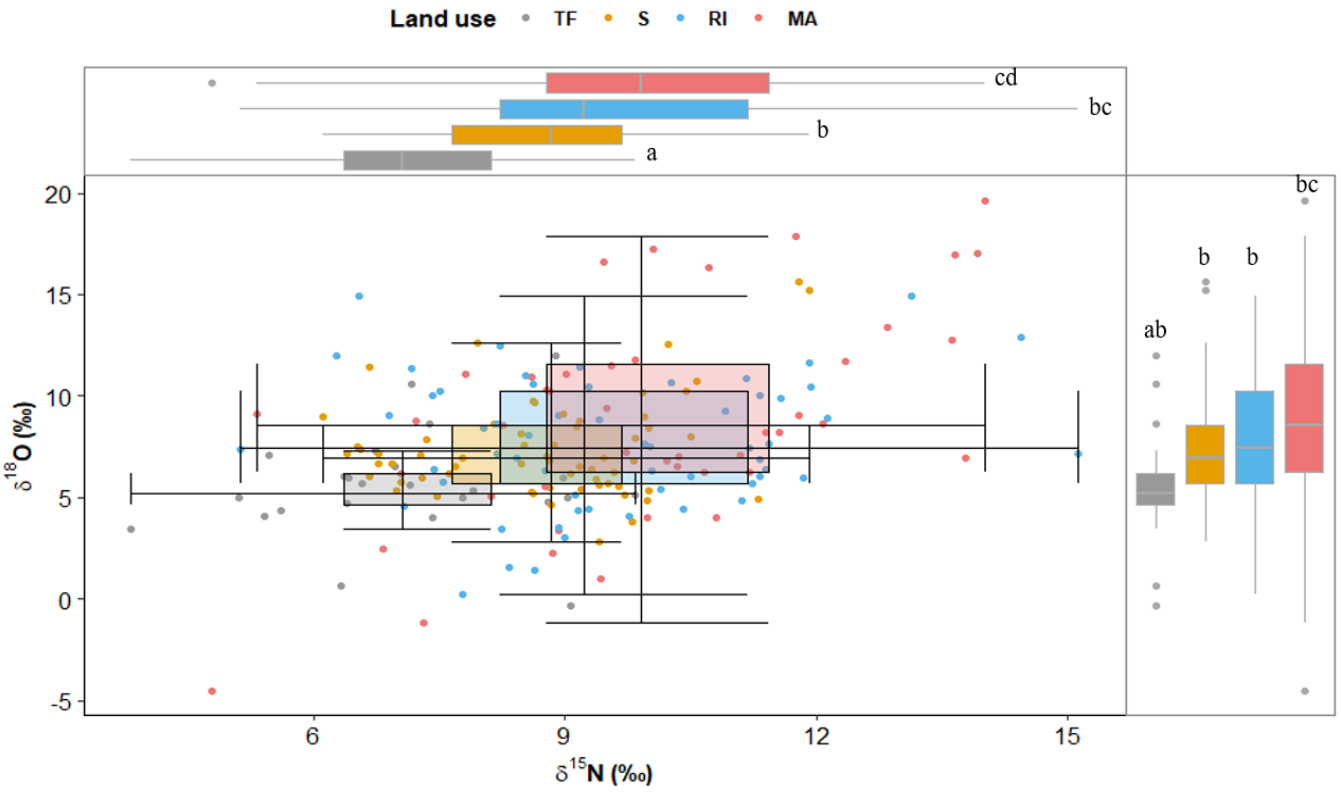

Figure 3.3. $\delta^{15}N$– and $\delta^{18}O$–NO_3^- ranges per land use class (MA, RI, S, TF) of the Nyando river basin; boxplots represent 25th, 50th, and 75th percentiles, whiskers represent 5th and 95th percentiles and dots represent outliers; letters represent ANOVA output with different letters indicating significant difference ($p < 0.05$) using Tukey HSD test

Figure 3.3 reveals a gradual increase in NO_3^- isotopic values from low levels in TF to higher levels in RI and MA; a pattern which indicates an increase in recycled NO_3^-, apparently driven by human activities. This spatial variation also enables the identification of the potential NO_3^- sources controlling these isotopic signatures.

$\delta^{15}N$–, $\delta^{18}O$–NO_3^- values for local NO_3^- sources were also determined. These sources were nitrate fertilizers (NF), ammonium in fertilizer/rain (NF&R), nitrate in precipitation (NP), soil nitrogen (SN), manure and sewage (M&S). As shown in Fig. 3.4a, the $\delta^{15}N$– and $\delta^{18}O$–NO_3^- values of the local sources were found to be within the literature range reported in Kendall et al. (2007), Mayer et al. (2001) and Xue et al.(2009).

On the other hand, composite samples from each land use (different seasons) were analyzed for B and $\delta^{11}B$ values. In addition, these values were also determined for the potential local

NO_3^- sources: manure, sewage and inorganic (solid) fertilizers. The B concentrations of the local NO_3^- sources ranged for the fertilizers (NPK, DAP, CAN) from 15 to 2500 μgL^{-1}, for manure from 127 to 581 μgL^{-1}, and for sewage from 25 to 46 $\mu g\ L^{-1}$. Boron concentrations in the surface water samples ranged from 2 to 14 $\mu g\ L^{-1}$ and were generally low, as also indicated by Tirez et al. (2010). The $\delta^{11}B$ value of fertilizers ranged from -4.3 to +7.8‰, of sewage from 16 to 22‰, and of manure from 31 to 37‰. The $\delta^{11}B$ values obtained in this study fall within the range of values reported in previous studies for inorganic fertilizers: -9 to +15‰ and for animal manure: +6.9 to +42.1‰ (Komor, 1997; Widory et al., 2013, 2005, 2004). However, sewage $\delta^{11}B$ values obtained in this study were higher than values reported in previous studies by Widory et al. (2013).

In Fig. 3.4a, a $\delta^{15}N–NO_3^-$ versus $\delta^{18}O–NO_3^-$ bi-plot of seasonal mean values per land use was plotted against source ranges of the potential local sources. Samples from MA, RI and S plotted predominantly in the manure & sewage source range but showed clear seasonal trends. However, for TF land use, samples plotted mainly in the soil N source range. The TF land use consisted of the Kipkoil forest (a pristine part of the Mau forest complex) and commercial tea farms in Tinderet, which also operate planted forests to supply wood for use in tea processing. Therefore, it seems that leaching of mineralized soil organic N was the main process controlling river NO_3^- input in TF. However, seasonal variation in TF is observed in Fig. 3.4a, whereby during the wet (PW, EW) seasons, samples plotted dominantly in the soil N source. On the other hand, during dry seasons (SW, D), TF samples plotted in the mixed range of soil N and manure & sewage sources. The decrease in soil N in the dry seasons can be attributed to reduced water discharge from the natural forest. In addition, domestic and animal wastes from small scale farmers who border the forest and practice mixed farming of tea, food crops and open grazing of dairy cows, may also contribute to the manure and sewage source observed during the dry seasons. Based on B data (Fig. 3.5), the TF station (F and T) samples had the lowest B concentrations ranging between 2 and 4 $\mu g\ L^{-1}$ being similar to B values (3.3 – 4.4 $\mu g\ L^{-1}$) reported by Widory et al. (2013) for a natural case study. In addition, mean $\delta^{11}B$ values of the

T (35‰) and F (45‰) stations fall in the wider range of $\delta^{11}B$ values, reported for natural environments and rainfall, ranging from 10 to +48‰ (Mather and Porteous, 2001; Millot et al., 2010; Widory et al., 2013). Therefore, the TF values can be taken to represent the natural B and $\delta^{11}B$ value ranges of the Nyando basin, upholding the NO_3^- isotope data indications that soil N (natural) is the main NO_3^- source in this land use.

The MA land use, which reported the highest NO_3^- concentrations (Fig. 3.2), showed relatively enriched $\delta^{15}N$ and $\delta^{18}O$ values (especially in the PW season) and data plotted predominantly in the manure and sewage source range during all seasons (Fig. 3.4a). In particular, MA3 samples (which drain a commercial flower farm) gave significantly high isotopic signatures ($\delta^{15}N$: +9.0 to +14.0; $\delta^{18}O$: +11.1 to +19.6‰) compared to the other samples of the entire basin. Given that the $\delta^{18}O$ values of the station (mean: 16.2±2.5‰) were within the NO_3^- fertilizer source range, it implies that leaching of NO_3^- from inorganic fertilizers applied on farms significantly contributes to river NO_3^- input. In addition, the flower farm has a water pond (see Fig. A1), located upstream of MA3. Therefore, the isotopic enrichment may be caused by *in-situ* denitrification taking place in the pond before water discharge into the river.

NO_3^- versus Cl^- correlation is an effective tool applied to determine mixing or denitrification processes and also useful in indicating anthropogenic sources of water solutes (Mengis et al., 1999; Widory et al., 2005). In the current study, both anions recorded significantly higher values in MA compared to the other land use classes (Table 3.1). However, they did not show any correlation implying that the NO_3^-/Cl^- ratio would not be a good indicator of mixing or denitrification processes in this area. However, the variation of NO_3^-/Cl^- molar ratios with Cl^- concentrations provides more insight to differentiate between inorganic fertilizers, sewage and manure sources of NO_3^- (Li et al., 2010; Liu et al., 2006; Meghdadi and Javar, 2018). In the current study, a plot of NO_3^-/Cl^- molar ratios versus Cl^- concentrations was generated (Fig. 3.4b) for the MA samples together with samples from sewage-contaminated streams in Kisumu city (Fig. 3.1a). Based on Fig. 3.4b, MA3 samples plot together showing a significantly higher NO_3^-/Cl^- ratio but low Cl^- concentrations, which is characteristic of the dominance of inorganic

fertilizers as sources of river water solute input (Liu et al., 2006). On the other hand, most of the other MA stations (MA1, MA2, MA4, MA5), together with the sewage contaminated streams, showed a low NO_3^-/Cl^- ratio, but a relatively high Cl^- concentration. Sewage and animal wastes have been found to be high in Cl^- concentrations and low in NO_3^-/Cl^- ratio (Chen et al., 2009; Liu et al., 2006; Zeng and Wu, 2015). The low NO_3^-/Cl^- ratio in sewage and animal wastes is partly because their nitrogen is more in the NH_4^+ form as opposed to the NO_3^- form (Chen et al., 2009). The MA2 and MA4 stations are located downstream of the Londiani and Kipkelion towns, respectively (Fig. 3.1b), while MA1 and MA5 locations are characterized by populated residences and mixed farming of food crops and free range livestock keeping. This, therefore, indicates that animal manure and/or sewage are the probable sources of river solutes in these four MA stations,

In order to overcome the limitations of $\delta^{15}N$-, $\delta^{18}O$– NO_3^- and hydro-chemistry data in discriminating between manure and sewage sources, the $\delta^{11}B$ analysis was integrated. From Fig. 3.5, B and $\delta^{11}B$ values in MA3 samples were in the natural NO_3^- source range for the Nyando basin. However, both $\delta^{15}N$-, $\delta^{18}O$– NO_3^- and hydrochemical data strongly indicate the inorganic fertilizer source in MA3. In addition, the significantly higher NO_3^- concentrations recorded in the MA3 station than anywhere else in the land use or basin, is consistent with an inorganic fertilizer source (Widory et al., 2013). This implies that both inorganic fertilizers and mineralized organic soil N (natural) are the main NO_3^- sources in MA3. But, *in situ* denitrification taking place in the water pond located upstream of MA3 (Fig. A1) causes isotopic enrichment ($\delta^{15}N$-, $\delta^{18}O$– NO_3^-), consequently blurring the natural source signal in Fig. 3.4a. On the other hand, an increase in B concentration was observed in the other four MA stations which are geographically located downstream of MA3. This means that, apart from background concentrations, B increase in the MA land use is controlled by either manure or sewage sources as opposed to inorganic fertilizer sources. However, the $\delta^{11}B$ values for the MA samples rule out the sewage source, implying that NO_3^- is mainly sourced from manure and/or natural (soil N) sources. Therefore, animal manure use (in small scale mixed farming

and animal feces from free-range livestock keeping) and leaching of mineralized soil organic N are the main sources of river NO_3^- input in these four MA stations.

NO_3^- sources in the sugarcane land use varied seasonally (Fig. 3.4a). During the SW and D seasons, S samples indicated a predominantly manure & sewage source while in the PW and EW seasons, they moved in the direction of NH_4^+ in the fertilizer and rainfall source range. Typically, urea is the most commonly used inorganic fertilizer in the sugarcane plantations (Nyilitya et al., 2020b) and is applied during the wet seasons, and therefore could be the probable cause of the alignment towards the NH_4^+ in fertilizer and rainfall source during PW and EW seasons. However, the dominance of manure & sewage NO_3^- source in this land use is due to domestic and industrial effluents from village residences and the Chemelil sugar industry complex (Fig. 3.1b), which houses a sugarcane factory, farm residences and schools. In addition, the practice of free-range livestock feeding and watering in rivers is common in the area, which leaves animal feces littering around the water points and eventually leaches NO_3^- into the river water. $\delta^{11}B$ data supports these findings and provides a more clear understanding of the seasonal variation in the NO_3^- sources (Fig. 3.5). It shows that sewage sources dominated the SW season, manure was the main source in the D season, while the soil N (natural) was dominant in the PW season.

For the RI land use, Fig. 3.4a shows that manure & sewage sources dominated the river NO_3^- in all seasons except the EW season when samples move in the direction of NH_4^+ in fertilizer and rainfall source range. The RI is a relatively densely populated and urbanized area of the Nyando basin which extends from the midstream of the Kipchorian tributary up to the Nyando wetland and river mouth. The area has industrializing towns including Muhoroni, Awasi and Ahero (Fig. 3.1b) with several industries including sugar, agrochemical, rice, lime, and cement factories. Mainly mixed farming of sugarcane, food crops and free-range livestock keeping are the common agricultural activities in this zone. Small scale farmers commonly use animal manure or sugarcane bagasse (compost manure made from sugarcane wastes) for soil fertility improvement. The urban centers lack formal sewage treatment facilities while effluent

treatment facilities of the sugarcane and allied industries are insufficient and ends up in discharging untreated sewage into the Nyando river (LVEMP, 2005). $\delta^{11}B$ data (Fig. 3.5), on the other hand, shows manure as the main anthropogenic NO_3^- source of river NO_3^- for the RI land use. However, seasonal patterns are evident: during wet seasons, a mixture of manure and natural sources (soil N) dominates, while in dry seasons, manure is the main source but with some level of contribution from sewage sources. This is expected because, as river water discharge declines during the dry season, natural NO_3^- sources from the upstream (TF) catchments decline, while anthropogenic sources (animal manure and sewage) remain constant and act as main sources of river solute inputs. Similarly, Lin et al. (2019) observed the dominance of urban wastewater NO_3^- sources in the upper Illinois River during the dry and low river flow season while agricultural NO_3^- sources dominated during the wet season.

The EW season in all land uses of the Nyando basin showed significantly lower $\delta^{15}N$ values ($p = 0.02$) compared to the other seasons (SW, PW, D) and water samples plotted in the soil N source range (Fig. 3.4a). In the Nyando basin, most food crops take 3 - 4 months to mature. Therefore, during the EW season, they are already harvested. This consequently leaves farm land bare and prone to erosion during this short rain season. In addition, most farmers do not cultivate in this season which means less agricultural inputs. Therefore, it implies that leaching of nitrified soil organic N, which may be enhanced by soil erosion, is the main pathway of river NO_3^- input during the EW season. This is supported by the $\delta^{11}B$ values (Fig. 3.5), in which the EW season samples analyzed for $\delta^{11}B$ (i.e. RI, MA) show values in the natural source range, indicating soil N was the dominant NO_3^- source in the basin in this season.

Therefore, through the integration of $\delta^{11}B$ data into the $\delta^{15}N$-, $\delta^{18}O$– NO_3^- and hydrochemical data, it appears that, manure and soil N (natural) are the dominant sources of river NO_3^- input in the Nyando river basin. However, sewage was the major source in the sugarcane land use during the SW season and also contributed to river NO_3^- in the residential & industrial land use during the D season. The findings in this study, to a much extend agrees with similar work in tropical river basins (Anornu et al., 2017; Minh et al., 2020). The study by Minh et al. (2020)

in the Day river basin of Vietnam reported the dominance of natural NO_3^- sources (i.e. soil and clean groundwater) in upstream catchments, dominance of sewage/manure in the midstream sections (discharging Hanoi city) especially in the dry season, while mineral fertilizers (urea) were the main NO_3^- source in the basin during the wet season. This is similar to the current spatiotemporal variations in NO_3^- sources observed in the Nyando basin. The study by Anornu et al. (2017) in the White Volta river basin in Ghana, identified animal manure and domestic sewage as the primary sources of NO_3^- contamination into surface water, which is similar to our study observations. This trend in the sub-Saharan African region, reflects to the rapid population growth being experienced there, which has not been matched with the corresponding investment in domestic/urban sewage management infrastructure leading to high discharge of untreated sewage into surface water resources (White et al., 2017). In addition, animal manure is the most commonly used agricultural input in sub-Saharan Africa due to its local availability and affordability to most households.

(a)

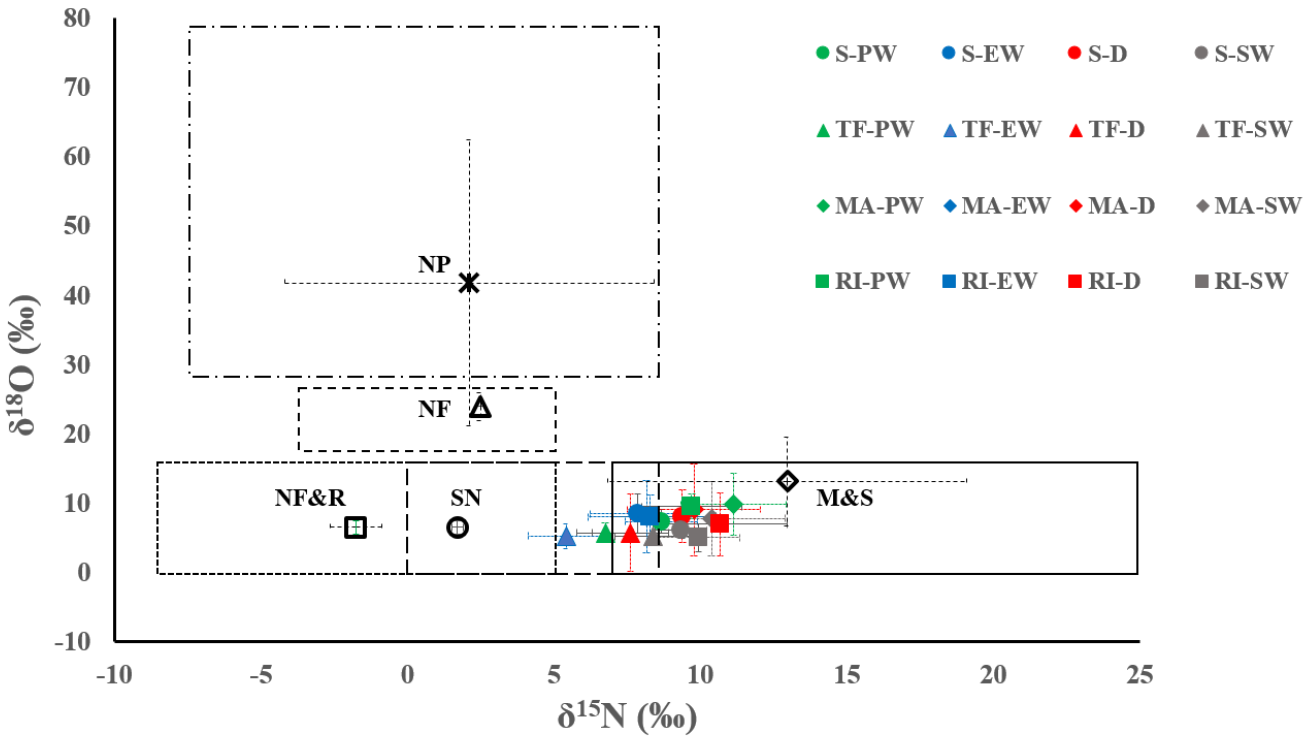

(b)

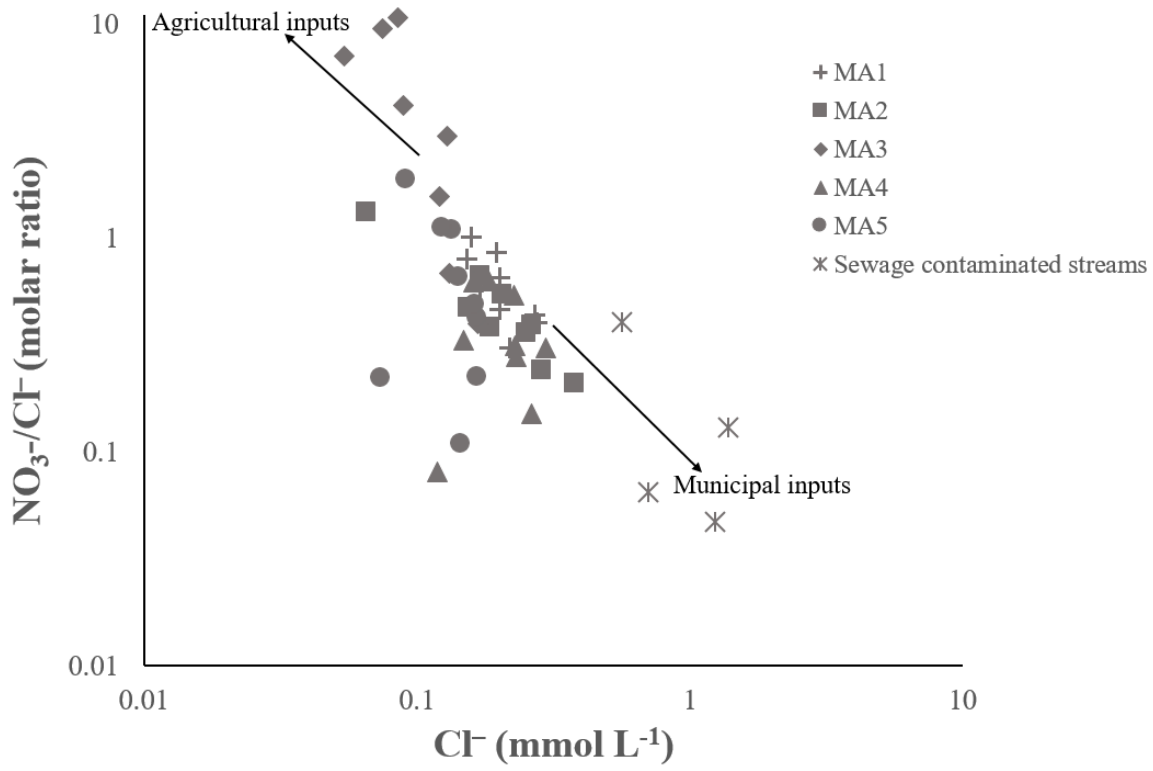

Figure 3.4. Mean $\delta^{15}N$– versus $\delta^{18}O$–NO_3^- values and standard deviations of Nyando river stations grouped into the four land use classes: S (circles), TF (triangles), MA (diamonds), RI (squares) and seasons represented by colours: SW (grey), PW (green), EW (blue) and D (red); $\delta^{15}N$– and $\delta^{18}O$–NO_3^- ranges of local NO_3^- sources: NO_3^- in precipitation (NP: black star), NO_3^- fertilizer (NF: open triangle), NH_4^+ in fertilizer and rainfall (NF&R: open square), soil N (SN: open circle), manure and sewage (M&S: open diamond) are within literature ranges (boxes) by (Kendall et al., 2007; Xue et al., 2009) (a); NO_3^-/Cl^- versus Cl^- log-log plot of the mixed agriculture (MA) samples and sewage-contaminated streams for identifying agricultural and municipal NO_3^- inputs (b).

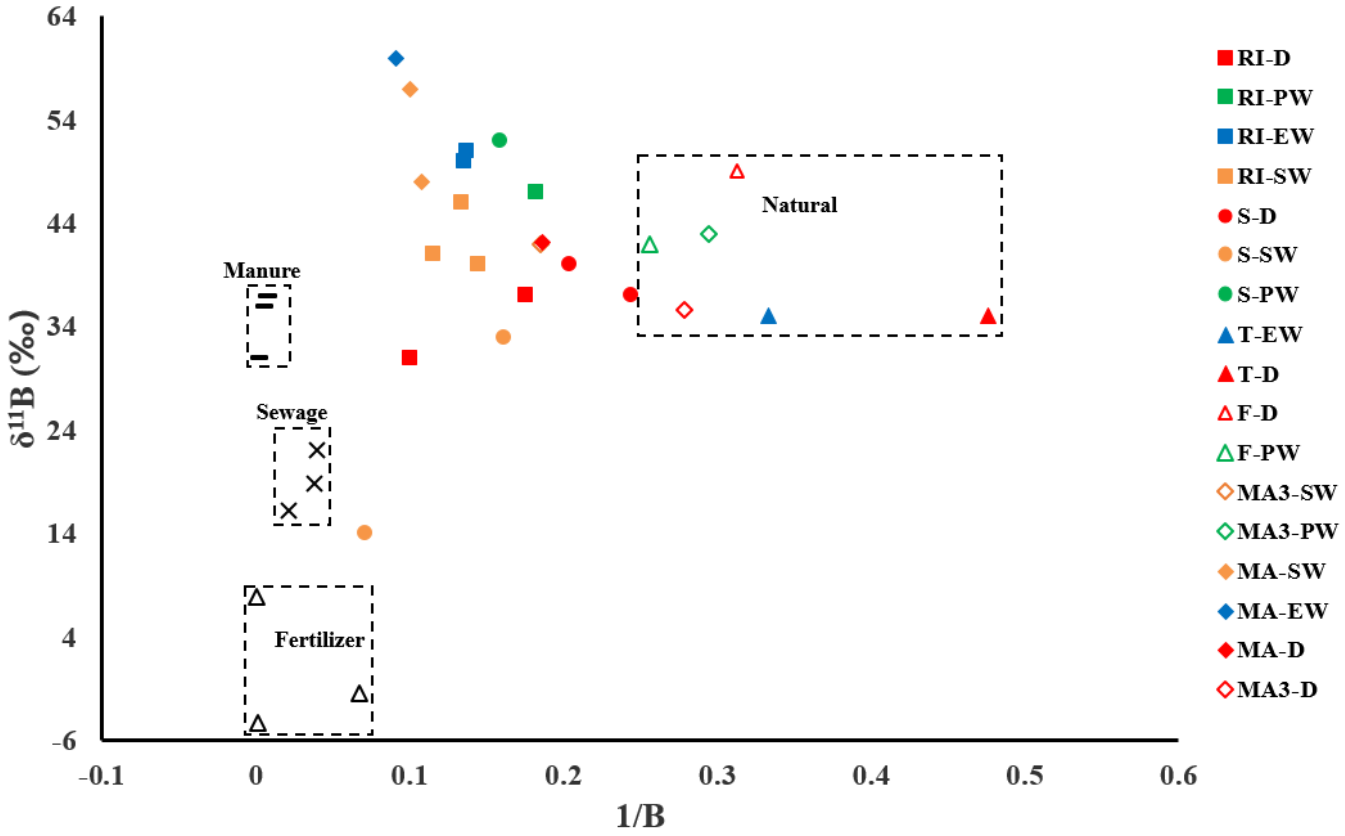

Figure 3.5. Plot of $\delta^{11}B$ versus 1/B of representative River Nyando samples selected spatially in the main land use classes: residential & industrial (RI), Sugarcane (S), tea (T), forest (F), mixed agriculture (MA); and seasons: start wet (SW), peak wet (PW), end wet (EW), dry (D); value ranges of local sources of manure, sewage and inorganic fertilizers are shown in boxes

3.3.4 Estimating proportional contribution of potential NO_3^- sources to the river nitrate

Multiple sources are involved as potential NO_3^- sources in the different land use areas of the Nyando basin. Although the multi-isotope ($\delta^{15}N$-, $\delta^{18}O$–NO_3^-, $\delta^{11}B$) approach has so far been successful in identifying the dominant sources of river NO_3^- for each land use, it is of greater benefit to estimate the quantities associated with the river NO_3^- sources for the targeted implementation of NO_3^- pollution control measures in the basin. Therefore, it was necessary to use a quantitative method based on the Bayesian isotopic mixing model (SIAR) to estimate the proportional contributions of these sources. Spatio-temporal $\delta^{15}N$-, $\delta^{18}O$–NO_3^- data of the

Nyando river were analyzed using mixSIAR to estimate the contribution of five potential NO_3^- sources: NP, NF, NF&R, SN, and M&S. Seasonal variations in source contribution in each land use area are presented in Fig. 3.6a–d. Each season represents at least two sampling campaigns (2SW, 3PW, 2EW, 2D) which had no significant differences ($p <= 0.05$) in their $\delta^{15}N$ or $\delta^{18}O$ values, i.e. SW1 and SW2 ($p = 0.4$); PW1 - PW3 ($P = 0.4, 0.5$); EW1 and EW2 ($p = 0.8, 0.08$) and D1 and D2 ($p = 0.4, 0.5$). The spatial NO_3^- source contributions in the whole basin are shown in Fig. 3.6e.

Figure 3.6a–c clearly shows that manure or sewage (M&S) was the dominant NO_3^- source in MA, RI and S land uses, in all seasons. However, based on $\delta^{11}B$ findings, it should be noted that manure was the dominant NO_3^- source over sewage. Therefore, in this case, manure has the highest contribution in the M&S source. In addition, the mixSIAR output and $\delta^{11}B$ findings are complementary regarding the observed seasonal patterns of source contribution in the three land use classes. For instance, for the RI and S land uses (Fig. 3.6b and c), there is a higher soil N source contribution during the wet seasons (PW, EW) relative to the dry seasons (SW, D). This is the same observation portrayed by $\delta^{11}B$ data (Fig. 3.5), where the natural source contribution was more dominant in RI and S during the wet seasons. The proportional NO_3^- source contribution in the three land use classes followed the order: M&S > SN > NF&R > NF > NP. However, for TF land use (Fig. 3.6d), the other potential sources (SN, NF&R, NF, NP) increased in proportional source contribution, while M&S decreased, and consequently, soil N became a co-dominating NO_3^- source in TF during especially the PW and EW seasons (Fig. 3.6d). This is also indicated in Fig. 3.5, because the B concentration and $\delta^{11}B$ values of TF samples are in the natural source range (Widory et al., 2013).

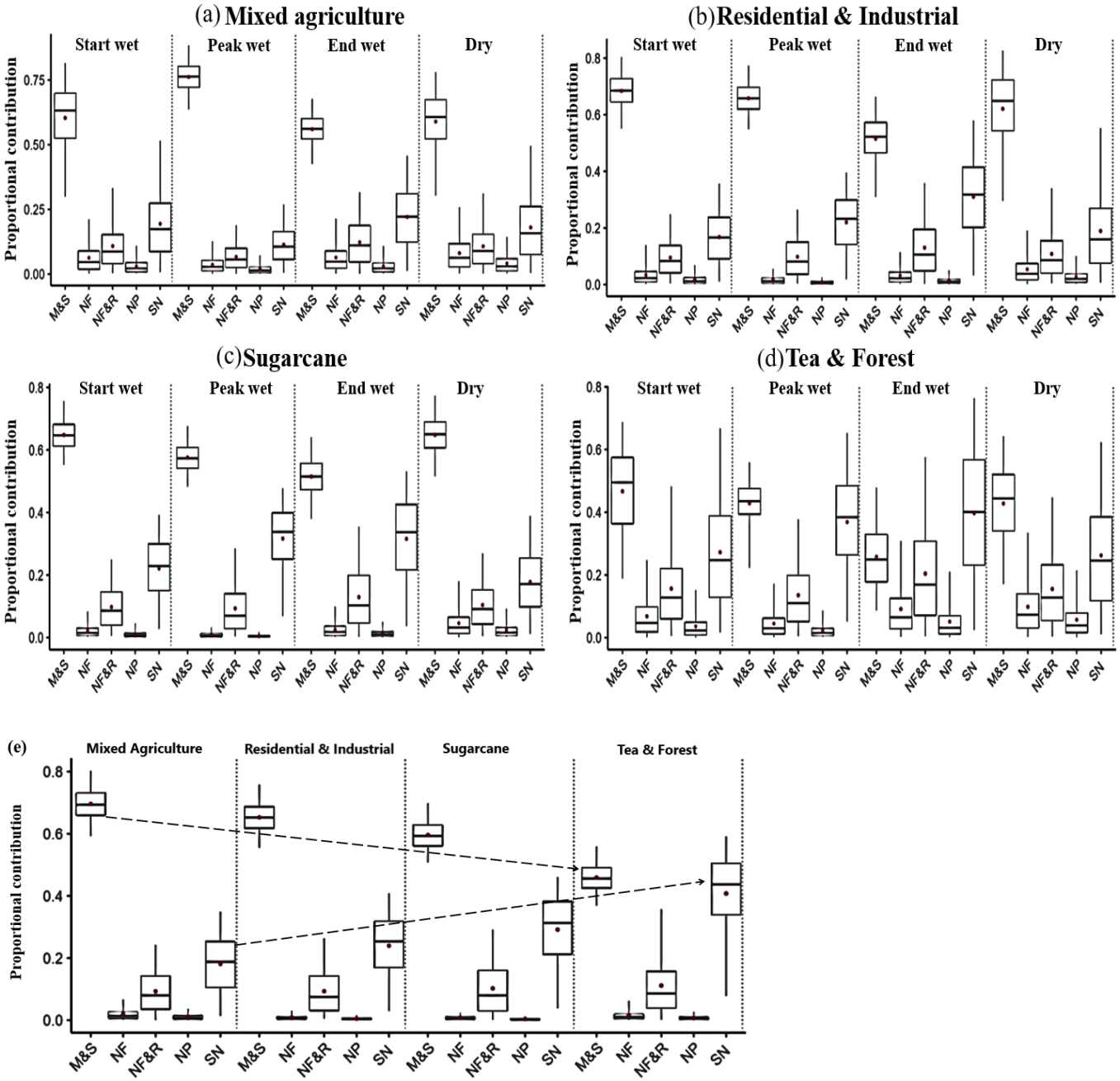

Figure 3.6. mixSIAR estimation of proportional contributions of local NO_3^- sources in the Nyando basin: seasonally in the four main land use classes (a - d); and the spatial NO_3^- source contribution in the whole basin (e); potential NO_3^- sources are manure & sewage (M&S), NO_3^- fertilizer (NF), NH_4^+ in fertilizer and/or rainfall (NF&R), NO_3^- in precipitation (NP), and soil N (SN); dotted arrows show a decrease in M&S source contribution corresponding to an increase in SN observed in the basin.

MixSIAR estimation of spatial NO_3^- source contributions to the whole basin (Fig. 3.6e) shows that, manure-dominant M&S is the leading source of the river NO_3^- input for each land use, contributing for 70% (MA), 65% (RI), S (60%) and TF (46%). Soil N ranked second with its

highest proportional contribution of 41% recorded for the TF land use, followed by 29% (S), 24% (RI) and 18% (MA). NF&R was third, contributing for about 10% NO_3^- for all land uses. This reflects the use of ammonium-based fertilizers in the basin as opposed to NF, which showed 1–2% contribution to the basin. NP was the least, contributing <1% in the whole basin. The contribution of inorganic fertilizers (NF&R or NF) in the Nyando basin is generally low compared to river basin studies in other regions, which reports inorganic fertilizers as largest contributor to river NO_3^- (Chen et al., 2009; Lin et al., 2019; Zhang et al., 2018a; Zhang et al., 2018b). This can be attributed to the relatively low inorganic fertilizer application rate in the larger part of the Nyando basin (generally < 50 kg N ha^{-1}), which when coupled with the inadequate sanitation systems and higher manure use, makes inorganic fertilizer contribution less significant. A clear spatial trend in the proportional contribution of the five potential sources to the Nyando basin is evident in Fig. 3.6e. The M&S source, which was highest for MA land use (characterized by a combination of commercial, mixed agriculture and urban effluents), decreased steadily moving to the TF land use (forests and commercial tea). The trend corresponds to a soil N source increase from the lowest proportional contribution in MA to the leading NO_3^- source for TF land use (Fig. 3.6e).

3.4 Conclusions

NO_3^- discharge in the Nyando basin varies spatially and is driven by intensive land use patterns. The combined application of multi-isotope ($\delta^{15}N$-, $\delta^{18}O$– NO_3^-, $\delta^{11}B$) data and mixSIAR reveals that animal manure, either from free range livestock keeping or manure application in mixed farming, is the dominant source of river NO_3^- in the basin. Soil N is the second most important source of river NO_3^-, especially in the tea and forest land use and in the whole basin during the agriculturally dormant short rainy season. However, sewage sources influence river NO_3^- during the dry seasons and especially for the sugarcane, residential & industrial land use classes where industries are located. On the other hand, inorganic fertilizers are the major sources of river NO_3^- in an area under commercial flower farming. Therefore, in order to control excess NO_3^- discharges and ensure sustainable water quality management in the basin,

good manure use guidelines and better animal husbandry methods like paddocking or zero grazing, which controls the spread of animal wastes should be adopted in the basin. In addition, technological advancement and expansion of the existing waste water treatment infrastructure is key for the control of the sewage sourced NO_3^- contamination of river water. Also, the restoration of previously degraded water sources (wetlands and forests) and improvement of land management practices is necessary for the control of soil erosion-driven NO_3^- losses.

Chapter 4. Tracking sources and fate of groundwater nitrate in Kisumu city and Kano plains in Lake Victoria basin, Kenya

This chapter has been published as

Nyilitya, B., Mureithi, S., Boeckx, P., 2020. Tracking sources and fate of groundwater nitrate in Kisumu city and Kano plains, Kenya. Water (Switzerland) 12, 1–18. https://doi:10.3390/w12020401

Abstract

Groundwater nitrate (NO_3^-) pollution sources and *in* situ attenuation were investigated in Kisumu city and Kano plains. Samples from 62 groundwater wells consisting of shallow wells (hand dug, depth <10 m) and boreholes (machine drilled, depth >15 m) were obtained during wet (May-July 2017) and dry (February 2018) seasons and analyzed for physicochemical and isotopic ($\delta^{15}N\text{-}NO_3^-$, $\delta^{18}O\text{-}NO_3^-$, $\delta^{11}B$) parameters. Groundwater NO_3^- concentrations ranged from < 0.04 to 90.6 mg L^{-1}. Boreholes in Ahero town, showed significantly higher NO_3^- (20.0 – 70.0 mg L^{-1}) than boreholes in the Kano plains (< 10.0 mg L^{-1}). Shallow wells in Kisumu gave significantly higher NO_3^- (11.4 – 90.6 mg L^{-1}) than those in the Kano plains (< 10.0 mg L^{-1}). About 63% of the boreholes and 75% of the shallow wells exceeded the drinking water WHO threshold for NO_3^- and NO_2^- (nitrite) during the study period. Mean $\delta^{15}N\text{-}NO_3^-$ values of 14.8±7.0 and 20.7±11.1‰, and $\delta^{18}O\text{-}NO_3^-$ values of 10.2±5.2 and 13.2±6.0‰ in wet and dry seasons, respectively, indicated manure and/or sewage as main sources of groundwater NO_3^-. However, a concurrent enrichment of $\delta^{15}N$ and $\delta^{18}O$ was observed, especially in the dry season, with a corresponding NO_3^- decrease, indicating *in situ* denitrification. In addition, partial nitrification of mostly sewage derived NH_4^+ appeared to be responsible for increased NO_2^- concentrations observed in the dry season. Specifically targeted $\delta^{11}B$ data indicated that sewage was the main source of groundwater NO_3^- pollution in shallow wells within Kisumu informal settlements, boreholes in Ahero, and public institutions in populated neighborhoods of Kano; while manure was the main source of NO_3^- in boreholes and shallow wells in the Kano and planned estates around Kisumu. Waste water sanitation systems in the region should be urgently improved to avoid further deterioration of groundwater sources.

Keywords: Kenya; Kisumu; Groundwater; Nitrate; Hydrochemistry; Denitrification

4.1 Introduction

Africa is quickly urbanizing with cities in Sub-Saharan Africa (SSA), reported to have grown at an average rate of 4.0% per annum over a period of 20 years, compared to the global average annual urban population growth rate of between 1.44 – 1.84 % (White et al., 2017). This rapid urbanization has put pressure on water service provision and sanitation infrastructure in SSA cities. Their sanitation infrastructure largely remains unchanged due to low capital investments, estimated at about 20% of the GDP. As utilities responsible for piped water and sanitation services struggle to meet the demand, community and private-owned groundwater wells becomes the alternative option, not only to the rural population but also to urban dwellers. At the same time, nitrate (NO_3^-) is emerging as the most widespread groundwater contaminant associated with anthropogenic activities. The World Health Organization (WHO) has put the maximum allowable concentration at 50 mg L^{-1} nitrate. This is because, high nitrate concentrations in water are both a health and environmental hazard promoting eutrophication, pose high risks to methemoglobinemia (blue baby syndrome) in infants and colorectal cancer (Kendall et al., 2007; Schullehner et al., 2018).

In Kisumu city, which is located at the shores of Lake Victoria, groundwater use for domestic, industrial, and agricultural purposes is high. This is driven by rapid urbanization and industrialization due to a vibrant sugarcane production industry and a high population density ranging 827 – 4737 people per square kilometer, compared to Kenya's average population density of 82 people per square kilometer (KNBS, 2019). The supply of Lake Victoria water to the city is limited because of the low production capacity of the city's water service provider grappling with increased treatment costs caused by pollution and eutrophication of Lake Victoria. This has made the piped lake water unaffordable to the majority of the residents in the city and its surrounding areas, leading to an increased reliance on hand dug shallow wells or community water supply boreholes. Because of the minimal costs involved in their construction, shallow wells are widely used amongst urban residents in Kisumu and their distribution and significance has been well documented (Wright et al., 2013). Despite the rapid expansion of the city, there has not been a corresponding investment in necessary waste management infrastructure, an occurrence which is characteristic of many other SSA cities (Wang et al., 2012). The situation has been worsened by proliferation of informal settlements (slums), which are not connected to any conventional sanitation system. The slum areas are characterized by the use of pit latrines, open defecation by both humans and animals and

landfills developing near groundwater resources. A similar sanitary situation is found in the rural Kano, although with a lower population density. In addition, the use of inorganic fertilizer and animal manure in the Kano area for sugarcane farming (Fig. 4.1) may be a potential source of groundwater nitrate contamination.

Despite the high risks to groundwater nitrate contamination, the available information on groundwater nitrate in this part of the Lake Victoria basin is scarce (Okotto-Okotto et al., 2015; Wright et al., 2013). Therefore, data on spatial nitrate distribution in the city and its surroundings is lacking and no study has attempted to identify the potential sources of groundwater nitrate or its fate. Coupling of hydrochemistry and nitrate isotopes ($\delta^{15}N$-, $\delta^{18}O$–NO_3^-) has demonstrated its usefulness in identifying potential NO_3^- sources in groundwater and surface water (Aravena et al., 1993). In addition, the use of $\delta^{15}N$-, $\delta^{18}O$–NO_3^- has proven to be a powerful method to pinpoint occurrence of NO_3^- transformation processes such as nitrification and denitrification, influencing the NO_3^- concentration in groundwater (Böttcher et al., 1990; Mengis et al., 1999). However, mixing of different NO_3^- sources can lead to modification of the isotopic composition of dissolved NO_3^- and at the same time, $\delta^{15}N$-, $\delta^{18}O$–NO_3^- cannot clearly distinguish manure from sewage nitrate sources, since both sources have overlapping isotopic signatures (Kendall et al., 2007). Similarly, N transformation via nitrification and denitrification results into isotopic fractionations which alter the isotopic signatures ($\delta^{15}N$, $\delta^{18}O$) of NO_3^-. These confounding factors complicate discrimination between multiple nitrate sources based on their isotopic composition. However, boron is ubiquitous tracer in nature and is usually found in groundwater as a minor constituent. The large range of boron isotope ($\delta^{11}B$) ratios, observed in nature, enables clear contrasts to be made between boron sources in groundwater. Furthermore, boron is not affected by N transformation processes and researchers have demonstrated the added value of combining nitrate and boron isotope ($\delta^{15}N$, $\delta^{18}O$-NO_3^-, $\delta^{11}B$) ratios in NO_3^- source discrimination (Seiler, 2005; Widory et al., 2013, 2005; Xue et al., 2013).

Together with providing baseline spatiotemporal water quality and isotopic data of the investigated area, this study seeks 1) to establish the potential sources of NO_3^- input into groundwater and 2) to assess *in situ* attenuation controlling groundwater NO_3^- concentration in the region. This information is paramount for policy development regarding groundwater use, sanitation, urban waste management and use of agricultural inputs in the region.

4.2 Materials and Methods

4.2.1 Study area

Kisumu city and the surrounding Kano plains are geographically located in a central plain surrounded by higher areas in the north-west (Kisian hill) and north-east (Nandi hills), bordering the Winam gulf of Lake Victoria (Fig. 4.1). The city lies between latitude 00°02'N – 00°11'S and longitude 34°35' – 34°55'E and covers approximately 417 km^2, and 35.5% is part of the Lake Victoria water body. The city has experienced a high population growth with a reported population of 567,963 according to the recent 2019 census (KNBS, 2019). It is Kenya's third largest city and the second most important city in the lake basin after Kampala (Juma et al., 2014). The area receives a mean annual rainfall of 1245 mm occurring in two seasons, long and short rains from March – July and September – November, respectively. In addition, the mean annual minimum and maximum temperatures in the area are 17.3 and 28.9°C, respectively (Mireri et al., 2007). The geology and hydrogeology of the study area has been described by Olago (2019). Kisumu city consists of fractured basalt overlain by pyroclastic deposits which results into perched/unconfined aquifers with a localized recharge (Wright et al., 2013). The unconfined aquifer comprises the shallow groundwater in the area which occurs at depths ranging between 5 and 25 m (Okotto-Okotto et al., 2015). The fractures act as pathways for groundwater flow and recharge, posing a great risk to groundwater pollution. Deeper aquifers (25 – 60 m) in the area occur in faulted and fractured hard rocks and sediments along the gulf, while thicker and well developed aquifers occur in the Kano area at depths greater than 150 m (Olago, 2019). A piezometric map of the study area by Oiro (2012) shows groundwater flows from the high altitude areas towards Lake Victoria as discharge point. This is in agreement with Olago (2019), who reported that the groundwater flow direction in the Kisumu regional aquifer is from the highland recharge areas towards the central part of the Kano plains and the lake.

Land use in the study area includes the urban and peri-urban zone, which is mainly concentrated in the Kisumu municipality, an area covering 297 km^2 (Mireri et al., 2007). The other urban centres are Ahero and Awasi which are situated in the Kano plains and lie along the busy Kisumu – Nairobi highway (Fig. 4.1(b)). Major industries include: cotton mills, breweries, cement factory, and several sugar milling and agro-chemical production industries. Urban agriculture and livestock keeping is common in the area and has been documented (Mireri et

al., 2007). Sugarcane farming is the main agricultural activity in the Kano area (Fig. 4.1), and is practiced under both small-scale mixed farming (with food crops: maize, sorghum, finger millet) and large-scale commercial farming. Irrigated rice farming is practiced in the Ahero area next to the river Nyando.

(a)

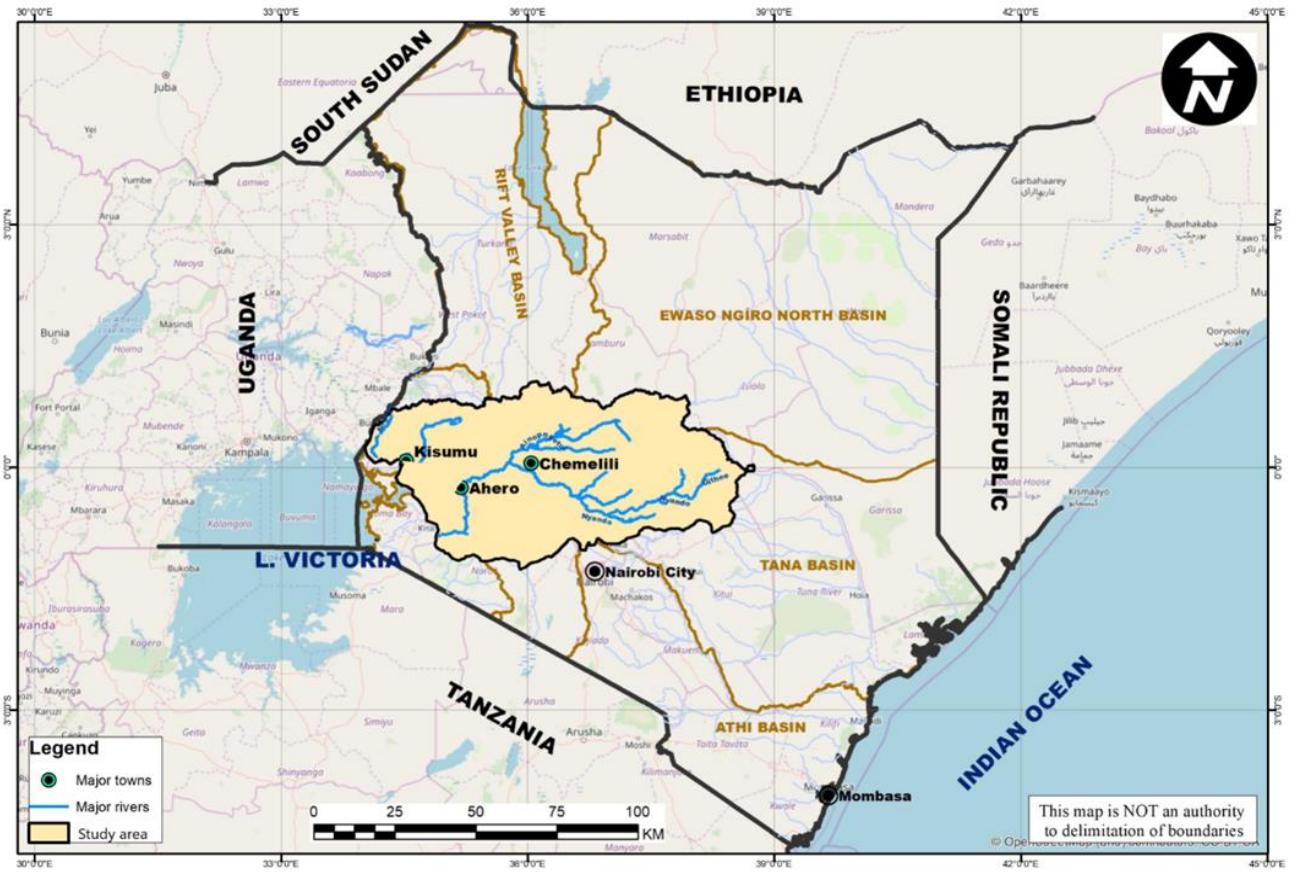

(b)

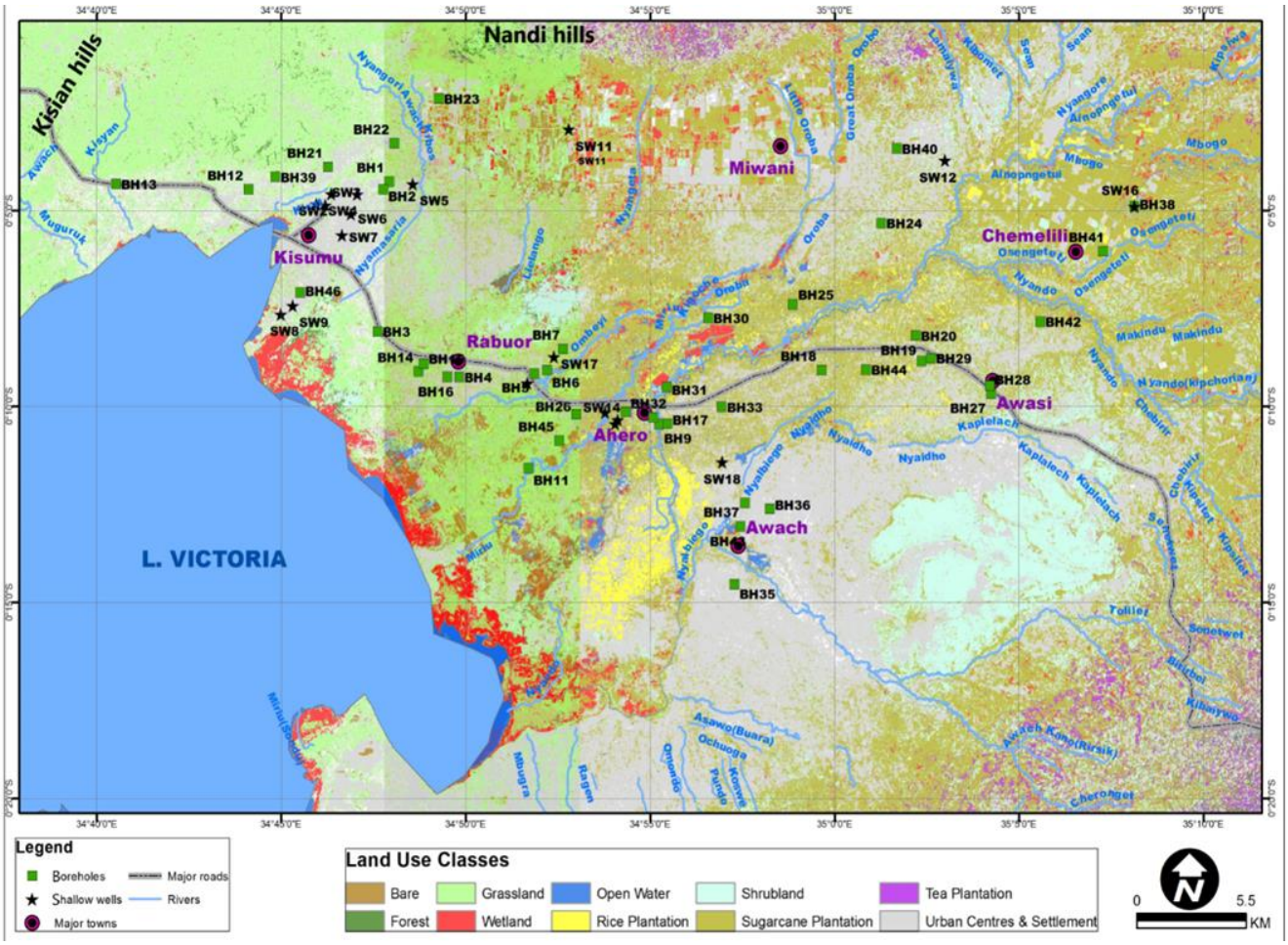

Figure 4.1. Study area map with inset: location of the study area in the Lake Victoria basin, Kenya (a); land use map indicating the spatial distribution of the groundwater sampling points represented by squares and stars for boreholes (BH) and shallow wells (SW), respectively (b).

4.2.2 Water sampling and analysis

In order to understand groundwater nitrate concentration, distribution, potential sources and fate, the study targeted both the shallow unconfined aquifer where shallow wells (SW) tap from, and the deeper unconfined and confined aquifers where the boreholes (BH) are sank at depths above 25 m. The groundwater points were mapped and selected in May 2017 in consultation with the Kisumu-based water resources authority (WRA) regional office. The aim was to identify production BHs and SWs spatially distributed and representative of the major land use patterns in the area (Fig. 4.1). The final list of sampling points included BHs and SWs in informal settlements (Ombuga, Nyalenda, Manyatta) and formal settlements (Migotsi, Kibos) of Kisumu city where groundwater use is high. In the Kano area, BHs and SWs were

selected from public institutions (e.g. schools), community donor funded projects, and private owned wells. A total of 62 groundwater production points were sampled during the wet season (May-July 2017) and in the dry season (February 2018).

During sampling, water samples were taken from production BHs and SWs. In case the well wasn't pumping prior to the sampling exercise, the well was purged to ensure the representativeness of a sample. Samples were first pre-filtered onsite using 11 µm filters (Whatman, GE Healthcare Life Sciences, Chicago, IL, USA) and then filled in a 200 ml PVC bottle after pre-rinsing with the sample water. Sample water was stored in an insulated cooler box containing ice cubes for transportation to the laboratory for physicochemical and isotopic analysis. Duplicate samples for cation analysis were taken in 100 mL HDPE bottles, pre-filtered and acidified to pH = 2 using diluted hydrochloric acid. *In situ* measurements included temperature (T), electrical conductivity (EC), pH and dissolved oxygen (DO). These *in situ* parameters (T, EC, pH, DO) were measured in every sampling station using a multi-parameter sensor (Multi3430, WTW, Germany). On the other hand, sampling of the potential NO_3^- sources (sewage, manure, inorganic fertilizers, precipitation, and soil nitrogen) for the determination of $\delta^{15}N$–, $\delta^{18}O$–NO_3^- and $\delta^{11}B$–B values was conducted during the field campaigns. Sewage effluents were sampled from the inlet point of sewage treatment plants located in major towns (Kisumu, Ahero), sugarcane factories (Muhoroni, Chemelil), agrochemical and lime factories. Manure samples were taken from cow, goat and sheep as animal droppings in the Kano area. Inorganic fertilizers samples of the commonly used types (CAN, DAP, NPK, urea) were purchased from farmers and suppliers in the basin. Precipitation samples were collected from rainfall stations in Ahero, Kakamega and Kericho towns, while soil N samples were collected by filtering suspended soil sediments in river water using 11 µm filters (Whatmann, GE Healthcare Life Sciences, Chicago, IL, USA). In the laboratory, all samples were filtered through 0.45 µm membrane filters and stored frozen (-17°C) awaiting analysis. Laboratory determination of Na^+, K^+, Ca^{2+}, Mg^{2+}, NH_4^+, NO_3^-, NO_2^-, Cl^- and SO_4^{2-} concentrations was carried out using an ion chromatograph (930 Compact IC Flex, Metrohm, Switzerland).

The $\delta^{15}N$– and $\delta^{18}O$–NO_3^- values were determined by the "Bacterial denitrification method" (Casciotti et al., 2002; Sigman et al., 2001; Xue et al., 2009), which allows simultaneous determination of $\delta^{15}N$ and $\delta^{18}O$ in N_2O produced from the conversion of NO_3^- by denitrifying

bacteria, which naturally lack N_2O-reductase activity. The $\delta^{15}N$ and $\delta^{18}O$ analysis of the produced N_2O was carried out using a trace gas preparation unit (ANCA TGII, SerCon, UK), coupled to an isotope ratio mass spectrometer (IRMS) (20-20, SerCon, UK). The N_2O sample was flushed out of the sample vial using a double-hole needle on an auto-sampler. Water was removed using a combination of nafion dryer and $MgClO_4$ scrubber. By cryogenic trapping and focusing, the N_2O was compressed onto a capillary column (CP-Poraplot Q 25 m, 0.32 mm id, 10 µm df, Varian, US) at 35°C and subsequently analyzed by IRMS. The subsequent stable isotope data were expressed as delta (δ) units in per mil (‰) notation relative to the respective international standards:

$$\delta_{sample}\ (‰) = \left[\frac{R_{sample}}{R_{standard}} - 1\right] \times 1000 \qquad 4.1$$

Where R_{sample} and $R_{standard}$ are the $^{15}N/^{14}N$ or $^{18}O/^{16}O$ ratio of the sample and the standard for $\delta^{15}N$ and $\delta^{18}O$, respectively. $\delta^{15}N$ values are reported relative to N_2 in atmospheric air (AIR) and $\delta^{18}O$ are reported relative to Vienna Standard Mean Ocean Water (VSMOW). Three internationally recognized reference standards, USGS32 (180.0 ± 1.0‰ for $\delta^{15}N$, 25.7 ± 0.4‰ for $\delta^{18}O$), USGS34 (-1.8 ± 0.2‰ for $\delta^{15}N$, -27.8 ± 0.4‰ for $\delta^{18}O$), and USGS35 (2.7 ± 0.2‰ for $\delta^{15}N$, 56.8 ± 0.3‰ for $\delta^{18}O$), were used to normalize the raw $\delta^{15}N$– and $\delta^{18}O$– NO_3^- values (based on a N_2O reference gas tank) to the AIR and VSMOW scale. USGS32 and USGS34 were used for normalization of the $\delta^{15}N$ value and USGS34 and USGS35 for the $\delta^{18}O$. The amount of NO_3^- in samples and references were matched (i.e. 20 nmol) which corrects for nonlinearity of the IRMS and blanks associated with the procedure. An in-house KNO_3 laboratory standard (9.9‰ for $\delta^{15}N$, 24.3‰ for $\delta^{18}O$), was analyzed together with the samples for quality control. Measurement batches were only accepted if measured $\delta^{15}N$ and $\delta^{18}O$ values of the laboratory standard were within 0.4 and 0.5 ‰ of our accepted values, respectively. If standard deviation on replicate samples was higher than 0.3 and 0.4 for $\delta^{15}N$ and $\delta^{18}O$, respectively, the sample was reanalyzed. This method is well explained in Casciotti et al. (2002) and Sigman et al. (2001).

The water analysis technique for B and $\delta^{11}B$ is well covered in Tirez et al. (2010). Samples underwent a two-step chemical purification using Amberlite IRA-743-selective resin (method adapted from Gaillardet and Allgre (1995)). First, the sample (pH = 7) was loaded on a Teflon PFA® column filled with 1 ml resin, previously cleaned with ultrapure water and 2 N ultrapure

NaOH. After cleaning the resin again with water and NaOH, the purified B was collected with 15 ml of sub-boiled HCl 2N. After neutralization of the HCl with Superpur NH_4OH (20%), the purified B was loaded again on a small 100 ml resin Teflon PFA® column. B was collected with 2 ml of HCl 2N. An aliquot corresponding to 2 mg of B was then evaporated below 70°C with mannitol ($C_6H_8(OH)_6$) in order to avoid B loss during evaporation (Ishikawa and Nakamura, 1990). The dry sample was loaded onto a tantalum (Ta) single filament with graphite (C), mannitol and cesium (Cs). $\delta^{11}B$ values were then determined by measuring the $Cs_2BO_2^+$ ion (Spivack et al., 1987; Spivack and Edmond, 1986) by a thermal ionization mass spectrometer. The analysis was ran in dynamic mode by switching between masses 308 and 309. Each analysis corresponded to 10 blocks of 10 ratios. Samples were always ran twice. Total B blank was less than 10 ng corresponding to a maximum contribution of 0.2%, which is negligible. Seawater (IAEA-B1) was purified regularly in the same way, in order to check for possible chemical fractionation due to an uncompleted recovery of B, and to evaluate the accuracy and reproducibility of the overall procedure (e.g. (Gonfiantini et al., 2003)). Reproducibility was obtained by repeated measurements of the NBS951, and the accuracy was controlled with the analysis of the IAEA-B1 seawater standard ($\delta^{11}B$=38.6±1.7‰). Similar to N and O, B isotope ratios were expressed in delta (δ) units and a per mil (‰) notation relative to an international standard, NBS951.

Statistical analysis for determining spatial-temporal differences in physico-chemical and isotopic parameters was performed using ANOVA with Tukey HSD tests, and $p < 0.05$ significance level was set to test significance between the parameter sets. Major ionic constituents were plotted in piper tri-linear diagrams (Piper, 1944) using the AquaChem (version 2014.2) software package. These are a combination of anion and cation triangles with a diamond shape between them which is used to plot the analysis. Piper diagrams helps in deciphering groundwater processes like mineralization, mixing, and in determining water types and water origin.

4.3 Results and discussion

4.3.1 Hydrochemistry

Table 4.1 presents a statistical summary of 16 hydro-chemical and 3 isotopic parameters for boreholes and shallow wells sampled during the wet and dry seasons. Water pH ranged from 6.1 to 10.1 and from 6.2 to 8.6 in boreholes and shallow wells, respectively. Two borehole samples (BH 27 & 28) exceeded the World Health Organization (WHO) pH limit (> 8.5) during both wet and dry seasons while shallow wells within Kisumu recorded a slightly acidic pH (< 6.5). High pH observed in BH 27 and 28, located in the Awasi area (Fig. 4.1b), is characteristic of cation exchange reactions where Ca^{2+} and/or Mg^{2+} in solution is exchanged with Na^{+} on clay minerals (Allen and Suchy, 2001). Replacement of Ca^{2+} by Na^{+} in solution results into a pH change, which is sanctioned by change in the equilibrium of the reaction:

$$CaCO_3 + CO_2(g) + H_2O = Ca^{2+} + 2HCO_3^- \quad 4.2$$

It shifts the equilibrium further to the right and increases the bicarbonate content and pH. This is supported by the significantly low Ca^{2+} ($p < 0.0001$) and Mg^{2+} ($p = 0.04$) values ranging from 1.1 to 1.7 mg L^{-1} and from 0.1 to 0.2 mg L^{-1}, respectively obtained in the two boreholes during the study period (Table A8 & A9). Consequently, high pH and low calcium levels favor the solubility of fluoride, and this accounts for the high fluoride levels (9.0 and 11.0 mg L^{-1}, respectively; Table A8) observed in the two Awasi boreholes. Generally, groundwater in the area has high fluoride levels as shown in Table 1 where mean values exceeds WHO limit (1.5 mg L^{-1}) for drinking water. This is a health risk since excessive intake of fluoride is known to cause dental/ skeletal fluorosis, cancer, low hemoglobin levels, osteoporosis, reduced immunity, and thyroid disorders (Barathi et al., 2019).

Water temperature ranged from 25.3 to 37.6°C and from 24.5 to 28.5°C in boreholes and shallow wells, respectively, and did not significantly differ by season. The EC values ranged from 295 to 2562 µS cm^{-1} in boreholes and from 248 to 1427 µS cm^{-1} in shallow wells portraying an increase in mineralization with well depth. On the other hand, dissolved oxygen (DO) values ranged from 1.4 to 6.8 mg O_2 L^{-1} in boreholes and from 1.2 to 9.8 mg O_2 L^{-1} in shallow wells. However, the wet season showed lower DO values than the dry season in both boreholes and shallow wells. This implies an increased oxygen consumption in the

groundwater most likely by dissolved organic carbon originating from contaminated surface water during the wet season.

Table 4.1. Statistical summary of hydro-chemical and isotopic parameters for boreholes (n=44) and shallow wells (n=18) sampled during wet and dry seasons. ± denotes standard deviation, WHO limit stands for World Health Organization standard limits for drinking water; DO stands for dissolved oxygen; p-value represents ANOVA (at $p < 0.05$ levels) output for testing differences of parameters between wet and dry seasons.

	Boreholes									Shallow wells								
	Wet			Dry			P value	WHO limit	Number Exceeded WHO	Wet			Dry			P value	WHO limit	Number Exceeded WHO
	Min	Mean	Max	Min	Mean	Max				Min	Mean	Max	Min	Mean	Max			
Physico-chemical parameters																		
pH (-)	7	7.6±0.7	10.1	6.1	7.4±0.6	9.6	0.23	6.5 - 8.5	4	6.3	7.1±0.7	8.6	6.2	7.0±0.6	8.2	0.70	6.5 - 8.5	10
Temp (°C)	25.3	28.0±2.2	37.6	25.7	28.1±1.9	36	0.84	-	0	25.1	26.4±0.9	28.2	24.5	26.2±1.0	28.5	0.43	-	0
EC (µS cm^{-1})	295	1091±390	2520	400	1052±383	2562	0.71	500	42	248	821±282	1420	290	785±3.02	1427	0.74	500	15
DO (mg O_2 L^{-1})	1.4	3.1±1.4	6.6	2	3.9±1.2	6.8	0.01	-	0	1.2	2.9±1.5	6.2	1.6	4.1±2.0	9.8	0.05	-	0
Cl^- (mg L^{-1})	1.6	22±21	80.1	0.1	29.4±39.7	156	0.29	250	0	1.7	32.0±22.8	75.5	2.8	41.5±34.3	103	0.33	250	0
SO_4^{2-} (mg L^{-1})	0.9	37±41	212	0.4	49.1±67.7	360	0.33	250	0	1.4	31±17	56.3	9	37±17.5	67.2	0.38	250	0
NO_3^- (mg L^{-1})	< 0.04	5.8±8.8	43.7	< 0.04	6.7±12.5	69.9	0.74	50	1	< 0.04	33.5±32.4	90.6	0.04	10.9±13.0	38.2	0.02	50	6
NO_2^- (mg L^{-1})	< 0.04	0.02±0.01	0.06	< 0.04	1.4±0.9	3.2	< 0.0001	0.2	27	< 0.04	0.04±0.04	0.15	< 0.04	0.6±0.8	2.2	0.006	0.2	6
HCO_3^- (mg L^{-1})	2.4	93±46	167	20.2	98.5±36.4	172	0.67	500	0	16.6	47±38	109	4.9	57.2±43.8	122	0.61	500	0
Na^+ (mg L^{-1})	33.6	190±92	452	29.8	186±98	461	0.86	250	0	41	112±75	311	31.1	98.3±63.0	236	0.60	250	0
K^+ (mg L^{-1})	4.9	23.6±15.5	66.5	3.5	23.3±14.7	67.9	0.90	250	0	1.3	22±15	55	3.1	23.8±17.8	62.1	0.75	250	0
Ca^{2+} (mg L^{-1})	1.11	23.9±16.6	74.7	1.2	23.2±13.3	60	0.85	75	0	2.5	26.6±14.2	51.7	7.7	24.7±12.2	42.4	0.70	75	0
Mg^{2+} (mg L^{-1})	0.1	6.1±7.1	31.3	0.04	7.4±7.8	30	0.46	50	0	0.4	8.0±6.8	30	1.8	7.1±3.8	12.9	0.68	50	0
NH_4^+ (mg L^{-1})	< 0.01	0.03±0.02	0.14	< 0.01	0.03±0.02	0.09	0.84	-	0	< 0.01	0.7±2.8	11.4	< 0.01	1.1±3.9	14.1	0.74	-	0
B (µg L^{-1})	16	24.5±7.5	34					-	0	20	23±4.2	26					-	0
F^- (mg L^{-1})	0.7	4.1±2.6	10.9					1.5	31	0.3	1.6±2.0	8.0					1.5	6
Isotopic parameters																		
$\delta^{15}N$ (‰)	4.1	12.6±6.2	25.8	6.9	15.5±6.0	32.2	0.06	-		8	19.5±5.8	28.9	12.4	33.6±11.5	51.8	0.0004	-	
$\delta^{18}O$ (‰)	-2.4	9±5.4	20.8	-1.7	11.1±5.5	24.1	0.13	-		7.5	13.3±4.0	19.8	12	18.0±4.8	29.3	0.0138	-	
$\delta^{11}B$ (‰)	23	30.3±6.3	36					-		16	25±12.7	34					-	

Nitrate showed a wide variation ranging from < 0.04 to 70.0 mg L^{-1} and from < 0.04 to 90.6 mg L^{-1} in boreholes and shallow wells, respectively (Table 4.1). Seasonally, NO_3^- concentrations in shallow wells were significantly higher in the wet season compared to the dry season with about 70% of shallow wells located in Kisumu city giving values above the WHO recommended limit (50 mg L^{-1}). Unlike NO_3^-, NO_2^- concentration was significantly

higher in the dry season than in the wet season for both boreholes and shallow wells with 60% of the samples exceeding the WHO limit (0.2 mg L^{-1}) during the dry season. The biogeochemical processes governing the NO_3^- and NO_2^- variations are discussed further in section 3.3. In general, about 63% of the boreholes and 75% of the shallow wells exceeded the WHO recommended limit values for NO_3^- and NO_2^- during the study period. Both boreholes and shallow wells showed similar concentrations of the major anions: Cl^-, SO_4^{2-}, HCO_3^- and the cations: Na^+, K^+, Ca^{2+}, Mg^{2+}, NH_4^+ during wet and dry seasons with values falling within the WHO limits for drinking water.

In Figure 4.2, water facies are presented in a Piper diagram (Piper, 1944) for the boreholes and shallow wells. The boreholes and shallow wells were grouped into spatial categories which also display similarities in hydro-chemical and isotopic parameters. These were: shallow wells located in Kisumu city (SW-Kisumu city); Shallow wells located in Kano plain (SW-Kano plain); boreholes located in Ahero town (BH-Ahero town), boreholes located in public institutions in highly populated neighborhoods (BH-Public) and boreholes located in the Kano plain (BH-Kano plain). It is clear that the groundwater positioning in the Piper diagram is mainly determined by hydrogeology and anthropogenic activities. A mineralization trend was observed (Fig. 4.2, cation triangle) from the low mineralized boreholes (BH: 13, 23, 41) located at the foot of the Nandi and Kisian hills (recharge areas) to highly mineralized boreholes located around Awasi town (BH: 27, 28). While this, on the one hand, represents cation exchange of Ca^{2+} by Na^+ in solution as discussed earlier, on the other hand, it is an indicator of the direction of groundwater recharge. According to Olago (2019), groundwater recharges from the high altitude areas of the Nandi hills towards the center of the Kano plain (Awasi). These boreholes located near the recharge zones (Fig. 4.1b) had a Ca^{2+}-Mg^{2+}-HCO_3^-, Na^+-Ca^{2+}-Mg^{2+}-HCO_3^- water type representing fresh and recharging groundwater (Ako et al., 2012). The same water type was obtained in BH 42, which by being located next to R. Nyando (Fig. 4.1b) reveals young/recharging water from the river (Nyilitya et al., 2016). However, the Awasi boreholes (BH: 27, 28) with a high pH showed a dominant Na^+-Cl^- water type by plotting on the far-right corner of the diamond. In addition, these boreholes had a low NO_3^- content (<1 mg L^{-1}), but relatively high EC (>1000 µS cm^{-1}), characterizing saline water (Allen and Suchy, 2001; Piper, 1944).

The shallow wells in the diamond grouped into two categories: a group consisting of the SW-Kisumu city showing a Na^+-K^+-Cl^--NO_3^- or Na^+-K^+-Cl^--SO_4^{2-} water type , and a group made of the SW-Kano plain showing a Na^+-K^+-HCO_3^- or Na^+-HCO_3^- water type. The majority of the BH-Kano plain, just like the shallow wells, had the Na^+-K^+-HCO_3^- and Na^+-HCO_3^- water type. Previous studies conducted in the study area by Oiro (2012) similarly report Na^+ and HCO_3^- as the dominant cation and anion respectively in borehole water. The study also observed high NO_3^- and SO_4^- levels in shallow wells located in Kisumu. This suggests that weathering of Na^+-K^+ containing alumino-silicate minerals is the major process contributing to the dominance of Na^+ and K^+ in the study area. In addition, the dissolution of CO_2 and carbonate during precipitation and infiltration in the unsaturated zone impart the bicarbonate character of the groundwater (Shanyengana et al., 2004). However, the dominance of NO_3^-, Cl^- and SO_4^{2-} anions observed in SW-Kisumu city suggests the influence of contaminated surface water, just as alluded in the previous study (Oiro, 2012). This is in agreement with a similar study by Kamtchueng et al. (2016) on surface and groundwater hydrogeochemistry around Lake Manoun, Cameroon. The study observed Na^+-K^+-Cl^--NO_3^- and Ca^{2+}-Mg^{2+}-Cl^--NO_3^- as the water types representing freshwater mixed with contaminated sources. The rest of the BH-Kano plain, BH-Public and BH-Ahero displayed a Na^+-K^+-Cl^--SO_4^{2-} or Na^+-K^+-Cl^--NO_3^- water type.

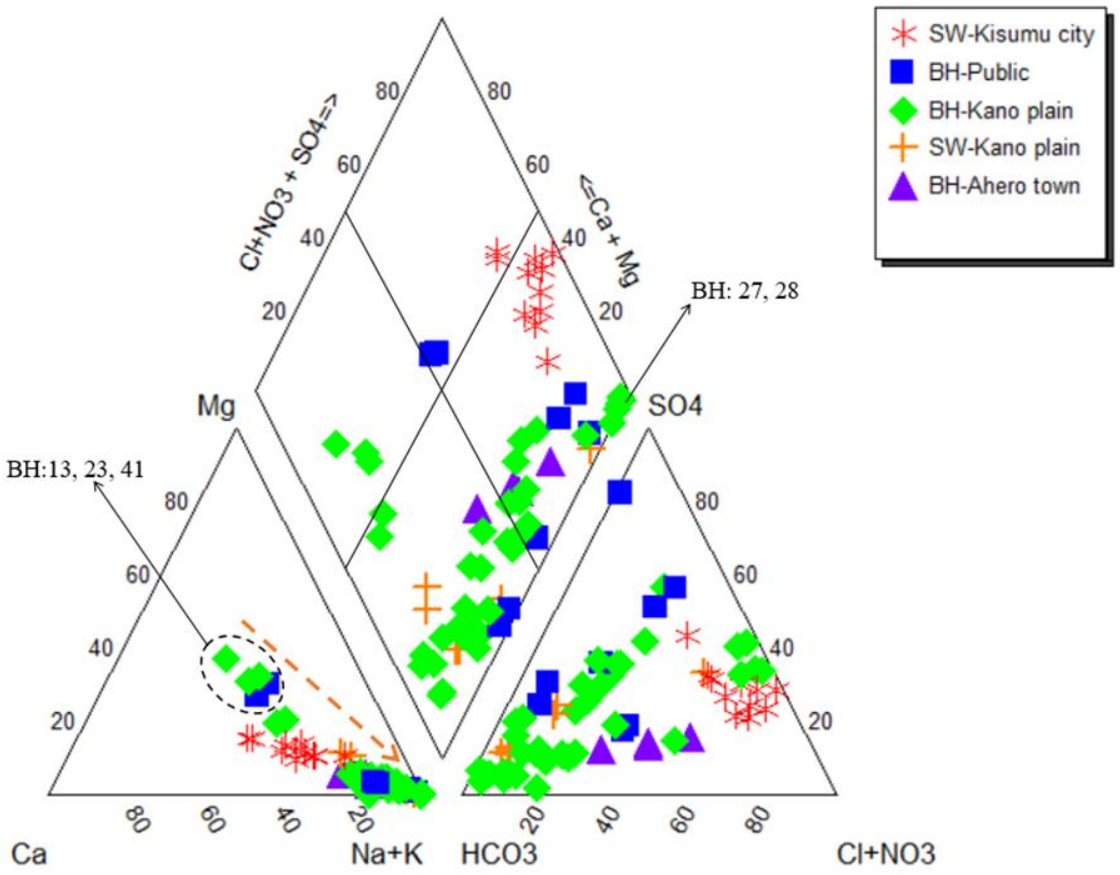

Figure 4.2. Piper diagram representation of major cations and anions (in % meqL^{-1}) for water characterization. Samples are categorized as, SW-Kisumu city: shallow wells located in Kisumu city; SW-Kano plain: shallow wells located in Kano plain; BH-Ahero town: boreholes located in Ahero town; BH-Public: boreholes in public institutions located in populated neighborhoods; and BH-Kano plain: boreholes located in the Kano plain. BH 13, 23, 41 are located near Nandi/ Kisian hills; BH 27 & 28 are located in Awasi town; dotted brown arrow shows increasing groundwater mineralization.

4.3.2 Spatial groundwater NO_3^- distribution and its controlling factors

Figure 4.3 presents the spatial NO_3^- concentration ranges (averaged over the wet and dry seasons) obtained in the boreholes and shallow wells. It was observed that the highest NO_3^- concentration in shallow wells, above the WHO limit (50 – 91 mg L^{-1}) were mainly recorded in Kisumu city. These accounts for 70% of the shallow wells sampled in the city and are located in informal settlements (Ombuga, Nyalenda, Manyatta) where locals depend on shallow groundwater because of low costs associated with their construction (Wright et al., 2013). The rest of the shallow wells in the city had NO_3^- concentrations ranging between 10 – 50 mg L^{-1}

and are situated in newly planned but also highly populated estates (Kibos, Migotsi). Kisumu is a densely populated city in Kenya with an average city population density of 2375 people per km^2, compared to Kenya's average density of 82 people per km^2 (KNBS, 2019). Because of the limited sewerage infrastructure network in Kisumu, untreated sewage discharges into urban streams is common. In addition, the majority of the urban population living in the informal settlements use pit latrines (Wright et al., 2013). This can easily result in leaching of NO_3^- into the unconfined shallow aquifer system of the city. The SW-Kano plain had lower NO_3^- concentrations with most these wells recording values < 10 mg L^{-1} except for SW 17, and 18 which gave > 10 mg L^{-1} during the wet season. During the dry season, however, a general decrease of NO_3^- concentrations was observed in shallow wells to values ranging between 0.04 and 38.2 mg L^{-1} (Table 4.1).

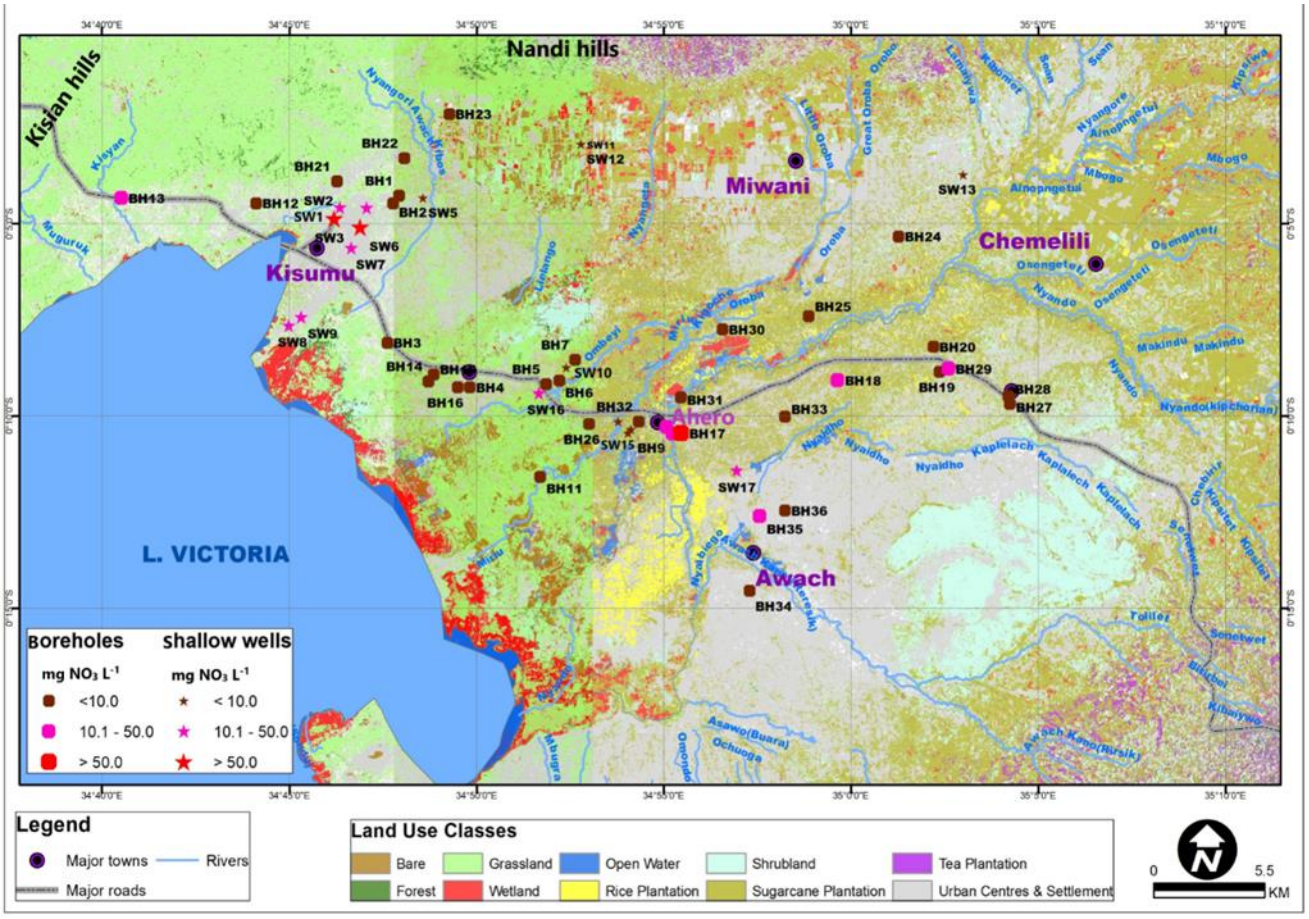

Figure 4.3. Spatial groundwater NO_3^- concentration (average of wet and dry seasons) map of the study area represented in ranges by bullet sizes; squares for boreholes, stars for shallow wells.

On the other hand, NO_3^- concentrations in boreholes varied spatially with BH-Ahero town samples recording significantly higher NO_3^- concentrations (20.0 – 69.9 mg L^{-1}) in both

seasons, than those located elsewhere in the study area. The relatively high NO_3^- in Ahero, where one exceeded the WHO threshold should raise concern regarding NO_3^- pollution management in the town because the three main water supply wells to the town were sampled. Two of them belong to the local water service provider and the third is run by a faith-based organization. Ahero is a highly populated town located along the busy Kisumu – Nairobi highway and totally lacking a conventional sewage management system. In addition, irrigation rice farming is the common agricultural activity around Ahero (See Fig. 4.1b) and uses water from the river Nyando, implying that the use of inorganic fertilizers (i.e. $(NH_4)_2SO_4$) may also be contributing to the observed NO_3^- levels. NO_3^- concentrations ranging from 10 to 50 mg L^{-1} in boreholes were measured in public schools and in a community water supply (BH: 7, 13, 18, 29, 35).

The lowest NO_3^- concentration in boreholes < 10 mg L^{-1} were recorded mainly in the less populated parts of the Kano plain, which spans from the outskirts of Kisumu, the sugarcane belt and the recharge areas near Nandi hills (Fig. 4.3). Based on Figure 4.2, the low groundwater NO_3^- range belongs to the Ca^{2+}-Mg^{2+}-HCO_3^- and Na^+-K^+-HCO_3^- water types which reveals either a dilution from the low NO_3^- recharging water or background NO_3^- levels. But, as water changes to Na^+-K^+-Cl^--SO_4^{2-} or Na^+-K^+-Cl^--NO_3^- type, NO_3^- concentration increases tremendously to levels > 20 mg L^{-1}. This points out to urbanization and human population pressure as the key drivers to groundwater NO_3^- increase in the study area. The low NO_3^- (<1 mg L^{-1}) reported in the Awasi boreholes (BH 27, 28) is due to its confined and thick aquifer occurring at depths greater than 150 m (Olago, 2019)

4.3.3 Use of multi isotope and hydro-chemical methods to track sources of groundwater nitrate contamination and removal

For the implementation of effective NO_3^- pollution control strategies, spatial water quality data alone is not sufficient without identifying the potential NO_3^- sources and associated biogeochemical processes controlling groundwater NO_3^- concentration. In order to identify the sources of groundwater NO_3^- input, $\delta^{15}N$-, $\delta^{18}O$-NO_3^- values of boreholes and shallow wells, in addition to those of the potential NO_3^- sources from the study area were determined. Isotopic values obtained for the local NO_3^- sources: manure and sewage, soil N, precipitation, NO_3^- fertilizer, and NH_4^+ in fertilizer and rainfall (Fig. 4.4) were found to be within the literature ranges (Kendall et al., 2007; Mayer et al., 2001; Xue et al., 2009). The $\delta^{15}N$-NO_3^- in boreholes

ranged from +4.1 to +25.8‰ and from +6.9 to +32.2‰ in wet and dry seasons, respectively. In shallow wells, $\delta^{15}N\text{-}NO_3^-$ ranged from +8.0 to +28.9‰ and from +12.4 to +51.8‰ during the wet and dry seasons, respectively (Table 4.1). $\delta^{18}O\text{-}NO_3^-$ in boreholes, on the other hand, ranged from -2.4 to +20.8‰ and from -1.7 to +24.1‰ during wet and dry seasons, respectively, while in shallow wells, it ranged from +7.5 to +19.8‰ and from +12 to +29.3‰ during the wet and dry seasons, respectively.

A $\delta^{15}N$ vs. $\delta^{18}O$ plot of the groundwater samples during wet and dry seasons (Fig. 4.4) clearly shows that the majority of the groundwater samples lie in the manure and/or sewage source range. However, a few exceptions of the BH-Kano plain samples (BH: 7, 18, 20) (see Fig. 4.3) plotted in the mixed soil N and NH_4^+ in fertilizer and rainfall source range during the wet season. Isotopic enrichment with population density is evident from Figure 4.4 as shown by all the SW-Kisumu city, BH-Public and BH-Ahero town samples. These are the high population density areas (827 – 4737 people per square kilometer) which gave significantly higher $\delta^{15}N$ values ($p < 0.0001$: wet & dry seasons) compared to the Kano plain (BH-Kano plain and SW-Kano plain), an area with a lower population density ranging 234 – 362 people per square kilometer (KNBS, 2019). In addition, the SW-Kisumu city and BH-Ahero town with enriched $\delta^{15}N$ also recorded relatively high NO_3^- concentrations above 20 mg L^{-1} (Fig. 4.3, 4.4). This is an indication that sewage, characteristically enriched in $\delta^{15}N$ (Xue et al., 2009), is likely the driving force to groundwater NO_3^- contamination in the major urban areas. A gradual enrichment in $\delta^{15}N$- and $\delta^{18}O\text{-}NO_3^-$ is observed in both boreholes and shallow wells moving from the wet to dry season (Fig. 4.4).

The isotopic enrichment observed in the dry season was accompanied by a NO_3^- decrease in all of the SW-Kisumu city samples and some of the BH-Kano plain (BH: 1, 7, 18, 20, 29) (Fig. 4.5). This indicates that *in situ* NO_3^- attenuation via denitrification is taking place in the groundwater points during the dry season. Kinetic isotope effects during denitrification preferably convert lighter isotopes (^{14}N and ^{16}O) to N_2 and N_2O, causing an enrichment of the heavy isotopes (^{15}N and ^{18}O) in the residual NO_3^- (Fukada et al., 2003; Mayer et al., 2002). It is also clear that denitrification was more pronounced in SW-Kisumu city, with high NO_3^- concentrations in the wet season.

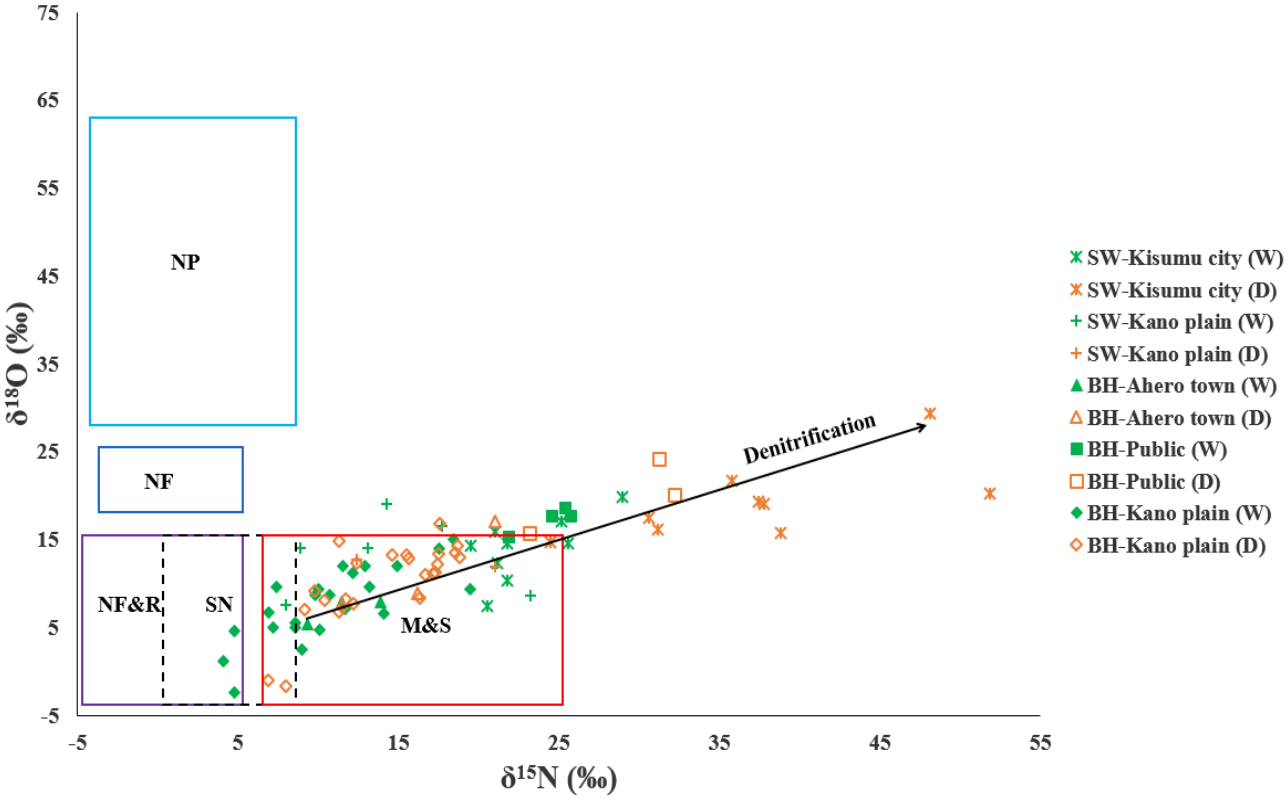

Figure 4.4. $\delta^{15}N$- vs. $\delta^{18}O$-NO_3^- plot of groundwater samples categorized as, SW-Kisumu city: shallow wells located in Kisumu city; SW-Kano plain: shallow wells in Kano plain; BH-Ahero town: boreholes in Ahero town; BH-Public: boreholes in public institutions located in populated neighborhoods; and BH-Kano plain: boreholes in Kano plain, during wet (green symbols) and dry (brown symbols) seasons. Boxes represent $\delta^{15}N$- and $\delta^{18}O$-NO_3^- ranges of local NO_3^- sources: NO_3^- in precipitation (NP), NO_3^- fertilizer (NF), NH_4^+ in fertilizer and rainfall (NF&R), soil N (SN), manure and sewage (M&S). Black arrow indicates a denitrification vector for the increasing $\delta^{15}N$ and $\delta^{18}O$

Based on Figure 4.4 and 4.5, it appears that denitrification may also be responsible for the low NO_3^- concentration (but high $\delta^{15}N$ and $\delta^{18}O$) values recorded in the BH-Public samples during both wet and dry seasons. In addition, a general linear relationship indicating an enrichment of $\delta^{15}N$ relative to $\delta^{18}O$ by a factor of between 1.3:1 and 2.1:1 supports evidence for *in situ* denitrification (Mengis et al., 1999). Figure 4.4 shows a linear relationship between $\delta^{15}N$ and $\delta^{18}O$ ($\delta^{18}O = 0.5\ \delta^{15}N + 2.9$, $R^2 = 0.7$) for all groundwater samples. The slope reveals an enrichment of $\delta^{15}N$ relative to $\delta^{18}O$ by a factor of 2:1 which is characteristic of denitrification (Mengis et al., 1999; Sacchi et al., 2013; Seiler, 2005). Previous work done in the region by Nyilitya et al. (2016) and involving one of the BH-Public wells (BH11, Fig. 4.3), obtained $\delta^{15}N$ and $\delta^{18}O$ values of 18±1.2‰ and 20±0.2‰ respectively for the well, and a corresponding NO_3^- concentration of 0.6 mg L^{-1}. In comparison to Nyando river and boreholes located in the

headwater catchments, the BH-Public well had low NO_3^- concentration and showed a linear isotopic enrichment which the authors attributed to denitrification.

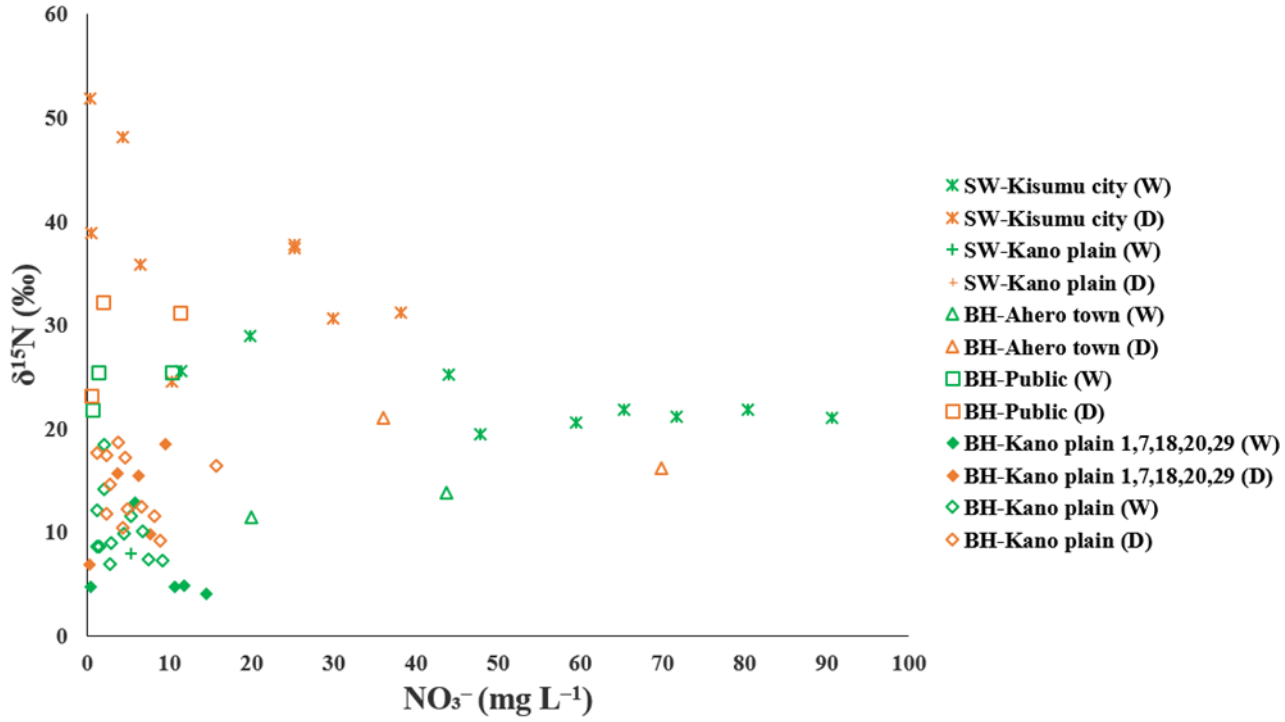

Figure 4.5. NO_3^- concentrations vs. $\delta^{15}N\text{-}NO_3^-$ of groundwater samples categorized as, SW-Kisumu city: shallow wells located in Kisumu city; SW-Kano plain: shallow wells in Kano plain; BH-Ahero town: boreholes in Ahero town; BH-Public: boreholes in public institutions located in populated neighborhoods; BH-Kano plain: boreholes in Kano plain; and BH-Kano plain 1,7,18,20,29: boreholes in Kano plain showing NO_3^- decrease with $\delta^{15}N\text{-}NO_3^-$ increase, during wet (green symbols) and dry (brown symbols) seasons.

A NO_3^- vs. Cl^- concentration plot is another effective tool to distinguish NO_3^- reduction by a biogeochemical processes from dilution (Altman and Parizek, 1995; Mengis et al., 1999). The method is quite useful in cases where two water masses from different groundwater flow paths containing different NO_3^- and Cl^- concentrations mix, and assumes that Cl^- is a conservative element unaffected by the biogeochemical processes occurring in groundwater (Altman and Parizek, 1995). A plot of NO_3^- vs. Cl^- is shown in Figure 4.6 and a theoretical dilution line generated by joining the largely unpolluted BH-Kano plain to most polluted SW-Kisumu city as end members. Any groundwater resulting from the mixing of the two end members should lie closely to this line. On the other hand, groundwater affected by NO_3^- removal via denitrification should appear below the theoretical dilution line due to NO_3^- removal alone (Mengis et al., 1999). In the current study, samples lying along this line consist of SW-Kisumu city (wet season) and BH-Ahero town (wet & dry seasons), both of which were on the high

NO_3^- and Cl^- concentration range. Along this line were also the boreholes in low NO_3^- and Cl^- concentration range which were located in the recharge (Nandi hills) areas and the sparsely populated parts of Kano. The samples plotting along the Cl^- axis (Fig. 4.6) which include the Awasi boreholes with high Cl^- but significantly low NO_3^- may mainly be portraying a salinization effect. At the same time several samples lie below the theoretical mixing line showing a significantly lower NO_3^- concentration than would be expected if dilution was the only controlling factor for NO_3^- concentration. Samples clearly indicating the NO_3^- reduction process of denitrification includes: all the SW-Kisumu city (dry season), BH-Public (BH: 11, 26, 32) and one of the BH-Kano plain (BH: 31). Together with the low NO_3^- concentration, the samples recorded highly enriched $\delta^{15}N$ values (Fig. 4.5), thus corroborating denitrification as a key process responsible for the NO_3^- reduction.

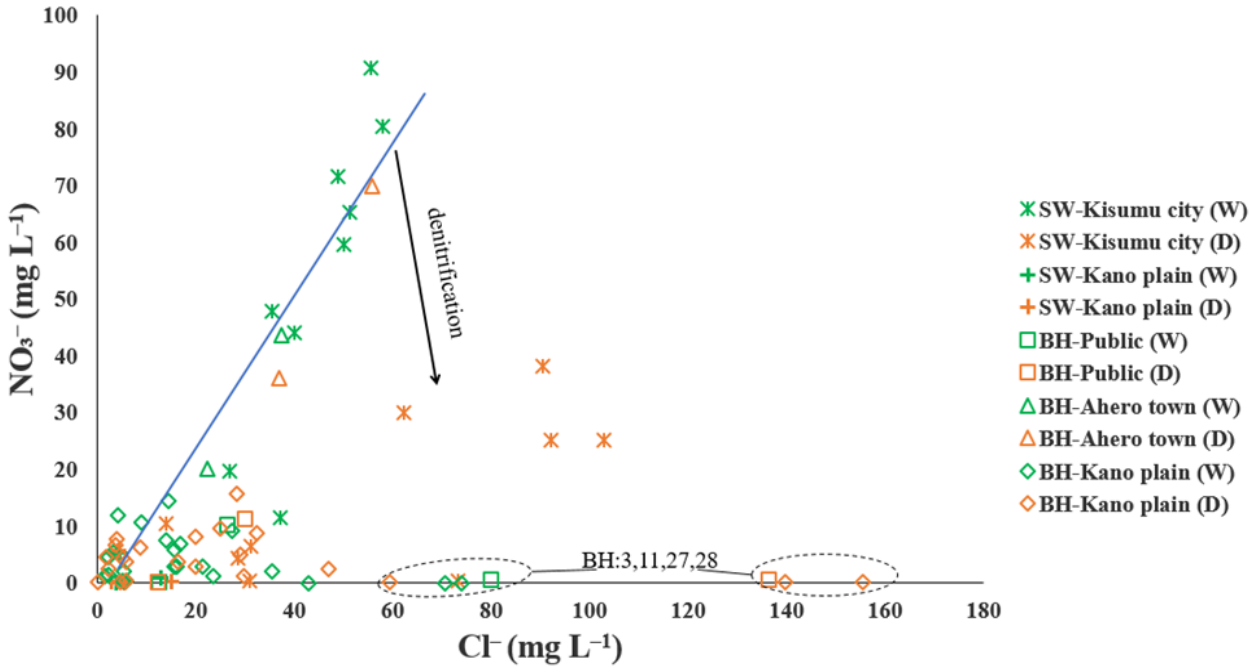

Figure 4.6. Cl^- vs. NO_3^- concentrations of groundwater samples. SW-Kisumu city: shallow wells located in Kisumu city; SW-Kano plain: shallow wells in Kano plain; BH-Ahero town: boreholes in Ahero town; BH-Public: boreholes in public institutions located in populated neighborhoods; and BH-Kano plain: boreholes in Kano plain, during wet (green symbols) and dry (brown symbols) seasons, for determination of NO_3^- removal mechanisms. Blue line is the dilution line, while the black arrow indicates samples undergoing NO_3^- removal through denitrification.

Based on Figures 4.4, 4.5 and 4.6, it can be concluded that denitrification was responsible for NO_3^- attenuation observed in all the SW-Kisumu city (dry season), BH-Public (both seasons) and several of the BH-Kano plain (BH: 1, 7, 18, 20, 29, & 31) samples. It is noteworthy that

the data indicates denitrification occurring in oxic conditions (DO ≥ 1.6 in dry season), however, it has been demonstrated that groundwater denitrifiers can be active in anoxic microsites while the bulk of groundwater is well oxygenated (Koba et al., 1997). In the case of BH-Ahero town, an increasing NO_3^- concentration corresponding to $\delta^{15}N$ increase was observed moving from wet to dry season (Fig. 4.5). This may mean that an enriched $\delta^{15}N$ source is responsible for the $\delta^{15}N$ enrichment as opposed to denitrification, which in this case should be urban sewage source. Furthermore, Figure 4.6 corroborates that denitrification may not be a major process in the BH-Ahero town samples (and confirms sewage source) because they plotted along the dilution line on the high NO_3^- and Cl^- concentration range in both seasons.

The significantly higher NO_2^- content, corresponding to lower NO_3^- content observed in the dry season indicates that denitrification may not be the only N conversion process taking place in groundwater in the study area. Partial nitrification occurs in waste water contaminated systems under high NH_4^+, high temperature and limited oxygen conditions which favours ammonium oxidizing bacteria but inhibits the nitrite oxidizing bacteria, resulting in accumulation of NO_2^- but reduced NO_3^- production in the system (Philips et al., 2002; Wyffels et al., 2003). The fact that most groundwater samples in this study plot in the manure & sewage source domain, coupled with the sanitation problem in the study area imply that sewage (urban and domestic) contamination of groundwater is common. This should result in elevated NH_4^+ concentrations. However, in this study NH_4^+ concentrations are generally low while NO_2^- concentrations are elevated (Table 4.1), indicating that (partial) nitrification is occurring. Although DO levels reported in this study (mean: 4.1 mg O_2 L^{-1}) are somewhat above the 1 mg O_2 L^{-1} threshold reported by Wyffels et al. (2003), for initiating partial nitrification to sustain NO_2^- accumulation, these were snapshot measurements and may therefore vary with time, location and depth. In addition, the relatively higher temperatures (mean: 26°C (SW) and 28°C (BH)) observed in this study is another favorable condition for the high rate of NO_2^- production witnessed (Pynaert et al., 2002; Wyffels et al., 2003). For instance, Pynaert et al. (2002) reported a temperature of 26 ± 1°C as favorable for the high activity of NH_4^+ oxidizing bacteria, resulting into high production of NO_2^-. Hence partial nitrification of sewage derived NH_4^+ may thus be another explanation for low NO_3^- and the significantly higher NO_2^- observed in the dry season. However, further studies are required to establish the inorganic nitrogen dynamics (e.g. nitrification, denitrification, annamox) in groundwater in the area.

To discriminate manure from sewage sources and at the same time overcome any bias in NO_3^- source apportionment, which might have been occasioned by denitrification, boron (B) isotopic values were determined for the three potential NO_3^- sources and for representative groundwater samples. B and $\delta^{11}B$ values were analyzed in a selection of representative groundwater samples from: Kisumu shallow wells located in the informal settlements (SWa); Kisumu shallow wells in newly planned estates (SWb); boreholes in public institutions located in populated neighborhoods (BH-Public); boreholes located in Kano plain (BH-Kano plain) and boreholes situated in the Ahero town (BH-Ahero town).

The boron concentration was highest in the inorganic fertilizers (15–2500 µg L^{-1}) followed by manure (127–581 µg L^{-1}), sewage (25–46 µg L^{-1}) and groundwater (16–34 µg L^{-1}). The $\delta^{11}B$ values of the three sources were: fertilizers ranging from -4.3 to +7.8‰; sewage from +16 to +22‰; and in manure from +31 to +37‰.The fertilizer and manure $\delta^{11}B$ values fall in the literature range of -9 to +15‰ reported by Widory et al. (2005) and Komor (1997) in fertilizers and +15.3 to +42.1‰ reported by Widory et al. (2004) in manure. The sewage $\delta^{11}B$ values obtained in this study were higher than values reported in previous studies (Widory et al., 2013) ranging from -3.5 to +13‰. However, $\delta^{11}B$ of our sources showed clear differences, which allowed contrasts to be made between the three sources.

A plot of $\delta^{11}B$ versus 1/B (Fig. 4.7) show the groundwater samples plot close to the sewage and manure source boxes. The SWa show a strong $\delta^{11}B$ signature of a sewage source while BH-Public and BH-Ahero town also align themselves to the sewage source. The BH-Kano plain and SWb showed a $\delta^{11}B$ signature similar to the manure sources. SWa are located in the densely populated informal settlements (Obunga, Nyalenda, Manyatta) of Kisumu city which lacks formal sanitation systems but are characterized by the use of pit latrines, open defecation and landfills (Okotto-Okotto et al., 2015). In addition, sewer contaminated surface water canals are common whose effluents together with the landfill and pit latrine wastes can easily leach NO_3^- into the city's shallow groundwater. BH-Public are situated in public institutions in populated neighborhoods while BH-Ahero town is located along the Kisumu – Nairobi highway. These two locations also have high pit latrine density (in every homestead and institution) while open surface channels drain the Ahero town effluents due to lack of conventional sewer system.

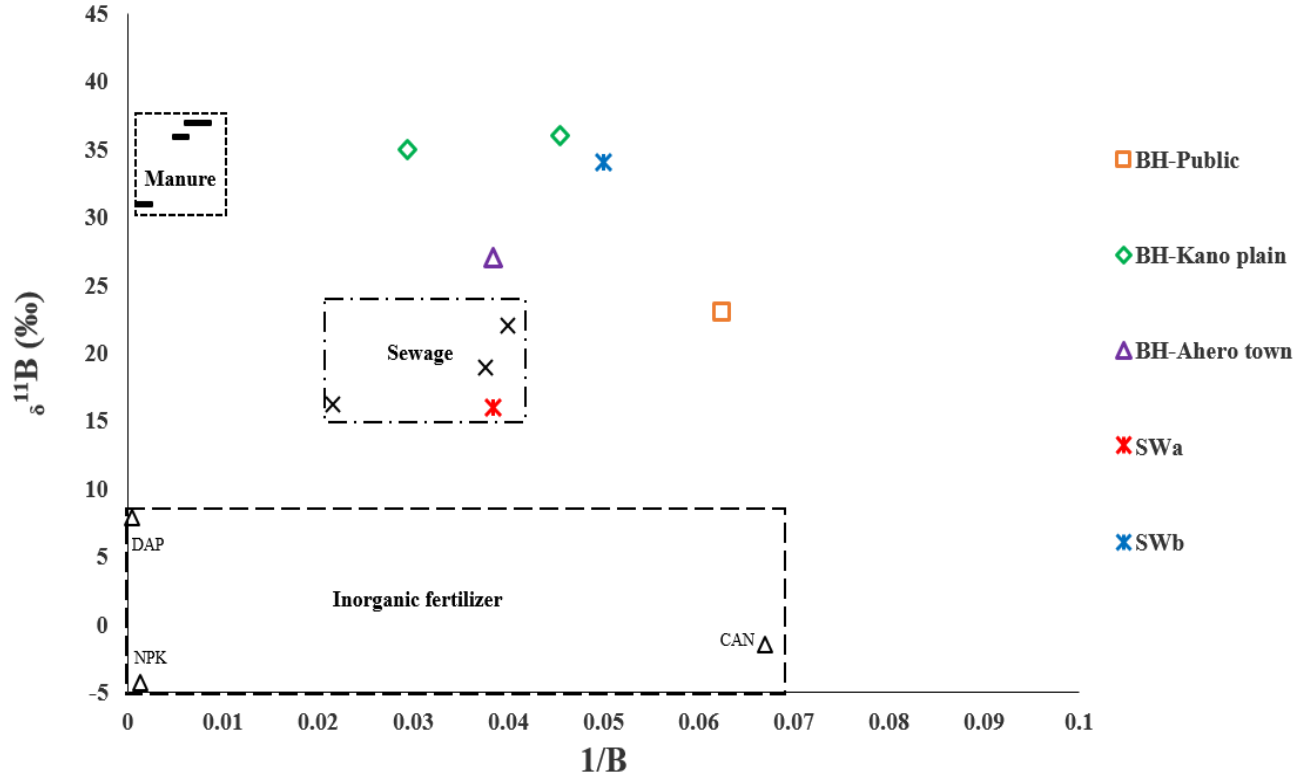

Figure 4.7. $\delta^{11}B$ versus 1/B concentration in selected borehole (BH) and shallow well (SW) samples. Value ranges of local sources of manure, sewage and inorganic fertilizer are shown in boxes. BH-Public: boreholes in public institutions located in populated neighborhoods (brown squares); BH-Kano plain: boreholes located in the rural Kano (green diamonds); BH-Ahero town: boreholes situated in Ahero town (purple triangles); SWa: Kisumu shallow wells located in informal settlements (red stars); SWb: Kisumu shallow wells located in newly planned estates (blue stars).

The lack of proper sanitation systems is the reason why sewage dominates groundwater NO_3^- input in the three locations. This agrees with the highly enriched $\delta^{15}N\text{-}NO_3^-$ values obtained in SWa, BH-Public and BH-Ahero town. SWb on the other hand are located in newly planned estates in Kisumu (Migotsi and Kibos) with high-rise apartments which are connected to the city sewer system. However, these estates neighbor the peri-urban zone of Kibos where small scale mixed farming and free-range livestock keeping are common. BH-Kano plain are situated in the rural parts of the Kano plain characterized by small scale mixed farming of food crops and livestock. Therefore, in the two locations (SWb, BH-Kano plain), animal manure use in farming and free-range livestock keeping, which leaves animal wastes littering streams and the land surface can easily leach NO_3^- into groundwater aquifers. The $\delta^{11}B$ data successfully disentangles the manure and sewage sources and augments hydrochemistry and NO_3^- isotope

findings in identifying the sources of groundwater NO_3^- contamination in Kisumu city and its surroundings.

4.4 Conclusions

A triple isotope approach indicated that NO_3^- contamination of groundwater in Kisumu city and its surrounding is largely driven by inadequate sewage infrastructure and animal manure application from either farming or free-range livestock keeping in the rural areas. However, *in situ* NO_3^- attenuation by denitrification and/or dilution concurrently helps to minimize the NO_3^- loading. On the other hand partial nitrification is likely responsible for accumulation of NO_2^- in the groundwater system. It is however, necessary to develop more process-based research for an in-depth understanding of groundwater N fate in the area. Expansion and improvement of waste water sanitation should urgently be implemented in the region to avoid further deterioration of groundwater sources.

Chapter 5. General conclusions and discussion

This study was motivated by the increasing eutrophication and siltation of the Lake Victoria water resources, which happens against the backdrop of insufficient nutrient data availability especially regarding riverine NO_3^- sources and discharge on the Kenyan side of the Lake. In the preceding Chapters, results of this study are elaborated based on the specific objectives of each research topic. This concluding chapter therefore, highlights the key findings based on the research questions, presents an integrated discussion and finally proposes remedial measures for informing policy, and identifies research and policy gaps for further work.

5.1 Key research findings

A summary of the key findings is presented in response to the research questions of each research chapter.

5.1.1 Land use controls Kenyan riverine nitrate discharge into Lake Victoria – Evidence from Nyando, Nzoia, and Sondu Miriu river basins

The main research questions were: (1) what is the role of land use on river NO_3^- concentrations and sources? (2) are biogeochemical processes affecting NO_3^- concentrations in rivers?

First, because of limited historical river NO_3^- data, in addition to the fact that this study was the first in the basin to integrate isotopic and hydrochemical techniques in water pollution studies, it was crucial to establish baseline hydrochemical and isotopic data. This is presented and discussed in chapter 2 for three river basins: Nyando, Nzoia, Sondu Miriu. Normally, water physico-chemistry is controlled by both natural solutes (from rainfall or geology) and anthropogenic activities. Therefore, spatial (basin-wide) river hydrochemistry data normally describes the key processes influencing the water quality and indicates the land use activities taking place in a river basin (Barakat et al., 2016; Kamtchueng et al., 2016; Zhang et al., 2009). From hydrochemistry data of the three rivers investigated, it is clear that land use patterns influence river water chemistry. This was displayed through hierarchical cluster analysis (HCA) of hydrochemical data from spatial sampling stations of the river basins (Chapter 2).

The HCA analysis resulted into distinct clusters, which matched the main land use characteristics in the river basins. Therefore, the main land use characteristics in the region were identified as: mixed agriculture (MA), residential & industrial (RI), sugarcane (S), tea with forests (TF), commercial agriculture (CA), urban (U), and tea (T).

It has been established that, riverine NO_3^- concentrations in the river basins varied with land use. For instance, the mixed agriculture land use of the Nyando basin, (characterized by mixed farming of crops, horticulture, and free-range livestock keeping) recorded significantly higher NO_3^- discharges compared to the other land use zones in the three river basins. In addition, the urban areas of the Nzoia river and the large-scale tea farming zone of the Sondu Miriu river recorded highest NO_3^- concentrations for their respective river basins. On the other hand, upstream land use zones of the river basins (like tea with forests in Nyando and Sondu Miriu) characterized by low human activities recorded lower NO_3^- concentrations. Therefore, this shows that human population density and intensive agricultural activities are substantially controlling the NO_3^- discharges into the rivers. The isotopic characterization of river water identified the potential sources of river NO_3^- input, which were also observed to vary with land use and river basin. *In situ* attenuation of NO_3^- is happening in the downstream catchments and is likely more intense in the dry season due to longer water residence time (Marwick et al., 2014; Mulholland et al., 2008).

In terms of quality, the river NO_3^- concentrations obtained in this study are below the WHO threshold value (50 mg L^{-1}) for potable use. In addition, other physicochemical parameters (Cl^-, SO_4^{2-}, HCO_3^-, Na^+, K^+, Ca^{2+}, Mg^{2+}, pH, temperature, electrical conductivity, dissolved oxygen) are generally within WHO limits for potable purposes. However, high water turbidity was observed in the rivers especially during the wet seasons.

The three rivers investigated in this study contributes approximately 60% of the total Kenyan catchment inflow into Lake Victoria (LVEMP, 2005). It was therefore necessary to determine their respective NO_3^- loads into the Lake for awareness creation regarding their potential impact

on the Lake water NO_3^- concentrations. This study has established that, the overall riverine NO_3^- delivery into the Lake is governed by river water discharge volumes, basin size, and season. That's why the largest (see chapter 1 for basin areas) and high water-yielding River Nzoia, recorded the highest NO_3^- delivery into the Lake, followed by Sondu Miriu and Nyando river basins in that order. The peak wet season exhibited highest NO_3^- delivery into the Lake attributed to farming activities, while the dry season showed the least. This agrees with earlier findings by Okungu and Opango (2004), which observed River Nzoia as the leading source of nutrient loading of Lake Victoria from the Kenyan side.

The LV basin in Kenya is characterized by a complex land use systems in which, agricultural activities, industries and residences are mixed, or small holder farms encroach forest and wetland areas. The Nyando river exemplifies these LV basin-Kenya land use characteristics, and was therefore selected as a case study for further NO_3^- source apportionment investigations.

5.1.2 Nitrate source apportionment in the complex Nyando tropical river basin in Kenya

The main research questions were: (1) what are the main sources of riverine NO_3^- input in the Lake Victoria basin, Kenya?, (2) what is the proportional contribution of different potential NO_3^- sources?, (3) what is the benefit of integrating isotopic, hydro-chemical and mixSIAR techniques in NO_3^- source apportionment of a tropical SSA river basin?

In a complex land use system like the Nyando river basin, it is complicated to identify clear nonpoint sources of pollution. That's why a multi-tracer technique was applied by coupling hydrochemistry, multi-isotope tracers and a mixSIAR model in this basin (chapter 3). The integration of multi-isotope, hydrochemistry and mixSIAR tools, was effective in constraining the potential sources of river NO_3^- input. The $\delta^{15}N$- and δ^{18}-NO_3^- of the local NO_3^- sources (nitrate fertilizers, ammonium in fertilizer and/or rain, nitrate in precipitation, soil nitrogen, manure and sewage) were determined and found to be within the literature range reported in Kendall et al. (2007), Mayer et al. (2001), and Xue et al. (2009). Boron isotope ($\delta^{11}B$) data was

quite applicable in this study and overcame the limitations faced using $\delta^{15}N$- and $\delta^{18}O$-NO_3^- to discriminate between manure and sewage sources.

The complementary $\delta^{11}B$ data clearly identified manure as the dominant source of river NO_3^- in the mixed agriculture land use of the Nyando basin. From Chapter 2, manure and/or sewage also dominated NO_3^- sources in the mixed agriculture land use zones of both Nzoia and Sondu Miriu river basins. In addition, manure was found to be a major NO_3^- source in the sugarcane and residential/industrial land use zones of the Nyando basin. Sewage was the dominant NO_3^- source in the urban centres of Nzoia and also dominated in the residential/industrial and sugarcane land uses of the Nyando basin during the dry seasons. Inorganic fertilizers on the other hand, were the main sources of river NO_3^- in the large-scale tea and commercial flower farming zones of the Sondu Miriu and Nyando river basins, respectively. Seasonally, inorganic fertilizers were observed to contribute significantly to river NO_3^- input during the wet season in the agriculture-dominated land uses (mixed agriculture, tea, sugarcane, commercial agriculture) of the three river basins. Nitrified organic soil N, on the other hand, was the main source of river NO_3^- input in the tea and forest land use of the Nyando and the small scale tea land use of the Sondu Miriu. The latter are situated in the upstream reaches, which are characterized by tea farms, forests and relatively low population density. Also, nitrified organic soil N was a key river NO_3^- source during the agriculturally dormant 'short rains' season. The Bayesian isotopic mixing model (mixSIAR) output in Chapter 3 augments the isotopic findings and shows that the sources of river NO_3^- follows the order: manure and/or sewage > soil N > ammonium in fertilizer and/or rain > nitrate fertilizer > nitrate in precipitation. Therefore, the application of multi-tracer techniques confirms that manure is the main source of river NO_3^- in the Lake Victoria basin in Kenya. Findings in this study closely match similar work in tropical river basins (Anornu et al., 2017; Minh et al., 2020). The study by Minh et al. (2020) in Day river basin of Vietnam reported dominance of manure and sewage sources during the dry season while inorganic fertilizers were the main river NO_3^- sources during the wet season. The

study by Anornu et al. (2017) in the White Volta river basin in Ghana, identified manure (human and animal wastes) as the dominant sources of NO_3^- contamination into surface water.

5.1.3 Tracking sources and fate of groundwater nitrate in Kisumu city and Kano plains in Lake Victoria basin, Kenya

The key research questions in this topic were: (1) what is the current status of groundwater quality regarding NO_3^-? (2) what are the dominant groundwater NO_3^- pollution sources? (3) Do *in situ* attenuation processes affect groundwater NO_3^- concentration?

Groundwater in the basin is the main water source to the urban slum dwellers and in the rural areas where surface water is inaccessible. In Kisumu and its surrounding Kano plains, groundwater is estimated to account for 30% of potable water supply (Olago, 2019). NO_3^- in groundwater varied spatially with shallow wells located in Kisumu city recording significantly high NO_3^- concentrations than those located in the rural Kano area. On the other hand, boreholes located in Ahero town had significantly higher NO_3^- concentration compared to those located in the rural Kano. About 63% of the boreholes and 75% of the shallow wells exceeded the drinking water WHO threshold for NO_3^- (50 mg L^{-1}) and NO_2^- (0.2 mg L^{-1}) during the study period. This indicates that groundwater NO_3^- concentration is controlled by human population density. However, a significant NO_3^- concentration decrease was observed in the groundwater during the dry season, but with a concomitant increase in NO_2^- concentration. In addition, high fluoride levels were obtained in this study. Mean fluoride values for both boreholes and shallow wells were above the 1.5 mg L^{-1} WHO threshold (Chapter 4). Therefore, the quality of groundwater in the area is generally not sufficient for potable purposes, unless it's treated before use.

Nitrate isotope data ($\delta^{15}N$- and $\delta^{18}O$-NO_3^-) indicated that manure and sewage were the main sources of groundwater NO_3^- input in the area of study. However, further analysis using $\delta^{11}B$ data confirmed that sewage was the dominant NO_3^- source in Kisumu's informal settlements, boreholes located in Ahero town and those located in populated neighborhoods of the Kano

plains. $\delta^{11}B$ data also confirmed that manure was the main NO_3^- source in boreholes and shallow wells located in the Kano area and those in planned estates around Kisumu. Enrichment of $\delta^{15}N$- and $\delta^{18}O$-NO_3^- corresponding to a NO_3^- concentration decrease was observed in the dry season indicating *in situ* denitrification might be responsible for this NO_3^- decrease. However, a partial nitrification process could be taking place concurrently, which might be responsible for the increase in NO_2^- concentrations observed in the dry season. But, this require further studies to be clearly defined.

5.2 Key factors influencing NO_3^- input into surface and groundwater in Lake Victoria basin, Kenya and the necessary remedial measures

This work has provided spatiotemporal whole-river NO_3^- distribution and source data (chapters 2 and 3), which highlights the specific land use zones experiencing increasing NO_3^- discharges and their potential sources. This is unlike previous studies in the Lake Victoria basin, Kenya which were limited to selected sub-basins (Jacobs et al., 2017; Kipkemboi et al., 2014; Masese et al., 2017; Mwanake et al., 2019; Nyairo et al., 2015; Triest et al., 2012). In comparison to other river basin studies in the sub-Saharan Africa (Table 5.1), mean river NO_3^- values obtained in this study are higher than those reported for R. Tana in Kenya (Bouillon et al., 2009), tropical rivers in Zambia (Kennedy et al., 2016), R. Pangani in Tanzania (Selemani et al., 2018), and Senegal river in West Africa (Mbaye et al., 2016). In addition, river NO_3^- in this study is in the range of values reported for the Vaal (Rensburg et al., 2019) and the Mvudi rivers (Edokpayi et al., 2015) of South Africa. However, the Athi-Galana-Sabaki (AGS) river basin in Kenya (Marwick et al., 2014) reported higher NO_3^- values, attributed to high sewage effluents from Nairobi city, where the river has its headwaters. It appears therefore, that river NO_3^- levels in Lake Victoria basin in Kenya tend towards the higher concentration range of SSA river basins.

Table 5.1. Comparison of mean (seasonal) river NO_3^- concentration ranges obtained in this study to other river basin studies in the sub-Saharan Africa region. NO_3^- values represent reported mean concentration range.

River	Country	Nitrate concentration (mg L^{-1})	Reference
Nyando Nzoia Sondu Miriu	Kenya	2.7 – 6.8 1.4 – 3.0 3.4 – 3.8	This study
Pangani	Tanzania	2.1 – 3.1	Selemani et al. 2018
Tana	Kenya	1.2 ± 1.6	Bouilloin et al. 2009
Tropical rivers in Zambia	Zambia	0.3 – 1.4	Kennedy et al. 2016
Athi-Galana-Sabaki	Kenya	8.0 – 12.0	Marwick et al. 2014
Senegal	Senegal	0.2 – 0.8	Mbaye et al. 2016
Vaal	South Africa	1.0 – 5.0	Rensburg et al. 2019
Mvudi	South Africa	1.9 – 8.1	Edokpayi et al. 2015

Conspicuously missing, however, in all these tropical African river basin studies is nutrient source apportionment investigations. Most studies have unjustifiably attributed increasing NO_3^- levels in the rivers to mainly agricultural inputs or urban effluents, without performing dedicated NO_3^- source discrimination amongst the potential sources in the basins (Edokpayi et al., 2015; Mbaye et al., 2016; Rensburg et al., 2019). Conversely, NO_3^- source apportionment has been well addressed in this study.

The increasing NO_3^- discharges observed especially in the highly populated and intensively farmed land use zones of the Lake Victoria basin in Kenya, gives a clear message that intervention measures should be implemented to reverse the trend. As earlier stated in Chapter 1, Lake Victoria Basin Commission (LVBC) coordinates environmental management activities in the basin. In the last decade, the activities of LVBC have been focused on catchment restoration and control of point (nutrient) sources, including: tree planting in deforested zones,

wetland reclamation, and rehabilitation of sewage treatment systems in major towns (WorldBank, 2018). However, the main challenge has been a lack of current long-term and spatiotemporal nutrient concentrations data of the river basins. Therefore, their interventions are based on relatively old nutrient monitoring data (COWI, 2002; LVEMP, 2005). The situation is even more complex due to the fact that dependency on nutrient monitoring data alone is insufficient in identifying the main sources of pollution to a water body (Widory et al., 2013). Unlike the situation in the LVB and the greater part of SSA, nitrate monitoring data and pollution source apportionment investigations in different water bodies are more widespread in other regions (Erostate et al., 2018; Li et al., 2010; Lin et al., 2019; Meghdadi and Javar, 2018; Panno et al., 2006; Soto et al., 2019; Widory et al., 2005; Xue et al., 2012; Zeng and Wu, 2015; Zhang et al., 2018b). As a result, a region like Europe, three decades ago developed and implemented the Nitrate Directive (1991) whose aim is to protect water resources from nitrate pollution sourced from agricultural inputs (EU, 2010). Nevertheless, this study significantly contributes to the pre-existing knowledge gap in the LVB by providing current spatiotemporal nutrient and physicochemical data. It also outlines the main sources of NO_3^- contamination in both surface and groundwater, as well as the proportional source contributions and distributions in surface water. In addition, an onset for a spatiotemporal river water monitoring network, which is based on major land use patterns has been established in this work for river basin monitoring. Such a network will optimize field monitoring campaigns and also enable early detection of pollution hotspots for timely implementation of remediation measures.

The main goal of this work has been targeted to identify the key sources of NO_3^- input into water resources. It has been well established in this study that, manure is a crucial source of NO_3^- input into river water in the Lake Victoria basin in Kenya. Animal manure is the most commonly used fertilizer for improving soil nutrients amongst the majority of farmers who practice mixed farming (Rufino et al., 2006). Since manure is produced at household level, it's freely available and the rates and frequency of application depend on individual farmers who, without guidelines may apply excessively. Nutrient uptake efficiencies from manure fertilizers

is a key factor determining its potential nutrient loss to the environment. Rufino et al. (2006) observed poor nitrogen uptake efficiency from manure in the region. The authors reported uptake of N in maize ranging from 3 – 49%, while in millet it ranged from 9 – 71%. It should be noted that, not all the N which fails to be taken up into plant tissues, is lost. Some is retained in the soil matrix or immobilized by micro-organisms. However, depending on the soil physicochemical characteristics, topography, rainfall intensity and soil cover/land use, low N uptake efficiency may lead to increased N losses to the environment (Xia et al., 2018). This may partly be the reason for the observed dominance of manure-sourced riverine NO_3^- reported in this study. In addition, the mode of manure application in the region is mostly broadcasting before planting. Such practices, especially on sloping and escarpment lands triggers high manure losses into rivers during wet seasons, which are characteristically stormy in the Lake Victoria basin in Kenya.

On the other hand, free range livestock keeping is the most common method of livestock farming amongst the rural-area residents in Kenya (Rufino et al., 2006). This facilitates the spread of animal excreta (feces and urine) over large tracts of land (including wetlands and forests) where the animals roam during feeding. For instance, with reference to a livestock ruminant distribution density map of Kenya (Figure 5.1, adopted from FAO 2017), livestock densities in Lake Victoria basin are in the higher ranges for the country, ranging 100 – 250 and > 250 heads km^{-2}. The 2006 Intergovernmental Panel on Climate Change (IPCC) guidelines for national greenhouse gas inventories, can be applied here to estimate the annual amounts of nitrogen (N) excreted by livestock in the basin. In this case, the Tier 1 approach (IPCC, 2006), was used for calculating the annual nitrogen excretion rates for each livestock type via the equation:

$$N_{ex(T)} = N_{rate\,(T)} * \frac{TAM}{1000} * 365 * n_T \qquad 5.1$$

Where: $N_{ex(T)}$ is the annual N excretion for livestock type T, kg N yr^{-1}; $N_{rate\ (T)}$ is the default N excretion rate, kg N (1000 kg animal mass)$^{-1}$ day^{-1}; TAM is the typical animal mass for livestock type T, kg animal^{-1}; and n_T is the total number of livestock type T in the basin.

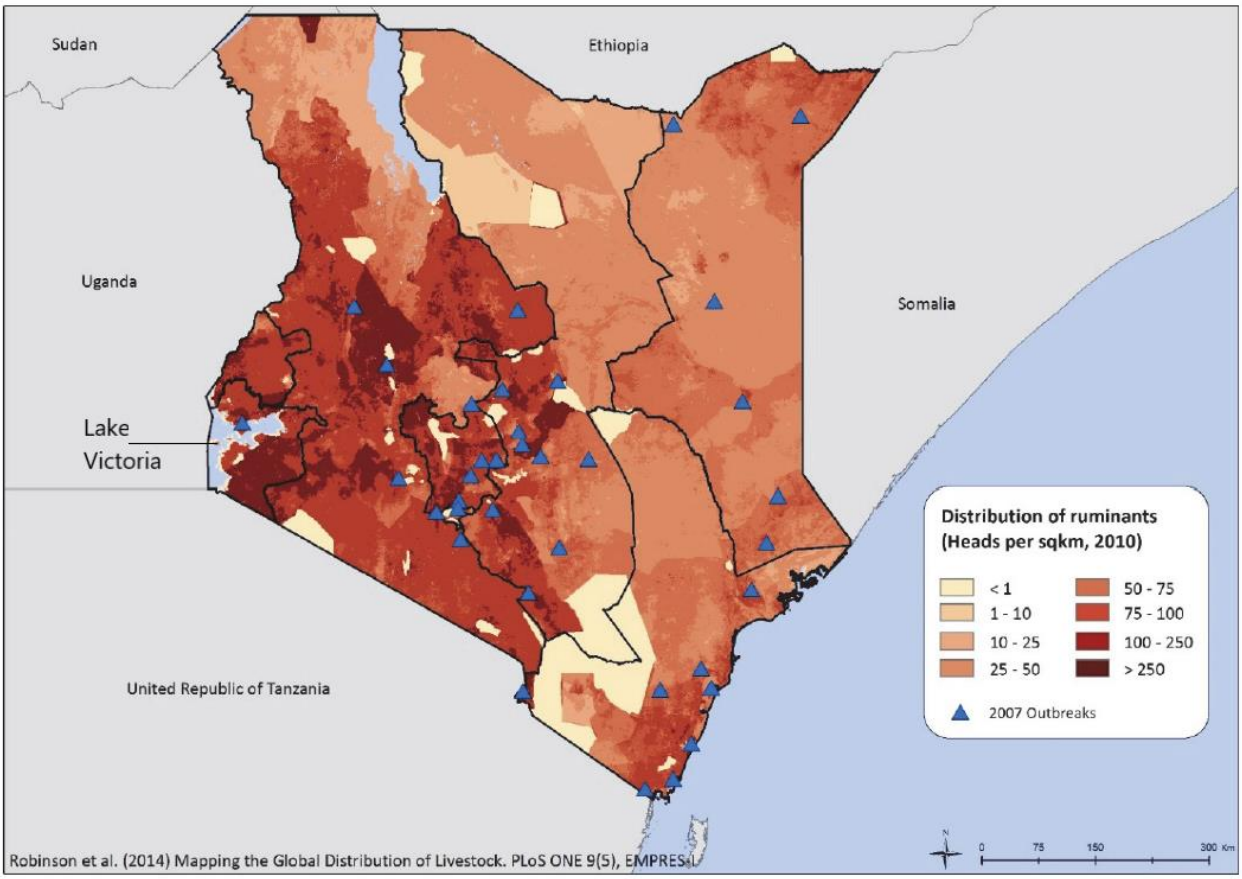

Figure 5.1 Livestock ruminant distribution map of Kenya, showing relatively higher density in the areas surrounding the Lake Victoria (Adopted from FAO, 2017; Robinson et al., 2014).

We used the default N_{rate} and TAM for African cattle, sheep and goats provided in IPCC (2006). In addition, the available Kenya National Bureau of Statistics (KNBS, 2009) figures for cattle, sheep and goats in the Lake Victoria basin counties of Kenya were used, and the $N_{ex(T)}$ for each of the three livestock types were determined using equation 5.1. Consequently, the sum total N excreted annually by these three most common livestock types in the basin per unit area amounts to approximately 63 kgs ha^{-1} yr^{-1}. This is the amount of N in animal manure, which is already more than double the average inorganic fertilizer N use in Kenya, estimated to be < 30 kg ha^{-1} (Masso et al., 2017). Most of this N is either applied in the farms as manure

or dropped on land surfaces (feces and urine) by the freely moving animals during feeding. The animal droppings will either leach or be deposited into rivers through runoff. In addition, the animals are watered directly inside the rivers and ends up contaminating the river water with these nitrogen-rich wastes.

Indeed, livestock keeping and manure use in agriculture are key for attaining Kenya's food security and economic growth goals. However, the impacts of manure and its potential threat to fresh water availability and security cannot be ignored given that Kenya is a water scarce country (JICA, 2013). Therefore, the following measures needs to be implemented: (1) development of 'good manure use guidelines' in order to optimize its use in agriculture while at the same time ensuring water resources quality, (2) enhancement of existing environmental and water resources management regulations by restricting the direct watering of livestock in surface water, (3) implementation of better animal husbandry methods which controls the spread of animal wastes, like paddocking or zero grazing. Such methods will not only control water pollution but also lead to improved livestock productivity.

Sewage is the other major source of NO_3^- contamination in both groundwater and surface water of the region. Sanitation is a major problem especially in the urban areas of the LV basin in Kenya. Although sewage treatment systems exists in the major towns (Kisumu, Eldoret, Kakamega, Bungoma), the high rate of urban population growth has not been matched with corresponding improvement in the sewage management infrastructure (White et al., 2017). As a result, the sewage systems are overstretched and often discharges partly treated waste water into fresh water resources (Juma et al., 2014). The sanitation situation in the towns is made worse by the proliferation of informal settlements, which are not connected to the formal sewage systems, but rely mainly on pit latrines (Okotto-Okotto et al., 2015; Wright et al., 2013). This ends up contaminating the surrounding groundwater as proven in this work by the high NO_3^- and sewage-contaminated groundwater in Kisumu city and Ahero town. In addition, waste water treatment plants of several manufacturing industries in the basin have been

reported to discharge high nutrient containing effluents into river basins and the Lake (LVEMP, 2005; Omosa et al., 2012).

Sanitation is a common problem in the Lake Victoria basin, and other studies in the basin have associated sewage as the main source of NO_3^- input into surface and groundwater (Kabenge et al., 2016; Nyenje et al., 2013, 2010). It is reported that in SSA cities, less than 30% of waste water is treated in formal sanitary facilities, while the remainder is disposed either through onsite systems (septic tanks, pit latrines) or directly into surface water resources (Nyenje et al., 2010; White et al., 2017). This common occurrence in SSA, according to White et al. (2017), is caused by rapid urban growth without proper planning and investment in infrastructural services. SSA cities have been growing fast, at an average rate of 4% compared to the global average of 1.5% (WHO, 2015). However, the overall capital investments in infrastructure remains low, at 20 % of GDP. Just as World Bank (2012) stated, there is a significant risk that cities in the SSA region may become locked up into a "grow dirty now, clean up later" development path. This is counterproductive in the long run because it leads to negative socio-economic impacts like: increased costs of water production, deterioration of human health, damage to infrastructure and loss of biodiversity. To some extent, these impacts are being witnessed already in the Lake Victoria basin, Kenya. There is therefore an urgent need for policy institutions to improve on their urban planning, development and environmental management decisions in order to contain sewage pollution of water resources.

For the protection of water resources from sewage pollution in the region, the following measures should be considered: (1) technological advancement and expansion of the existing waste water treatment infrastructure in order to serve the unconnected areas, especially the urban slums, (2) environmental and sanitation awareness campaigns to slum dwellers and provision of incentives to develop formal (but affordable) housing, (3) a ban on both the construction of pit latrines and the potable use of shallow groundwater in cities, (4) formal treatment of borehole water before use, and (5) expansion of the surface water (i.e. from Lake Victoria) treatment capacity to increase water supply in slums and rural areas. In addition,

manufacturing industries in the LVBK should have an operational effluent treatment system while those with existing systems needs technological advancement. The sugar-based industries, have an opportunity in their effluent to produce biogas energy by investing in recent technologies or by linking-up with research institutions.

Soil N was the other key NO_3^- source in surface water after manure or sewage. Because of the human encroachment in forests, wetlands and historical deforestation (LVBC, 2007; Raburu et al., 2012), soil erosion rates tremendously increased in river basins resulting in high sedimentation at the river mouths and the Winam gulf (ICRAF, 2003). Mineralization followed by nitrification is a potential process which takes place in the sediment/water interface and the produced NO_3^- dissolves into the river water column. Therefore, sedimentation potentially increases the river NO_3^- levels. In addition, farming on escarpment and un-terraced lands results in high soil loss through erosion during wet seasons. Consequently, soil erosion aggravates the loss of soil N into surface water. Therefore, concerted efforts by all stakeholders in natural resources are required in order to restore the affected water sources and wetlands like, Mau forest complex, Mt. Elgon forests, Cherengani hills, Kakamega forests, and Nyando and Yala wetlands. This entails intervention measures like resettlement of small holder farmers from forest reserves and wetlands, tree planting and wetland restoration. The existing land and water resources policies in Kenya clearly defines forest reserves and riparian areas as protected lands. However, implementation of these policies have been hampered by lack of political will and land grabbing. These policies needs to be implemented in order to control the soil and nutrient losses being experienced in Lake Victoria basin in Kenya.

Inorganic fertilizers dominated river NO_3^- input in the large-scale tea farms of the Sondu Miriu basin, and commercial farms, e.g. flower production. The farms are operated by multi-national firms (e.g. Unilever, Finlays, etc.) and experience intensive use of inorganic fertilizers to maximize crop productivity. It was also expected that inorganic fertilizers dominates river NO_3^- in the sugarcane land use of the Nyando and the commercial agriculture land use of the Nzoia basin. However, this was not the case. As reported in chapter 2, nitrogen fertilizer application

rates in the commercial tea and horticulture farms were high (ranging between 38 and 75 kg N ha^{-1}) compared to the rates applied in the sugarcane and commercial agriculture land use zones (< 30 kg N ha^{-1}). In addition, the latter zones are intermixed with human settlements, urban centres and agro-based industries which leads to the dominance of manure or sewage sources as opposed to inorganic fertilizers. It appears therefore, that the rate of fertilizer application in addition to presence or absence of other potential NO_3^- sources are controlling factors.

Inorganic fertilizer use in sub-Saharan Africa is low and most of the countries have not even been able to meet the 50 kg nutrients ha^{-1} target set in the 2006 Abuja declaration. For instance the average inorganic fertilizer use in Kenya, is estimated to be < 30 kg nutrients ha^{-1} (Masso et al., 2017). However, as observed in this study, the distribution of fertilizer use varies widely, with the commercial farms having higher use rates, while the small-scale farms (which form the majority) have relatively low use rates. There is therefore, need for the development and implementation of fertilizer use and management guidelines in the basin. First of all, such guidelines should be aligned to the 4R nutrient concept which ensures improved nutrient use efficiency and environmental sustainability (Johnston and Bruulsema, 2014). The 4R nutrient guideline refers to, applying the Right source of nutrients, at the Right rate, at the Right time, and in the Right place. Due to the different application rates observed in the basin, fertilizer management practices may vary with the location. The commercial tea and horticultural farms should develop a centralized waste water treatment and management system to treat their waste water before discharging into rivers. Specifically, commercial farms under intensive use of inorganic fertilizers and other agrochemicals (e.g. greenhouse farming) should install tile drainage systems to collect all farm drainage water for treatment. However, these would require efficient monitoring (for compliance) by the responsible agricultural, water and environmental regulatory authorities in Kenya. Although inorganic fertilizer-use in small to medium scale farms is currently low, it is expected to increase because of the food security goals of the country. Therefore, early development of best fertilizer management practices, and awareness creation to farmers, would ensure minimum nutrient losses into river water.

5.3 Research gaps and future perspectives

5.3.1 Biogeochemistry research

The overall objective of this work was to identify and apportion the sources of excess NO_3^- discharge into the water resources of Lake Victoria basin in Kenya. This information is useful to underpin decision support tools for improved nutrient management in the basin. Here, substantial data and information has been generated for the inorganic nutrient species (NO_3^-, NO_2^-, NH_4^+, and PO_4^-) in the Kenyan part of the basin. However, these are just a fraction of the total nitrogen (N) and phosphorus (P) lost through the river basins. Further studies should be undertaken in the basin to monitor dissolved organic nitrogen (DON), dissolved organic phosphorus (DOP), inorganic and dissolved organic carbon (DOC) which have not been covered in this work. Additionally, in view of the high rate of soil erosion and sedimentation experienced in the basin (chapter 1), studies on the particulate inorganic and organic nutrients (N, P, C) are long overdue. Therefore, in efforts towards establishing a riverine nutrient distribution map and budget for the Kenyan side of the basin, the following future study approach is proposed:

(1) Studying the spatiotemporal concentrations, discharge and cycling of dissolved organic N, P and C in addition to the particulate N, P, and C in the Nyando, Nzoia, and Sondu Miriu river basins;
(2) Determination of nutrient sources, distribution, discharge and cycling in the remaining rivers of the Lake Victoria basin in Kenya (chapter 1), i.e. Rivers: Yala, Gucha, Mara, Sio, North Awach and South Awach;
(3) Generating a riverine nutrient distribution map and budget for the Lake Victoria basin in Kenya and proposing policy guidelines.

Phosphorus is the other major nutrient associated with the eutrophication of the Lake Victoria (Gikuma-Njuru and Hecky, 2005; Lung'ayia et al., 2001; Sitoki et al., 2010), therefore, the understanding of its potential sources of pollution will greatly boost nutrient control efforts in

the basin. Future nutrient pollution source monitoring studies should integrate the stable isotope of phosphate ($\delta^{18}O\text{-}PO_4^{3-}$) for tracking sources of phosphorus discharge into surface and groundwater in the basin. Unlike N and C, phosphorus has only one stable isotope (^{31}P), therefore P-isotopes cannot be used to understand P systematics in the environment in a similar manner as used for N and C. However, P occurs in nature primarily as *ortho*phosphate (PO_4^{3-}) which permits use of the stable isotope ratios of oxygen in PO_4^{3-} as a potential stable isotope tracer of P in the environment (Davies et al., 2014; Jaisi and Blake, 2014; McLaughlin et al., 2006). Research studies have demonstrated that different phosphate sources (inorganic fertilizers, sewage, detergents, manure) have distinguishable $\delta^{18}O\text{-}PO_4^-$ values, and by tracking of $\delta^{18}O\text{-}PO_4^-$ in water, contrasts have been made between its potential sources (Granger et al., 2017; Tian et al., 2016; Young et al., 2009). In addition, $\delta^{18}O\text{-}PO_4^-$ values helps in understanding the biogeochemical cycling of P in the environment (Davies et al., 2014; Jaisi and Blake, 2014; McLaughlin et al., 2006).

Biogeochemical processes of inorganic N species (nitrification, denitrification, annamox, etc.) have been identified as potential processes influencing NO_3^- concentration in water resources of the basin. In this work, the occurrence of denitrification as potential process attenuating NO_3^- in surface and groundwater was tested through laboratory incubation experiments of river bed sediments, isotopic ($\delta^{15}N\text{-}NO_3^-$ versus $\delta^{18}O\text{-}NO_3^-$) and hydrochemical ($NO_3^-$ versus Cl^-) correlations. However, these processes require further studies. For rivers and wetlands, studies can be carried out using ^{15}N as a tracer for determination of a single or simultaneously occurring biogeochemical processes under relatively natural conditions. The technique entails the introduction of a known quantity of ^{15}N (normally $^{15}NO_3^-$) into a wetland or riverbed system (e.g. sediment core), and then measuring the concentration of the produced ^{15}N-labelled N_2 gas (Huygens et al., 2013). The N_2 production shows an active NO_3^- reduction process via denitrification and/or annamox, whose relative potential contributions can be determined (Risgaard-Petersen et al., 2003; Thamdrup and Dalsgaard, 2002). Further confirmation of the

annamox process by this technique is done by the introduction of a known quantity of $^{15}NH_4^+$ into the system followed by the determination of ^{15}N in the produced N_2 gas.

Nitrous oxide (N_2O) is a potential product of the denitrification process, and a greenhouse gas linked with the depletion of the stratospheric ozone. Greenhouse gas emission investigations should be incorporated in future studies in order to understand the significance of the basin in terms of greenhouse gas emissions. The key wetlands, like the Nyando and Yala, should be targeted for biogeochemical investigations and greenhouse gas emission studies in order to establish their N-removal and -retention capacity and significance as nutrient buffer zones. Similarly, process-based studies (nitrification, denitrification, annamox) should be conducted in different groundwater aquifer systems in the basin. All these biogeochemical investigations should establish the favorable or limiting conditions required for the processes to take place and test for the nitrifying, denitrifying and anammox microbial community composition.

5.3.2 Sustainable management

The sustainable use and protection of the Lake Victoria basin water resources in Kenya and other countries can only be achieved through a robust framework of integrated and adaptive water resources management planning. One of the principles of Integrated Water Resources Management (IWRM) is the devolvement of decision-making to the lowest appropriate level, and recommends that, the river basin should be the logical unit for water resources management (Lankford et al., 2007). According to the Kenyan Water Law (Water Act 2016, Section 27), the management of river basins is under the Basin Water Resources Management Committee, which works under the regulations made by the Water Resources Authority (WRA). However, there is no clear or specific strategy for sustainable river basin management. There is need, therefore, to develop a river basin management plan in order to promote water resources management and service provision at the river basin unit. This minimizes red tape procedures characteristic of centralized systems and enables timely identification of problems and formulation of solutions that work effectively. Therefore, the implementation of a river basin

management plan would be a key milestone towards achieving the sustainable development goal number six ("universal access to water and sanitation") in the country. However, the development of an effective and integrated river basin management plan should be informed by scientific data and information. From the experience gained through this work in the Lake Victoria basin, and with reference to frameworks from developing countries (Avagyan et al., 2014; Lankford et al., 2007), the first important and scientifically-informed step in a river basin management plan should be as follows.

5.3.2.1 River basin characterization

This is a multi-disciplinary review of physical, biological, geographic, social, economic and water use aspects of a river basin. It involves maps describing location, hydrography, topography, ecology, vegetation and climate data of the basin. A description of the geology, hydrogeology (major aquifers, springs, and wells), soils, and land use characteristics with maps is very important. Spatiotemporal water quality data of surface water in the basin (rivers, lakes), and groundwater (boreholes, springs) should be well presented and analyzed. It should highlight both the point and nonpoint sources of pollutants in the basin. Socio-economic characterization of the river basin on the other hand, includes a description of the pressures on a basin's water resources, like human population density, agricultural and industrial development, economic activities and infrastructure. These factors are the key drivers determining the water use and allocation in a river basin. Water use characterization should include abstraction and wastewater discharge data by the main sectors of water use in the basin including, municipal, domestic, agricultural, industrial, fisheries, recreational and hydropower. This socio-economic characterization should assess the employment, income, and the water resource impacts on the main sectors of the economy in the river basin. The water use characterization, land use characteristics and river hydrology are main factors which affect water quality and quantity of the river basin. This has been manifested in this study where urbanization and intensive agricultural practices (like commercial tea and flower farming) were

the lead drivers of increasing NO_3^- deposition in surface and groundwater. Therefore, the Ministry responsible for water resources management in Kenya should lead the process of developing the river basin management plan.

5.3.2.2 River basin monitoring

In the Lake Victoria basin and generally the Kenyan water sector, there is currently a weak framework for surveillance and monitoring of water resources, leading to irregular and inadequate data (NWP, 2019). Therefore, an effective water resources monitoring programme, covering both surface and groundwater (quality and quantity) needs to be operationalized. The programme for surface water should at least be composed of:

1) Set up a spatial (land use-based) water sampling network, which should include at least three stations in every land use zone as identified in this work (Chapter 2);
2) Carry out sampling campaigns during four seasons of a hydrological year: the start of wet season, the peak of wet season, end of the wet season, and the dry season;
3) Perform *in situ* measurements (water discharge, pH, electrical conductivity, temperature, dissolved oxygen, alkalinity) and perform physicochemical (mainly: chloride, nitrate, phosphate, ammonium, sulphate, bicarbonate, sodium, potassium, calcium, magnesium), organic matter (TOC, BOD, COD) and bacteriological analysis (total coliform, fecal coliform, and E. coli);
4) Information on land use changes, water use, and socio-economic data in the river basin should be collected and updated.

Groundwater monitoring programme on the other hand, should include at least:

1) Establish a spatial network of sampling stations which represent the main aquifer systems in the basin;
2) To conduct sampling campaigns at least once during the wet and dry seasons;

3) Sampling should include *in situ* measurements (water level, pH, electrical conductivity, temperature, dissolved oxygen, alkalinity), physicochemical (chloride, nitrate, phosphate, ammonium, sulphate, bicarbonate, sodium, potassium, calcium, magnesium) and bacteriological (total coliform, fecal coliform, E. coli) analysis;
4) At least one groundwater well specifically designed for monitoring and fitted with a piezometer should be developed in each of the main aquifer systems.

Additionally, an efficient water resources data and information management system requires investment in the necessary laboratory infrastructure and technical personnel, which needs improvement in Kenya.

5.3.2.3 Nitrate Policy

This study has reported high NO_3^- and NO_2^- concentrations above WHO threshold in groundwater. For surface water, an increasing NO_3^- concentration trend was observed relative to previous studies, while some land use zones had significantly high NO_3^- concentration values. It would therefore be prudent to start developing a specifically targeted NO_3^- pollution control policy for the Lake Victoria basin. A good example is the European Nitrate Directive which was established in 1991 to protect water quality across Europe by preventing NO_3^- from agricultural sources polluting surface and groundwater and promoting good farming practices (EU, 2010). A starting point for a Lake Victoria Nitrate Directive (LVND) would be to map and identify nitrate vulnerable zones in the basin. From this work, Kisumu city's shallow groundwater system showed high vulnerability to NO_3^- pollution, while based on the Lake's Limnology studies, the Winam gulf (Kenya) and Murchison gulf (Uganda) are the most highly degraded parts of the Lake in terms of water quality (Gikuma-Njuru et al., 2013b; Kabenge et al., 2016). The other step is to identify the main sources of NO_3^- contamination in these areas. From this work, manure has been identified as a major source of riverine NO_3^- input while sewage was the main NO_3^- pollution source in Kisumu groundwater. Therefore, the nitrate directive would outline control measures for each identified vulnerable zone based on its key

NO_3^- pollution sources. However, the LVND would require more NO_3^- concentrations and source data and identification of nitrate vulnerable zones especially for other key river basins like River Kagera, which contributes approximately 33.5% of total riverine inflow and it's a trans boundary river. This calls for replication of similar studies in major river basins of the Lake's riparian countries. The LVND could be developed and implemented through the Lake Victoria Basin Commission, which coordinates water resources management and development in the basin.

5.3.3 Related initiatives

Indeed, this work has pioneered recent nutrient studies in the Lake Victoria basin, and further nitrogen studies have started in the greater Lake Victoria basin and the tropical Africa to address the nitrogen data and information deficiency. In these studies, my affiliate institutions (Ghent University, University of Nairobi, Ministry of Water and Irrigation) are leading their respective countries and disciplines. The studies include:

1. The International Nitrogen Management Systems (INMS, http://www.inms.international/) have started a case study in the larger Lake Victoria basin region to improve the understanding of the nitrogen cycle and investigate practices and management policies at the local, national and regional levels with a view to reducing the negative impacts of reactive nitrogen on the ecosystems within the Lake Victoria Basin. The University of Nairobi leads the water quality component;
2. The International Atomic Energy Agency (IAEA, https://www.iaea.org/services/coordinated-research-activities) coordinated research projects: "Isotopes to study nitrogen pollution and eutrophication of rivers and lakes" and "Global Monitoring of Nitrogen Isotopes in Atmospheric Waters". Ghent University (ISOFYS) and University of Nairobi are the lead collaborating institutions of the respective projects;

3. Integrated Nitrogen Management Studies (https://h2020-insa.aeris-data.fr/) is an EU (H2020-MSCA-RISE) funded project aiming to build a network of scientists from Europe and Africa working on different aspects of the nitrogen budget in Africa, in order to produce a nitrogen assessment for Africa. Ghent University (ISOFYS) and the Ministry of Water and Irrigation (Kenya) are the collaborating institutions in their respective countries.

References

Agwanda, P.O., Iqbal, M.M., 2019. Engineering Control of Eutrophication: Potential Impact Assessment of Wastewater Treatment Plants Around Winam Gulf of Lake Victoria in Kenya. J. Coast. Res. 91, 221–225. https://doi.org/10.2112/SI91-045.1

Ako, A.A., Shimada, J., Hosono, T., Kagabu, M., Ayuk, A.R., Nkeng, G.E., Eyong, G.E.T., Takounjou, A.L.F., 2012. Spring water quality and usability in the Mount Cameroon area revealed by hydrogeochemistry. Environ. Geochem. Health 34, 615–639. https://doi.org/10.1007/s10653-012-9453-3

Allen, D.M., Suchy, M., 2001. Geochemical evolution of groundwater on Saturna Island, British Columbia. Can. J. Earth Sci. 38, 1059–1080. https://doi.org/10.1139/e01-007

Altman, S.J., Parizek, R.R., 1995. Dilution of Nonpoint-Source Nitrate in Groundwater. J. Environ. Qual. 24, 707–718. https://doi.org/10.2134/jeq1995.00472425002400040023x

Anornu, G., Gibrilla, A., Adomako, D., 2017. Science of the Total Environment Tracking nitrate sources in groundwater and associated health risk for rural communities in the White Volta River basin of Ghana using isotopic approach (δ 15 N , δ 18 O \. Sci. Total Environ. 603–604, 687–698. https://doi.org/10.1016/j.scitotenv.2017.01.219

Aravena, R., Evans, M.. L., Cherry, J.A., 1993. Stable Isotopes of Oxygen and Nitrogen in Source Identification of Nitrate from Septic Systems.pdf. Groundwater 31, 180–186.

Arbuckle, T.E., Sherman, G.J., Corey, P.N., Walters, D., Lo, B., 1988. Water Nitrates and CNS Birth Defects: A Population-Based Case-Control Study. Arch. Environ. Health 43, 162–167.

Avagyan, A., Arakelyan, A., Yeritsian, H., Manandyan, H., 2014. The principles of guideline for the river basin management planning in Armenia. https://doi.org/10.13140/2.1.2886.7367

Barakat, A., El Baghdadi, M., Rais, J., Aghezzaf, B., Slassi, M., 2016. Assessment of spatial and seasonal water quality variation of Oum Er Rbia River (Morocco) using multivariate statistical techniques. Int. Soil Water Conserv. Res. 4, 284–292. https://doi.org/10.1016/j.iswcr.2016.11.002

Barathi, M., Kumar, A.S.K., Rajesh, N., 2019. Impact of fluoride in potable water – An outlook on the existing defluoridation strategies and the road ahead. Coord. Chem. Rev. 387, 121–128. https://doi.org/10.1016/j.ccr.2019.02.006

Bassett, R.L., Buszka, P.M., Davidson, G.R., Chong-Diaz, D., 1995. Identification of Groundwater Solute Sources Using Boron Isotopic Composition. Environ. Sci. Technol. 29, 2915–2922.

Bauters, M., Drake, T.W., Verbeeck, H., Bodé, S., Hervé-Fernández, P., Zito, P., Podgorski, D.C., Boyemba, F., Makelele, I., Ntaboba, L.C., Spencer, R.G.M., Boeckx, P., 2018. High fire-derived nitrogen deposition on central African forests. Proc. Natl. Acad. Sci. U. S. A. 115, 549–554. https://doi.org/10.1073/pnas.1714597115

Benkovitz, C.M., Scholtz, M.T., Pacyna, J., Tarrasón, L., Dignon, J., Voldner, E.C., Spiro,

P.A., Logan, J.A., Graedel, T.E., 1996. Global gridded inventories of anthropogenic emissions of sulfur and nitrogen. J. Geophys. Res. Atmos. 101, 29239–29253. https://doi.org/10.1029/96JD00126

Blackmer, A., Bremner, J., 1977. Nitrogen isotope discrimination in denitrification of nitrate in soils. Soil Biol. Biochem 9, 73–77.

Böttcher, J., Strebel, O., Voerkelius, S., Schmidt, H.L., 1990. Using isotope fractionation of nitrate-nitrogen and nitrate-oxygen for evaluation of microbial denitrification in a sandy aquifer. J. Hydrol. 114, 413–424. https://doi.org/10.1016/0022-1694(90)90068-9

Bouillon, S., Abril, G., Borges, A. V., Dehairs, F., Govers, G., Hughes, H.J., Merckx, R., R. Meysman, F.J., Nyunja, J., Osburn, C., Middelburg, J.J., 2009. Distribution, origin and cycling of carbon in the Tana River (Kenya): a dry season basin-scale survey from headwaters to the delta. Biogeosciences 6, 2475–2493. https://doi.org/10.5194/bg-6-2475-2009

Bremner, J., Lopez-Carr, D., Zvoleff, A., Narcisa Pricope, 2013. Using New Methods and Data to Assess and Address Population, Fertility, and Environment links in the Lake Victoria Basin, in: XXVII IUSSP International Population Conference, 26 - 31st August 2013, Busan, South Korea. Busan, South Korea, pp. 55–60.

Brender, J.D., Weyer, P.J., Romitti, P.A., Mohanty, B.P., Shinde, M.U., Vuong, A.M., Sharkey, J.R., Dwivedi, D., Horel, S.A., Kantamneni, J., Huber, J.C., Zheng, Q., Werler, M.M., Kelley, K.E., Griesenbeck, J.S., Zhan, F.B., Langlois, P.H., Suarez, L., Canfield, M.A., 2013. Prenatal nitrate intake from drinking water and selected birth defects in offspring of participants in the national birth defects prevention study. Environ. Health Perspect. 121, 1083–1089. https://doi.org/10.1289/ehp.1206249

Casciotti, K.L., Sigman, D.M., Hastings, M.G., Böhlke, J.K., Hilkert, A., 2002. Measurement of the oxygen isotopic composition of nitrate in seawater and freshwater using the denitrifier method. Anal. Chem. 74, 4905–4912. https://doi.org/10.1021/ac020113w

Cedergren, M., Selbing, A., Lofman, O., Kallen, B., 2002. Chlorination Byproducts and Nitrate in Drinking Water and Risk for Congenital Cardiac Defects. Environ. Res. 89, 124–130.

Chen, F., Jia, G., Chen, J., 2009. Nitrate sources and watershed denitrification inferred from nitrate dual isotopes in the Beijiang River, south China. Biogeochemistry 94, 163–174. https://doi.org/10.1007/s10533-009-9316-x

Chen, Y., Randerson, J.T., Werf, G.R.V.N.D.E.R., Morton, D.C., Mu, M., Kasibhatla, P.., 2010. Nitrogen deposition in tropical forests from savanna and deforestation fire.pdf. Glob. Chang. Biol. 16, 2024–2038.

COWI, consulting engineers, 2002. Integrated Water Quality / Limnology Study for Lake Victoria. Lake Victoria Environmental Management Project, Part II Technical Report.

Cox, B.A., 2003. A review of currently available in-stream water-quality models and their applicability for simulating dissolved oxygen in lowland rivers. Sci. Total Environ. 314–316, 335–377. https://doi.org/10.1016/S0048-9697(03)00063-9

CRA, Commission of Revenue Allocation, 2011. Kenya County Fact Sheets, Kenya Bureau

of Statistic [WWW Document].
Davies, C.L., Surridge, B.W.J., Gooddy, D.C., 2014. Phosphate oxygen isotopes within aquatic ecosystems: Global data synthesis and future research priorities. Sci. Total Environ. 496, 563–575. https://doi.org/10.1016/j.scitotenv.2014.07.057
Dhondt, K., Boeckx, P., Van Cleemput, O., Hofman, G., 2003. Quantifying nitrate retention processes in a riparian buffer zone using the natural abundance of 15N in NO3-. Rapid Commun. Mass Spectrom. 17, 2597–2604. https://doi.org/10.1002/rcm.1226
Do, H.T., Lo, S.L., Chiueh, P. Te, Thi, L.A.P., Shang, W.T., 2011. Optimal design of river nutrient monitoring points based on an export coefficient model. J. Hydrol. 406, 129–135. https://doi.org/10.1016/j.jhydrol.2011.06.012
Edokpayi, J.N., Odiyo, J.O., Msagati, T.A.M., Potgieter, N., 2015. Temporal variations in physico-chemical and microbiological characteristics of mvudi river, South Africa. Int. J. Environ. Res. Public Health 12, 4128–4140. https://doi.org/10.3390/ijerph120404128
Erostate, M., Huneau, F., Garel, E., Lehmann, M.F., Kuhn, T., Aquilina, L., Vergnaud-Ayraud, V., Labasque, T., Santoni, S., Robert, S., Provitolo, D., Pasqualini, V., 2018. Delayed nitrate dispersion within a coastal aquifer provides constraints on land-use evolution and nitrate contamination in the past. Sci. Total Environ. 644, 928–940. https://doi.org/10.1016/j.scitotenv.2018.06.375
EU, 2010. The EU Nitrates Directive [WWW Document].
FAO, 2017. Africa Sustainable Livestock (ASL) 2050 Country Brief: Kenya. FAO 49, 0–8.
Fukada, T., Hiscock, K.M., Dennis, P.F., Grischek, T., 2003. A dual isotope approach to identify denitrification in groundwater at a river-bank infiltration site. Water Res. 37, 3070–3078. https://doi.org/10.1016/S0043-1354(03)00176-3
Gaillardet, J., Allgre, C.J., 1995. Boron isotopic compositions of corals : Seawater or diagenesis record? Earth Planet. Sci. Lett. 136, 665–676.
Galloway, J.N., Townsend, A.R., Erisman, J.W., Bekunda, M., Cai, Z., Freney, J.R., Martinelli, L.A., Seitzinger, S.P., Sutton, M.A., 2008. Transformation of the Nitrogen Cycle : Recent trends, questions and potential solutions. Science (80-.). 320, 889–892. https://doi.org/10.1126/science.1136674
Galy-Lacaux, C., Delon, C., 2014. Nitrogen emission and deposition budget in West and Central Africa. Environ. Res. Lett. 9, 125002. https://doi.org/10.1088/1748-9326/9/12/125002
Gao, L., Li, D., 2014. A review of hydrological/water-quality models. Front. Agric. Sci. Eng. 1, 267–276. https://doi.org/10.15302/J-FASE-2014041
Gikuma-Njuru, P., Guildford, S.J., Hecky, R.E., Kling, H.J., 2013a. Strong spatial differentiation of N and P deficiency, primary productivity and community composition between Nyanza Gulf and Lake Victoria (Kenya, East Africa) and the implications for nutrient management. Freshw. Biol. 58, 2237–2252. https://doi.org/10.1111/fwb.12205
Gikuma-Njuru, P., Hecky, R.E., 2005. Nutrient concentrations in Nyanza Gulf, Lake Victoria, Kenya: Light limits algal demand and abundance. Hydrobiologia 534, 131–140. https://doi.org/10.1007/s10750-004-1418-9

Gikuma-Njuru, P., Hecky, R.E., Guildford, S.J., Macintyre, S., 2013b. Spatial variability of nutrient concentrations, fluxes, and ecosystem metabolism in Nyanza Gulf and Rusinga Channel, Lake Uictoria (East Africa). Limnol. Oceanogr. 58, 774–789. https://doi.org/10.4319/lo.2013.58.3.0774

Glibert, P.M., Seitzinger, S., Heil, C.A., Burkholder, J.M., Parrow, M.W., Codispoti, L.A., Kelly, V., 2005. The role of eutrophication in the global proliferation of harmful algal blooms. Oceanography 18, 198–209. https://doi.org/10.5670/oceanog.2005.54

Gonfiantini, R., Tonarini, S., Gröning, M., Adorni-Braccesi, A., Al-Ammar, A.S., Astner, M., Bächler, S., Barnes, R.M., Bassett, R.L., Cocherie, A., Deyhle, A., Dini, A., Ferrara, G., Gaillardet, J., Grimm, J., Guerrot, C., Krähenbühl, U., Layne, G., Lemarchand, D., Meixner, A., Northington, D.J., Pennisi, M., Reitznerová, E., Rodushkin, I., Sugiura, N., Surberg, R., Tonn, S., Wiedenbeck, M., Wunderli, S., Xiao, Y., Zack, T., 2003. Intercomparison of boron isotope and concentration measurements. Part II: Evaluation of results. Geostand. Newsl. 27, 41–57. https://doi.org/10.1111/j.1751-908X.2003.tb00711.x

Gophen, M., Ochumba, P., Kaufman, L., 1995. Some aspects of perturbation in the structure and biodiversity of the ecosystem of Lake Victoria (East Africa). Aquat. Living Resour. 8, 27–41.

Granger, S.J., Heaton, T.H.E., Pfahler, V., Blackwell, M.S.A., Yuan, H., Collins, A.L., 2017. The oxygen isotopic composition of phosphate in river water and its potential sources in the Upper River Taw catchment, UK. Sci. Total Environ. 574, 680–690. https://doi.org/10.1016/j.scitotenv.2016.09.007

Hill, A.R., 1996. (1996) Nitrate Removal in Stream Riparian Zones. J. Environ. Qual. 25, 743–755.

Huygens, D., Trimmer, M., Rütting, T., Müller, C., Heppell, C.M., Lansdown, K., Boeckx, P., 2013. Biogeochemical Nitrogen Cycling in Wetland Ecosystems: Nitrogen-15 Isotope Techniques, in: DeLaune, R.D., Reddy, K.R., Richardson, C.J., Megonigal, J.P. (Eds.), Methods in Biogeochemistry of Wetlands. Soil Science Society of America, WI 53711-5801, USA, pp. 553–591. https://doi.org/10.2136/sssabookser10.c30

ICRAF, 2003. Global Environment Facility. Project proposal for a Full Sized Project. Nairobi, Kenya.

IPCC, 2007. Climate Change 2007: Synthesis Report. Contribution of Working Groups I, II and III to the Fourth Assess- ment Report of the Intergovernmental Panel on Climate Change [Core Writing Team, Pachauri, R.K and Reisinger, A. (eds.)]. IPCC, Geneva, Switzerland, Intergovernmental Panel on Climate Change (IPCC,2007).

IPCC, 2006. 2006 IPCC Guidelines for National Greenhouse Gas Inventories, Chapter 10 Emissions From Livestock and Manure Management [Core Authors: Dong, H., Mangino, J., McAllister, T.], Volume 4: Agriculture, Forestry and Other Land Use.

Ishikawa, T., Nakamura, E., 1990. Suppression of boron volatilization from a hydrofluoric acid solution using a boron-mannitol complex. Anal. Chem. 62, 2612–2616. https://doi.org/10.1021/ac00222a017

Jacobs, S.R., Breuer, L., Butterbach-Bahl, K., Pelster, D.E., Rufino, M.C., 2017. Land use affects total dissolved nitrogen and nitrate concentrations in tropical montane streams in Kenya. Sci. Total Environ. 603–604, 519–532. https://doi.org/10.1016/j.scitotenv.2017.06.100

Jaisi, D.P., Blake, R.E., 2014. Advances in Using Oxygen Isotope Ratios of Phosphate to Understand Phosphorus Cycling in the Environment, 1st ed, Advances in Agronomy. Elsevier Inc. https://doi.org/10.1016/B978-0-12-800137-0.00001-7

JICA, Japan International Cooperation Agency, 2013. National Water Master Plan 2030, Ministry of Environment, Water & Natural Resources. Nairobi.

Johnes, P.J., 1996. Evaluation and management of the impact of land use change on the nitrogen and phosphorus load delivered to surface waters: The export coefficient modelling approach. J. Hydrol. 183, 323–349. https://doi.org/10.1016/0022-1694(95)02951-6

Johnston, A.M., Bruulsema, T.W., 2014. 4R nutrient stewardship for improved nutrient use efficiency. Procedia Eng. 83, 365–370. https://doi.org/10.1016/j.proeng.2014.09.029

Juma, D.W., Wang, H., Li, F., 2014. Impacts of population growth and economic development on water quality of a lake: Case study of Lake Victoria Kenya water. Environ. Sci. Pollut. Res. 21, 5737–5746. https://doi.org/10.1007/s11356-014-2524-5

Kabenge, M., Wang, H., Li, F., 2016. Urban eutrophication and its spurring conditions in the Murchison Bay of Lake Victoria. Environ. Sci. Pollut. Res. 23, 234–241. https://doi.org/10.1007/s11356-015-5675-0

Kamtchueng, B.T., Fantong, W.Y., Wirmvem, M.J., Tiodjio, R.E., Takounjou, A.F., Ndam Ngoupayou, J.R., Kusakabe, M., Zhang, J., Ohba, T., Tanyileke, G., Hell, J. V., Ueda, A., 2016. Hydrogeochemistry and quality of surface water and groundwater in the vicinity of Lake Monoun, West Cameroon: approach from multivariate statistical analysis and stable isotopic characterization. Environ. Monit. Assess. 188, 524. https://doi.org/10.1007/s10661-016-5514-x

Kansiime, F., Kateyo, E., Oryem-Origa, H., Mucunguzi, P., 2007. Nutrient status and retention in pristine and disturbed wetlands in Uganda: Management implications. Wetl. Ecol. Manag. 15, 453–467. https://doi.org/10.1007/s11273-007-9054-6

Kellman, L.M., Hillaire-Marcel, C., 2003. Evaluation of nitrogen isotopes as indicators of nitrate contamination sources in an agricultural watershed. Agric. Ecosyst. Environ. 95, 87–102. https://doi.org/10.1016/S0167-8809(02)00168-8

Kendall, C., Elliott, E.M., Wankel, S.D., 2007. Tracing anthropogenic inputs of nitrogen to ecosystems, in: Michener, R., Lajtha, K. (Ed.), Stable Isotopes in Ecology and Environmental Science,. Blackwell Publishing Ltd., Oxford, UK, pp. 375 – 449.

Kennedy, M.P., Lang, P., Tapia Grimaldo, J., Varandas Martins, S., Bruce, A., Lowe, S., Dallas, H., Davidson, T.A., Sichingabula, H., Briggs, J., Murphy, K.J., 2016. The Zambian Macrophyte Trophic Ranking scheme, ZMTR: A new biomonitoring protocol to assess the trophic status of tropical southern African rivers. Aquat. Bot. 131, 15–27. https://doi.org/10.1016/j.aquabot.2016.01.006

Kipkemboi, J., McClain, M.E., Gettel, G.M., Irvine, K., Masese, F.O., Kitaka, N., 2014. Litter processing and shredder distribution as indicators of riparian and catchment influences on ecological health of tropical streams. Ecol. Indic. 46, 23–37. https://doi.org/10.1016/j.ecolind.2014.05.032

KNBS, Kenya National Bureau of Statistics, 2019. 2019 Kenya Population and Housing Census Volume I : Population By County and Sub-County [WWW Document].

KNBS, Kenya National Bureau of Statistics, 2009. Livestock population by type and district 2009 [WWW Document].

Koba, K., Tokuchi, N., Wada, E., Nakajima, T., Iwatsubo, G., 1997. Intermittent denitrification: The application of a 15N natural abundance method to a forested ecosystem. Geochim. Cosmochim. Acta 61, 5043–5050. https://doi.org/10.1016/S0016-7037(97)00284-6

Kolding, J.P., Zwieten, P., Mkumbo, O., Silsbe, G., Hecky, R.E., 2008. Are the Lake Victoria fisheries threatened by exploitation or eutrophication? Towards an ecosystem based approach to management., in: Bianchi, R., Kjoldal, H.R. (Eds.), The Ecosystem Approach to Fisheries. CABI Publishing, Rome, pp. 309–354.

Komor, S.C., 1997. Boron Contents and Isotopic Compositions of Hog Manure, Selected Fertilizers, and Water in Minnestoa. J. Environ. Qual. 26, 1212–1222. https://doi.org/10.2134/jeq1997.00472425002600050004x

Lankford, B., Merrey, D., Cour, J., Hepworth, N., 2007. From Integrated to Expedient: An Adaptive Framework for River Basin Management in Developing Countries. Integrated Water Management Institute, Colombo, Sri Lanka. https://doi.org/http://dx.doi.org/10.3910/2009.110

Li, S.L., Liu, C.Q., Lang, Y.C., Zhao, Z.Q., Zhou, Z.H., 2010. Tracing the sources of nitrate in karstic groundwater in Zunyi, Southwest China: A combined nitrogen isotope and water chemistry approach. Environ. Earth Sci. 60, 1415–1423. https://doi.org/10.1007/s12665-009-0277-0

Lin, J., Böhlke, J.K., Huang, S., Gonzalez-meler, M., Sturchio, N.C., 2019. Seasonality of nitrate sources and isotopic composition in the Upper Illinois River. J. Hydrol. 568, 849–861. https://doi.org/10.1016/j.jhydrol.2018.11.043

Liu, C.Q., Li, S.L., Lang, Y.C., Xiao, H.Y., 2006. Using δ15N- and δ18O-values to identify nitrate sources in karst ground water, Guiyang, Southwest China. Environ. Sci. Technol. 40, 6928–6933. https://doi.org/10.1021/es0610129

Lund, L.J., Horne, A.J., Williams, A.E., 1999. Estimating denitrification in a large constructed wetland using stable nitrogen isotope ratios. Ecol. Eng. 14, 67–76. https://doi.org/10.1016/S0925-8574(99)00020-8

Lung'ayia, H., Sitoki, L., Kenyanya, M., 2001. The nutrient enrichment of Lake Victoria (Kenyan waters). Hydrobiologia 458, 75–82. https://doi.org/10.1023/A:1013128027773

LVBC, 2007. Lake Victoria Basin Commission (LVBC). Regional trans-boundary diagnostic analysis of the Lake Victoria basin Report. Kisumu, Kenya.

LVEMP, 2006. Lake Victoria Environmental Management Project (LVEMP). Assessment of

the potential of land suitability mapping with environmental overlays and potential usefulness of spatial planning for managing the Lake Victoria basin. Nairobi, Kenya.
LVEMP, 2005. Lake Victoria Environmental Management Project (LVEMP). Kenya National Water Quality synthesis Report. Kisumu, Kenya.
Maghanga, J.K., Kituyi, J.L., Kisinyo, P.O., Ng'Etich, W.K., 2013. Impact of nitrogen fertilizer applications on surface water nitrate levels within a Kenyan tea plantation. J. Chem. 2013, 1–4. https://doi.org/10.1155/2013/196516
Mariotti, A; Germon, J; Lecrerc, A., 1982. Nitrogen isotope fractionation associated with the NO2 - N2O step of denitrifcation in soils. Can. J. Soil Sci. 62, 227–241.
Marwick, T.R., Tamooh, F., Ogwoka, B., Teodoru, C., Borges, A. V., Darchambeau, F., Bouillon, S., 2014. Dynamic seasonal nitrogen cycling in response to anthropogenic N loading in a tropical catchment, Athi-Galana-Sabaki River, Kenya. Biogeosciences 11, 443–460. https://doi.org/10.5194/bg-11-443-2014
Masese, F.O., Salcedo-Borda, J.S., Gettel, G.M., Irvine, K., McClain, M.E., 2017. Influence of catchment land use and seasonality on dissolved organic matter composition and ecosystem metabolism in headwater streams of a Kenyan river. Biogeochemistry 132, 1–22. https://doi.org/10.1007/s10533-016-0269-6
Masso, C., Baijukya, F., Ebanyat, P., Bouaziz, S., Wendt, J., Bekunda, M., Vanlauwe, B., 2017. Dilemma of nitrogen management for future food security in sub-Saharan Africa-a review. Soil Res. 55, 425–434. https://doi.org/10.1071/SR16332
Mather, J.D., Porteous, N.C., 2001. The geochemistry of boron and its isotopes in groundwaters from marine and non-marine sandstone aquifers. Appl. Geochemistry 16, 821–834. https://doi.org/10.1016/S0883-2927(00)00072-X
Matiatos, I., 2016. Nitrate source identification in groundwater of multiple land-use areas by combining isotopes and multivariate statistical analysis: A case study of Asopos basin (Central Greece). Sci. Total Environ. 541, 802–814. https://doi.org/10.1016/j.scitotenv.2015.09.134
Mattikalli, N.M., Richards, K.S., 1996. Estimation of surface water quality changes in response to land use change: Application of the export coefficient model using remote sensing and geographical information system. J. Environ. Manage. https://doi.org/10.1006/jema.1996.0077
Mayer, B., Bollwerk, S.M., Mansfeldt, T., Hütter, B., Veizer, J., 2001. The oxygen isotope composition of nitrate generated by nitrification in acid forest floors. Geochim. Cosmochim. Acta 65, 2743–2756. https://doi.org/10.1016/S0016-7037(01)00612-3
Mayer, B., Van Breemen, N., Howarth, R.W., Seitzinger, S., Billen, G., Lajtha, K., Nadelhoffer, K.J., Van Dam, D., Hetling, L.J., Nosal, M., Paustian, K., Boyer, E.W., Goodale, C.L., 2002. Sources of nitrate in rivers draining sixteen watersheds in the northeastern U.S.: Isotopic constraints. Biogeochemistry 57–58, 171–197.
Mbaye, M.L., Gaye, A.T., Spitzy, A., Dähnke, K., Afouda, A., Gaye, B., 2016. Seasonal and spatial variation in suspended matter, organic carbon, nitrogen, and nutrient concentrations of the Senegal River in West Africa. Limnologica 57, 1–13.

https://doi.org/10.1016/j.limno.2015.12.003
McLaughlin, K., Cade-Menun, B.J., Paytan, A., 2006. The oxygen isotopic composition of phosphate in Elkhorn Slough, California: A tracer for phosphate sources. Estuar. Coast. Shelf Sci. 70, 499–506. https://doi.org/10.1016/j.ecss.2006.06.030
Meghdadi, A., Javar, N., 2018. Quantification of spatial and seasonal variations in the proportional contribution of nitrate sources using a multi-isotope approach and Bayesian isotope mixing model. Environ. Pollut. 235, 207–222. https://doi.org/10.1016/j.envpol.2017.12.078
Mengis, M., Schiff, S., Harris, M., English, M., Aravena, R., Elgood, R., Maclean, A., 1999. Multiple geochemical and isotopic approaches for assesing groundwater nitrate elimination in a riparian zone. Groundwater 37, 448–457.
Mfumu Kihumba, A., Vanclooster, M., Ndembo Longo, J., 2017. Assessing groundwater vulnerability in the Kinshasa region, DR Congo, using a calibrated DRASTIC model. J. African Earth Sci. 126, 13–22. https://doi.org/10.1016/j.jafrearsci.2016.11.025
Millot, R., Petelet-Giraud, E., Guerrot, C., Négrel, P., 2010. Multi-isotopic composition (δ7Li-δ11B-δD-δ18O) of rainwaters in France: Origin and spatio-temporal characterization. Appl. Geochemistry 25, 1510–1524. https://doi.org/10.1016/j.apgeochem.2010.08.002
Min, J.H., Yun, S.T., Kim, K., Kim, H.S., Hahn, J., Lee, K.S., 2002. Nitrate contamination of alluvial groundwaters in the Nakdong River basin, Korea. Geosci. J. 6, 35–46.
Minh, L.T.N., Nga, D.T., Matiatos, I., Panizzo, V.N., Duc, T.A., 2020. Stable isotopes as an effective tool for N nutrient source identification in a heavily urbanized and agriculturally intensive tropical lowland basin. Biogeochemistry 149, 17–35. https://doi.org/10.1007/s10533-020-00663-w
Mireri, C., Atekyereza, P., Kyessi, A., Mushi, N., 2007. Environmental risks of urban agriculture in the Lake Victoria drainage basin: A case of Kisumu municipality, Kenya. Habitat Int. 31, 375–386. https://doi.org/10.1016/j.habitatint.2007.06.006
Mulholland, P.J., Helton, A.M., Poole, G.C., Hall, R.O., Hamilton, S.K., Peterson, B.J., Tank, J.L., Ashkenas, L.R., Cooper, L.W., Dahm, C.N., Dodds, W.K., Findlay, S.E.G., Gregory, S. V., Grimm, N.B., Johnson, S.L., McDowell, W.H., Meyer, J.L., Valett, H.M., Webster, J.R., Arango, C.P., Beaulieu, J.J., Bernot, M.J., Burgin, A.J., Crenshaw, C.L., Johnson, L.T., Niederlehner, B.R., O'Brien, J.M., Potter, J.D., Sheibley, R.W., Sobota, D.J., Thomas, S.M., 2008. Stream denitrification across biomes and its response to anthropogenic nitrate loading. Nature 452, 202–205. https://doi.org/10.1038/nature06686
Musungu, P.C., Lalah, J.O., Jondiko, I.O., Ongeri, D.M.K., 2014. The impact of nitrogenous and phosphorous nutrients from selected point sources in Kisumu City on River Kisat and Nyalenda Wigwa Stream before their discharge into Winam Gulf, Lake Victoria. Environ. Earth Sci. 71, 5121–5127. https://doi.org/10.1007/s12665-013-2915-9
Muyodi, F.J., Bugenyi, F.W.B., Hecky, R.E., 2010. Experiences and lessons learned from interventions in the Lake Victoria Basin: The Lake Victoria environmental management

project. Lakes Reserv. Res. Manag. 15, 77–88. https://doi.org/10.1111/j.1440-1770.2010.00425.x

Mwanake, R.M., Gettel, G.M., Aho, K.S., Namwaya, D.W., Masese, F.O., Butterbach-Bahl, K., Raymond, P.A., 2019. Land Use, Not Stream Order, Controls N2O Concentration and Flux in the Upper Mara River Basin, Kenya. J. Geophys. Res. Biogeosciences 124, 3491–3506. https://doi.org/10.1029/2019JG005063

Nestler, A., Berglund, M., Accoe, F., Duta, S., Xue, D., Boeckx, P., Taylor, P., 2011. Isotopes for improved management of nitrate pollution in aqueous resources: Review of surface water field studies. Environ. Sci. Pollut. Res. 18, 519–533. https://doi.org/10.1007/s11356-010-0422-z

Ntiba, M.J., Kudoja, W.M., Mukasa, C.T., 2001. Management issues in the Lake Victoria watershed. Lakes Reserv. Res. Manag. 6, 211–216. https://doi.org/10.1046/j.1440-1770.2001.00149.x

NWP, 2019. National Water Policy (Draft), Ministry of Water & Sanitation, Republic of Kenya. https://doi.org/10.1017/S0022278X00014853

Nyairo, W.N., Owuor, P.O., Kengara, F.O., 2015. Effect of anthropogenic activities on the water quality of Amala and Nyangores tributaries of River Mara in Kenya. Environ. Monit. Assess. 187. https://doi.org/10.1007/s10661-015-4913-8

Nyeko-Ogiramoi, P., Willems, P., Ngirane-Katashaya, G., 2013. Trend and variability in observed hydrometeorological extremes in the Lake Victoria basin. J. Hydrol. 489, 56–73. https://doi.org/10.1016/j.jhydrol.2013.02.039

Nyenje, P.M., Foppen, J.W., Kulabako, R., Muwanga, A., Uhlenbrook, S., 2013. Nutrient pollution in shallow aquifers underlying pit latrines and domestic solid waste dumps in urban slums. J. Environ. Manage. 122, 15–24. https://doi.org/10.1016/j.jenvman.2013.02.040

Nyenje, P.M., Foppen, J.W., Uhlenbrook, S., Kulabako, R., Muwanga, A., 2010. Eutrophication and nutrient release in urban areas of sub-Saharan Africa - A review. Sci. Total Environ. 408, 447–455. https://doi.org/10.1016/j.scitotenv.2009.10.020

Nyilitya, B., Mureithi, M.S., Boeckx, P., 2016. Tracking sources of excess nitrate discharge in Lake Victoria , Kenya for improved Nitrogen use efficiency in the catchment, in: Proceedings of the 2016 International Nitrogen Initiative Conference, “Solutions to Improve Nitrogen Effieciency for the World”, Melbourne, Australia, 4 - 8 December, 2016.

Nyilitya, B., Mureithi, S., Boeckx, P., 2020a. Tracking Sources and Fate of Groundwater Nitrate in Kisumu City and Kano Plains , Kenya. Water 12, 1–18. https://doi.org/doi:10.3390/w12020401

Nyilitya, B., Mureithi, S., Boeckx, P., 2020b. Land use controls Kenyan riverine nitrate discharge into Lake Victoria – evidence from Nyando , Nzoia and Sondu Miriu river catchments. Isotopes Environ. Health Stud. 56, 170–192. https://doi.org/10.1080/10256016.2020.1724999

Ochumba, P., Kibaara, D., 1989. Observations on blue-green algal blooms in the open waters

of Lake Victoria, Kenya. Afr. J. Ecol. 27, 23–34.
Ochumba, P.B.O., 1990. Massive fish kills within the Nyanza Gulf of Lake Victoria, Kenya. Hydrobiologia 208, 93–99. https://doi.org/10.1007/BF00008448
Odada, E.O., Olago, D.O., Ochola, W.O., 2006. Environment for Development: An Ecosystems Assessment of Lake Victoria Basin, Unep/Pass.
Oiro, S.O., 2012. The hydrogeology and groundwater quality assessment of Kisumu town area in Kenya. MSc. thesis, Ghent University, Belgium. https://doi.org/10.1016/j.ejrad.2007.09.008
Okotto-Okotto, J., Okotto, L., Price, H., Pedley, S., Wright, J., 2015. A longitudinal study of long-term change in contamination hazards and shallow well quality in two neighbourhoods of Kisumu, Kenya. Int. J. Environ. Res. Public Health 12, 4275–4291. https://doi.org/10.3390/ijerph120404275
Okungu, J., Opango, P., 2004. Pollution loads into Lake Victoria from the Kenyan catchment [WWW Document].
Olago, D.O., 2019. Constraints and solutions for groundwater development, supply and governance in urban areas in Kenya. Hydrogeol. J. 27, 1031–1050. https://doi.org/10.1007/s10040-018-1895-y
Olang, L.O., Fürst, J., 2011. Effects of land cover change on flood peak discharges and runoff volumes: Model estimates for the Nyando River Basin, Kenya. Hydrol. Process. 25, 80–89. https://doi.org/10.1002/hyp.7821
Omosa, I.B., Wang, H., Cheng, S., Li, F., 2012. Sustainable tertiary wastewater treatment is required for water resources pollution control in Africa. Environ. Sci. Technol. 46, 7065–7066. https://doi.org/10.1021/es3022254
Owor, M., Taylor, R., Mukwaya, C., Tindimugaya, C., 2011. Groundwater/surface-water interactions on deeply weathered surfaces of low relief: Evidence from Lakes Victoria and Kyoga, Uganda. Hydrogeol. J. 19, 1403–1420. https://doi.org/10.1007/s10040-011-0779-1
Panno, S., Hackley, K., Kelly, W., Hwang, H.-H., 2006. Isotopic Evidence of Nitrate Sources and Denitrification in the Mississippi River, Illinois. J. Environ. Qual. 35, 495–504. https://doi.org/10.2134/jeq2005.0012
Parnell, A.C., Inger, R., Bearhop, S., Jackson, A.L., 2010. Source partitioning using stable isotopes: Coping with too much variation. PLoS One 5, 1–6. https://doi.org/10.1371/journal.pone.0009672
Pejman, A.H., Nabi Bidhendi, G.R., Karbassi, A.R., Mehrdadi, N., Esmaeili Bidhendi, M., 2009. Evaluation of spatial and seasonal variations in surface water quality using multivariate statistical techniques. Int. J. Environ. Sci. Technol. 6, 467–476. https://doi.org/10.1007/BF03326086
Philips, S., Wyffels, S., Sprengers, R., Verstraete, W., 2002. Oxygen-limited autotrophic nitrification/denitrification by ammonia oxidisers enables upward motion towards more favourable conditions. Appl. Microbiol. Biotechnol. 59, 557–566. https://doi.org/10.1007/s00253-002-1059-8

Piña-Ochoa, E., Álvarez-Cobelas, M., 2006. Denitrification in aquatic environments: A cross-system analysis. Biogeochemistry 81, 111–130. https://doi.org/10.1007/s10533-006-9033-7

Piper, A.., 1944. A Graphical Procedure in the Geochemical Interpretation of Water Analysis. Trans. Am. Geophys. Union 25, 914–923. https://doi.org/http://dx.doi.org/10.1029/TR025i006p00914

Pynaert, K., Wyffels, S., Sprengers, R., Boeckx, P., Van Cleemput, O., Verstraete, W., 2002. Oxygen-limited nitrogen removal in a lab-scale rotating biological contactor treating an ammonium-rich wastewater. Water Sci. Technol. 45, 357–363. https://doi.org/10.2166/wst.2002.0369

Raburu, P., Okey-Owuor, J., Kwena, F., 2012. Community Based Approach to the Management of Nyando Wetland, Lake Victoria Basin, Kenya, First. ed. KDC-VIRED-UNDP, Nairobi.

Rensburg, S., Barnard, S., Booyens, S., 2019. Comparison of phytoplankton assemblages in two differentially polluted streams in the Middle Vaal Catchment, South Africa. South African J. Bot. 125, 234–243. https://doi.org/10.1016/j.sajb.2019.07.036

Risgaard-Petersen, N., Nielsen, L.P., Rysgaard, S., Dalsgaard, T., Meyer, R.L., 2003. Application of the isotope pairing technique in sediments where anammox and denitrification coexist. Limnol. Oceanogr. Methods 1, 63–73. https://doi.org/10.4319/lom.2011.1.63

Robinson, T.P., William Wint, G.R., Conchedda, G., Van Boeckel, T.P., Ercoli, V., Palamara, E., Cinardi, G., D'Aietti, L., Hay, S.I., Gilbert, M., 2014. Mapping the global distribution of livestock. PLoS One 9, 1–13. https://doi.org/10.1371/journal.pone.0096084

Rufino, M.C., Rowe, E.C., Delve, R.J., Giller, K.E., 2006. Nitrogen cycling efficiencies through resource-poor African crop-livestock systems. Agric. Ecosyst. Environ. 112, 261–282. https://doi.org/10.1016/j.agee.2005.08.028

Sacchi, E., Acutis, M., Bartoli, M., Brenna, S., Delconte, C.A., Laini, A., Pennisi, M., 2013. Origin and fate of nitrates in groundwater from the central Po plain: Insights from isotopic investigations. Appl. Geochemistry 34, 164–180. https://doi.org/10.1016/j.apgeochem.2013.03.008

Scheren, P.A.G.M., Zanting, H.A., Lemmens, A.M.C., 2000. Estimation of water pollution sources in Lake Victoria, East Africa: Application and elaboration of the rapid assessment methodology. J. Environ. Manage. 58, 235–248. https://doi.org/10.1006/jema.2000.0322

Schullehner, J., Hansen, B., Thygesen, M., Pedersen, C.B., Sigsgaard, T., 2018. Nitrate in drinking water and colorectal cancer risk: A nationwide population-based cohort study. Int. J. Cancer 143, 73–79. https://doi.org/10.1002/ijc.31306

Seiler, R.L., 2005. Combined use of 15N and 18O of nitrate and 11B to evaluate nitrate contamination in groundwater. Appl. Geochemistry 20, 1626–1636. https://doi.org/10.1016/j.apgeochem.2005.04.007

Selemani, J.R., Zhang, J., Muzuka, A.N.N., Njau, K.N., Zhang, G., Mzuza, M.K., Maggid, A., 2018. Nutrients' distribution and their impact on Pangani River Basin's ecosystem–Tanzania. Environ. Technol. (United Kingdom) 39, 702–716. https://doi.org/10.1080/09593330.2017.1310305

Shanyengana, E.S., Seely, M.K., Sanderson, R.D., 2004. Major-ion chemistry and ground-water salinization in ephemeral floodplains in some arid regions of Namibia. J. Arid Environ. 57, 211–223. https://doi.org/10.1016/S0140-1963(03)00095-8

Shepherd, K., Walsh, M., Mugo, F., Ong, C., Svan-Hansen, T., Swallow, B., Awiti, A., Hai, M., Nyantika, D., Ombalo, D., Grunder, M., Mbote, F., Mungai, D., 2000. Improved Land Management in the Lake Victoria Basin: Linking Land and Lake, Research and Extension, Catchment and Lake Basin. International Centre for Research in Agroforestry., Nairobi.

Shirazi, S.M., Imran, H.M., Akib, S., 2012. GIS-based DRASTIC method for groundwater vulnerability assessment: A review. J. Risk Res. 15, 991–1011. https://doi.org/10.1080/13669877.2012.686053

Sigman, D.M., Casciotti, K.L., Andreani, M., Barford, C., Galanter, M., Böhlke, J.K., 2001. A bacterial method for the nitrogen isotopic analysis of nitrate in seawater and freshwater. Anal. Chem. 73, 4145–4153. https://doi.org/10.1021/ac010088e

Simiyu, B.M., Oduor, S.O., Rohrlack, T., Sitoki, L., Kurmayer, R., 2018. Microcystin Content in Phytoplankton and in Small Fish from Eutrophic Nyanza Gulf, Lake Victoria, Kenya. Toxins (Basel). 10, 1–19. https://doi.org/10.3390/toxins10070275

Sitoki, L., Gichuki, J., Ezekiel, C., Wanda, F., Mkumbo, O.C., Marshall, B.E., 2010. The environment of Lake Victoria (East Africa): Current status and historical changes. Int. Rev. Hydrobiol. 95, 209–223. https://doi.org/10.1002/iroh.201011226

Soto, D.X., Koehler, G., Wassenaar, L.I., Hobson, K.A., 2019. Spatio-temporal variation of nitrate sources to Lake Winnipeg using N and O isotope (δ15N, δ18O) analyses. Sci. Total Environ. 647, 486–493. https://doi.org/10.1016/j.scitotenv.2018.07.346

Spivack, A., Edmond, J., 1986. Determination of Boron Isotope Ratios by Thermal Ionization Mass Spectrometry of the Dicesium Metaborate Cation,. Anal. Chem 58, 31. https://doi.org/10.1021/ac00292a010.

Spivack, A., Palmer, M., Edmond, J., 1987. The sedimentary cycle of the boron isotopes. Geochim. Cosmochim. Acta 51, 1939–1949. https://doi.org/10.1016/0016-7037(87)90183-9

Spruill, T.B., Showers, W.J., Howe, S.S., 2002. Application of Classification-Tree Methods to Identify Nitrate Sources in Ground Water. J. Environ. Qual. 31, 1538–1549.

Stager, J.C., Hecky, R.E., Grzesik, D., Cumming, B.F., Kling, H., 2009. Diatom evidence for the timing and causes of eutrophication in lake victoria, east africa. Hydrobiologia 636, 463–478. https://doi.org/10.1007/s10750-009-9974-7

Talling, J.F., 1966. The annual cycle of stratification and phytoplankton growth in Lake Victoria (East Africa). Int. Rev. Hydrobiol. 51, 545–621.

Thamdrup, B., Dalsgaard, T., 2002. Production of N2 through Anaerobic Ammonium

Oxidation Coupled to Nitrate Reduction in Marine Sediments. Appl. Environ. Microbiol. 68, 1312 LP – 1318. https://doi.org/10.1128/AEM.68.3.1312-1318.2002

Tian, L., Guo, Q., Zhu, Y., He, H., Lang, Y., Hu, J., Zhang, H., Wei, R., Han, X., Peters, M., Yang, J., 2016. Research and application of method of oxygen isotope of inorganic phosphate in Beijing agricultural soils. Environ. Sci. Pollut. Res. 23, 23406–23414. https://doi.org/10.1007/s11356-016-7482-7

Tirez, K., Brusten, W., Widory, D., Petelet, E., Bregnot, A., Xue, D., Boeckx, P., Bronders, J., 2010. Boron isotope ratio (δ11B) measurements in Water Framework Directive monitoring programs: Comparison between double focusing sector field ICP and thermal ionization mass spectrometry. J. Anal. At. Spectrom. 25, 964–974. https://doi.org/10.1039/c001840f

Triest, L., Lung'ayia, H., Ndiritu, G., Beyene, A., 2012. Epilithic diatoms as indicators in tropical African rivers (Lake Victoria catchment). Hydrobiologia 695, 343–360. https://doi.org/10.1007/s10750-012-1201-2

Twesigye, C.K., 2011. The Impact of Land Use Activities on Vegetation Cover and Water Quality in the Lake Victoria Watershed. Open Environ. Eng. J. 4, 66–77. https://doi.org/10.2174/1874829501104010066

UNEP, WHRC, 2007. Reactive Nitrogen in the Environment; Too Much or too Little of a Good Thing. United Nations Environ. Program. 1–56.

Vengosh, A., Heumann, K.G., Juraske, S., Kasher, R., 1994. Boron Isotope Application for Tracing Sources of Contamination in Groundwater. Environ. Sci. Technol. 28, 1968–1974.

Verschuren, D., Johnson, T.C., Kling, H.J., Edgington, D.N., Leavitt, P.R., Brown, E.T., Talbot, M.R., Hecky, R.E., 2002. History and timing of human impact on Lake Victoria, East Africa. Proc. R. Soc. B Biol. Sci. 269, 289–294. https://doi.org/10.1098/rspb.2001.1850

Wang, H., Wang, T., Toure, B., Li, F., 2012. Protect lake victoria through green economy, public participation and good governance. Environ. Sci. Technol. 46, 10483–10484. https://doi.org/10.1021/es303387v

Wells, N.S., Clough, T.J., Johnson-Beebout, S.E., Elberling, B., Baisden, W.T., 2019. Effects of denitrification and transport on the isotopic composition of nitrate (δ 18 O, δ 15 N) in freshwater systems. Sci. Total Environ. 651, 2228–2234. https://doi.org/10.1016/j.scitotenv.2018.10.065

White, R., Turpie, J., Gwyneth, L., 2017. Greening Africa ' s Cities:Enhancing the relationship between urbanization, environmental assets and ecosystem services. World Bank, Washingt. DC, USA 1–73.

WHO, World Health Organization, 2015. Urban Population Growth [WWW Document].

Widory, D., Kloppmann, W., Chery, L., Bonnin, J., Rochdi, H., Guinamant, J.L., 2004. Nitrate in groundwater: An isotopic multi-tracer approach. J. Contam. Hydrol. 72, 165–188. https://doi.org/10.1016/j.jconhyd.2003.10.010

Widory, D., Petelet-Giraud, E., Brenot, A., Bronders, J., Tirez, K., Boeckx, P., 2013.

Improving the management of nitrate pollution in water by the use of isotope monitoring: the δ ^{15}N, δ ^{18}O and δ ^{11}B triptych. Isotopes Environ. Health Stud. 49, 29–47. https://doi.org/10.1080/10256016.2012.666540

Widory, D., Petelet-Giraud, E., Négrel, P., Ladouche, B., 2005. Tracking the sources of nitrate in groundwater using coupled nitrogen and boron isotopes: A synthesis. Environ. Sci. Technol. 39, 539–548. https://doi.org/10.1021/es0493897

WorldBank, 2018. Lake Victoria Environmental Management Project: Project Information Document/Integrated Safeguards Data Sheet (PID /ISDS). World Bank 21.

WorldBank, 2012. Inclusive Green Growth: the pathway to sustainable development, The World Bank. https://doi.org/10.1596/978-0-8213-9551-6

Worthington, E.B., 1930. Observations on the temperature, hydrogen-ion concentration, and other physical conditions of the Victoria and Albert Nyanzas. Int. Rev. Hydrobiol. 24, 328–357.

Wright, J.A., Cronin, A., Okotto-Okotto, J., Yang, H., Pedley, S., Gundry, S.W., 2013. A spatial analysis of pit latrine density and groundwater source contamination. Environ. Monit. Assess. 185, 4261–4272. https://doi.org/10.1007/s10661-012-2866-8

Wyffels, S., Boeckx, P., Pynaert, K., Verstraete, W., Van Cleemput, O., 2003. Sustained nitrite accumulation in a membrane-assisted bioreactor (MBR) for the treatment of ammonium-rich wastewater. J. Chem. Technol. Biotechnol. 78, 412–419. https://doi.org/10.1002/jctb.808

Xia, X., Zhang, S., Li, S., Zhang, Liwei, Wang, G., Zhang, Ling, Wang, J., Li, Z., 2018. The cycle of nitrogen in river systems: Sources, transformation, and flux. Environ. Sci. Process. Impacts 20, 863–891. https://doi.org/10.1039/c8em00042e

Xue, D., Botte, J., De Baets, B., Accoe, F., Nestler, A., Taylor, P., Van Cleemput, O., Berglund, M., Boeckx, P., 2009. Present limitations and future prospects of stable isotope methods for nitrate source identification in surface- and groundwater. Water Res. 43, 1159–1170. https://doi.org/10.1016/j.watres.2008.12.048

Xue, D., De Baets, B., Van Cleemput, O., Hennessy, C., Berglund, M., Boeckx, P., 2013. Classification of Nitrate Polluting Activities through Clustering of Isotope Mixing Model Outputs. J. Environ. Qual. 42, 1486. https://doi.org/10.2134/jeq2012.0456

Xue, D., De Baets, B., Van Cleemput, O., Hennessy, C., Berglund, M., Boeckx, P., 2012. Use of a Bayesian isotope mixing model to estimate proportional contributions of multiple nitrate sources in surface water. Environ. Pollut. 161, 43–49. https://doi.org/10.1016/j.envpol.2011.09.033

Yevenes, M.A., Soetaert, K., Mannaerts, C.M., 2016. Tracing nitrate-nitrogen sources and modifications in a stream impacted by various land uses, south Portugal. Water (Switzerland) 8, 1–18. https://doi.org/10.3390/w8090385

Young, M.B., McLaughlin, K., Kendall, C., Stringfellow, W., Rollog, M., Elsbury, K., Donald, E., Paytan, A., 2009. Characterizing the oxygen isotopic composition of phosphate sources to aquatic ecosystems. Environ. Sci. Technol. 43, 5190–5196. https://doi.org/10.1021/es900337q

Zeng, H., Wu, J., 2015. Tracing the nitrate sources of the Yili River in the Taihu Lake watershed: A dual isotope approach. Water (Switzerland) 7, 188–201. https://doi.org/10.3390/w7010188

Zhang, F., Jin, Z., Yu, J., Zhou, Y., Zhou, L., 2015. Hydrogeochemical processes between surface and groundwaters on the northeastern Chinese Loess Plateau: Implications for water chemistry and environmental evolutions in semi-arid regions. J. Geochemical Explor. 159, 115–128. https://doi.org/10.1016/j.gexplo.2015.08.010

Zhang, Y., Shi, P., Li, F., Wei, A., Song, J., Ma, J., 2018a. Quantification of nitrate sources and fates in rivers in an irrigated agricultural area using environmental isotopes and a Bayesian isotope mixing model. Chemosphere 208, 493–501. https://doi.org/10.1016/j.chemosphere.2018.05.164

Zhang, M., Zhi, Y., Shi, J., Wu, L., 2018b. Apportionment and uncertainty analysis of nitrate sources based on the dual isotope approach and a Bayesian isotope mixing model at the watershed scale. Sci. Total Environ. 639, 1175–1187. https://doi.org/10.1016/j.scitotenv.2018.05.239

Zhang, Q., Li, Z., Zeng, G., Li, J., Fang, Y., Yuan, Q., Wang, Y., Ye, F., 2009. Assessment of surface water quality using multivariate statistical techniques in red soil hilly region: A case study of Xiangjiang watershed, China. Environ. Monit. Assess. 152, 123–131. https://doi.org/10.1007/s10661-008-0301-y

Zhou, M., Brandt, P., Pelster, D., Rufino, M.C., Robinson, T., Butterbach-Bahl, K., 2014. Regional nitrogen budget of the Lake Victoria Basin, East Africa: Syntheses, uncertainties and perspectives. Environ. Res. Lett. 9. https://doi.org/10.1088/1748-9326/9/10/105009

Appendices

Table A1. Physicochemical data of the spatial sampling stations in the Nyando catchment during the start wet (SW), peak wet (PW), end wet (EW) and the dry (D) seasons

Start wet season

Land use	Station ID	Na^{+} (mgL^{-1})	K+ (mgL-1)	Ca^{2+} (mgL^{-1})	Mg^{2+} (mgL^{-1})	Cl^{-} (mgL^{-1})	NO_3^{-} (mgL^{-1})	SO_4^{-} (mgL^{-1})	pH (-)	EC ($\mu S\ cm^{-1}$)	Temp (°C)	DO ($mg\ O_2\ L^{-1}$)	$\delta^{15}N$ (‰)	$\delta^{18}O$ (‰)
Sugarcane	S1	15.6	5.3	9.6	14.4	2.9	0.8	0.4	8.2	304	25.7	5.8	8.9	6.5
	S2	17.2	5.3	12.3	8.0	2.8	0.4	0.4	8.2	280	22.4	5.4	9.0	9.1
	S3	16.0	5.5	9.8	11.9	1.4	0.6	0.3	8.4	320	22.7	6.2	8.8	5.5
	S4	15.4	5.4	8.3	12.7	1.8	1.0	0.4	8.5	328	23.0	5.8	9.4	5.9
	S5	19.2	9.0	13.4	8.0	2.9	0.9	0.4	8.0	334	20.8	5.7	7.3	7.1
	S6	13.5	4.8	6.8	10.1	3.1	1.8	0.7	8.5	288	20.5	3.2	9.6	6.2
	S7	17.0	8.0	13.1	14.4	1.4	0.4	0.5	8.4	403	26.5	6.1	9.6	5.5
Tea & Forest	TF1	7.6	3.6	9.6	8.2	2.0	2.9	1.3	8.2	194	16.6	4.5	8.8	4.8
	TF2	7.6	4.3	10.7	9.1	2.0	2.1	0.6	8.1	206	18.0	5.0	6.4	4.7
	TF3	7.3	4.0	10.6	7.9	2.2	2.5	1.1	7.8	188	20.8	4.3	9.0	5.0
Mixed agriculture	MA1	14.9	6.4	6.3	1.5	6.0	6.1	3.0	5.1	114	18.4	6.0	8.9	3.4
	MA2	16.1	7.0	5.8	1.6	6.6	4.4	3.1	6.0	124	18.7	5.6	8.9	2.3
	MA3	21.3	7.2	9.2	6.4	3.1	-	1.6	5.8	221	18.9	6.0	13.9	17.0
	MA4	36.6	10.5	7.3	2.5	4.2	0.6	1.8	6.1	254	24.0	6.2	9.4	1.0
	MA5	15.9	11.4	9.0	1.9	4.4	8.5	2.7	7.5	168	22.9	5.3	5.3	9.1
Residential & Industrial	RI1	47.2	9.9	8.5	9.7	4.3	1.1	1.1	8.4	434	25.4	5.7	11.8	6.0
	RI2	30.8	8.4	9.6	7.3	3.7	1.0	1.2	8.4	321	27.6	4.8	8.2	3.4
	RI3	15.7	12.9	12.7	5.3	3.5	3.2	3.2	7.8	240	25.3	4.4	8.2	8.6
	RI4	28.3	19.8	14.8	7.7	3.9	1.9	1.4	7.8	476	27.9	5.3	9.1	4.5
	RI5	30.3	13.4	11.2	10.3	4.3	0.9	1.2	7.8	356	26.7	4.9	7.8	0.2
	RI6	21.2	16.6	12.5	6.4	4.7	2.8	2.7	8.0	299	27.3	5.7	9.2	4.4
	RI7	20.4	16.0	13.0	6.3	3.9	2.3	2.0	7.7	292	28.8	4.8	9.3	4.4

Table A1 (cont.): Peak wet season

Land use	Station ID	Na^+ (mgL^{-1})	K^+ (mgL-1)	Ca^{2+} (mgL^{-1})	Mg^{2+} (mgL^{-1})	Cl^- (mgL-1)	NO_3^- (mgL^{-1})	SO_4^- (mgL^{-1})	pH (-)	EC ($\mu S\ cm^{-1}$)	Temp (°C)	DO ($mg\ O_2\ L^{-1}$)	$\delta^{15}N$ (‰)	$\delta^{18}O$ (‰)
Sugarcane	S1	9.5	2.6	10.8	8.6	3.0	2.4	0.9	7.9	231	21.0	7.3	7.4	7.9
	S2	15.6	3.5	7.6	6.4	2.9	3.4	0.8	8.1	272	20.9	7.7	10.0	8.4
	S3	16.0	4.6	8.6	7.4	3.3	3.1	1.3	8.3	280	21.4	7.5	8.8	6.8
	S4	16.1	4.7	7.6	7.5	2.6	2.6	1.1	8.4	280	21.8	7.5	9.1	6.2
	S5	17.6	3.8	7.1	6.9	2.4	1.6	0.4	8.1	299	21.7	7.4	10.0	9.0
	S6	14.8	4.4	11.0	5.7	3.9	3.5	1.9	8.3	236	18.9	7.8	9.2	8.8
	S7	11.2	4.5	13.6	9.7	2.7	2.5	1.5	8.4	323	21.9	7.2	10.2	12.5
Tea & Forest	TF1	7.3	1.5	10.2	5.4	3.2	3.3	1.5	7.8	147	16.1	7.7	7.4	8.6
	TF2	6.5	2.4	9.5	5.1	1.7	2.5	0.6	7.8	137	16.6	7.7	5.1	8.6
	TF3	5.9	2.3	9.0	5.6	2.7	3.8	1.6	7.8	148.	19.6	7.2	6.4	5.0
Mixed agriculture	MA1	17.3	5.4	7.5	1.6	5.4	7.6	2.4	7.3	146	15.2	7.3	9.6	11.5
	MA2	16.9	5.9	6.3	2.4	9.3	6.4	3.9	7.2	149	15.8	7.0	9.5	9.4
	MA3	18.9	5.5	6.8	2.9	4.6	5.6	1.3	7.4	168	19.4	6.7	14.0	19.6
	MA4	19.5	6.8	8.6	1.8	8.2	4.0	4.4	7.8	180	18.8	7.4	8.8	10.3
	MA5	11.9	6.6	9.0	3.0	5.9	2.3	2.9	7.8	153	16.5	7.6	11.8	9.1
Residential & Industrial	RI1	25.5	5.9	11.3	4.7	4.5	1.7	1.2	8.2	271	20.3	7.5	10.3	10.7
	RI2	21.7	5.9	10.8	3.4	6.2	3.3	2.3	8.2	216	22.5	7.3	8.9	9.1
	RI3	14.3	4.8	10.8	2.9	4.1	1.4	2.0	7.6	162	21.9	6.8	6.3	12.0
	RI4	21.5	8.5	11.7	4.0	7.0	3.6	3.1	7.9	241	22.7	6.7	9.3	10.5
	RI5	16.2	6.6	13.5	4.1	5.0	1.5	2.0	7.8	215	20.3	7.9	8.0	8.4
	RI6	16.3	6.1	11.0	3.8	4.4	2.8	2.2	8.0	213	22.6	7.0	9.2	11.4
	RI7	17.0	6.1	11.8	3.8	5.0	1.9	2.0	7.9	216	23.0	6.9	8.6	10.6

Table A1 (cont.): End wet season

Land use	Station ID	Na^{+} (mgL^{-1})	K+ (mgL-1)	Ca^{2+} (mgL^{-1})	Mg^{2+} (mgL^{-1})	Cl^{-} (mgL^{-1})	NO_3^{-} (mgL^{-1})	SO_4^{-} (mgL^{-1})	pH (-)	EC ($\mu S\ cm^{-1}$)	Temp (°C)	DO ($mg\ O_2\ L^{-1}$)	$\delta^{15}N$ (‰)	$\delta^{18}O$ (‰)
Sugarcane	S1	10.0	3.6	18.1	9.6	1.0	0.3	0.2	8.3	259	24.9	7.2	7.9	12.7
	S2	14.2	3.7	10.6	5.9	1.6	1.3	0.3	8.2	253	20.5	7.9	8.6	9.6
	S3	14.6	4.7	12.4	6.2	4.1	2.7	1.7	8.4	242	20.5	7.8	6.1	9.0
	S4	14.2	4.6	12.4	6.1	3.6	2.4	1.5	8.2	242	20.7	7.8	8.1	8.7
	S5	16.6	4.4	15.0	7.3	3.7	2.3	1.0	8.2	300	20.3	8.2	7.6	6.2
	S6	13.5	4.5	13.6	4.8	4.0	2.7	1.7	8.4	205	18.6	7.8	9.1	8.5
	S7	10.2	5.4	21.9	9.6	2.4	1.2	1.4	8.3	304	22.5	7.1	10.5	8.0
Tea & Forest	TF1	5.6	2.4	11.6	5.6	1.4	1.9	1.0	7.9	137	16.2	7.7	5.4	4.1
	TF2	6.0	3.0	10.8	4.9	2.2	2.9	1.2	7.6	134	15.8	7.8	3.8	3.4
	TF3	5.8	2.5	13.3	5.9	2.2	2.5	1.9	8.1	153	18.2	7.5	7.0	6.6
Mixed agriculture	MA1	16.5	11.3	5.9	1.4	6.9	10.4	4.1	7.5	143	15.3	7.0	8.1	5.1
	MA2	17.2	11.0	8.3	1.9	8.9	5.6	4.6	7.5	167	14.6	6.8	9.8	11.8
	MA3	15.9	6.5	12.2	4.9	4.3	11.6	1.7	7.5	196	16.7	7.0	9.0	11.1
	MA4	25.3	8.6	9.6	2.5	5.3	3.1	3.0	8.3	225	18.2	7.4	6.8	2.4
	MA5	14.5	7.2	9.7	2.4	2.6	1.0	0.7	7.7	183	16.2	7.1	7.3	-1.1
Residential & Industrial	RI1	20.2	7.0	12.4	4.3	5.1	3.8	2.6	8.3	232	19.6	7.5	8.4	6.9
	RI2	19.0	6.6	15.5	4.2	5.8	3.4	3.1	8.4	218	22.4	7.3	9.4	8.8
	RI3	17.3	10.7	12.7	5.3	5.1	1.8	2.7	7.8	247	22.5	6.7	7.5	5.8
	RI4	21.3	17.5	18.1	5.5	6.2	2.6	2.9	8.0	287	23.4	4.1	8.6	8.1
	RI5	19.1	10.1	14.9	5.0	5.1	3.4	2.5	7.9	259	21.4	7.4	9.0	3.1
	RI6	18.9	9.1	17.2	5.1	2.9	1.1	1.6	8.0	248	23.0	6.6	7.1	4.5
	RI7	17.8	9.8	13.8	5.4	3.8	2.0	1.5	8.0	258	23.6	6.6	8.8	6.3

Table A1 (cont.): Dry season

Land use	Station ID	Na^{+} (mgL^{-1})	K+ (mgL-1)	Ca^{2+} (mgL^{-1})	Mg^{2+} (mgL^{-1})	Cl^{-} (mgL^{-1})	NO_3^{-} (mgL^{-1})	SO_4^{-} (mgL^{-1})	pH (-)	EC ($\mu S\ cm^{-1}$)	Temp (°C)	DO ($mg\ O_2\ L^{-1}$)	$\delta^{15}N$ (‰)	$\delta^{18}O$ (‰)
Sugarcane	S1	12.9	4.1	14.2	13.2	2.7	0.6	0.6	8.1	330	22.1	7.8	9.8	3.8
	S2	15.5	4.2	13.7	7.1	2.3	1.5	0.4	8.3	274	20.7	8.0	8.6	9.7
	S3	16.6	4.9	16.4	10.4	3.3	1.4	0.8	8.6	323	21.3	8.1	10.4	10.2
	S4	17.0	5.2	11.2	11.0	3.5	1.4	0.9	8.5	333	23.0	7.4	8.5	7.6
	S5	16.8	5.2	17.6	8.1	3.1	1.2	0.4	8.4	329	22.9	7.1	9.4	2.8
	S6	15.7	4.8	11.3	8.4	3.9	1.9	1.1	8.5	285	19.0	7.7	8.6	9.7
	S7	15.3	7.2	18.5	14.0	2.5	1.4	1.0	8.5	424	23.4	7.3	11.8	15.6
Tea & Forest	TF1	6.9	2.5	9.4	7.6	1.5	1.9	1.5	8.1	193	15.2	7.7	6.6	5.7
	TF2	6.8	2.8	9.2	7.7	1.7	1.5	1.2	8.1	187	15.5	7.8	7.2	10.6
	TF3	6.6	2.6	10.3	7.5	1.5	1.6	1.3	7.9	186	17.9	7.3	8.9	12.0
Mixed agriculture	MA1	15.8	6.3	5.9	1.4	7.1	8.1	4.0	7.5	141	15.4	7.1	8.6	11.0
	MA2	16.4	7.0	6.6	1.6	7.3	7.0	3.3	7.7	152	15.5	7.2	8.8	10.2
	MA3	20.9	5.9	11.1	5.7	4.6	-	4.7	7.1	235	18.1	5.1	9.5	16.6
	MA4	33.6	10.7	8.1	2.6	9.3	2.4	5.1	8.6	266	22.1	6.9	12.4	11.7
	MA5	23.1	11.3	14.3	4.0	5.1	1.0	2.3	8.0	299	20.7	7.1	4.8	-4.5
Residential & Industrial	RI1	35.7	11.6	16.4	9.4	6.0	1.0	1.7	8.4	424	21.4	6.7	10.9	9.3
	RI2	32.6	9.4	13.6	8.4	5.3	0.4	1.9	8.6	376	25.4	7.6	12.1	8.9
	RI3	26.1	19.8	19.7	10.1	5.8	0.2	1.9	8.3	400	22.6	7.7	8.3	1.6
	RI4	35.2	69.4	26.2	12.7	12.3	0.1	2.7	8.1	621	27.0	0.1	8.2	12.5
	RI5	24.7	20.4	18.5	9.8	5.6	0.5	1.4	8.3	389	23.2	6.8	15.1	7.2
	RI6	26.6	20.2	18.0	9.2	5.9	0.3	2.3	8.3	399	26.0	5.6	11.1	4.8
	RI7	26.8	20.2	18.6	9.6	6.4	0.2	2.3	7.9	412	25.7	3.5	8.6	1.4

Table A2. Physicochemical data of the spatial sampling stations in the Sondu Miriu River catchment during the start wet (SW), peak wet (PW), end wet (EW) and the dry (D) seasons

Start wet season

Land use	Station ID	Na^{+} (mgL^{-1})	K+ (mgL-1)	Ca^{2+} (mgL^{-1})	Mg^{2+} (mgL^{-1})	Cl^{-} (mgL^{-1})	NO_3^{-} (mgL^{-1})	SO_4^{-} (mgL^{-1})	pH (-)	EC ($\mu S\ cm^{-1}$	Temp (°C)	DO ($mg\ O_2\ L^{-1}$)	$\delta^{15}N$ (‰)	$\delta^{18}O$ (‰)
Tea	T1	4.8	3.9	3.4	0.9	1.9	2.1	1.0	7.5	52	21	7	7.6	6.1
	T2	5.2	4.1	3.3	1.0	2.1	2.3	1.2	7.5	59	20	7	6.4	6.4
	T3	2.8	3.2	2.4	0.7	1.5	1.6	0.7	7.6	38	21	7	5.3	4.7
	T4	9.3	3.6	2.9	1.1	2.4	3.3	1.4	7.5	57	24	5	8.4	6.0
	T5	8.0	4.6	4.2	1.1	2.4	1.5	1.1	7.2	66	17	7	8.7	3.6
	T6	5.8	4.3	4.8	1.1	2.0	1.7	1.1	7.0	59	19	6	6.4	2.9
Tea & Urban	TU1	9.2	3.2	3.6	0.8	1.8	3.8	0.7	7.2	67	19	6	7.7	5.9
	TU2	5.5	3.7	3.6	0.8	2.7	6.8	1.5	7.0	60	22	7	9.6	7.8
Mixed agriculture	MA1	7.9	4.3	4.8	1.5	3.5	4.3	2.0	7.8	82	26	5	8.7	5.5
	MA2	8.7	4.6	6.1	1.6	3.7	4.3	2.2	7.2	92	27	5	9.0	6.4
	MA3	10.2	6.3	5.6	1.4	4.3	3.7	2.6	7.4	103	24	5	9.6	8.3
	MA4	9.4	5.2	6.2	1.6	4.4	5.6	2.6	7.8	100	24	4	9.1	5.1

Table A2 (cont.): Peak wet season

Land use	Station ID	Na^+ (mgL^{-1})	K+ (mgL-1)	Ca^{2+} (mgL^{-1})	Mg^{2+} (mgL^{-1})	Cl^- (mgL^{-1})	NO_3^- (mgL^{-1})	SO_4^- (mgL^{-1})	pH (-)	EC ($\mu S\ cm^{-1}$	Temp (°C)	DO (mg O_2 L^{-1})	$\delta^{15}N$ (‰)	$\delta^{18}O$ (‰)
Tea	T1	4.1	1.9	1.8	BDL	1.7	2.5	0.5	7.0	39.7	15.8	8.2	5.5	5.9
	T2	4.6	2.2	2.0	BDL	2.1	2.9	0.7	7.2	43.3	15.7	8.1	6.8	6.8
	T3	3.4	1.6	2.4	BDL	2.0	2.4	0.7	7.0	30.1	15.4	8.3	6.1	7.6
	T4	4.6	1.9	2.0	BDL	2.2	3.0	0.6	7.2	43.0	18.4	8.1	4.7	5.4
	T5	4.8	2.2	2.4	BDL	2.2	2.8	0.7	7.2	45	17.7	8.1	6.7	7.4
	T6	3.6	1.6	1.8	BDL	1.8	2.6	0.5	7.0	33	14.9	8.2	4.9	5.4
Tea & Urban	TU.1	5.3	2.2	2.5	BDL	2.3	5.2	0.5	6.7	52.1	16.1	7.3	6.8	11.6
	TU.2	5.0	2.1	2.4	BDL	3.4	8.0	0.8	6.9	46.6	16.5	7.9	6.4	10.1
Mixed agriculture	MA.1	5.4	2.2	2.2	BDL	2.6	3.6	0.8	6.9	51.9	19.9	7.7	6.9	10.9
	MA.2	6.2	2.2	2.9	BDL	2.8	3.6	0.9	7.0	57.5	21.9	7.3	9.1	13.7
	MA.3	6.4	2.9	2.7	BDL	3.3	3.5	1.1	7.1	60.1	17.8	7.7	9.1	6.7
	MA.4	7.6	2.8	3.5	BDL	3.0	3.3	1.0	7.5	71.1	19.5	7.9	7.7	7.0

Table A2 (cont.): End wet season

Land use	Station ID	Na^+ (mgL^{-1})	K+ (mgL-1)	Ca^{2+} (mgL^{-1})	Mg^{2+} (mgL^{-1})	Cl^- (mgL^{-1})	NO_3^- (mgL^{-1})	SO_4^- (mgL^{-1})	pH (-)	EC ($\mu S\ cm^{-1}$	Temp (°C)	DO ($mg\ O_2\ L^{-1}$)	$\delta^{15}N$ (‰)	$\delta^{18}O$ (‰)
Tea	T1	3.6	2.5	2.1	BDL	2.2	3.2	1.2	6.9	37.5	18.7	7.6	6.1	7.7
	T2	4.1	2.7	2.3	BDL	2.0	2.7	1.0	6.9	41.5	16.9	7.8	6.3	6.3
	T3	2.8	1.9	2.1	BDL	2.0	2.6	1.0	6.6	29.9	17.9	7.6	2.8	2.2
	T4	4.2	2.4	2.6	BDL	2.3	3.9	1.2	7.5	42.8	18.8	8.1	7.1	8.6
	T5	4.1	2.7	2.3	BDL	2.3	2.7	1.5	6.8	39.0	18.1	7.6	5.9	5.1
	T6	4.4	2.8	2.7	BDL	2.3	4.1	1.4	6.7	44.6	17.8	7.6	7.3	9.4
Tea & Urban	TU1	4.7	2.6	3.1	BDL	2.4	6.1	1.0	7.0	51.2	16.6	7.4	8.5	10.8
	TU2	4.1	2.5	2.9	BDL	2.6	6.1	1.2	6.8	45.6	18.1	7.6	8.1	9.5
Mixed agriculture	MA1	4.6	2.9	2.7	BDL	2.6	3.6	1.0	7.9	47.4	21.1	8.0	7.6	8.5
	MA2	5.2	2.9	3.3	0.8	2.7	3.8	1.4	7.2	52.4	22.0	7.5	7.2	5.4
	MA3	4.8	3.6	3.1	BDL	2.3	2.3	1.3	7.0	50.3	19.7	7.4	7.7	7.4
	MA4	6.5	3.5	4.1	BDL	3.5	4.0	1.7	8.0	66.6	22.5	7.6	7.6	8.2

Table A2 (cont.): Dry season

Land use	Station ID	Na^{+} (mgL^{-1})	K+ (mgL-1)	Ca^{2+} (mgL^{-1})	Mg^{2+} (mgL^{-1})	Cl^{-} (mgL^{-1})	NO_3^{-} (mgL^{-1})	SO_4^{-} (mgL^{-1})	pH (-)	EC ($\mu S\ cm^{-1}$)	Temp (°C)	DO ($mg\ O_2\ L^{-1}$)	$\delta^{15}N$ (‰)	$\delta^{18}O$ (‰)
Tea	T1	4.1	2.6	2.3	0.6	1.5	3.0	0.8	7.0	45.2	18.1	8.0	6.6	8.5
	T2	4.3	2.8	2.3	0.6	1.5	2.8	0.9	7.4	48.3	16.2	7.9	6.3	9.5
	T3	2.7	2.0	1.8	0.5	1.1	2.7	0.6	7.2	35.3	15.5	8.2	5.8	7.8
	T4	4.7	2.6	2.9	0.7	1.7	3.4	0.8	7.2	49.9	21.0	8.0	7.7	9.7
	T5	4.5	2.9	2.3	0.6	1.9	3.8	1.2	7.1	49.0	15.3	8.1	7.5	9.9
	T6	4.5	2.8	3.1	0.8	1.5	2.2	0.9	6.6	47.9	15.7	7.5	7.1	7.7
Tea & Urban	TU1	5.6	2.5	2.4	0.6	1.6	5.4	0.5	6.5	54.3	16.5	7.6	6.8	11.1
	TU2	4.7	2.8	2.5	0.6	2.1	6.9	0.8	7.2	54.7	19.5	7.7	7.1	11.1
Mixed agriculture	MA1	5.6	2.9	3.4	1.0	1.8	2.7	0.9	8.1	63.4	21.4	8.1	9.0	8.3
	MA2	10.7	3.2	4.4	1.2	3.1	3.3	1.5	6.8	94.2	23.3	6.9	8.3	9.7
	MA3	7.0	3.8	6.2	1.2	4.1	4.1	3.6	7.2	66.0	22.0	7.3	8.3	6.7
	MA4	7.2	3.7	5.1	1.4	2.8	3.5	1.3	8.0	84.2	21.9	8.0	9.0	8.9

Table A3. Physicochemical data of the spatial sampling stations in the Nzoia catchment during the start wet (SW), peak wet (PW), end wet (EW) and the dry (D) seasons

Start wet season

Land use	Station ID	Na^+ (mgL^{-1})	K+ (mgL-1)	Ca^{2+} (mgL^{-1})	Mg^{2+} (mgL^{-1})	Cl^- (mgL^{-1})	NO_3^- (mgL^{-1})	SO_4^- (mgL^{-1})	pH (-)	EC ($\mu S\ cm^{-1}$)	Temp (°C)	DO ($mg\ O_2\ L^{-1}$)	$\delta^{15}N$ (‰)	$\delta^{18}O$ (‰)
Commercial agriculture	CA1	5.3	2.7	7.2	3.8	2.5	4.1	1.6	7.2	95	22.8	6.4	8.5	4.4
	CA2	9.6	3.8	7.3	2.8	3.9	4.7	1.7	7.6	110	23.9	6.7	7.0	6.0
	CA3	10.3	3.2	9.6	4.0	2.9	5.9	1.8	7.6	148	23.9	6.5	9.4	7.9
	CA4	12.0	4.2	10.7	4.8	5.5	2.0	1.3	7.8	166	24.0	5.5	8.4	4.5
	CA5	8.4	3.4	8.2	3.5	3.2	3.9	1.8	8.6	138	24.6	7.8	8.2	5.6
	CA6	8.6	4.4	8.3	3.4	3.0	3.7	1.6	8.3	124	26.5	6.7	7.5	2.4
	CA7	7.7	2.8	6.6	2.6	2.6	5.0	3.1	7.4	94	26.5	6.0	6.2	5.1
	CA8	8.2	4.2	7.7	2.8	3.3	1.6	2.0	7.1	107	25.8	4.3	10.7	8.7
	CA9	6.5	2.0	6.3	2.9	2.2	6.0	2.2	7.3	88	24.6	7.5	7.4	5.9
	CA10	7.7	3.2	9.9	4.0	3.2	2.3	1.1	7.6	133	22.8	6.2	8.4	4.8
Mixed agriculture	MA1	5.1	2.8	6.6	3.1	1.8	2.3	0.8	6.9	86	22.0	6.4	5.9	5.2
	MA2	6.8	3.4	6.5	2.3	2.9	2.1	1.1	7.6	87	21.8	6.3	6.0	3.3
	MA3	30.8	4.0	3.1	1.1	4.5	0.4	0.7	7.4	160	16.5	6.0	6.6	3.5
	MA4	10.0	4.0	5.4	1.5	1.8	0.7	0.2	7.2	89	17.0	6.8	5.6	0.2
	MA5	14.6	4.2	6.7	2.0	3.9	2.0	1.0	7.4	116	22.3	4.6	8.4	6.3
	MA6	9.6	3.0	3.3	1.6	1.7	1.0	0.6	7.9	94	24.5	5.9	7	4.3
	MA7	8.1	4.0	3.3	1.1	3.1	2.1	1.0	7.2	71	17.0	6.1	14.2	13.7
Urban	U1	21.0	5.8	12.2	7.9	12.3	2.8	3.8	8.2	274	24.0	6.4	8.8	5.1
	U2	21.8	8.3	9.9	2.2	12.9	0.4	3.5	7.7	206	26.6	3.0	10.7	5.6
	U3	18.8	6.8	11.0	4.9	10.8	2.7	3.9	8.4	260	22.3	7.7	8.7	5.2
	U4	13.7	6.4	11.0	4.6	7.1	4.9	4.4	7.8	185	22.6	6.1	10.6	5.6

Table A3 (cont.): Peak wet season

Land use	Station ID	Na^{+} (mgL^{-1})	K+ (mgL-1)	Ca^{2+} (mgL^{-1})	Mg^{2+} (mgL^{-1})	Cl^{-} (mgL^{-1})	NO_3^{-} (mgL^{-1})	SO_4^{-} (mgL^{-1})	pH (-)	EC ($\mu S\ cm^{-1}$)	Temp (°C)	DO ($mg\ O_2\ L^{-1}$)	$\delta^{15}N$ (‰)	$\delta^{18}O$ (‰)
Commercial agriculture	CA1	5.5	1.2	4.9	2.9	2.7	3.0	0.7	7.2	84	20.0	7.6	8.3	9.7
	CA2	10.6	2.7	6.3	2.3	3.8	1.7	1.0	7.8	114	19.8	8.3	10.1	12.1
	CA3	9.0	3.0	10.9	3.7	2.4	3.7	0.6	7.6	113	20.0	7.3	9.2	10.7
	CA4	12.6	3.4	10.1	3.9	0.2	0.3	0.0	7.2	161	19.2	6.2	5.5	14.9
	CA5	10.5	3.0	4.5	1.3	4.2	0.7	0.8	7.9	89	19.8	7.7	11.9	12.2
	CA6	6.9	2.0	8.1	2.9	1.3	0.6	0.3	7.7	106	23.0	7.3	8.6	12.6
	CA7	9.9	2.5	5.9	2.5	4.2	1.4	1.4	7.4	112	21.4	7.1	8.6	11.7
	CA8	10.5	2.7	6.5	2.4	3.5	0.9	0.8	7.5	117	21.3	7.4	10.8	11.6
	CA9	11	2.9	8.2	3.0	3.2	1.7	0.9	7.4	89	22.5	7.5	7.4	11.4
	CA10	7.8	2.3	6.0	2.6	2.4	1.3	0.5	7.5	109	20.8	7.4	8.9	11.9
Mixed agriculture	MA1	4.7	1.4	3.4	1.6	2.2	2.2	0.6	7.0	60	19.6	7.2	6.1	14.5
	MA2	6.5	1.8	5.8	1.9	2.3	0.6	1.3	6.9	78	18.7	6.2	8.7	11.7
	MA3	9.1	2.3	2.6	0.9	2.8	0.1	0.2	6.9	67	16.8	7.1	6.4	13.9
	MA4	10.0	3.3	4.0	1.0	2.4	0.4	0.4	7.5	82	17.8	7.5	3.2	13.0
	MA5	9.8	2.7	3.8	1.2	2.8	0.2	0.2	7.3	87	18.7	7.6	5.8	13.1
	MA6	4.6	2.0	6.5	2.0	2.5	0.1	0.8	7.3	79	17.0	7.6	6.5	14.7
	MA7	7.5	2.2	4.3	1.4	2.5	0.6	0.6	7.1	76	18.1	7.2	6.1	13.5
Urban	U1	20.1	4.0	10.7	4.9	2.2	0.4	0.3	7.7	222	18.3	7.4	6.2	9.1
	U2	11.7	4.2	5.2	1.2	7.7	4.8	2.8	7.3	105	18.0	7.4	14.3	14.0
	U3	11.8	3.8	5.3	1.4	4.8	2.9	1.1	7.1	111	18.7	7.4	10.3	3.7
	U4	14.5	4.0	7.1	2.5	4.9	2.7	1.4	7.3	145.6	18.3	7.4	10.3	8.9

Table A3 (cont.): End wet season

Land use	Station ID	Na^{+} (mgL^{-1})	K+ (mgL-1)	Ca^{2+} (mgL^{-1})	Mg^{2+} (mgL^{-1})	Cl^{-} (mgL^{-1})	NO_3^{-} (mgL^{-1})	SO_4^{-} (mgL^{-1})	pH (-)	EC ($\mu S\ cm^{-1}$)	Temp (°C)	DO ($mg\ O_2\ L^{-1}$)	$\delta^{15}N$ (‰)	$\delta^{18}O$ (‰)
Commercial agriculture	CA1	5.4	2.3	5.2	2.9	4.4	3.3	30.7	7.4	78	20.1	7.5	7.7	5.6
	CA2	10.8	3.3	9.0	3.1	4.9	2.8	6.4	8.0	122	20.0	8.1	8.3	-0.9
	CA3	10.8	3.1	15.3	5.8	5.3	6.3	7.0	7.7	180	20.8	7.2	9.9	6.7
	CA4	11.6	3.8	11.8	4.2	7.5	2.0	6.9	7.3	151	18.5	6.6	8.0	3.3
	CA5	10.8	3.7	5.7	1.9	5.6	3.0	7.5	7.7	101	20.3	7.4	10.7	3.0
	CA6	5.9	3.0	5.4	2.6	4.7	1.7	6.7	7.8	92	21.1	7.5	5.4	-2.2
	CA7	8.9	2.9	6.7	2.7	5.4	2.6	6.6	7.4	104	22.6	6.9	7.8	5.3
	CA8	10.4	3.5	8.4	2.9	5.7	2.4	7.8	7.5	117	21.8	7.2	5.4	-4.8
	CA9	6.5	2.0	5.7	3.0	3.8	2.8	7.5	7.4	92	23.7	7.2	8.0	5.4
	CA10	6.4	2.2	8.0	4.1	3.7	1.9	6.9	7.5	131	18.9	7.4	8.4	3.2
Mixed agriculture	MA1	5.6	1.8	5.0	2.8	3.3	2.5	6.9	7.2	79	20.3	7.4	8.4	3.6
	MA2	7.1	2.3	6.6	2.4	4.2	2.6	9.6	7.1	95	17.7	7.2	6.1	1.6
	MA3	9.7	2.8	3.0	1.2	3.2	0.3	6.9	7.1	79	18.1	7.4	7.6	2.8
	MA4	9.6	3.6	3.6	1.2	4.0	0.5	5.9	7.8	83	18.5	7.6	9.0	3.6
	MA5	11.3	3.5	4.9	1.7	5.1	0.9	7.9	7.7	99	18.9	7.6	10.7	-6.4
	MA6	3.0	2.0	5.5	1.8	2.7	0.8	7.5	7.8	62	14.0	8.3	4.3	-5.4
	MA7	7.0	3.2	3.1	0.9	3.9	1.8	9.5	6.8	64	18.4	7.5	12.1	8.7
Urban	U1	20.8	5.3	9.4	5.9	13.1	2.5	7.3	7.7	222	17.6	7.5	9.0	1.9
	U2	11.9	5.7	4.6	1.5	8.5	4.4	5.9	8.0	112	20.2	7.6	14.5	2.8
	U3	13.1	5.0	5.9	2.1	7.9	6.2	6.1	7.1	123	18.9	7.3	9.8	-1.7
	U4	12.4	4.9	12.8	5.0	7.5	3.6	6.6	7.5	184	18.6	7.3	11.6	5.2

Table A3 (cont.): Dry season

Land use	Station ID	Na^{+} (mgL^{-1})	K+ (mgL-1)	Ca^{2+} (mgL^{-1})	Mg^{2+} (mgL^{-1})	Cl^{-} (mgL^{-1})	NO_3^{-} (mgL^{-1})	SO_4^{-} (mgL^{-1})	pH (-)	EC ($\mu S\ cm^{-1}$)	Temp (°C)	DO ($mg\ O_2\ L^{-1}$)	$\delta^{15}N$ (‰)	$\delta^{18}O$ (‰)
Commercial agriculture	CA1	5.7	1.7	7.6	4.5	2.0	3.3	0.5	7.7	114	19.4	7.7	8.2	11.3
	CA2	11.1	2.9	9.3	3.9	3.5	2.8	0.9	8.2	147	21.5	8.2	10.7	10.6
	CA3	11.6	3.5	13.5	6.1	2.8	3.7	0.7	8.1	204	21.2	8.2	8.6	10.6
	CA4	11.5	2.7	11.4	4.9	2.8	1.6	0.4	7.8	170	18.8	7.1	8.8	10.0
	CA5	12.2	3.6	6.7	2.6	4.2	4.8	0.9	8.1	122	19.5	8.6	14.0	9.3
	CA6	7.7	2.9	9.7	3.9	2.5	2.5	0.9	7.7	128	22.4	7.6	7.1	5.5
	CA7	10.0	2.6	8.0	4.1	3.1	2.3	1.1	7.8	137	24.7	6.6	10.2	6.9
	CA8	10.5	2.9	9.7	3.9	3.1	2.1	0.8	8.0	142	22.5	6.0	11.0	10.0
	CA9	7.9	1.6	9.2	4.6	2.2	2.8	0.7	7.9	121	22.0	7.4	8.8	10.1
	CA10	7.7	3.1	10.8	4.7	2.7	0.9	0.8	7.8	157	20.3	7.4	9.8	11.9
Mixed agriculture	MA1	5.6	2.3	7.0	4.1	2.4	1.9	0.4	7.6	105	19.0	8.7	8.3	10.6
	MA2	7.2	1.8	7.3	2.6	1.8	3.0	0.6	7.5	96	18.2	7.4	5.8	7.6
	MA3	15.9	2.9	4.0	1.2	1.7	0.5	0.2	7.2	111	15.6	7.3	7.5	7.4
	MA4	9.5	3.2	4.1	1.3	1.9	0.5	0.4	7.2	88	15.5	7.6	10.2	9.4
	MA5	13.7	4.2	8.0	2.2	3.5	1.0	0.5	7.4	122	19.0	6.8	10.0	4.8
	MA6	4.5	2.6	7.8	2.4	1.7	1.2	1.0	7.2	82	19.4	7.2	5.2	4.9
	MA7	10.3	4.6	5.0	1.5	3.7	6.7	1.6	6.6	98	15.6	5.8	16.5	19.2
Urban	U1	17.0	3.2	11.7	6.6	6.0	3.5	2.1	8.0	240	19.8	7.6	7.6	9.1
	U2	22.6	7.8	9.9	2.3	11.3	1.4	2.8	7.8	206	17.5	6.4	16.2	15.4
	U3	20.9	9.4	15.0	4.2	13.2	9.6	4.8	8.2	196	19.0	7.4	16.0	6.9
	U4	13.9	4.2	13.0	5.8	3.4	2.7	0.7	8.0	212	18.7	8.0	12.5	11.3

Table A4. Nitrate and isotope results from laboratory incubations of Nyando and Sondu Miriu River bed sediments for determination of denitrification enrichment factors

	Time (Hours)	0	4	8	24	30	48	%Carbon
Nyando (MA4)	NO_3^-(mgL^{-1})	9.5	6.9	4.4	0.1	-	-	4
	$\delta^{15}N$(‰)	13.7	22.6	25.8	-	-	-	
	$\delta^{18}O$(‰)	12.1	19.7	23.6	-	-	-	
Nyando (MA5)	NO_3^-(mgL^{-1})	79	77	58	51	33	2	6
	$\delta^{15}N$(‰)	6.5	7.6	9.8	13.8	22.3	-	
	$\delta^{18}O$(‰)	22.9	23.4	25.3	30.3	36.6	-	
Sondu wetland (near TU1)	NO_3^-(mgL^{-1})	78	74	68	64	51	-	8
	$\delta^{15}N$(‰)	5.0	-	6.9	8.7	9.4	-	
	$\delta^{18}O$(‰)	23.3	-	23.4	25.2	26.7	-	
Sondu (MA1)	NO_3^-(mgL^{-1})	23.0	22.5	21.4	12.4	11.7	10.7	0.8
	$\delta^{15}N$(‰)	9.5	9.9	11.5	23.6	24.8	26.1	
	$\delta^{18}O$(‰)	24.0	23.4	26.7	38.1	39.1	39.4	
Sondu (TU2)	NO_3^-(mgL^{-1})	20.4	20.4	20.0	11.3	9.9	7.8	1
	$\delta^{15}N$(‰)	9.4	10.1	11.2	28.1	31.2	36.9	
	$\delta^{18}O$(‰)	24.3	25.7	26.7	41.7	45.1	50.3	

Table A5. The spatial distribution of NO_3^- concentration (mg L^{-1}) in R. Nyando during the nine season monitoring period (2016 – 2018). Values < 0.04 indicate attributes below detection limit; "–" represents samples not analyzed

Land use	Station ID	Station name	Latitude (South)	Longitude (East)	Peak wet/2016	End wet/2016	Dry/ 2016	Start wet/2017	Peak wet/2017	End wet/2017	Dry/ 2017	Start wet/2018	Peak wet/2018
Mixed Agriculture	**MA1**	R. Masaita upstream	0.135	35.608	7.6	10.4	8.1	6.1	5.8	7.3	9.9	6.9	4.1
	MA2	R. Masaita at Londiani	0.163	35.584	6.4	5.6	7.0	4.4	4.3	5.4	7.1	4.9	4.5
	MA3	Finlays stream	0.142	35.534	5.6	11.6	23.8	22.9	23.7	26.9	44.2	56.3	4.1
	MA4	R. Kipchorian at Kipkelion	0.207	35.462	4.0	3.1	2.5	0.6	7.5	6.2	4.5	5.7	7.1
	MA5	R. Tugunon	0.255	35.415	2.3	1.0	1.0	8.5	5.8	10.5	4.4	5.0	9.1
Residential & Industrial	**RI1**	R. Namuting	0.204	35.348	1.7	3.8	1.0	1.1	3.5	5.9	4.1	5.8	6.7
	RI2	R. Nyando- upstrm Muhoroni	0.163	35.196	3.3	3.4	0.4	1.0	5.7	7.5	1.0	7.3	6.7
	RI3	R. Nyando at Ahero	0.172	34.921	1.4	1.8	0.2	3.2	4.9	5.5	3.2	5.1	5.2
	RI4	R. Nyando - dstrm Muhoroni	0.166	35.162	3.6	2.6	0.1	< 0.04	5.2	7.2	2.1	6.7	7.3
	RI5	R. Nyando at Ogilo	0.126	35.001	1.5	3.4	0.5	0.9	4.3	5.2	2.4	6.4	4.2
	RI6	R. Nyando at wetland	0.286	34.889	2.8	1.1	0.3	2.8	2.9	5.6	1.1	5.1	3.8
	RI7	R. Nyando mouth	0.286	34.854	1.9	2.0	0.2	2.3	2.6	5.5	3.3	4.2	2.2
Sugarcane	**S1**	R. Mbogo	0.099	34.751	2.4	0.3	0.1	< 0.04	2.5	4.4	2.0	3.2	2.9
	S2	R. Ainapsiwa dstrm	0.028	35.175	3.4	1.3	1.5	0.4	4.0	5.6	4.1	4.1	7.4
	S3	R. Ainamotua at confluence	0.029	35.174	3.1	2.7	1.4	0.6	3.4	4.5	3.3	3.5	3.4
	S4	R. Ainapngetuny dstrm	0.030	35.179	2.6	2.4	1.4	1.0	3.0	4.1	3.0	3.3	5.3
	S5	R. Ainapsiwa upstrm	0.011	35.194	1.6	2.3	1.2	0.9	3.0	4.7	3.8	4.1	6.7
	S6	R. Ainapngetuny midstream	0.001	35.292	3.5	2.7	1.9	1.8	3.3	4.0	3.5	2.7	5.4
	S7	R. Koru	0.173	35.263	2.5	1.2	1.4	0.4	2.7	4.8	2.3	6.2	6.3
	S8	R. Ainamotua at Kibigori	0.076	35.056	–	–	2.1	0.8	3.1	4.6	1.5	3.5	4.7
Tea & Forest	**TF1**	R. Mbogo at Kipkoil forest	0.065	35.334	3.3	1.9	1.9	2.9	3.6	4.0	4.5	2.3	4.1
	TF2	R. Ainapngetuny at Tinderet	0.021	35.369	2.5	2.9	1.6	2.1	2.0	4.4	2.8	1.6	4.2
	TF3	R. Mbogo at Mbogo valley	0.070	35.307	3.8	2.5	1.6	2.5	4.3	< 0.04	4.2	2.6	5.2

Table A6. The spatial $\delta^{15}N–NO_3^-$ values (‰) in R. Nyando during the nine season monitoring period (2016 – 2018). "–" represents samples not analyzed

Land use	Station ID	Peak wet/2016	End wet/2016	Dry/ 2016	Start wet/2017	Peak wet/2017	End wet/2017	Dry/ 2017	Start wet/2018	Peak wet/2018
Mixed Agriculture	**MA1**	9.6	8.1	8.6	8.9	8.8	8.3	11.2	10.2	10.8
	MA2	9.5	9.8	8.8	8.9	10.0	7.8	10.7	11.6	10.4
	MA3	14.0	9.0	9.5	13.9	13.7	10.1	11.8	10.7	12.9
	MA4	8.8	6.8	12.4	9.4	9.7	7.2	10.3	11.1	11.4
	MA5	11.8	7.3	4.8	5.3	12.1	7.0	–	13.8	13.6
Residential & Industrial	**RI1**	10.3	8.4	10.9	11.8	10.5	7.4	10.1	11.2	11.3
	RI2	8.9	9.4	12.1	8.2	10.0	6.9	–	11.4	11.4
	RI3	6.3	7.5	8.3	8.2	10.0	5.1	–	11.3	11.6
	RI4	9.3	8.6	8.2	–	9.9	8.2	8.9	9.8	11.9
	RI5	8.0	9.0	15.1	7.8	7.4	6.5	13.1	9.1	11.2
	RI6	9.2	7.1	11.1	9.2	7.5	14.4	–	10.4	11.2
	RI7	8.6	8.8	8.6	9.3	7.2	8.5	–	11.3	11.9
Sugarcane	**S1**	7.4	7.9	9.8	–	6.9	7.5	–	8.6	8.8
	S2	10.0	8.6	8.6	9.0	6.6	6.8	–	9.5	9.7
	S3	8.8	6.1	10.4	8.8	7.0	6.7	–	10.0	9.4
	S4	9.1	8.1	8.5	9.4	6.5	7.1	–	9.8	8.9
	S5	10.0	7.6	9.4	7.3	7.3	6.7	–	10.0	9.3
	S6	9.2	9.1	8.6	9.6	8.5	6.4	9.9	11.3	9.2
	S7	10.2	10.5	11.8	9.6	8.5	6.8	8.8	9.2	9.8
	S8	–	–	7.8	8.6	7.7	11.9	–	9.5	10.6
Tea & Forest	**TF1**	7.4	5.4	6.6	8.8	6.7	5.5	9.1	9.0	7.4
	TF2	5.1	3.8	7.2	6.4	5.6	–	6.3	7.2	6.4
	TF3	6.4	7.0	8.9	9.0	7.9	–	–	9.8	7.8

Table A7. The spatial $\delta^{18}O–NO_3^-$ values (‰) in R. Nyando during the nine season monitoring period (2016 – 2018). "–" represents samples not analyzed

Land use	Station ID	Peak wet/2016	End wet/2016	Dry/ 2016	Start wet/2017	Peak wet/2017	End wet/2017	Dry/ 2017	Start wet/2018	Peak wet/2018
Mixed Agriculture	**MA1**	11.5	5.1	11.0	3.4	5.5	8.5	6.3	6.8	4.0
	MA2	9.4	11.8	10.2	2.3	4.0	11.1	6.2	8.2	7.0
	MA3	19.6	11.1	16.6	17.0	17.0	17.3	17.8	16.3	13.4
	MA4	10.3	*2.4*	11.7	1.0	7.2	8.8	6.5	7.1	8.2
	MA5	9.1	-1.1	-4.5	9.1	8.6	6.2	–	6.9	12.8
Residential & Industrial	**RI1**	10.7	6.9	9.3	6.0	6.0	6.4	5.4	5.7	10.0
	RI2	9.1	8.8	8.9	3.4	7.5	9.0	–	6.4	7.7
	RI3	12.0	5.8	1.6	8.6	6.3	7.3	–	6.0	9.9
	RI4	10.5	8.1	12.5	–	7.6	7.2	3.6	4.1	10.5
	RI5	8.4	3.1	7.2	0.2	10.0	14.9	14.9	5.1	7.5
	RI6	11.4	4.5	4.8	4.4	10.3	12.9	–	4.4	10.9
	RI7	10.6	6.3	1.4	4.4	11.4	11.0	–	6.9	11.6
Sugarcane	**S1**	7.9	12.7	3.8	–	6.6	5.1	–	5.3	7.0
	S2	8.4	9.6	9.7	9.1	7.3	6.7	–	7.0	5.1
	S3	6.8	9.0	10.2	5.5	5.4	11.4	–	4.8	5.6
	S4	6.2	8.7	7.6	5.9	7.5	5.8	–	6.8	7.6
	S5	9.0	6.2	2.8	7.1	6.0	6.0	–	5.3	6.4
	S6	8.8	8.5	9.7	6.2	8.1	7.2	10.1	4.9	5.4
	S7	12.5	8.0	15.6	5.5	6.7	7.2	4.7	6.5	8.0
	S8	–	–	7.0	5.2	6.5	15.2	–	5.7	10.7
Tea & Forest	**TF1**	8.6	4.1	5.7	4.8	7.3	7.1	-0.3	6.0	4.0
	TF2	5.0	3.4	10.6	4.7	4.4	–	0.6	5.6	6.0
	TF3	6.1	6.6	12.0	5.0	5.3	–	–	5.2	5.0

Figure A1. Aerial photo of commercial flower farming in upper reaches of the Nyando-Kipchorian River, showing the location of the water pond upstream of the MA3 station.

Table A8. Hydro-chemical and isotopic parameters for shallow wells (SW) and boreholes (BH) in Kisumu and the Kano plains during the wet season (May-July, 2017); values < 0.04 for NO_2^- and NO_3^-, and < 0.01 for NH_4^+ indicate attributes below detection limit; "–" represents samples not analyzed

Station ID	pH (-)	EC (µS cm^{-1})	Temp (ºC)	DO (mg L^{-1})	F^- (mgL^{-1})	Cl^- (mgL^{-1})	NO_2^- (mgL^{-1})	NO_3^- (mgL^{-1})	SO_4^- (mgL^{-1})	HCO_3^- (mgL^{-1})	Na^+ (mgL^{-1})	NH_4^+ (mgL^{-1})	K^+ (mgL^{-1})	Ca^{2+} (mgL^{-1})	Mg^{2+} (mgL^{-1})	$\delta^{15}N$ (‰)	$\delta^{18}O$ (‰)
SW1	6.3	900	25.1	1.8	0.4	55.7	0.04	90.6	48.4	19.7	75.7	0.02	36.3	47.9	10.8	21.0	15.9
SW2	6.3	578	26.4	2.2	0.6	35.5	< 0.04	47.9	35.1	–	50.6	< 0.01	22.5	31.4	6.9	19.5	14.3
SW3	6.4	997	26.3	1.9	0.8	58.1	0.08	80.4	52.2	30.3	78.5	0.48	55.0	51.7	13.5	21.8	14.5
SW4	6.4	433	26.2	2.0	0.4	27.0	< 0.04	19.8	33.5	23.7	40.9	0.04	23.4	22.8	4.4	28.9	19.8
SW5	6.8	540	26.1	1.2	0.3	37.3	0.15	11.4	36.6	25.7	43.0	0.03	11.7	35.7	8.6	25.6	14.5
SW6	6.3	740	27.4	2.2	0.4	48.9	< 0.04	71.7	43.9	–	67.3	0.01	29.5	37.6	9.3	21.2	12.3
SW7	6.7	916	26	2.1	0.4	51.4	0.06	65.3	38.0	29.8	81.6	11.4	39.4	34.3	8.7	21.8	10.3
SW8	7.0	830	25.8	4.0	0.9	50.1	0.13	59.5	56.3	–	99.6	< 0.01	27.4	36.0	6.2	20.5	7.5
SW9	6.3	591	27.1	2.3	0.4	40.0	< 0.04	44.0	44.7	19.6	56.3	< 0.01	26.8	26.3	6.8	25.2	17.1
SW10	8.0	912	27.6	3.9	3.3	4.5	< 0.04	5.3	14.8	–	169	0.02	17.1	15.6	4.2	8.0	7.5
SW11	7.6	865	26.3	2.6	1.6	5.6	< 0.04	0.2	11.5	109	177	0.03	5.9	13.4	3.7	13.1	14.0
SW12	7.1	814	25.7	1.3	1.0	3.8	< 0.04	< 0.04	10.8	86.6	119	0.09	3.4	23.5	10.3	–	–
SW13	7.5	885	25.3	4.4	0.7	1.7	< 0.04	2.6	1.4	–	82.0	0.01	7.0	24.8	30.0	8.9	8.7
SW14	8.6	248	25.8	1.8	2.1	5.6	< 0.04	< 0.04	7.6	–	52.1	< 0.01	1.3	2.5	0.4	–	–
SW15	7.5	970	26.6	2.8	2.8	13.0	< 0.04	0.8	28.7	109	214	0.02	4.4	7.1	1.5	23.2	16.5
SW16	7.4	1302	27.7	6.2	3.5	75.5	< 0.04	57.6	49.5	–	180	0.01	25.2	34.2	9.4	17.7	19.1
SW17	7.8	1420	28.2	6.2	8.0	18.4	0.06	11.6	23.4	16.6	311	0.06	36.2	6.5	0.9	14.3	8.7
BH1	7.1	747	30	2.2	3.2	15.7	< 0.04	5.8	10.6	91.3	139	0.02	17.5	24.7	3.0	12.9	12.0
BH2	7.3	727	25.3	5.1	3.2	15.6	< 0.04	2.8	10.2	–	136	0.01	14.7	23.1	2.0	10.0	9.3
BH3	7.4	1434	27.2	2.4	1.8	42.8	< 0.04	0.0	84.4	120	241	0.02	14.9	42.0	8.9	–	–
BH4	7.5	1215	27.5	3.2	3.9	27.4	0.04	9.1	58.4	118	220	0.03	23.5	32.8	5.4	7.2	5.1
BH5	7.5	947	28	2.3	3.0	1.6	< 0.04	1.2	3.8	117	159	0.05	32.0	27.2	4.7	8.6	5.5
BH6	7.5	985	28.1	2.4	2.4	2.4	< 0.04	1.5	4.9	124	171	0.03	24.0	31.3	4.2	8.6	5.0
BH7	7.8	883	28.3	4.0	5.3	4.3	< 0.04	11.8	11.9	99.3	168	0.01	19.6	16.6	3.4	4.8	4.6
BH9	7.4	1064	29	3.7	2.4	22.4	0.04	20.0	17.9	106	162	0.01	25.7	39.2	7.1	11.5	7.9

BH10	7.7	1074	29	5.9	2.7	26.0	< 0.04	22.8	28.6	–	164	0.03	31.2	33.2	6.4	9.3	5.3
BH11	7.1	2520	28	1.7	2.9	80.1	< 0.04	0.7	212.3	119	452	0.04	49.1	58.0	10.2	21.9	15.3
BH12	7.4	295	26	2.3	1.5	8.7	< 0.04	4.5	23.1	–	33.6	0.14	4.9	19.5	2.1	19.5	9.3
BH13	7.1	950	26.8	2.2	1.3	26.4	0.06	10.2	22.1	77.1	82.7	0.00	6.1	54.9	29.2	25.4	18.6
BH14	7.8	1268	28.1	2.6	5.8	16.2	< 0.04	2.8	42.4	–	269	0.03	13.5	13.8	2.8	6.9	6.7
BH15	7.6	1300	28	1.4	3.9	23.5	< 0.04	1.1	57.3	128	266	0.02	12.1	18.5	4.8	12.1	11.1
BH16	7.5	1148	28.8	2.1	2.4	26.1	< 0.04	< 0.04	57.5	–	71.8	0.09	18.4	74.7	31.3	–	–
BH17	7.6	1202	27.7	5.3	4.6	37.6	< 0.04	43.7	27.6	107	194	0.02	52.2	30.1	4.0	13.9	7.9
BH18	7.5	1113	27.7	2.1	2.7	14.5	0.04	14.5	37.7	122	180	0.02	46.7	30.8	8.6	4.1	1.1
BH19	7.5	743	26.6	1.9	2.1	5.3	< 0.04	2.1	12.2	–	82.4	0.06	16.8	38.0	5.2	18.4	15.0
BH20	7.6	1057	27	5.8	2.8	5.9	< 0.04	0.4	21.4	129	196	0.03	35.2	19.3	5.9	4.8	-2.4
BH21	7.0	536	27.8	1.8	2.5	15.8	< 0.04	2.0	5.5	–	89.6	0.08	19.0	11.6	1.1	17.5	14.0
BH22	7.2	1224	37.6	1.8	8.1	27.7	< 0.04	< 0.04	20.1	2.4	282	0.03	7.5	3.6	0.3	–	–
BH23	7.0	484	26.1	4.4	0.7	3.4	< 0.04	5.4	0.9	45.1	34.4	< 0.01	5.9	27.2	16.2	11.5	11.9
BH24	7.4	638	27.5	6.7	0.9	2.2	< 0.04	4.5	2.7	56.6	52.7	< 0.01	12.5	30.5	12.2	9.8	8.7
BH25	7.2	1013	26.2	2.0	3.8	5.1	< 0.04	0.4	21.3	–	219	0.02	14.5	7.0	2.2	13.2	9.6
BH26	7.6	1701	26.7	3.3	10.5	_	0.04	1.4	69.4	17.5	370	0.05	15.3	10.7	3.6	24.6	17.7
BH27	10.2	1080	31.2	3.5	9.0	70.8	< 0.04	< 0.04	71.9	7.7	187	0.00	7.8	1.1	0.2	–	–
BH28	10.1	1065	31.5	2.3	10.9	73.9	< 0.04	< 0.04	74.8	14.2	174	< 0.01	6.1	1.5	0.1	–	–
BH29	6.9	943	27.8	3.1	1.6	9.0	< 0.04	10.7	6.7	92.2	136	< 0.01	15.4	24.5	7.5	14.9	12.0
BH30	7.6	1045	25.9	2.0	5.7	2.8	< 0.04	< 0.04	6.1	128	213	0.06	18.2	12.1	4.2	–	–
BH31	7.3	1577	28	3.6	7.2	35.4	< 0.04	2.0	84.8	–	290	0.04	34.4	20.4	5.8	14.1	6.6
BH32	8.2	1378	27	1.8	6.2	12.7	< 0.04	0.1	48.1	167	318	0.06	14.0	5.2	1.4	25.8	20.8
BH33	7.3	1144	28.1	3.9	4.1	21.3	< 0.04	2.9	38.9	103	173	0.02	66.5	19.1	4.4	9.0	2.4
BH34	7.5	1247	26.6	2.3	–	–	–	–	–	–	246	0.03	38.7	9.8	1.0	10.7	8.7
BH35	7.6	1034	27.5	5.1	2.4	14.0	< 0.04	7.4	12.9	99.9	182	0.03	39.8	11.6	1.8	7.4	9.6
BH36	7.4	1245	28.7	3.3	6.8	16.8	< 0.04	6.8	13.7	143	225	0.04	45.1	12.7	2.1	10.1	4.7

Table A9. Hydro-chemical and isotopic parameters for shallow wells (SW) and boreholes (BH) in Kisumu and the Kano plains during the dry season (February, 2018); values < 0.04 for NO_2^- and NO_3^- , and < 0.01 for NH_4^+ indicate attributes below detection limit; "–" represents samples not analyzed

Station ID	pH (-)	EC (µS cm^{-1})	Temp (ºC)	DO (mg O_2 L^{-1})	Cl^- (mgL^{-1})	NO_2^- (mgL^{-1})	NO_3^- (mgL^{-1})	SO_4^- (mgL^{-1})	HCO_3^- (mgL^{-1})	Na^+ (mgL^{-1})	NH_4^+ (mgL^{-1})	K^+ (mgL^{-1})	Ca^{2+} (mgL^{-1})	Mg^{2+} (mgL^{-1})	$\delta^{15}N$ (‰)	$\delta^{18}O$ (‰)
SW1	6.4	861	25.1	2.6	90.4	0.15	38.2	67.2	20.1	79.0	0.01	36.7	40.7	10.6	31.2	16.1
SW2	6.5	290	25.7	2.4	14.0	0.42	10.3	28.5	–	31.1	< 0.01	15.2	12.2	2.9	24.5	14.7
SW3	6.7	895	26.1	4.2	92.2	0.12	25.2	58.6	4.9	77.9	0.21	48.7	39.2	12.9	37.8	19.1
SW4	6.2	417	26.1	1.6	31.1	< 0.04	0.4	27.5	–	41.5	0.07	20.6	23.8	4.7	38.8	15.8
SW5	6.7	655	24.5	2.4	73.4	< 0.04	0.4	46.2	36.6	50.7	0.03	9.6	42.4	10.0	51.8	20.2
SW6	6.4	673	26.8	4.5	62.2	0.12	30.0	49.2	–	62.7	< 0.01	26.9	30.5	8.4	30.6	17.4
SW7	6.6	978	25.6	2.9	103.0	0.41	25.2	54.6	52.7	93.5	14.1	43.5	37.3	10.2	37.4	19.4
SW8	7.6	1177	24.8	3.7	28.7	< 0.04	4.4	46.9	25.2	129.1	0.07	62.1	30.5	12.4	48.1	29.3
SW9	6.4	377	28.5	9.8	31.1	0.06	6.4	45.5	–	37.8	< 0.01	20.3	16.0	4.5	35.8	21.6
SW10	8.2	835	27.3	6.2	4.3	1.74	5.7	17.9	–	170.6	0.03	16.2	7.7	2.9	12.4	12.7
SW11	7.4	882	26.3	4.1	5.5	1.96	0.04	13.6	111.3	188.1	0.03	6.0	12.7	3.8	–	–
SW12	7.3	772	26.1	3.2	2.8	1.07	0.3	9.0	85.3	125.8	0.03	3.1	20.1	9.5	–	–
SW15	7.6	1024	26.7	3.7	15.0	2.20	0.3	37.4	121.7	235.7	0.06	4.6	9.3	1.8	–	–
SW18	7.0	830	25.5	3.4	44.6	0.15	6.1	19.3	–	–	–	–	–	–	–	–
BH1	7.1	731	28.9	3.4	16.3	< 0.04	3.7	11.8	83.3	131.6	0.02	17.5	18.1	3.0	15.7	12.8
BH2	7.4	734	36.0	5.1	0.1	< 0.04	0.04	–	82.1	135.7	0.03	16.3	13.5	1.7	–	–
BH3	7.1	1276	26.3	2.3	59.5	1.93	< 0.04	121.2	111.2	235.0	0.04	14.9	36.8	9.4	–	–
BH4	7.2	1210	28.5	2.5	32.5	1.96	8.8	75.8	111.0	218.2	0.04	23.5	25.1	5.2	9.2	7.0
BH5	7.3	936	28.3	4.0	5.1	1.70	4.4	5.9	106.7	150.9	0.03	31.1	20.2	5.5	10.4	8.1
BH6	7.3	978	28.0	3.7	2.2	1.87	2.4	5.9	114.4	168.8	0.03	23.9	21.5	4.1	11.7	8.2
BH7	7.7	878	28.0	4.9	3.9	1.63	7.7	11.9	104.1	172.1	0.02	19.4	15.3	3.0	9.8	9.2
BH9	7.2	1129	29.0	4.3	36.8	1.80	36.0	23.7	100.1	172.5	0.03	27.2	25.8	6.7	21.0	17.1
BH11	7.1	2562	29.0	2.6	136.5	2.03	0.5	359.9	119.4	461.0	0.09	48.6	52.7	9.5	23.1	15.8

BH13	6.8	924	26.8	3.0	29.9	0.06	11.3	26.4	82.4	77.8	0.02	6.3	43.1	30.0	31.2	24.1
BH14	7.7	1262	27.5	4.9	20.0	2.31	2.8	64.5	25.4	276.1	0.06	14.0	10.3	2.9	14.6	13.2
BH15	7.3	1286	27.6	2.9	29.7	0.06	1.2	84.3	131.7	266.7	0.05	12.3	16.0	4.9	17.6	16.8
BH16	7.2	920	28.0	4.1	20.8	< 0.04	2.4	73.7	–	39.4	< 0.01	14.8	59.9	23.5	–	–
BH17	7.4	1262	27.7	5.9	55.9	< 0.04	69.9	37.8	95.9	196.8	0.02	53.1	19.7	4.0	16.2	8.9
BH18	7.2	979	28.5	2.9	8.8	0.11	6.3	14.3	109.5	153.7	0.02	29.7	25.1	0.0	15.5	13.3
BH19	7.4	723	26.9	4.4	5.9	0.76	3.7	11.7	–	80.3	0.02	16.8	32.1	5.3	18.7	14.3
BH20	7.4	1044	27.2	6.0	5.9	2.24	0.3	27.6	123.3	193.0	0.04	34.5	16.6	5.9	6.9	-1.1
BH23	6.7	482	26.0	4.4	3.7	1.04	6.6	1.0	53.4	37.4	< 0.01	6.0	24.9	17.5	12.4	12.3
BH24	7.3	779	29.6	6.1	1.9	0.92	4.6	2.7	72.7	67.9	0.01	16.0	34.3	15.6	17.2	11.1
BH25	7.7	1007	25.7	2.9	4.6	1.44	0.04	26.0	126.6	225.7	0.04	14.8	8.6	2.2	–	–
BH26	7.7	1790	26.7	2.9	40.4	3.17	1.9	103.7	163.9	381.5	0.09	14.6	10.9	3.4	32.2	20.1
BH27	9.6	1103	32.0	2.7	139.8	0.43	0.04	106.3	38.7	218.5	0.02	10.6	1.2	0.18	–	–
BH28	9.6	1066	31.4	2.7	155.5	0.17	0.04	117.5	20.2	205.6	0.01	7.7	1.7	0.15	–	–
BH29	7.4	940	29.0	5.3	24.9	1.28	9.6	21.7	89.4	158.7	0.03	13.4	21.5	5.8	18.5	13.5
BH30	7.7	1044	26.1	2.7	1.4	2.15	0.1	7.2	130.6	219.7	0.05	18.6	12.3	4.3	–	–
BH31	7.5	1535	27.5	4.0	47.1	2.51	2.4	126.9	–	297.8	0.06	36.4	23.7	6.2	17.5	12.2
BH32	8.1	1360	26.1	3.2	12.4	2.69	0.1	67.3	172.0	327.1	0.08	14.3	4.8	1.3	–	–
BH33	7.2	1125	28.1	4.8	29.0	1.46	4.9	58.6	102.9	174.8	0.03	67.9	24.2	4.3	12.2	7.8
BH35	7.7	1037	27.3	5.4	28.2	1.32	15.7	30.5	99.2	182.6	0.04	40.6	17.0	1.8	16.4	8.4
BH36	7.4	1256	28.7	3.9	20.1	2.58	8.2	17.1	134.1	234.9	0.05	49.1	16.3	1.9	11.5	7.3
BH38	6.8	964	27.5	3.2	56.9	2.06	9.2	24.8	77.7	131.3	0.03	20.2	27.4	5.4	17.3	11.3
BH39	7.0	727	28.1	4.7	1.4	1.89	0.9	3.8	–	167.8	0.03	25.9	31.9	6.8	8.0	-1.7
BH40	7.0	727	26.7	4.6	4.2	1.66	5.0	0.4	–	62.2	< 0.01	3.5	35.4	24.3	11.3	6.8
BH41	7.1	748	26.4	3.7	1.9	1.09	3.0	3.7	65.0	29.8	< 0.01	12.4	38.0	25.4	17.5	13.4
BH42	7.5	1386	28.7	2.0	1.3	2.86	3.5	7.7	–	59.2	0.01	13.3	37.4	14.9	11.3	14.8
BH43	7.1	944	29.7	3.2	8.4	1.51	7.3	9.3	–	307.0	0.08	38.1	10.0	0.8	16.7	11.0
BH44	7.3	1219	28.6	2.9	40.2	0.06	3.4	64.6	–	144.5	0.02	19.9	26.8	7.7	18.8	13.0

Curriculum Vitae

PERSONAL INFORMATION

Name	Benjamin Kyalo Nyilitya
Date of birth	23rd December 1973
Place of birth	Machakos, Kenya
Nationality	Kenyan
Address	P O Box 7456-00200, Nairobi
Telephone	+254720981209
Email	kyalob73@yahoo.com
Civil status	Married

EDUCATION

2016 – 2020	PhD in Bioscience Engineering-Environmental Science & Technology Department of Green Chemistry & Technology (ISOFYS) Faculty of Bioscience Engineering, Ghent University
2004 – 2007	Master of Science in Nuclear Science Institute of Nuclear Science & Technology University of Nairobi
1994 – 1998	Bachelor of Science (Chemistry) University of Nairobi
1989 – 1992	Kenya Certificate of Secondary Education Pope Paul VI Seminary, Machakos

PROFESSIONAL EXPERIENCE

2019 - Current	Principal Chemist Department of National Water Resources Management Ministry of Water, Sanitation & Irrigation
2013 - 2018	Senior Chemist, Department of National Water Resources Management Ministry of Water, Sanitation & Irrigation
2008 – 2012	Chemist 1 Department of National Water Resources Management Ministry of Water, Sanitation & Irrigation

2005 – 2007	Research Assistant Institute of Nuclear Science & Technology University of Nairobi

Master Thesis Supervision

Nicholas Ouma (2017). Nitrate source apportionment in surface water of a tropical river basin: physicochemical and isotopic tracer approach. MSc. Physical Land Resources, Ghent University, Belgium

Joyce Irungu (2018). Nitrate source apportionment, fractionation, and removal mechanism using stable isotopes in River Sondu Miriu – Lake Victoria catchment, Kenya. MSc. Environmental Sanitation, Ghent University, Belgium

Grants

- Awarded VLIRUOS (Belgium) scholarship to study PhD in Bioscience Engineering, at Ghent University (2016 - 2020)
- Awarded the University of Nairobi Gandhi Smarak Nidhi Scholarship to study Msc. Nuclear science (2004-2005)

SCIENTIFIC PUBLICATION

Peer-reviewed indexed articles

1st Author

- Nyilitya, B., Mureithi, S., Boeckx, P., 2020. Land use controls Kenyan riverine nitrate discharge into Lake Victoria – evidence from Nyando, Nzoia and Sondu Miriu river catchments, *Isotopes in Environmental and Health Studies*, 56:2, 170-192, DOI: 10.1080/10256016.2020.1724999
- Nyilitya, B., Mureithi, S., Boeckx, P., 2020. Tracking Sources and Fate of Groundwater Nitrate in Kisumu City and Kano Plains, Kenya. *Water* 12, 1–18. DOI:10.3390/w12020401

2nd Author

- D. M. Maina, L. W. Njenga, J. M. Onyari and B. N. Kyalo, Trace Element Concentrations in Some Traditional Diets Consumed in Selected Parts of Eastern Province of Kenya, *Journal of Environmental Protection*, Vol. 3 No. 7, 2012, pp. 617-623. DOI: 10.4236/jep.2012.37075.

Conference Contributions

- Nyilitya, B., Irungu, J., Mureithi, S., Boeckx, P., 2019. Nitrate source apportionment in river Sondu Miriu, Kenya. *General Assembly of the European Geosciences Union* (EGU). 7 –12th April 2019, Vienna-Austria. **Poster presentation**
- Nyilitya, B., Mureithi, S., Boeckx, P., 2017. Stable isotope forensics for improved management of nitrate pollution in the Lake Victoria catchment. *Lake Victoria basin*

environmental research and scientific conference, 15 – 16th February 2017, Mwanza-Tanzania. **Oral Presentation**

- Nyilitya, B., Mureithi, M.S., Boeckx, P., 2016. Tracking sources of excess nitrate discharge in Lake Victoria, Kenya for improved Nitrogen use efficiency in the catchment. *2016 International Nitrogen Initiative Conference, "Solutions to Improve Nitrogen Effieciency for the World"*, 4 – 8th December, 2016, Melbourne, Australia. **Oral presentation**
- Nyilitya, B., Mureithi, S., Boeckx, P., 2015. Use of δ^{15}N- and δ^{18}O-NO_3^- for tracing nitrate pollution sources in Lake Victoria catchment, Kenya. *The TropiLakes 2015 Conference*, 23 – 29th September 2015, Bahir Dar, Ethiopia. **Oral presentation**
- Nyilitya B. K, Omondi C. O, Karicho B. M, Mbugua A. Water Resources Assesment for Lamu Port using Isotope Hydrology. Presented in the *1st Science, Technology & Innovation week,* 7th- 11th May 2012, Nairobi, Kenya. **Oral presentation**

International Fellowships & Research Stay

- IAEA fellow at the Isotope Bioscience Laboratory (ISOFYS), Faculty of bio-science engineering, Ghent University, Belgium. To develop skills in isotope hydrology and applications of stable nitrogen isotopes in water pollution studies, bacterial denitrification method and isotope ratio mass spectrometry, 4th May- 3rd July 2015
- Research Stay for PhD proposal development at ISOFYS, Gent University- Belgium. Nov/ 2011 - Feb/ 2012. Funded by VLIRUOS - Belgium.
- IAEA fellow at the Centre for Atomic Physics, University of Lisbon, Portugal. Performing laboratory tests using the Total X-ray Fluorescence Spectroscopy (TXRF), April - June 2009.